INFORMATION TO USERS

This manuscript has been reproduced from the microfilm master. UMI films the text directly from the original or copy submitted. Thus, some thesis and dissertation copies are in typewriter face, while others may be from any type of computer printer.

The quality of this reproduction is dependent upon the quality of the copy submitted. Broken or indistinct print, colored or poor quality illustrations and photographs, print bleedthrough, substandard margins, and improper alignment can adversely affect reproduction.

In the unlikely event that the author did not send UMI a complete manuscript and there are missing pages, these will be noted. Also, if unauthorized copyright material had to be removed, a note will indicate the deletion.

Oversize materials (e.g., maps, drawings, charts) are reproduced by sectioning the original, beginning at the upper left-hand corner and continuing from left to right in equal sections with small overlaps. Each original is also photographed in one exposure and is included in reduced form at the back of the book.

Photographs included in the original manuscript have been reproduced xerographically in this copy. Higher quality 6" x 9" black and white photographic prints are available for any photographs or illustrations appearing in this copy for an additional charge. Contact UMI directly to order.

U·M·I

University Microfilms International
A Bell & Howell Information Company
300 North Zeeb Road, Ann Arbor, MI 48106-1346 USA
313/761-4700 800/521-0600

Order Number 9325165

Syntheses and investigations of electron acceptor substituted barbaralanes

Win, War War, Ph.D.

City University of New York, 1993

U·M·I
300 N. Zeeb Rd.
Ann Arbor, MI 48106

A

SYNTHESES AND INVESTIGATIONS OF ELECTRON ACCEPTOR SUBSTITUTED BARBARALANES

by

WAR WAR WIN

A dissertation submitted to the Graduate Faculty in Chemistry in partial fulfillment of the requirements for the degree of Doctor of Philosophy, The City University of New York

1993

This manuscript has been read and accepted for the Graduate Faculty in Chemistry in satisfaction of the dissertation requirement for the degree of Doctor of Philosophy.

3-8-93
Date

Dr. Klaus G. Grohmann
Chair of Examining Committee

3/9/93
Date

Dr. Richard Pizer
Executive Officer

Dr. Richard W. Franck
Supervisory Committee

Dr. William F. Berkowitz
Supervisory Committee

THE CITY UNIVERSITY OF NEW YORK

Abstract

SYNTHESES AND INVESTIGATIONS OF
ELECTRON ACCEPTOR SUBSTITUTED BARBARALANES

by

War War Win

Advisor: Professor Klaus G. Grohmann

The fundamental work of Doering and Roth in discovering the degenerate Cope rearrangement in homotropilidene **I** is one of the milestones of organic chemistry.

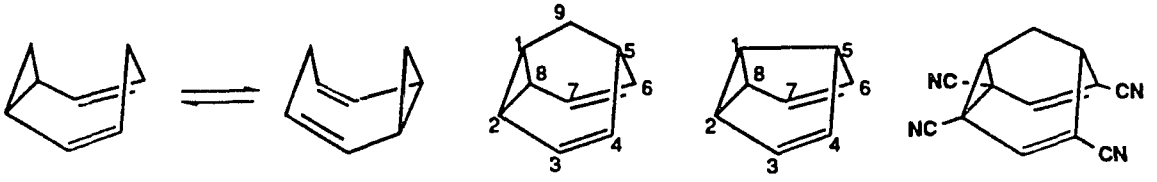

I **II** **III** **IV**

This project will focus on our attempts to reduce the activation energies for the Cope rearrangements of barbaralane **II** and semibullvalene **III**, which have the essential structure element of the homotropilidene system **I**. The activation energies of the Cope rearrangement of compounds **II** and **III** are 7.6 kcal/mol and 5.4 kcal/mol respectively. Theory has predicted that the activation energy of the Cope rearrangement of compound **III** would be lowered by substituting electron acceptors at C_2, C_4, C_6 and C_8 positions.

Furthermore, Hoffmann and Stohrer reported that four cyano groups at C_2, C_4, C_6 and C_8 positions would lower the activation energy of compounds **II** and **III** by 9.6 kcal/mol, making the 2,4,6,8-tetracyanobarbaralane **IV** an important target molecule. As the direct access to compound **IV** is difficult, we have investigated other pathways toward **IV** via 2,4,6,8-tetracarbomethoxy-barbaralane **V**.

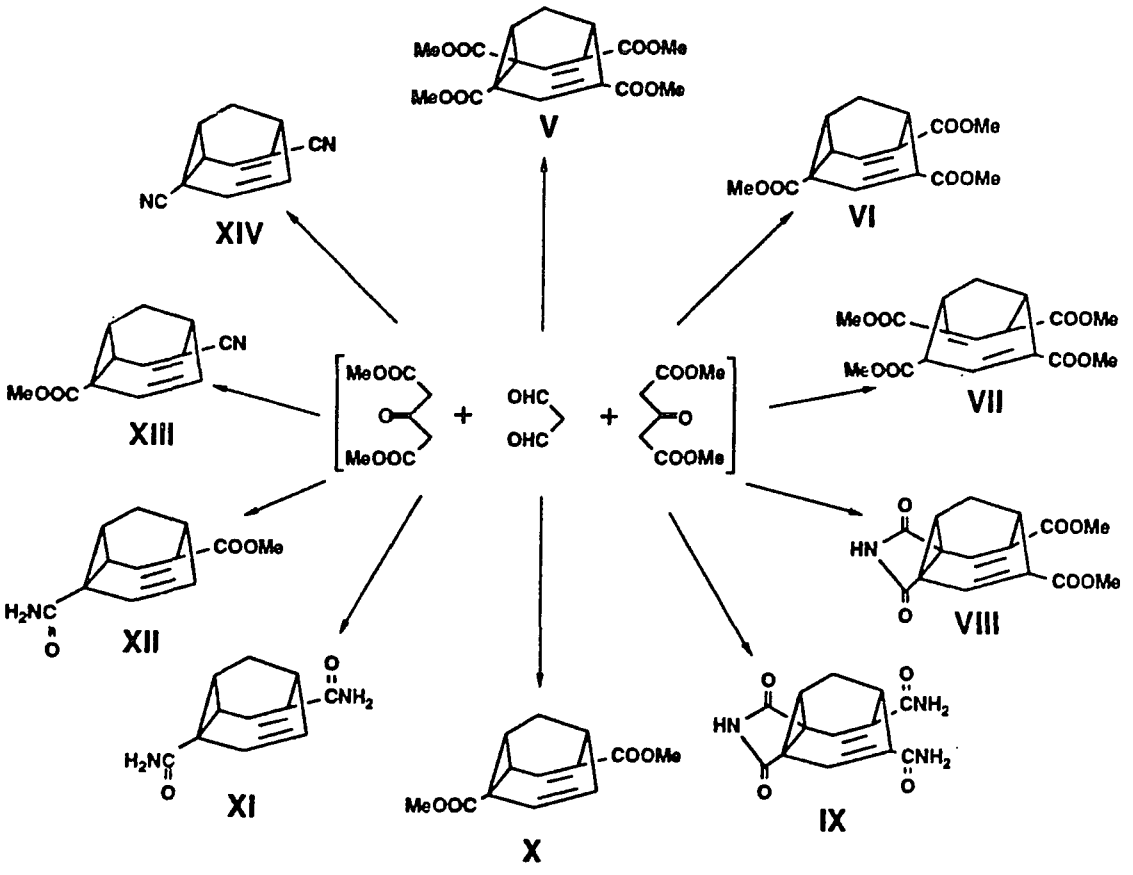

Electron Acceptor Substituted Barbaralanes

Synthesized via the Weiss Reaction

A new synthetic approach toward electron acceptor substituted barbaralanes has been described in this thesis. Strong equilibrium preferences are observed for compounds **VI**, **VIII**, **IX** and **XIII** with the equilibrium on the site of the most electron acceptor substituents on the double bond. Lowering of the activation energy of the Cope rearrangement is observed for the dynamic barbaralanes **V**, **X**, **XI**, **XII** and **XIV**. The dynamic behavior of compounds **V**, **X** and **XII**, as determined by variable temperature X-ray, NMR and IR spectroscopy, has been studied.

ACKNOWLEDGEMENTS

I would like to express my profound gratitude and indebtedness to my thesis advisor Professor Klaus G. Grohmann, for giving me the opportunity to be a member of his group and for his invaluable guidance, advice and encouragement throughout the entire process of this research work. His continuous support and intellectual discussions made the years of my graduate career pleasant and fruitful.

I am also grateful to Professors Richard W. Franck and William F. Berkowitz for their invaluable suggestions, comments and encouragement during the course of this work.

It is a pleasure to acknowledge Professor Max Diem for his helpful comments in FT-IR studies.

I take this opportunity to express my sincere thanks to Mr. Louis J. Todaro at Hoffmann-La Roche for his invaluable contribution for the X-ray crystal structure analysis on the chemistry of the electron acceptor substituted barbaralanes and for his various support.

I extend my thanks to Dr. Michael Blumenstein for his special help in recording NMR spectra.

Special thanks go to Dr. Thanos Karydas for his invaluable suggestions.

Finally, I would like to acknowledge my heartfelt gratitude to Mr. Phillip K. Young and Mrs. Ellen H. Young, Ms. Hla Yin, Dr. Htwe Yin and all of my colleagues for their kind support.

TO MY PARENTS

TABLE OF CONTENTS

CHAPTER 3

CHAPTER 4

LIST OF FIGURES

CHAPTER 1

CHAPTER 2

CHAPTER 3

CHAPTER 4

CHAPTER 5

LIST OF SCHEMES

CHAPTER 2

LIST OF TABLES

CHAPTER 1

CHAPTER 4

CHAPTER 6

Pages corresponding to spectral data available for compounds listed in chapters 2, 3 and 4

#	Structure	mp(°C)	NMR					IR/FT-IR		X-ray	UV	Vibrat. Anal.
			^{1}H		^{13}C							
			1-D	2-D	RT	Varia. Temp.	CP-MAS	Sol:	Solid			
5-a		100-102	218					238				
18		99-100	163		164	170	172	157	158 & 159	46, 147 & 244	45	154
23		~20	174		175	177						
26	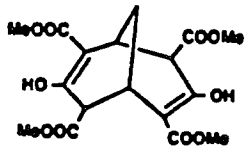	183-185	30		31							
27	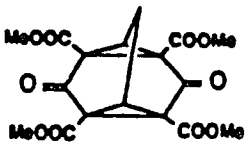	245-246	219					239		33 & 255		

Pages corresponding to spectral data available for compounds listed in chapters 2, 3 and 4

#	Structure	mp(°C)	NMR					IR/FT-IR		X-ray	UV	Vibrat. Anal.
			^{1}H		^{13}C							
			1-D	2-D	RT	Varia. Temp.	CP-MAS	Sol:	Solid			
28-a	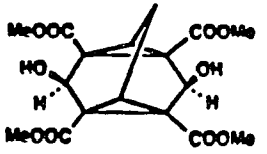	185-186	220					240		37, 38 & 261		
30		158-159	221		232			48		49 & 262	45	
31-a		105-107	52		53			241		58 & 268		
57	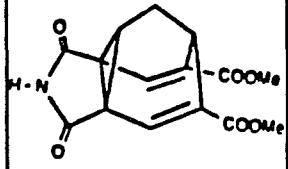	267-269	70		71				242	72 & 274		
58	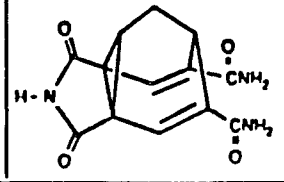	> 300	73									

Pages corresponding to spectral data available for compounds listed in chapters 2, 3 and 4

#	Structure	mp(°C)	NMR					IR/FT-IR		X-ray	UV	Vibrat. Anal.
			^{1}H		^{13}C							
			1-D	2-D	RT	Varia. Temp.	CP-MAS	Sol:	Solid			
67	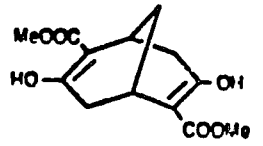	149-151	78		79							
68	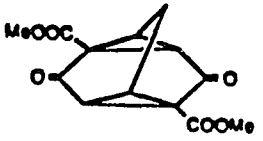	133-135	83									
76	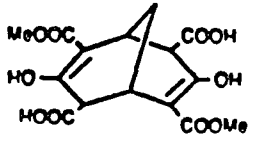	115-140	222									
81	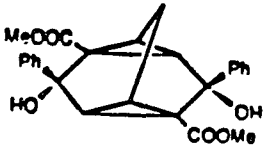		89							90 & 280		
85-c	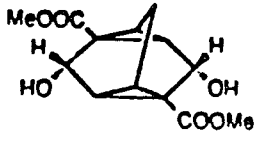	143-145	223							94 & 286		

Pages corresponding to spectral data available for compounds listed in chapters 2, 3 and 4

#	Structure	mp(°C)	NMR					IR/FT-IR		X-ray	UV	Vibrat. Anal.
			^{1}H		^{13}C							
			1-D	2-D	RT	Varia. Temp.	CP-MAS	Sol:	Solid			
86	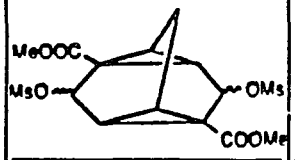	liq.	96									
87	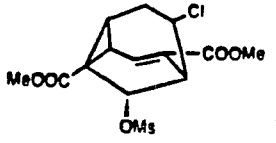	130-133	224									
88	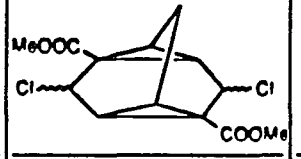	liq.	98									
89	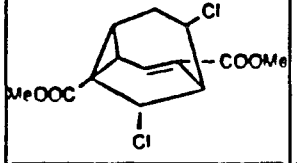	96-98	225									
91	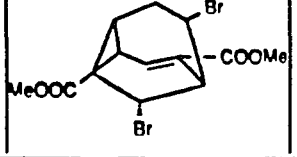	121-123	104	107						105 & 287		

Pages corresponding to spectral data available for compounds listed in chapters 2, 3 and 4

#	Structure	mp(°C)	NMR					IR/FT-IR		X-ray	UV	Vibrat. Anal.
			^{1}H		^{13}C							
			1-D	2-D	RT	Varia. Temp.	CP-MAS	Sol:	Solid			
94		> 280	113									
95-a		165-166	115 & 180		117 & 181	182				118 & 288		
96-a		107-108	226	124	233	125		126		127 & 294		
102	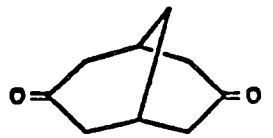	215-220	227		234							
104	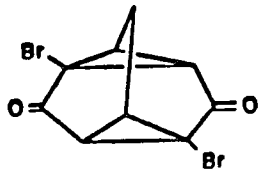	203-205	228									

Pages corresponding to spectral data available for compounds listed in chapters 2, 3 and 4

#	Structure	mp(°C)	NMR					IR/FT-IR		X-ray	UV	Vibrat. Anal.
			^{1}H		^{13}C							
			1-D	2-D	RT	Varia. Temp.	CP-MAS	Sol:	Solid			
114	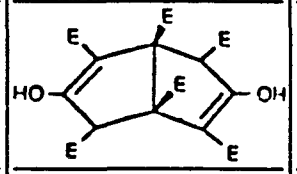	210-213	229		235					141 & 300		
115	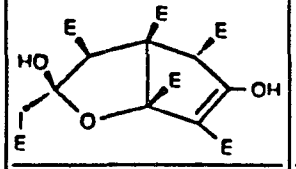	174-175	230		236					142 & 306		

CHAPTER 1

1.0. INTRODUCTION

1.1. Background

The Cope rearrangement (3,3-sigmatropic shift) which involves a bond breaking of one σ bond and the formation of another is one of the best studied reactions.[1] The most obvious feature of the Cope rearrangement is its inherent symmetry. The rearrangement of 1,5-hexadiene is the archetypical example of this type of chemistry[2] (Figure 1). The transformation, **1-a** to itself **1-b**, involves no structural change: the Cope rearrangement is degenerate.

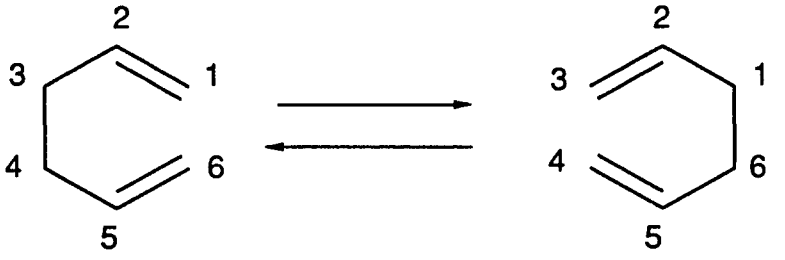

1-a 1-b

Figure 1: The Cope Rearrangement of 1,5-Hexadiene

The interconversion of bicyclo[5,1,0]octa-2,5-diene (homotropilidene) **2-a** to the superimposable mirror image of itself **2-b** also represents such a fully symmetrical, completely reversible Cope rearrangement[3] (Figure 2).

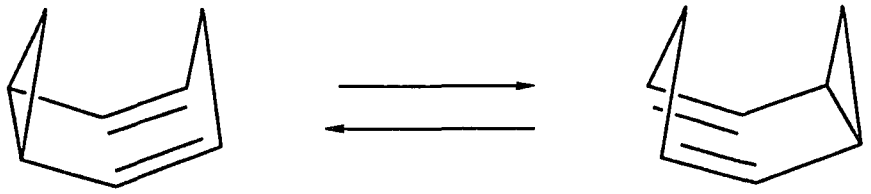

2-a 2-b

Figure 2: The Cope Rearrangement of Homotropilidene

Three principle structures have been considered for the transition state of the Cope rearrangement in the 1,5-hexadiene and homotropilidene system[4,5] (Table 1):

(1) the diallyl structure **A** with bond breaking as the initial step,

(2) the structure **B** with synchronous bond making and breaking,

(3) the 1,4-diradical ("diyl") structure **C** with bond formation as the initial step.

Table 1: Three Possible Transition States of 1,5-Hexadiene and Homotropilidene

Structure	Initial Step	1,5-Hexadiene	Homotropilidene
A	bond breaking	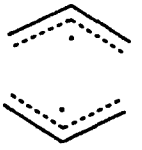	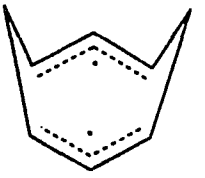
B	synchronous	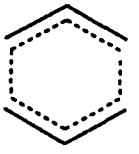	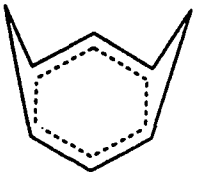
C	bond formation	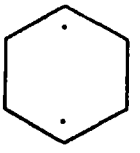	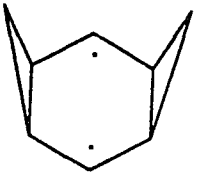

The structure of the transition state for this rearrangement has been studied by many chemists. Gajewski[6] as well as others concluded that the nature of the transition state depends upon the substituents and geometric constraints present in the molecule. A study by Dewar and Wade[7] assessed the effects of substituents on the rate of Cope

rearrangement in the 1,5-hexadiene system. They carried out the studies on 2-phenyl- and 2,5-diphenyl-1,5-hexadiene and postulated a biradicalroid (type **C**) intermediate for this reaction. They found a 69 and 4900 times rate increase, when compared with the parent, respectively. In contrast, homotropilidene should represent the extreme case for a rearrangement involving a transition state like **A** because (a) bond breaking as the initial step parallels with the relief of strain of the cyclopropane ring (transition state **A** or **B** of the homotropilidene), and (b) bond formation leads to a second strained three-membered ring (transition state **C** of the homotropilidene).

Among the various questions raised about the transition state of the Cope rearrangement, one that received considerable attention dealt with the chair/boat nature of the transition state. Doering[8] approached the problem from an experimental point of view, while Hoffmann and Woodward[9] attacked it theoretically. Both studies led to the conclusions that the chair conformation is the preferred conformation of the transition state for the Cope rearrangement in molecules free of geometric constraints; however, in bridged cyclic compounds the rearrangement has to proceed via the boat transition state.

The free energies of activation for the Cope rearrangement of 1,5-hexadiene and homotropilidene are 35.5 kcal/mol[10] and 13.7 kcal/mol[11] respectively, but, there are some bridged compounds for which this energy is much smaller. As shown in Table 2, the bridged homotropilidenes such as bullvalene, barbaralane, and semibullvalene, are of particular interest.

Table 2: Free Energies of Activation ($\Delta G^{\neq}$) in Bridged Homotropilidenes

Compound	$\Delta G^{\neq}$(kcal/mol)
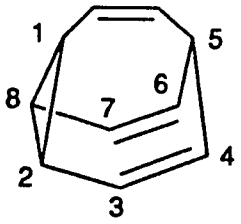 Bullvalene	12.8[12]
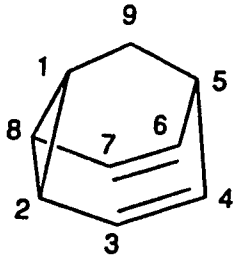 Barbaralane	7.6 [4,13]
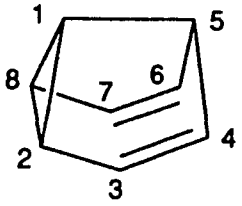 Semibullvalene	5.4[14]

Among them the activation energy of semibullvalene is the lowest on record.

If one looks at the Kekulé structures of benzene as the most extreme case of a rapidly rearranging cyclohexatriene system (Figure 3), then the proposed hypothetical "transition state", benzene itself, has a lower energy than either Kekulé structure and thus, is the actual ground state of the molecule.[15]

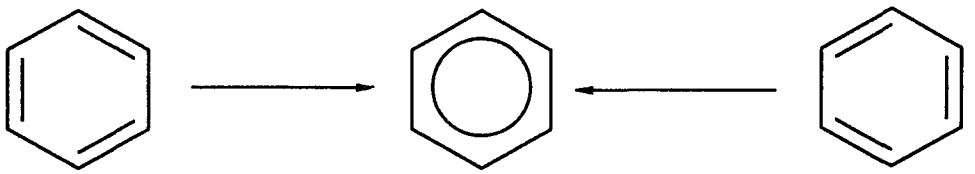

Figure 3: Benzene: The Transition State of the cyclohexatriene

Extension of this reasoning led many chemists to postulate methods of lowering the energy barrier in other systems. As mentioned in Table 2, the free energy of activation for the degenerate Cope rearrangement of the barbaralane is 7.6 kcal/mol. The potential energy diagram of the Cope rearrangement of barbaralane via the transition state can be illustrated schematically below (Figure 4).

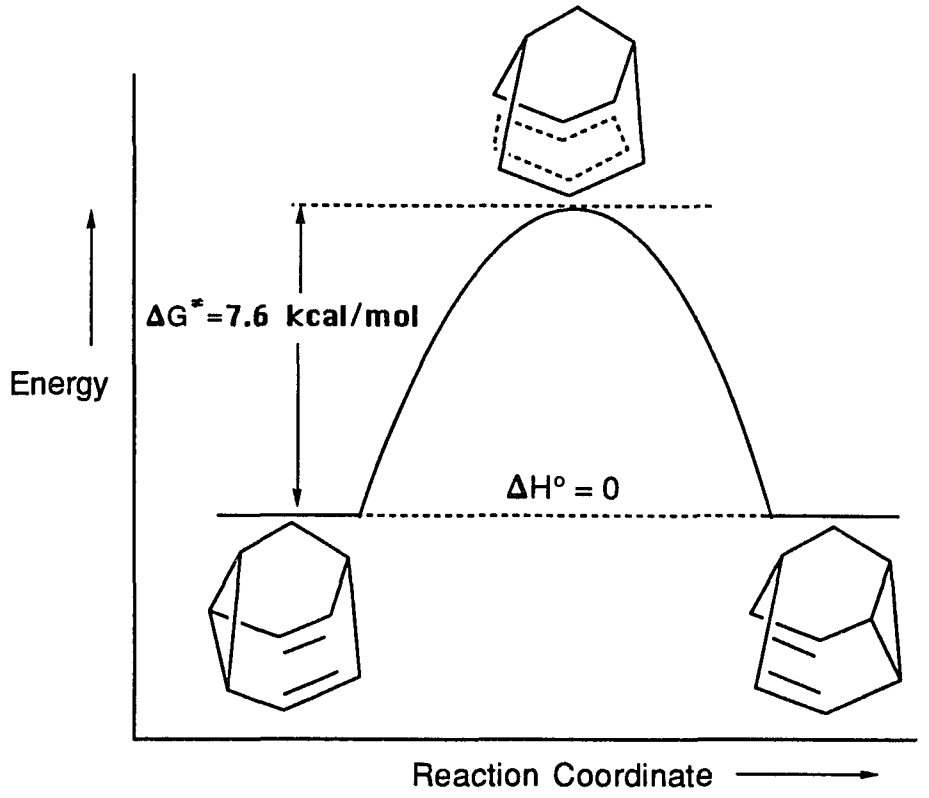

Figure 4: Degenerate Cope Rearrangement of Barbaralane

The degenerate Cope rearrangement of barbaralane was thought to be a synchronous reaction with a homoaromatic transition state.

The concept of homoaromaticity, introduced into organic chemistry by W. von E. Doering and S. Winstein, has stimulated and intrigued many researchers. A homoaromatic molecule is defined as an aromatic system whose σ-skeleton may be interrupted by an sp^3-carbon bridge at one or more sites resulting in mono- , bis- , tris- , etc., homoaromatic species and which still retains its aromatic character.[16]

Based on this concept, the transition state of the barbaralane **3** has been considered as bishomobenzene **3b** (Figure 5).

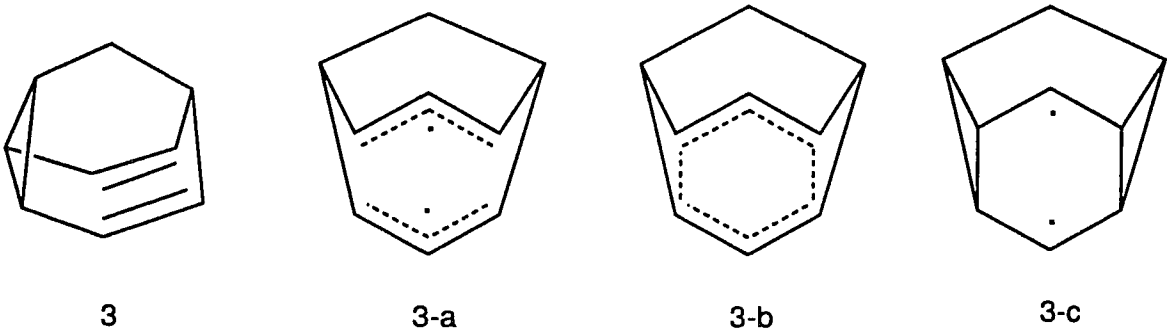

Figure 5: Three Possible Transition States for Barbaralane

If the transition state of the barbaralane **3** were bishomobenzene, it should have negative activation energy barrier. However, the reported energy barrier of barbaralane **3** is 7.6 kcal/mol which is found experimentally.[4] In order to achieve such a stage of perfection, we need to attack the problem of reducing the activation energy of the Cope rearrangement of barbaralane **3** to a negative number. Thus, the prospect of further lowering the activation energy by stabilizing the transition state , or destabilizing the ground state, or by some combination of both, and thus reaching a "transition state" of lower energy than the "ground state" is a challenge, and if successful would yield the first neutral bishomoaromatic molecule.

The concept of homoaromaticity initiated an impressive amount of both experimental and theoretical work.[17] While a large number of homoaromatic ions have been prepared and characterized, no neutral homoaromatic molecule has so far been reported.[16,17]

1.2. Theoretical Predictions And Previous Syntheses

In the early 1970's, theoreticians utilized several different methods to calculate the geometries of the ground and transition states for the bullvalene series and made predictions about the energies of activation for the Cope rearrangement. Dewar and Schoeller used MINDO/2 to study the Cope rearrangement in the bullvalene, barbaralane and semibullvalene.[18] They obtained an activation energy of 5.9 kcal/mol for the Cope rearrangement of barbaralane and calculated a transition state geometry where C_2-C_8 and C_4-C_6 bonds (The numbering system of barbaralane is shown in Table 2, p. 5.) were 1.720Å apart. Since MINDO/2 overestimates the stability of cyclic compounds, the calculated energy of activation was thought to be somewhat low.

In a later study by Dewar and Lo utilizing the data from MINDO/2 and applying an energy partitioning technique[19], they calculated an activation energy of 6.5 kcal/mol for the barbaralane.

The exchange rate constants for the Cope rearrangement in barbaralane were determined at several temperatures by Doering and co-workers[13] which led to an activation energy (E_{act}) of 8.6 ± 0.2 kcal/mol at 298K. The free energy of activation ($\Delta G^{\neq}$) at −77°C was 7.8 kcal/mol[20],while the enthalpy ($\Delta H^{\neq}$) and entropy ($\Delta S^{\neq}$) of activation were 9.8 ± 0.3 kcal/mol and 11.5 ± 0.3 eu, respectively.[21]

According to theoretical studies by Hoffmann and Stohrer using EHMO- theory[15] and by Dewar and co-workers using MINDO/2[19], it was

predicted that π-electron donors in positions 1 and 5, and π-electron acceptors in positions 2, 4, 6, and 8 will lower the activation energy for the Cope rearrangement in semibullvalene by destabilizing the ground state and stabilizing the transition state (Figure 6).

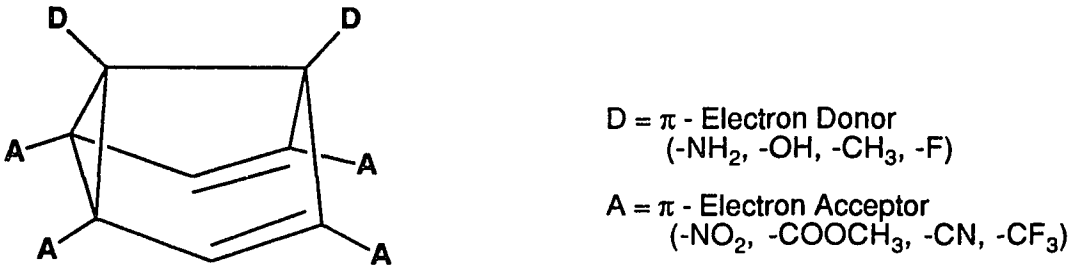

Figure 6: Hoffmann and Dewar's Design of Delocalized Bishomoaromatic Semibullvalene

Hoffmann also described that four cyano substituents in positions 2, 4, 6, and 8 were calculated to decrease $\Delta G^{\neq}$ by 9.6 kcal/mol[15] with respect to the unsubstituted molecules, such as semibullvalene and barbaralane, thus reaching negative values. After substitution, the transition states for tetracyanosemibullvalene and tetracyano-barbaralane would therefore be lower in energy than the ground state. In other words, within a given system this would cross the bridge from valence tautomerism, characterized by a positive activation energy, to resonance, with formally a negative activation energy (Figures 7 and 8).

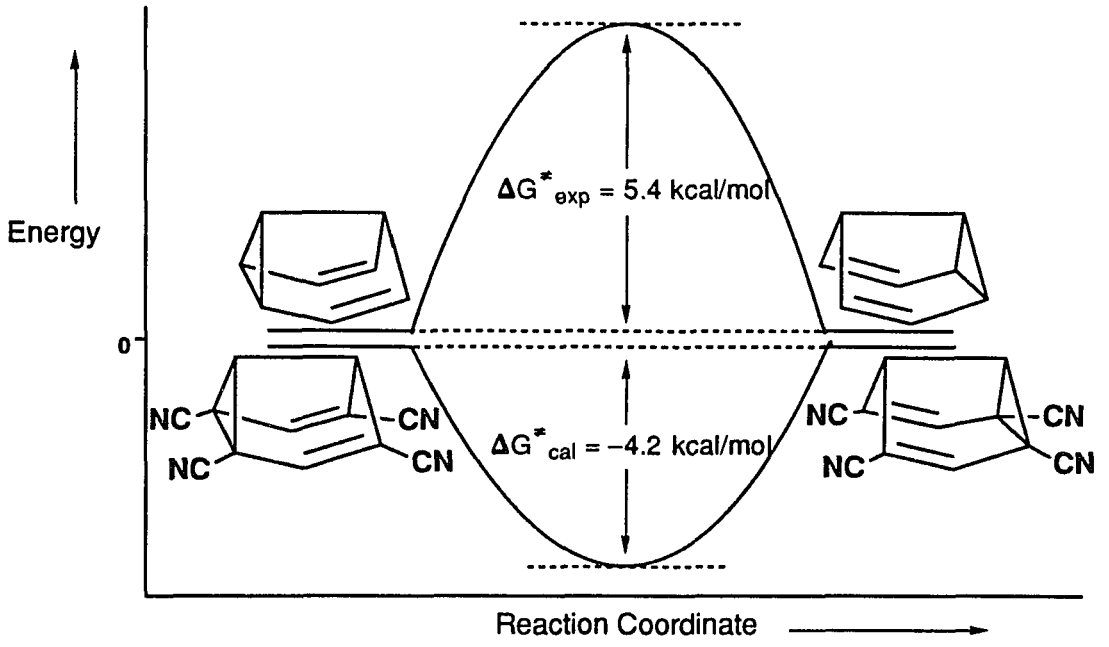

Figure 7: Potential energy diagram of 2,4,6,8-tetracyanosemibullvalene

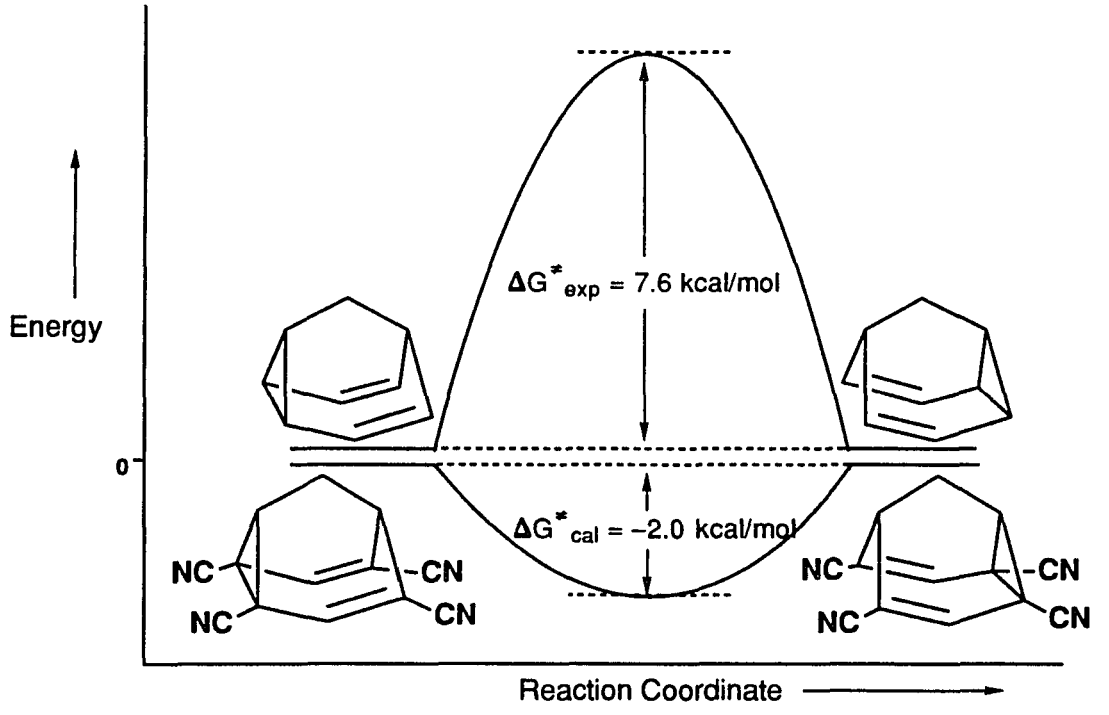

Figure 8: Potential energy diagram of 2,4,6,8-tetracyanobarbaralane

In 1983, Dannenberg, Miller and Grohmann [22] reported a MNDO-CI studies of the Cope rearrangements of unsubstituted semibullvalene and 2,4-dicyano-, 2,6-dicyano-, 3,7-dicyano-, and 2,4,6,8-tetracyano-semibullvalene. The calculated activation energy for semibullvalene is 5.7 kcal/mol, in good agreement with experiment. The differences in the energies between the delocalized and localized structures are 8.9, −0.2, 9.8, and −4.7 kcal/mol, respectively, for the cyano derivatives. Thus, 2,6-dicyanosemibullvalene (E_{act}= −0.2 kcal/mol) should have classical and delocalized structures of approximately equal energy. Since 2,4,6,8-tetracyanosemibullvalene has the activation energy of −4.7 kcal/mol, it is clearly predicted to have a homoconjugated ground state. This MNDO-CI calculations of the localized and delocalized structures of cyano-substituted semibullvalenes essentially agree with the earlier studies.[15]

In 1981, L. S. Miller[23] of our laboratory synthesized the first donor-acceptor substituted semibullvalene and determined the free energy of activation for a rapid degenerate Cope rearrangement of 1,5-dimethyl-2,4,6,8-tetracarbomethoxysemibullvalene **4** (Figure 9). Dynamic ^{13}C-NMR studies yielded an estimated activation energy for this molecule of 3.8 ± 0.3 kcal/mol. A significant decrease of the activation energy for the Cope rearrangement (1.6 kcal/mol) is observed, as predicted.

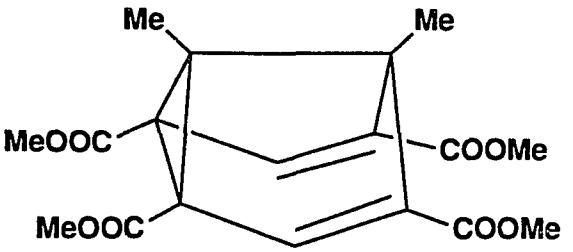

4

Figure 9: 1,5-Dimethyl-2,4,6,8-tetracarbomethoxysemibullvalene

Quast and co-workers also reported an analogous decrease in activation energies for the degenerate Cope rearrangement of 2,6-dicyano-[24] and 2,6-diphenylbarbaralane[25] **5-a and 5-b** (Figure 10). They determined the energy barriers from ^{13}C-NMR line width measurements and found 5.78 kcal/mol for the former and 5.16 kcal/mol for the latter. Their results show that 2,6-diphenylbarbaralane possesses an even lower activation barrier towards degenerate Cope rearrangement than 2,6-dicyanobarbaralane because phenyl groups stabilize the transition state.

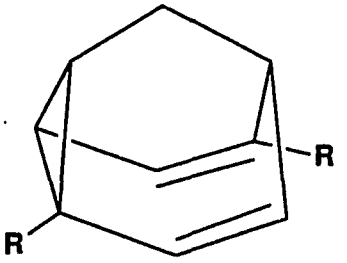

5-a: R = CN

5-b: R = Ph

Figure 10: 2,6-Disubstituted Barbaralanes

In this connection, the activation energy of the Cope rearrangement for 3,7-disubstituted barbaralanes is of interest. The activation parameters for the degenerate Cope rearrangement of parent barbaralane and three 3,7-disubstituted barbaralanes, such as 3,7-dicyano- , 3,7-dibromo- , and 3,7-dimethylbarbaralane (**6-a, 6-b, and 6-c**) have been determined by Günther and co-workers[4] (Figure 11). They investigated the substituent effects on rate constants of fluxional systems by dynamic ^{13}C FT-NMR spectroscopy. For the parent system, $\Delta G^{\neq}_{298} = 7.6$ kcal/mol. Substitution of barbaralane at the 3,7-positions leads to very small changes for the activation parameters of its valence tautomerism, in accord with earlier estimates obtained for substituents like Cl and OCH_3 by Hoffmann.[26]

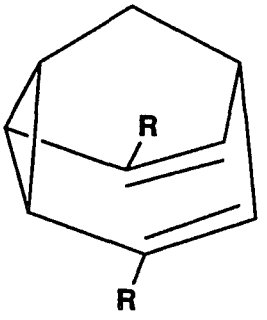

6-a: R = CN

6-b: R = Br

6-c: R = CH_3

Figure 11: 3,7-Disubstituted Barbaralanes

The degenerate Cope rearrangement of 3,7-diphenylbarbaralane **7** (Figure 12) has been analysed by Kessler and Ott.[5] Their results showed that substitution in the 3,7-positions of the barbaralane by phenyl groups increases the energy barrier by 1.7 kcal/mol. They assumed that the experimental observation of increasing in the barrier could be related

to an effect of electron donating groups (such as methyl or phenyl) on the basis of the increase in electron density in the transition state.

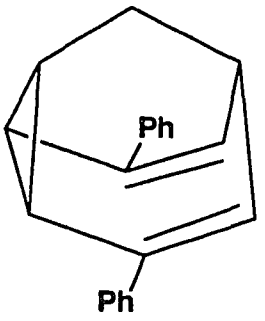

7

Figure 12: 3,7-Diphenylbarbaralane

Studies on the heteroatom-substituted barbaralanes have been reported. The temperature dependence of the ^{13}C-NMR spectra of 3,7-diethoxy-1,5-dimethyl-2,4,6,8-tetraazabarbaralane **8** (Figure 13) has been analysed in the temperature range of 298-210K by Gompper and co-workers.[27] The energy barrier of **8** is found to be higher by 1.68 kcal/mol with respect to the unsubstituted barbaralane, this is due to the combined effect of 4-N, 2-OEt and 2-Me.

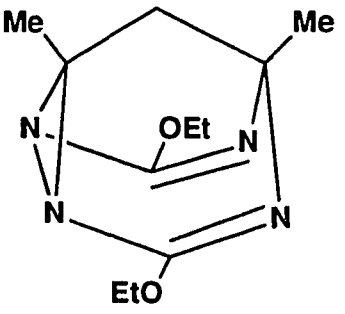

8

Figure 13: 3,7-Diethoxy-1,5-dimethyl-2,4,6,8-tetraazabarbaralane

Furthermore, Barton et al.[28] studied the rapid degenerate Cope rearrangement of 9-silabarbaralane **9** (Figure 14) at room temperature and they found out that both pmr and cmr spectra illustrated 9-silabarbaralane to be completely frozen at −70°C.

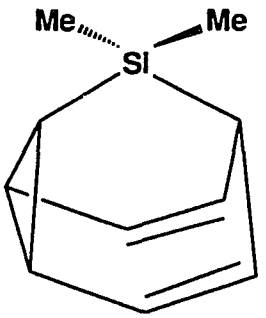

9

Figure 14: 9-Silabarbaralane

Anastassiou and co-workers prepared the thermally unstable, unsubstituted 9-azabarbaralane **10-a** and its N-methyl derivative **10-b** (Figure 15) and found that the nitrogen lone pair exerts a destabilizing effect on the 9-azabarbaralane system.[29] They reported the dynamic character of **10-a** ($\Delta G^{\neq}_{305} \approx 22$ kcal/mol) and its increasing thermal stability in acid media.

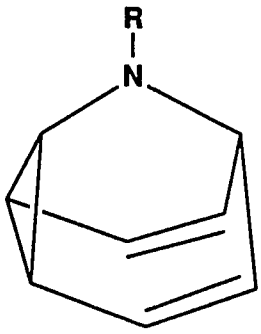

10-a: R = H

10-b: R = CH_3

Figure 15: 9-Azabarbaralane **10-a** and its N-methyl derivative **10-b**

9-Thiabarbaralane **11**, whose ^{1}H-NMR spectrum is analogous to that described[30] for barbaralone, was prepared by Anastassiou et al.[31] (Figure 16). They described that the pronounced insolubility of **11** in such media as acetone and carbondisulfide at temperature below −30°C frustrated all attempts at assessing the activation parameters of its valence bond isomerism.

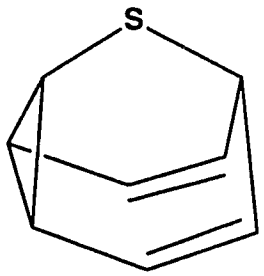

11

Figure 16: 9-Thiabarbaralane

Katz and co-workers[32] prepared 9-phosphabarbaralane **12-b** from the bridged phosphine **12-a** upon irradiation with ultraviolet light (Figure 17). Their synthetic route toward **12-b** seems shorter than others that have given barbaralanes.[13,33] The oxide of **12-b** shows at room temperature an NMR spectrum similar to that of parent barbaralane[13]: with the phosphorus spin decoupled besides phenyl protons. The kinetic parameter, estimated as E_{act} = 7.0 kcal/mol, is similar to that for the unsubstituted hydrocarbon.[13]

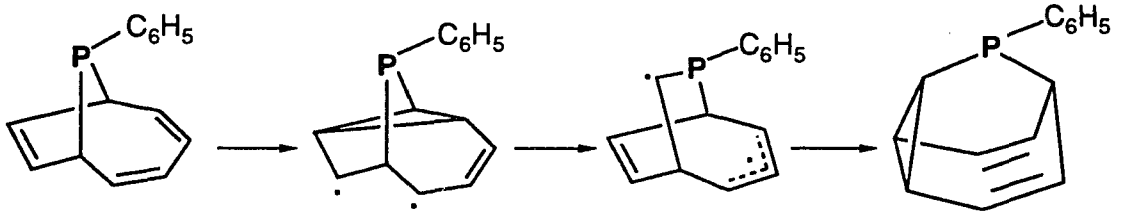

12-a 12-b

Figure 17: 9-Phosphabarbaralane

A 9-phospheniumbarbaralane salt **13** (Figure 18) has been synthesized and investigated by Baxter and co-workers.[34] In the solid state, it exhibits bond distances closely resembling the expected values for Cope transition state by showing very similar C_2-C_8 and C_4-C_6 distances (C_2-C_8 = 1.949Å and C_4-C_6 = 2.054Å respectively). But, qualitative evaluation of the dynamic NMR behavior in solution indicated with the estimated Cope energy barrier of 12 ± 1.7 kcal/mol.

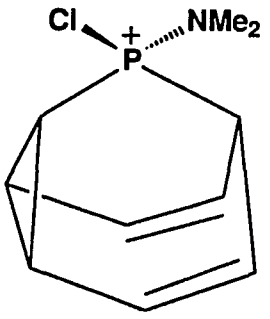

13

Figure 18: 9-Phospheniumbarbaralane

As predicted theoretically by Hoffmann[15] and Dewar[19,35] and done experimentally by many researchers,[18-37] 1, 5-donor-2, 4, 6, 8-acceptor-substitution is the only effective approach towards a barbaralane or a semibullvalene with a negative activation energy , in other words, to a neutral bishomoaromatic structure. Here is a very intriguing and different concept involving destabilization of the ground state by strain, stabilization of the transition state through extended conjugation as well, resulting in the establishment of a strained aromatic (4n + 2) perimeter. This possibility was first discussed by Hoffmann and Stohrer[15] for the unknown system **14** (Figure 19), predicted not to exist as a 2,8-4,6-bisetheno bridged semibullvalene **14** but as a strained bridged [10]annulene **15**. For the related molecule, the bridged [14]annulene structure **16** was established mainly by NMR data.[38]

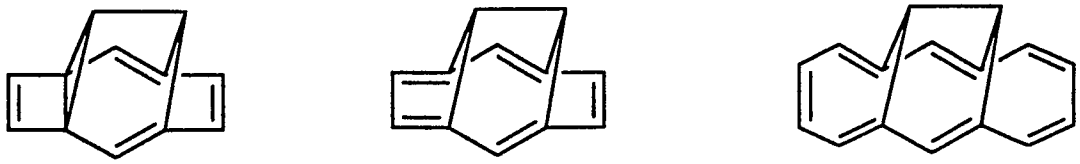

14 15 16

Figure 19: 2,8-4,6-Doubled Bridged Semibullvalenes

In 1988, Williams and Kurtz[39] carried out a theoretical investigation of the effects of small-ring annelation at the termini of the semibullvalene nucleus (Figure 20).

17-a 17-b

Figure 20: Small-ring Annelation in Semibullvalene

They used MNDO (plus 2 × 2 CI) as well as AM1 and predicted stabilization of the delocalized **17-b** over the localized bridged semibullvalene **17-a** by 10.73 kcal/mol.

1.3. Scope of the Present Research Work

By long tradition, theoretical predictions stimulate experimental work. In fact, Hoffmann and Dewar's design of delocalized homoaromatic semibullvalenes presents a considerable experimental challenge which is getting more attention in our laboratory. After studying the substituent effects in semibullvalene by L. S. Miller[23] and R. Iyengar,[40] we have chosen to study the effect of substituents in barbaralane system (Figure 21) since, unlike the semibullvalene system which is known to rearrange readily to cyclooctatetraenes.

The successful synthesis of 1,5-dimethyl-2,4,6,8-tetracarbomethoxy-semibullvalene **4** and its characterization as a molecule approaching the bishomoaromatic transition state prompted us to investigate the related barbaralane system, 2,4,6,8-tetracarbomethoxybarbaralane **18**. The four carbomethoxy groups are good π-electron acceptors and therefore predicted to lower the activation energy as demonstrated in the semibullvalene case. Compound **18** could be the key compound in the preparation of other substituted barbaralanes.

Conversion of ester functional groups of **18** into linear nitrile groups is well documented. Theoretical results indicating that suitably substituted derivatives – for example, 2,4,6,8-tetracyanosemibullvalene – might show "negative activation energies" for their hypothetical valence tautomerism, i.e., homoaromatic character,[15,19] have motivated us to test this prediction experimentally by using barbaralane as a model molecule.

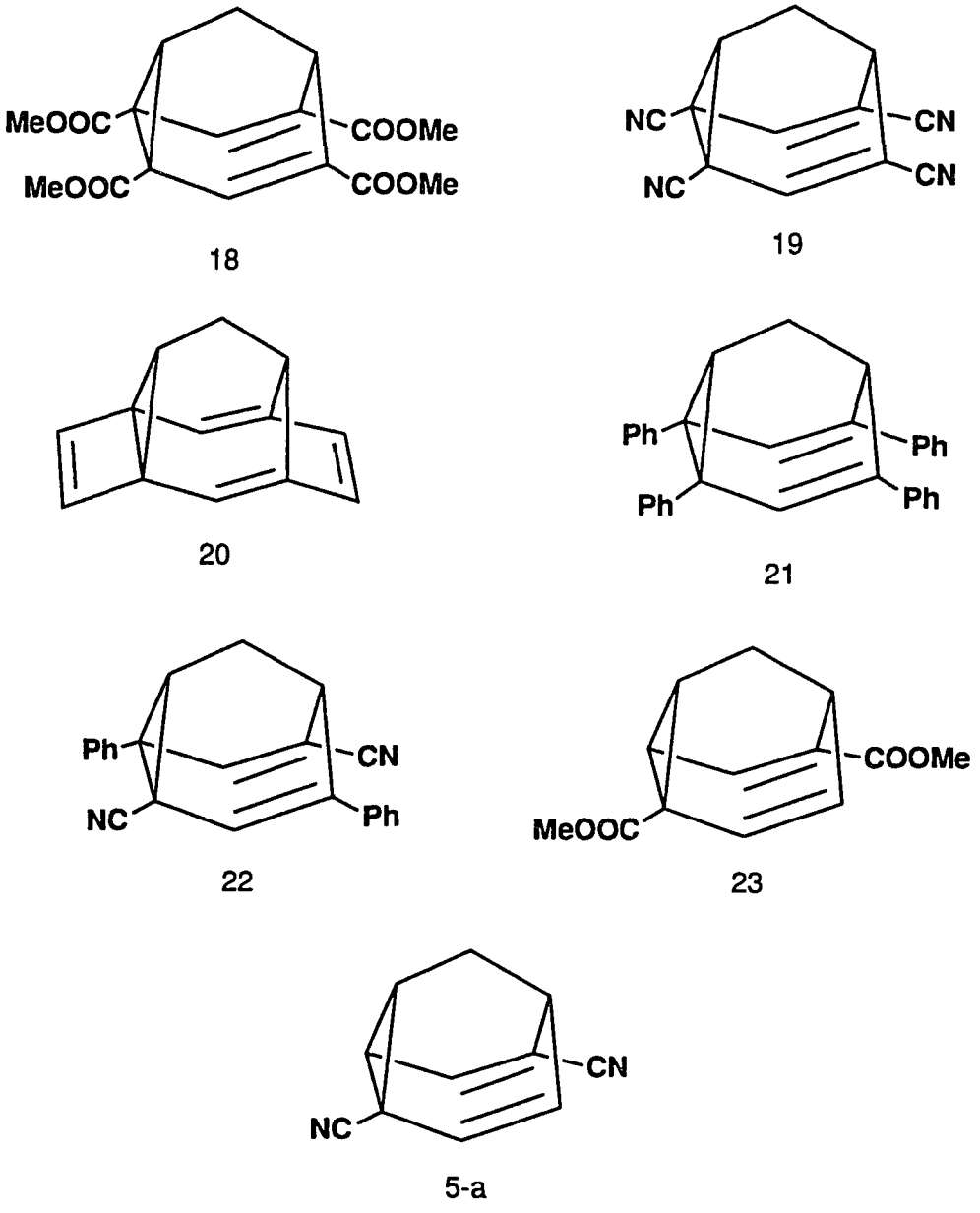

Figure 21: Electron Acceptor Substituted Barbaralanes and Bridged Barbaralane

In order to test the theoretical investigation of the stabilization effect of small-ring annelation at the termini of the barbaralane nucleus, 2,8 and 4,6-symmetrically bridged barbaralane like **20** could be synthesized by using 2,4,6,8-tetracarbomethoxybarbaralane **18** as the starting material.

We also considered that the route which led to 2,4,6,8-tetracarbomethoxy-barbaralane **18** could be modified to investigate 2,4,6,8-tetraphenyl-barbaralane **21**, 2,6-dicycno-4,8-diphenyl-barbaralane **22** and 2,6-dicarbomethoxybarbaralane **23**.

Quast et al. developed the synthetic pathway for 2,6-dicyanobarbaralane **5-a** by using Meerwein's diketone, bicyclo[3.3.0]-nonane-2,6-dione, as a precursor.[24] In contrast, **5-a** could also be synthesized by our new efficient method where 2,6-dicarbomethoxy-triasterane-3,7-dione will be starting material.

In this context the Cope activation barrier lowering effect of electron acceptor or bridged substituents at C_2, C_4, C_6, C_8 positions of barbaralane skeleton is of particular interest. High resolution variable temperatures X-ray crystal structure determination, variable temperatures solution and solid-state ^{13}C-NMR measurements, and variable temperatures solution and solid-state IR studies provide powerful tools for such investigations. Hopefully, our approach will offer a possible synthetic route to the hypothetical homoaromatic barbaralane / semibullvalene of Hoffmann and Dewar.[15,19]

CHAPTER 2

2.0.0. SYNTHESES, RESULTS, AND DISCUSSIONS

2.1.1. Synthesis of 2,4,6,8-Tetracarbomethoxy-barbaralane (18)

Theoretical studies on the Cope activation barrier of semibullvalene by Hoffmann[15] and Dewar[19] suggested that electron donor substituents at C-1,5 and/or electron acceptor substituents at C-2,4,6,8 should decrease the activation energy of the Cope rearrangement. In order to prove Hoffmann's and Dewar's theoretical predictions, L. S. Miller and R. Iyengar have synthesized and investigated 1,5-dimethyl- and 1,5-annulated 2,4,6,8-tetracarbomethoxysemibullvalene.[23,40] Their well-developed synthetic routes promised to provide the most straightforward access to 2,4,6,8-tetracarbomethoxybarbaralane **18** (Figure 22).

The starting material, 2,4,6,8-tetracarbomethoxy-bicyclo[3.3.1]-nonane-3,7-dione **26**, used in the synthesis of compound **18** could be prepared by the method of Bertz[41] and Sands.[42] Bromination and cyclization (elimination of HBr) of dienol **26**, and reduction of tetracyclic diketone **27** with triisobutylaluminum in dry toluene[43] should give exo,exo-diol **28-a**. Reaction of **28-a** with two equivalents of methanesulfonyl chloride should provide the dimesylate **29**. The expected pathway for the conversion of the dimesylate to the compound **18** would be via the diiodide could be accomplished using NaI in dry

acetone and this reagent possibly would react further to facilitate the 1,4-elimination reaction.

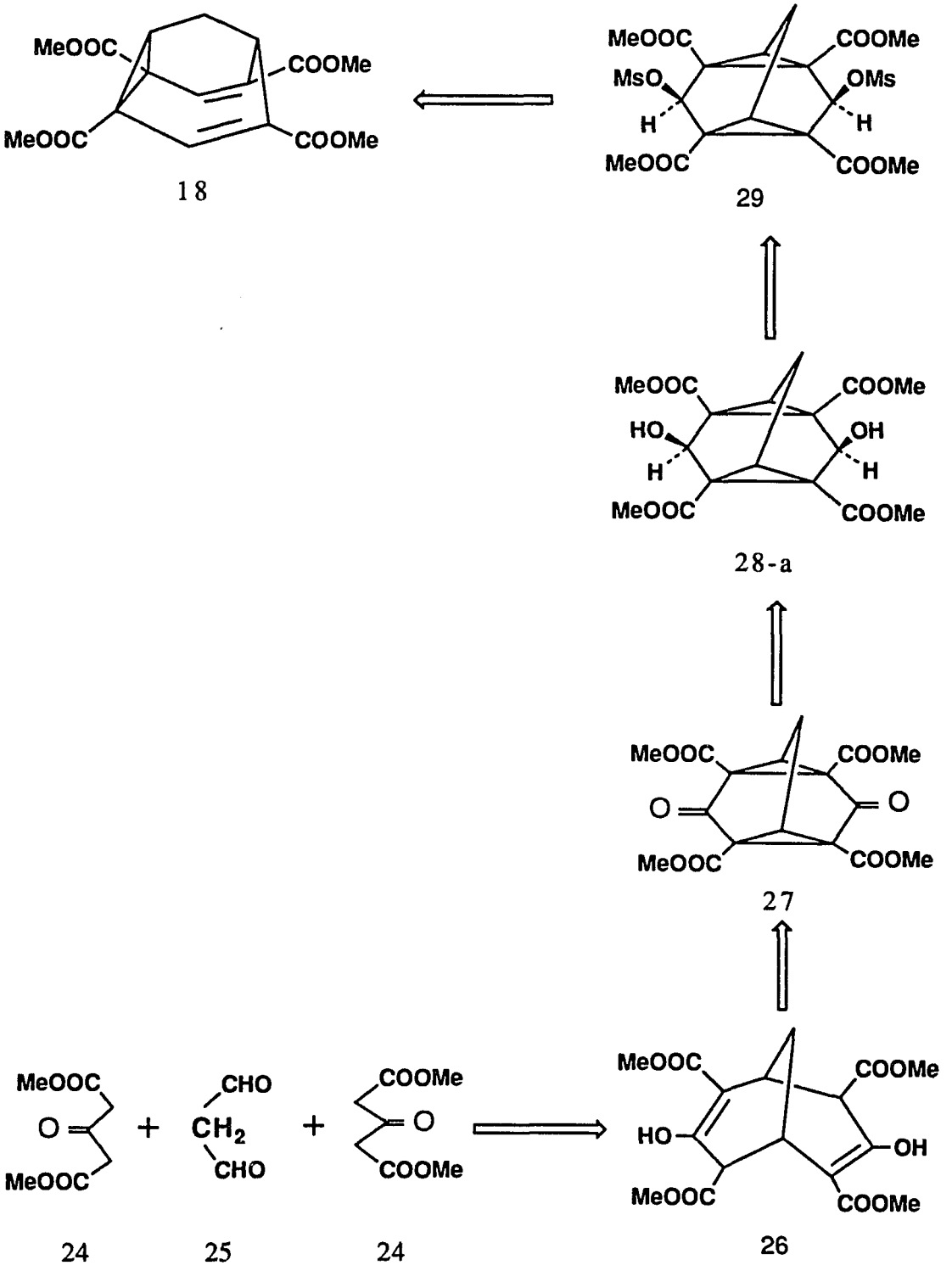

Figure 22: Retrosynthetic Analysis for **18**

Even if the last step does not occur with NaI in acetone, we felt confident that we could modify some other reagents to effect this transformation.

We have synthesized compound **18** in an efficient four-step sequence which for the first time enabled us to obtain a qualitative evaluation of the predicted substituent effect in the tetrasubstituted barbaralane system.[15,19] The synthetic route of **18** is outlined in Scheme 1.

Starting material in the synthesis of **18** is 2,4,6,8-tetracarbomethoxy-bicyclo[3.3.1]nonane-3,7-dione **26** (in its enol form) obtained according to Bertz[41] from malondialdehyde **25** and dimethyl 1,3-acetonedicarboxylate **24**. The accepted mechanism involves two sequences of aldolization, elimination, and Michael addition (Scheme 2).

In the feasible mechanism, initial 1:1 ratio of **24** to **25** aldol condensation leads to adduct **32** which will easily lose one molecule of water forming the intermediate **33** followed by Michael addition of another molecule of dimethyl 1,3-acetonedicarboxylate **24** to form **34**. It can continuously undergo the second sequence of intramolecular aldol condensation, elimination of water, and consecutive intramolecular Michael addition which leads to **26** via **35** and **36**. Bertz[41] proposed that the last three steps (**34** → **35** → **36** → **26**) are undoubtedly faster than the first three (**24** + **25** → **32** → **33** → **34**), as they are all unimolecular, whereas two of the first three are bimolecular.

Scheme 1

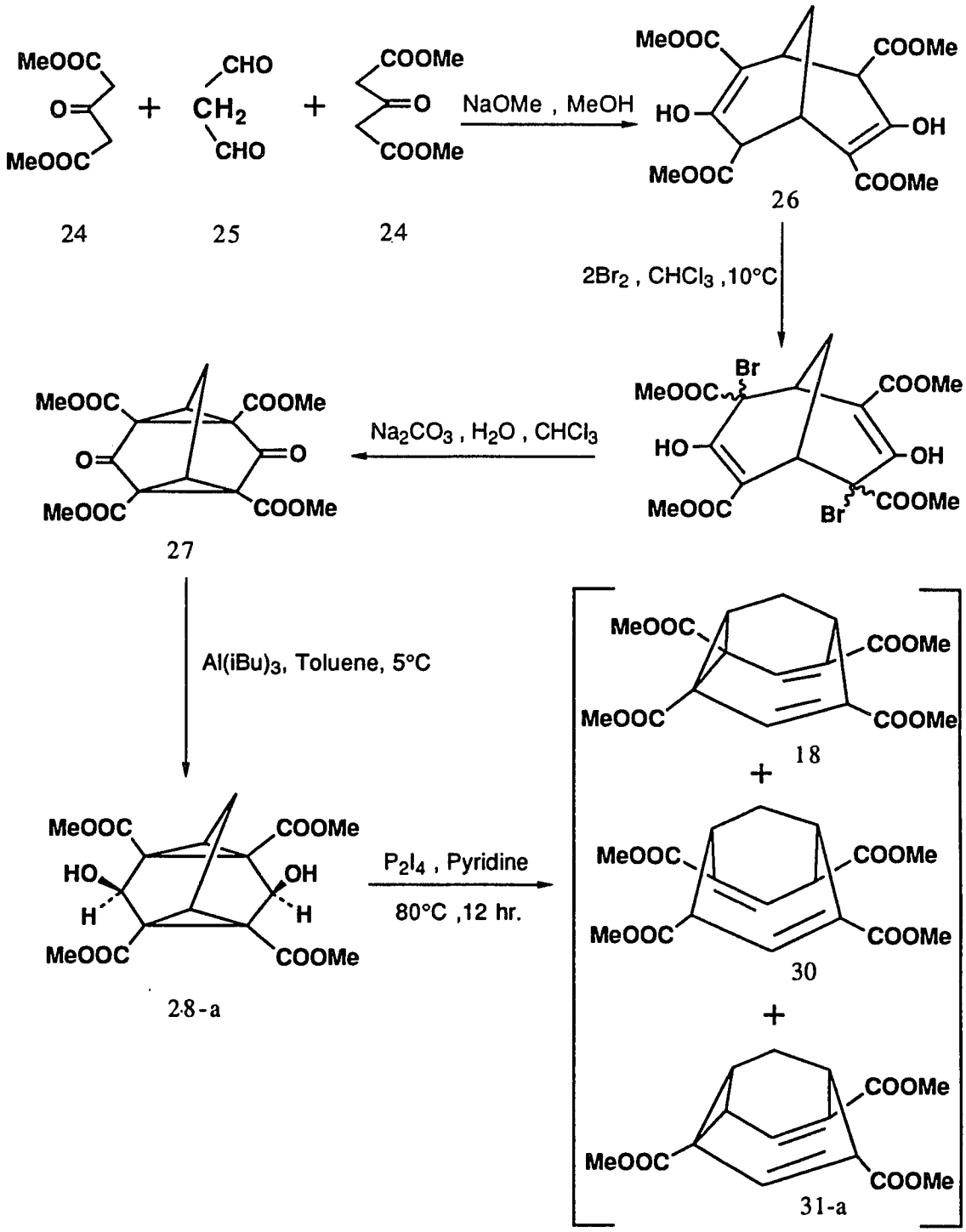
MeOOC
O
MeOOC
CHO
CH2
CHO
COOMe
O
COOMe
NaOMe , MeOH
MeOOC
COOMe
HO
OH
MeOOC
COOMe
26
24
25
24
2Br2 , CHCl3 ,10°C
Br
MeOOC
COOMe
HO
OH
MeOOC
Br
COOMe
Na2CO3 , H2O , CHCl3
MeOOC
COOMe
O
O
MeOOC
COOMe
27
Al(iBu)3, Toluene, 5°C
MeOOC
COOMe
HO
OH
H
H
MeOOC
COOMe
P2I4 , Pyridine
80°C ,12 hr.
28-a
MeOOC
COOMe
MeOOC
COOMe
18
+
MeOOC
COOMe
MeOOC
COOMe
30
+
COOMe
MeOOC
COOMe
31-a

Scheme 2

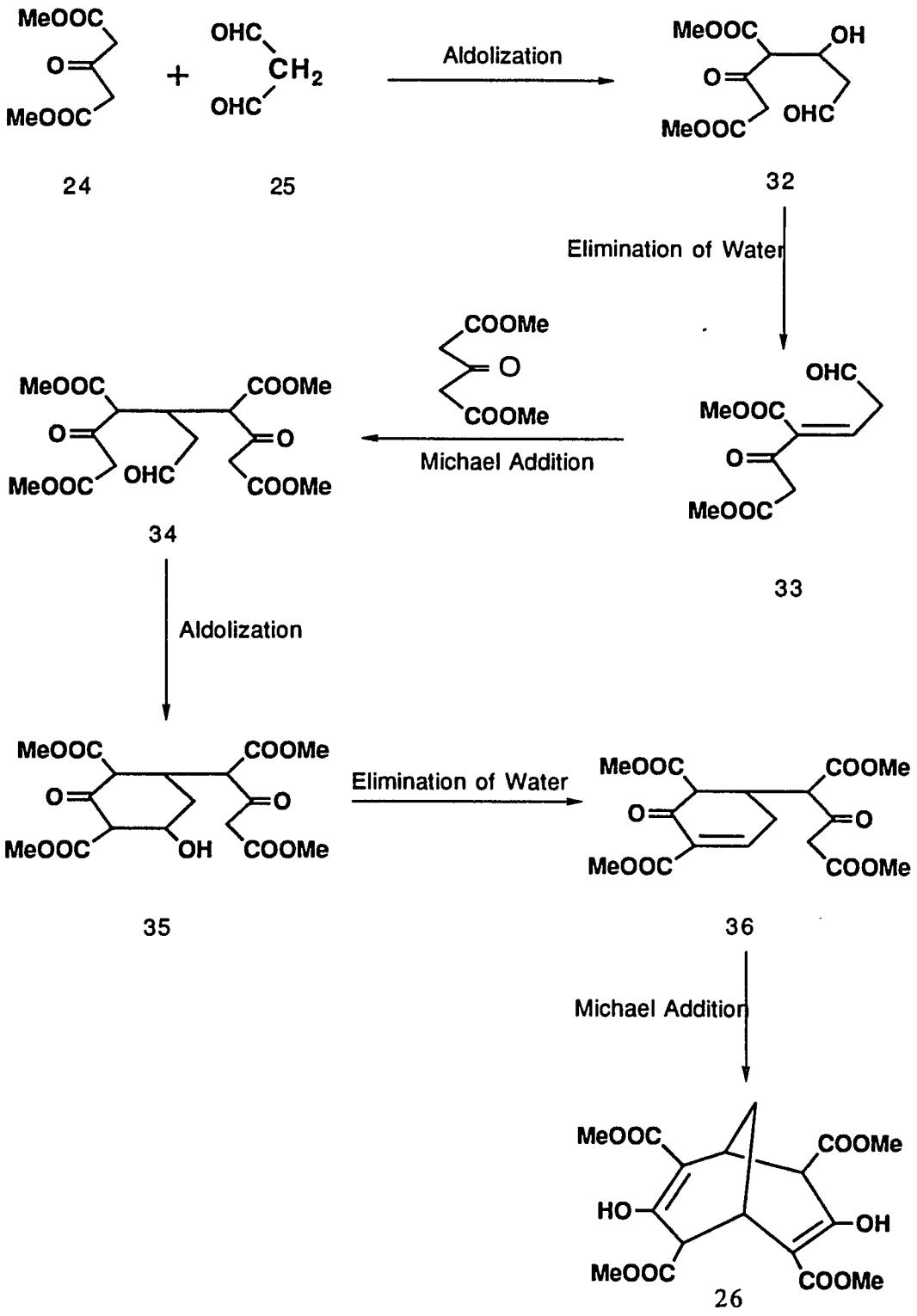
MeOOC
O
MeOOC
OHC
CH2
OHC
Aldolization
MeOOC
OH
O
MeOOC
OHC
24
25
32
Elimination of Water
COOMe
O
COOMe
Michael Addition
MeOOC
COOMe
O
MeOOC
OHC
COOMe
OHC
MeOOC
O
MeOOC
34
33
Aldolization
MeOOC
COOMe
O
MeOOC
OH
COOMe
Elimination of Water
MeOOC
COOMe
O
MeOOC
O
COOMe
35
36
Michael Addition
MeOOC
COOMe
HO
OH
MeOOC
COOMe
26

Preparative scale reactions for product **26** were carried out with a 2:1 ratio of **24** to **25** at pH 8 by stirring at room temperature for 4 days. After acidification, filtration, and digestion with methanol, 65% of white solid **26** was isolated. Recrystallization of the crude compound **26** from methanol gave white crystals, mp: 183-185°C, well above the reported values of 175-176°C[41] and 179.1°C[42].

The ^{1}H-NMR spectrum of **26** in chloroform-d consists of a 2H triplet at δ 1.95 (J 2.9 Hz), another 2H triplet at δ 3.24 (J 2.9 Hz), a 2H broad singlet at δ 3.30, and three singlets at δ 3.78 (6H), 3.85 (6H), and 12.35 (2H). The peak for the enol hydroxy hydrogens at δ 12.35 disappears upon the addition of D_2O. Its ^{13}C-NMR spectrum also shows the peaks at δ 22.4, 30.1, 50.3, 52.1, 52.6, 102.0, 168.1, 170.7 and 171.8 ppm respectively. The structure of **26** is confirmed by the detailed study of Bertz[41].

The next step, bromination of **26**, was attempted by using two different methods. One, as shown in Scheme 1, bromination of **26** in methylene chloride with two equivalents of bromine gave a dibromide which was not characterized. Treatment of the latter in the separatory funnel with saturated sodium carbonate solution led to the elimination of HBr, forming the highly symmetrical tetracyclic diketotetraester **27** in 74% yield: mp 245-246°C.

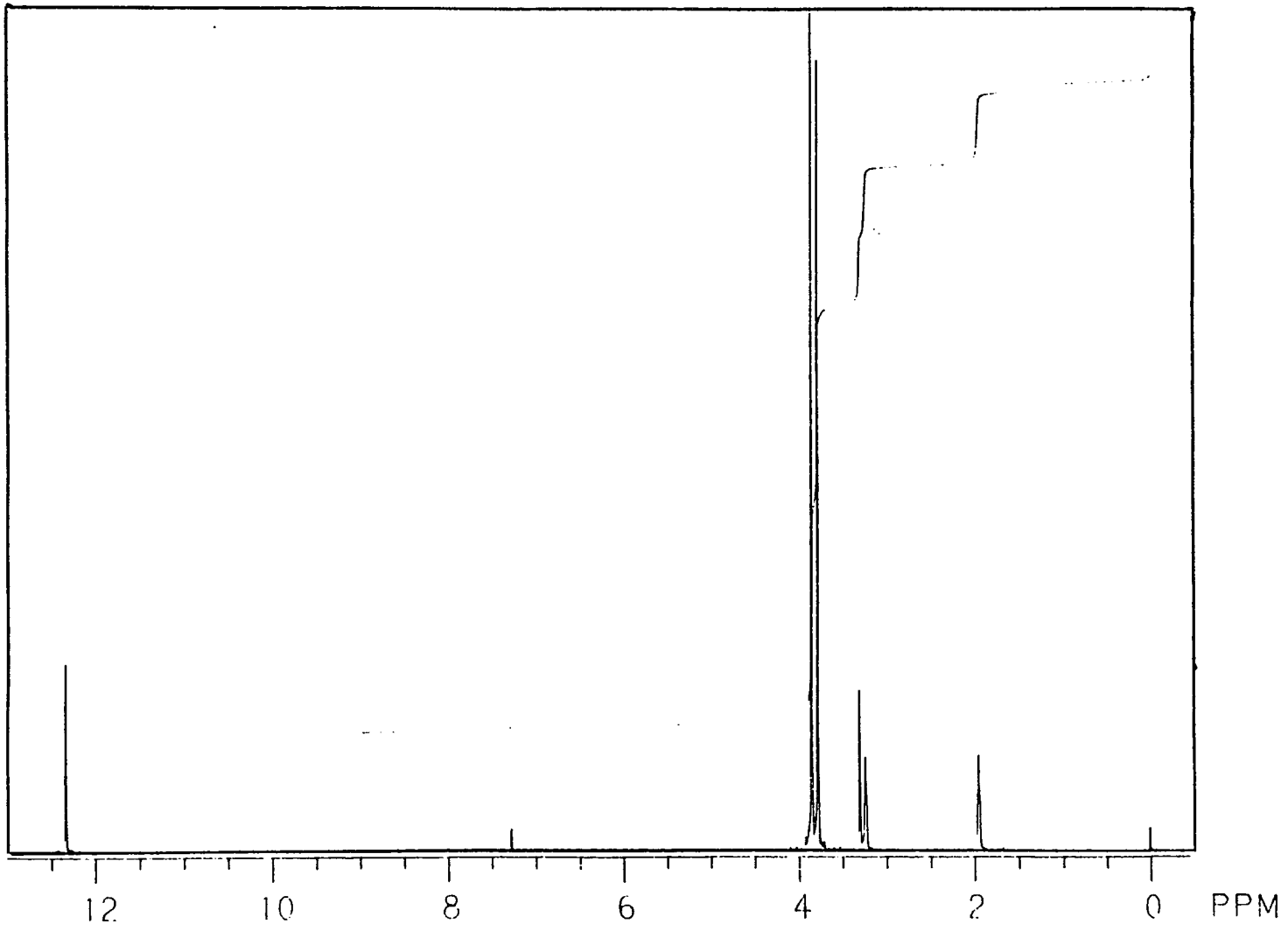

Figure 23: ^{1}H-NMR spectrum of **26**

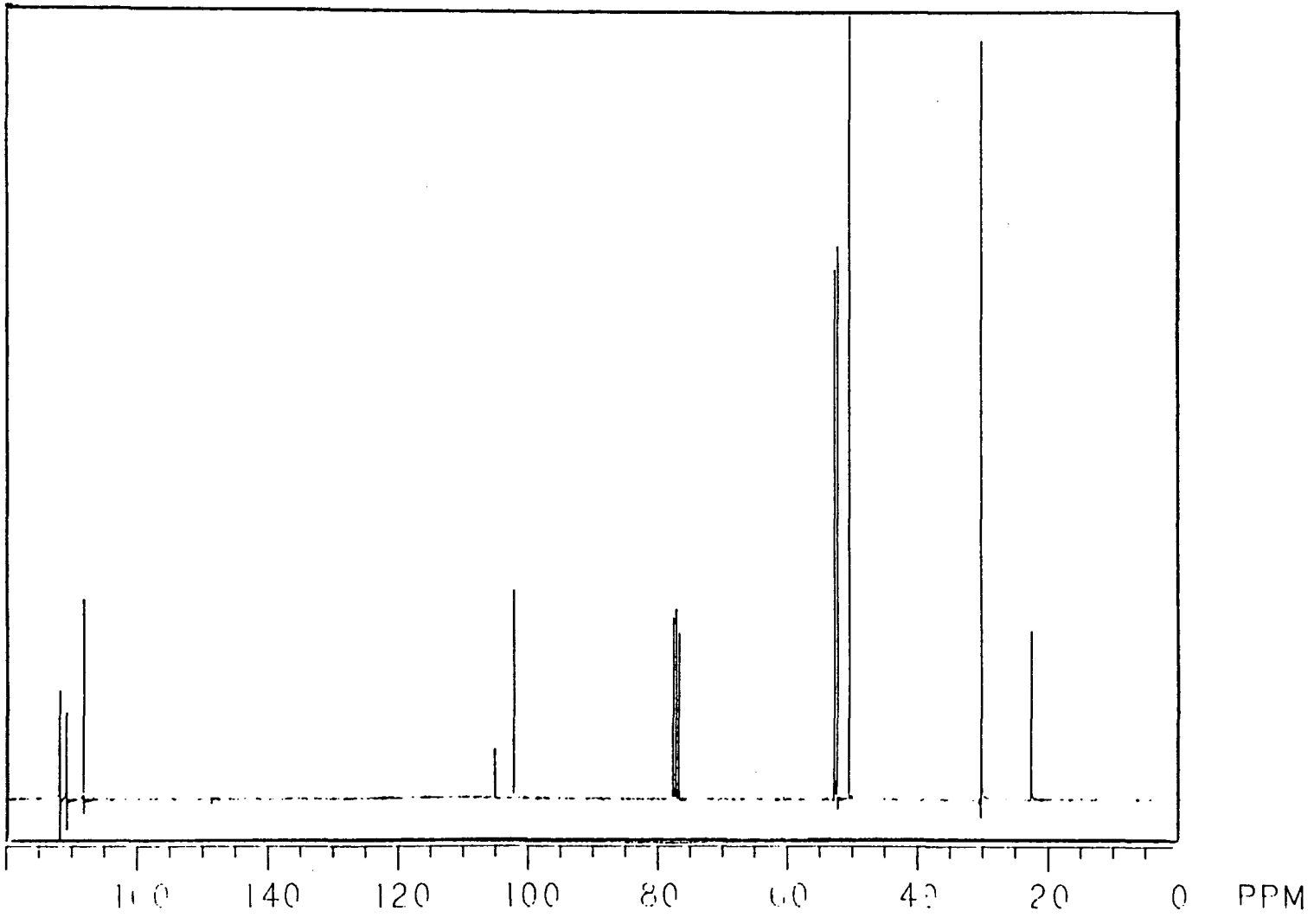

Figure 24: ^{13}C-NMR spectrum of **26**

And two..., as shown in Figure 25, the bisenol tetraester **26** in methylene chloride was treated with 4.5 equivalents of triethylamine at 0°C for two hours to form dienolate. Continuous bromination-debromination was achieved by using 2.2 equivalents of bromine in methylene chloride. The tetracyclic diketotetraester **27** was isolated in 91% yield, mp: 245-246°C.

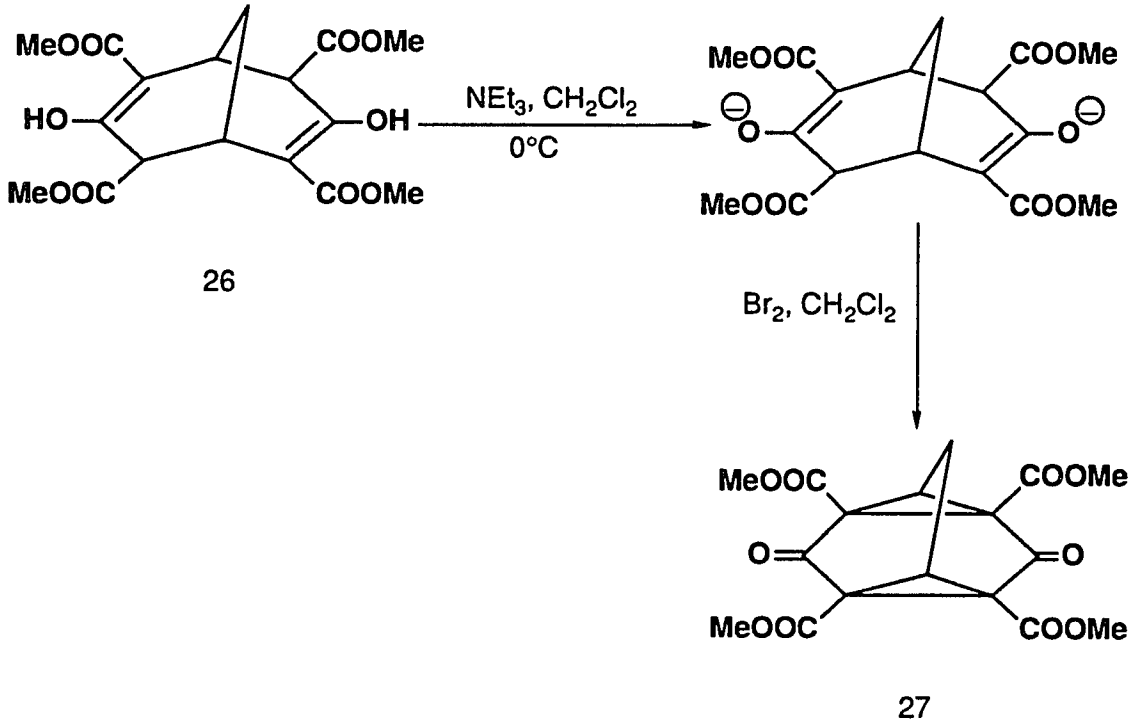

Figure 25: Alternative Approach Toward **27**

The ^{1}H and ^{13}C NMR data for compound **27** verified its structure and symmetry. The ^{1}H NMR consisted of a 2H triplet at δ 2.59 (J 2.45 Hz), another 2H triplet at δ 3.41 (J 2.45 Hz), and a 12H singlet at δ 3.79. The ^{13}C proton decoupling NMR analysis showed 6 peaks at δ 16.0, 39.2, 49.1, 53.8, 164.0, and 186.8.

X-ray diffraction analysis has been performed on **27** which provides unequivocal proof of structure.

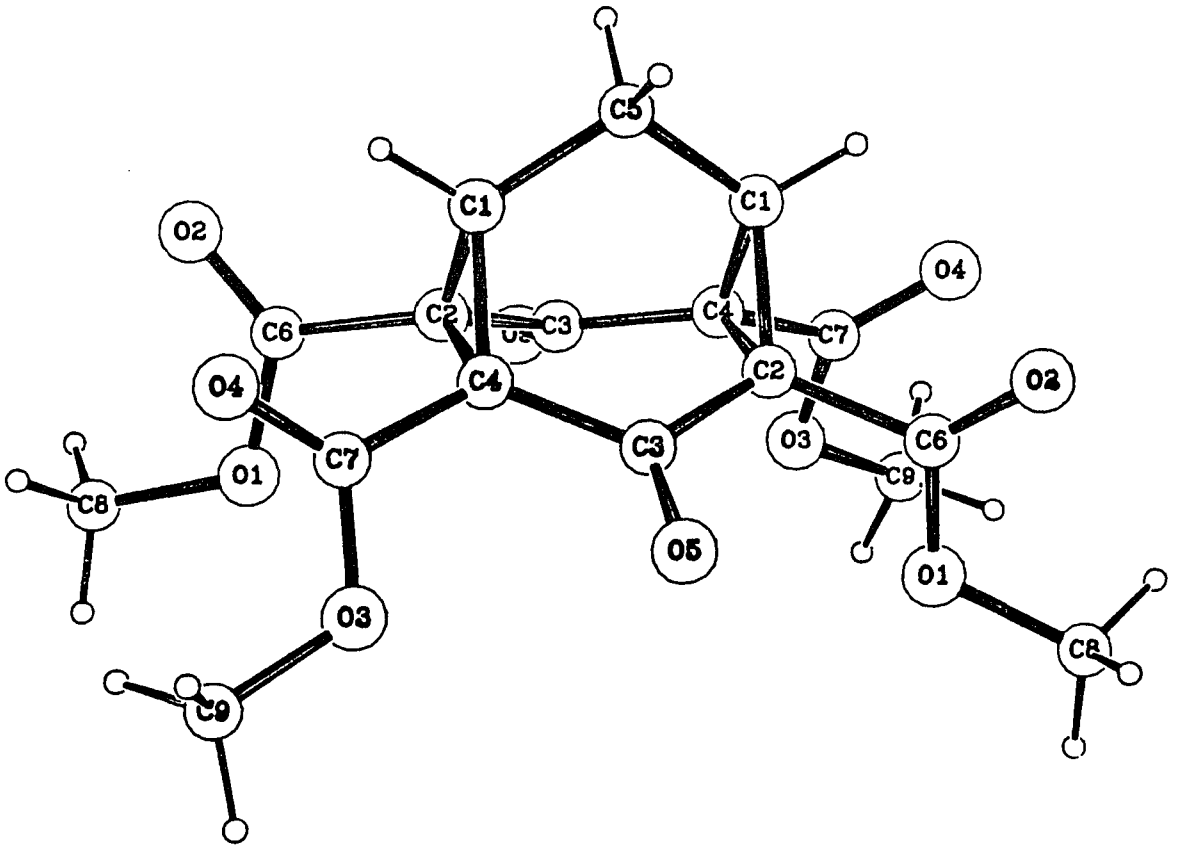

Figure 26: X-ray Crystal Structure of **27**

The next step in the synthetic scheme involved the reduction of the ketone groups of the tetracyclic β-keto tetraester **27** to alcohols **28**. It

is necessary to reduce one group in a molecule without affecting another reducible group. Clearly, there are a number of reagents which would accomplish the reduction of ketone while still leaving the carbomethoxy groups and the ring system intact. However, stereochemistry of the product diol became an important factor. It is apparent that three different diols (**28-a**, **28-b**, and **28-c**) could form in the reduction reaction(Figure 27).

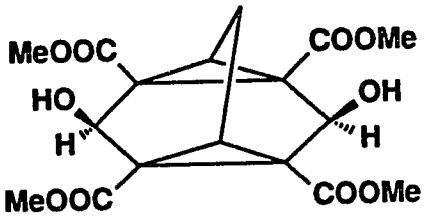

exo,exo-diol 28-a

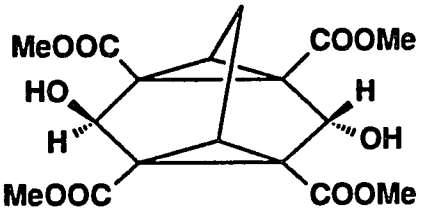

exo,endo-diol 28-b

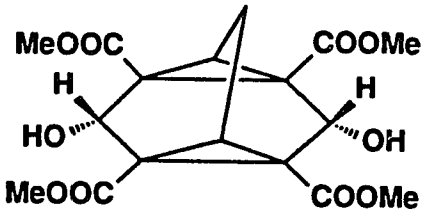

endo,endo-diol 28-c

Figure 27: Three Different Diols

Paquette and co-workers had reduced the bishomoquinone **18** with LAH and $NaBH_4$ (Figure 28). They found that LAH reduction produced a

mixture of diols whose major component was exo,endo diol **38-a**. When they used $NaBH_4$, they obtained a different mixture of diols in which exo,exo isomer **38-b** predominated.[44]

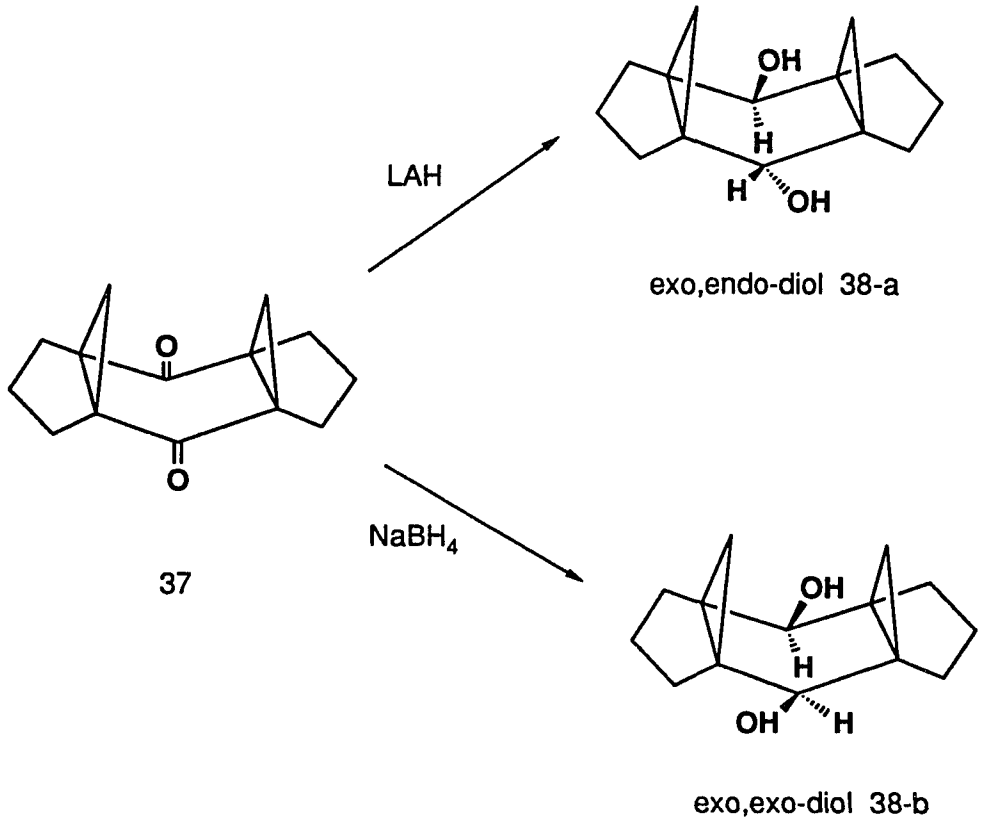

Figure 28: Reduction of Bishomoquinone

In a related system, L. S. Miller[23] reported that aluminum isopropoxide reduction of tetracyclic diketone **39** produced a single

product **40** which, in addition to having been reduced, was also transesterified. When she used $NaBH_4$, she obtained the endo,endo product **41-a**. In the case of triisobutylaluminum reduction, exo,exo diol **41-b** was isolated (Figure 29).

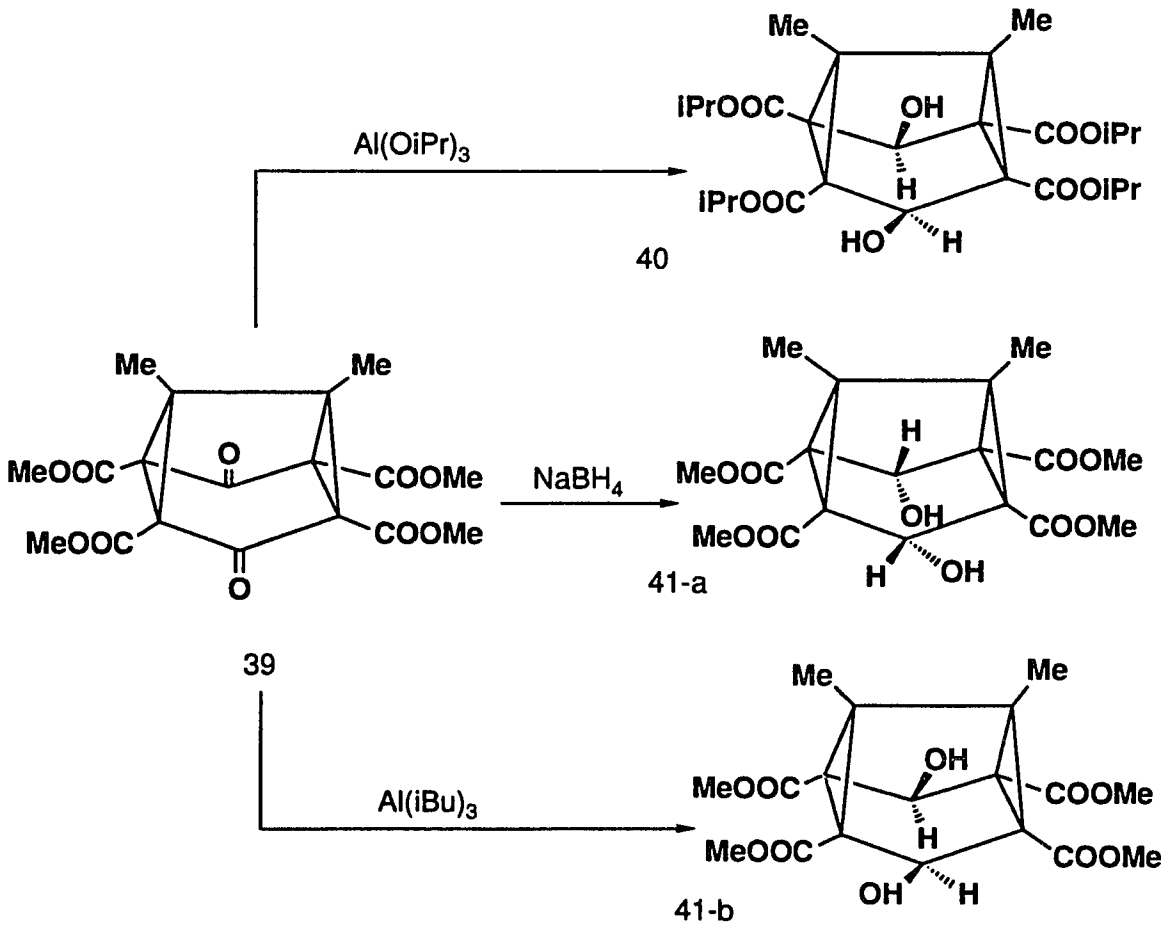

Figure 29: Reduction of **39**

Reduction of tetracyclic β-keto tetraester **27** with $Al(iBu)_3$ in dry toluene[43] (Scheme 1, p. 27) gave the symmetrical exo,exo diol **28-a** in

79% yield, mp: 185-186°C, after crystallization. The structure of **28-a** was conclusively proven as exo,exo by X-ray crystallography (Figure 30 and 31). Reduction of compound 27 with $NaBH_4$ gave the mixture of diols (**28-a**, **28-b** and **28-c**).

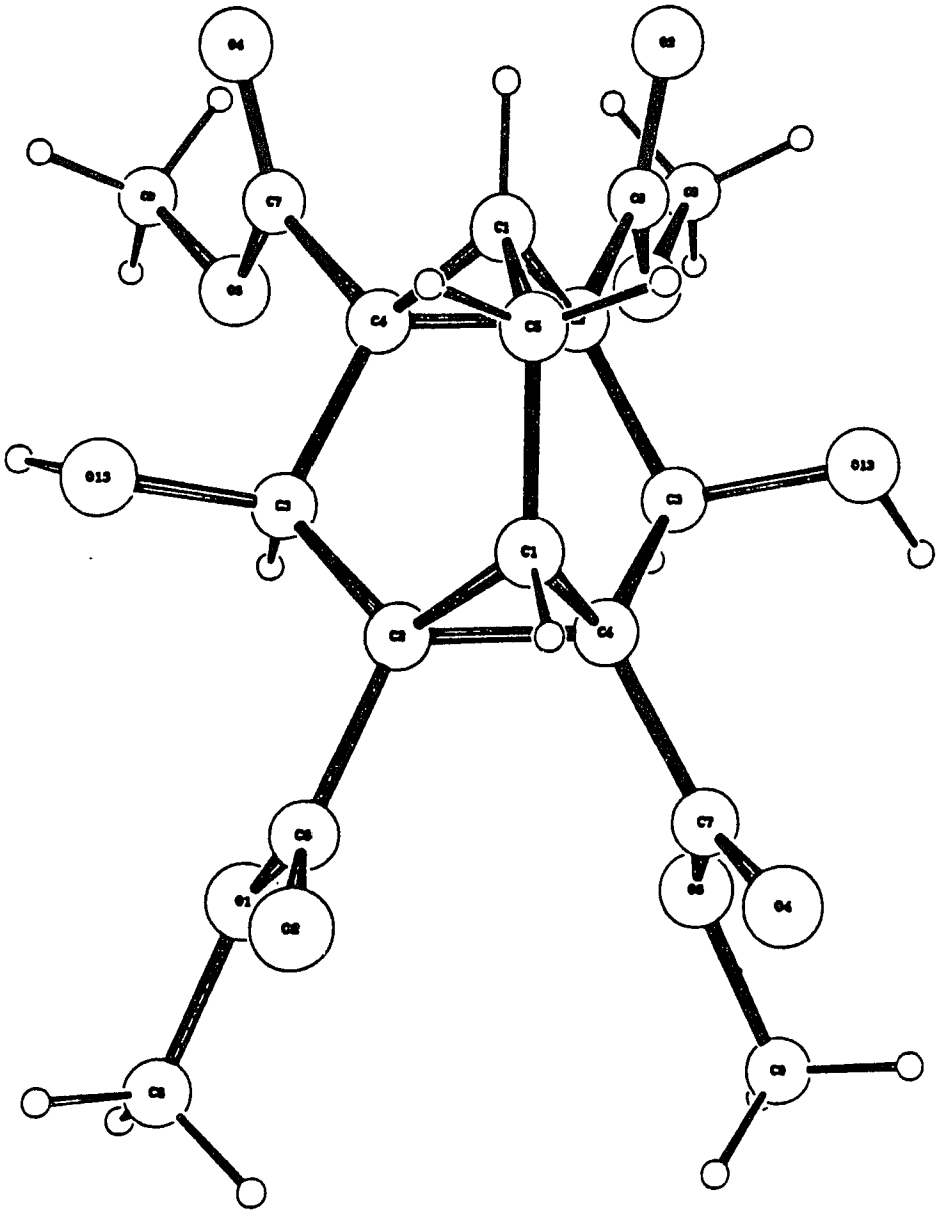

Figure 30: X-ray Crystal Structure of **28-a**

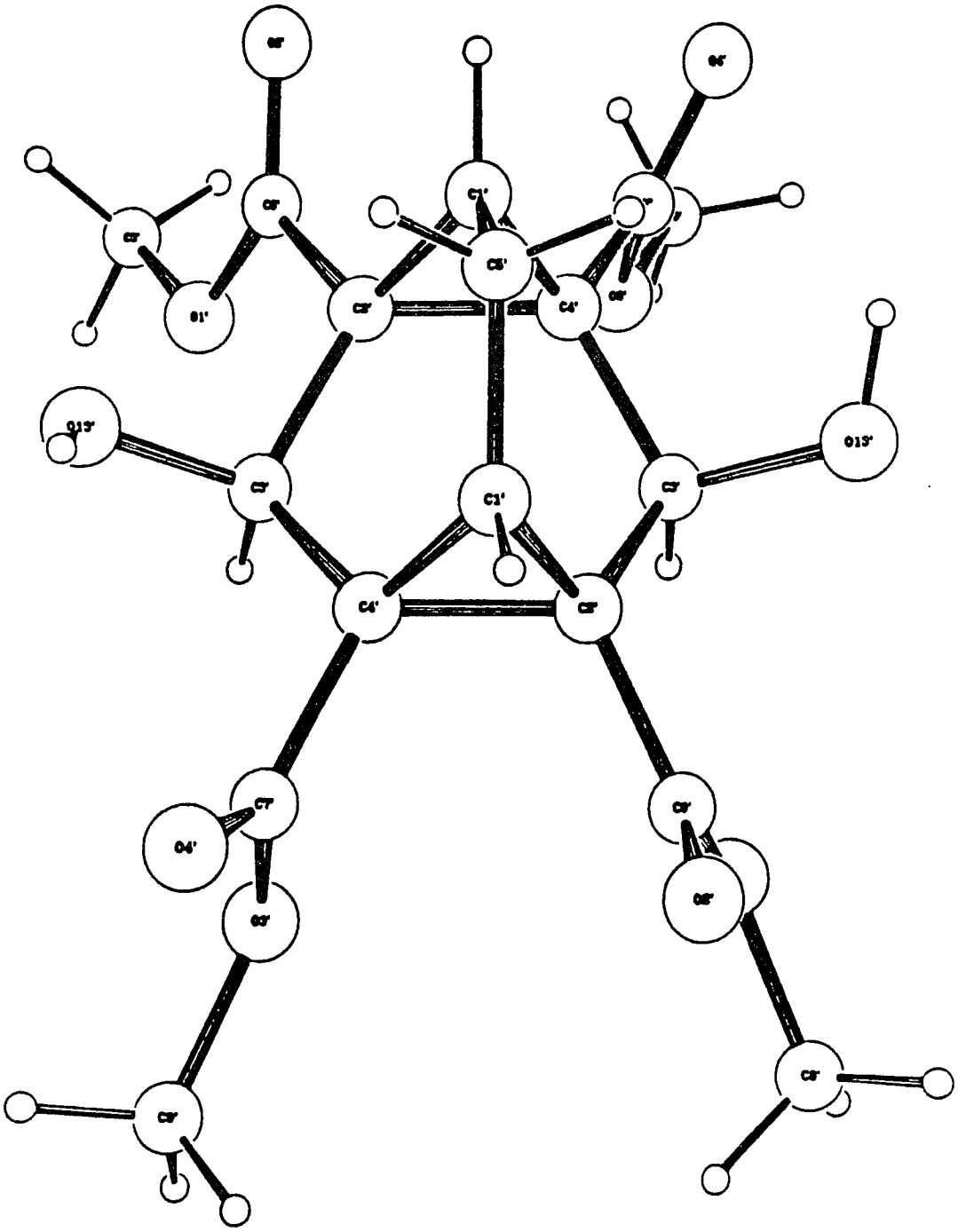

Figure 31: X-ray Crystal Structure of **28-a**

After characterization of the diol **28-a**, it was then essential to find appropriate reaction conditions in order to effect a 1,4-Grob type elimination[45,46] which would yield the desired product, 2,4,6,8-tetracarbomethoxybarbaralane **18,** in one or two steps.

There is precedence in the literature for this type of reaction. Substituted polycyclic hydrocarbons have been converted into homohypostrophene and hypostrophene (Figure 32) by the use of KI in polyhydrogen fluoride,[47] NaI in HMPA,[48] t-BuLi,[49] NaK alloy in THF,[49] and Na in liquid NH_3.[49] When ditosylate or diol was the precursor molecule, the diiodo substituted product was always isolated along with the desired diene.

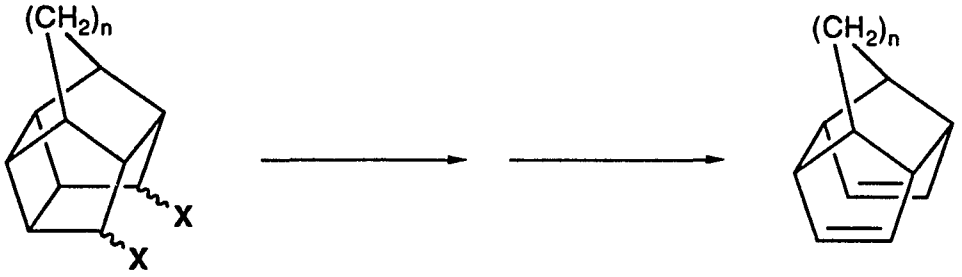

n = 0, 1

X = OTs, OH, I

Figure 32: 1,4-Elimination of Polycyclic Hydrocarbons

Research in our laboratory[23] had produced in preparation of 1,5-dimethyl-2,4,6,8-tetracarbomethoxysemibullvalene **4** in a two-step sequence: mesylation of the diol **42** followed by NaI, in dry acetone, induced Grob-fragmentation (Figure 33). This sequence could be used in a modified form for the synthesis of **18**.

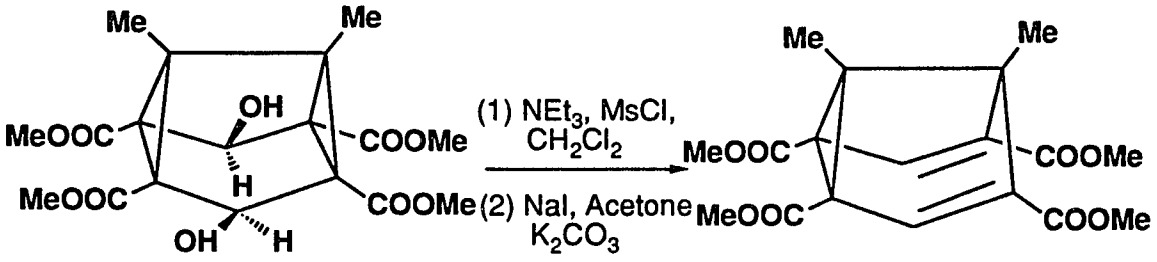

42 4

Figure 33: NaI in Acetone Induced Grob-Fragmentation in the Synthesis of **4**

Winstein et al.[50] had utilized lithium amalgam or sodium in liquid NH_3 to effect a homoconjugative elimination of a dichloride **44** in the synthesis of tetramethylhomotropilidene **45** (Figure 34).

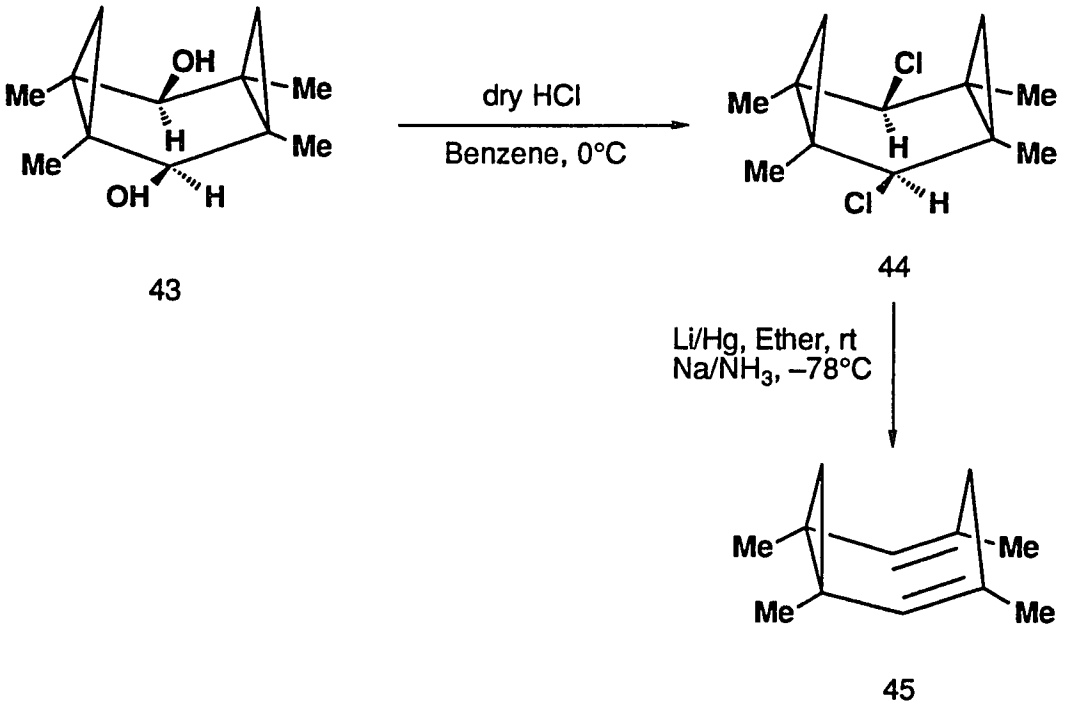

Figure 34: Homoconjugative Elimination of a Dichloride **44**

In a related system, Kessler[5] and Japanese chemists[51] have presented a homo-1,4-elimination of 1,2-di-(α-hydroxybenzyl)-cyclopropane **46** by the use of Kuhn-Winterstein reagent[52] (diphosphorus tetraiodide) in the presence of pyridine to provide trans,trans-diene **47** in about 50% yield (Figure 35). A complex mixture was obtained when stannous chloride in acid was used.

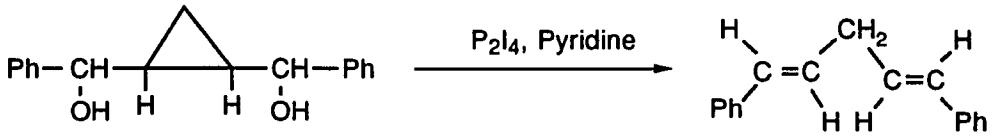

Figure 35: Homo-1,4-elimination of Dihydroxycyclopropane **46**

The expected pathway for the conversion of the diol **28-a** into a dimesylate **29** followed by the NaI in dry acetone induced Grob-fragmentation to form **18** (Figure 22, p. 25) did not succeed. In that case, a compound corresponding to a monomesylate was obtained.

Here, we would like to report a novel cyclopropane ring opening reaction, a homo-1,4-elimination of **28-a** by the use of P_2I_4 to afford 2,4,6,8-tetracarbomethoxybarbaralane **18** (Scheme 1, p. 27).

Diphosphorus tetraiodide (P_2I_4), a well characterized, stable, orange gold, crystalline solid as a powerful reagent in organic synthesis, was prepared by two methods.[53,54] In the first approach, PCl_3 and KI were refluxed in ether under argon and the resulting P_2I_4 was promptly used in the reaction without removal of the solvent. The second method, however, was more hazardous and less convenient where elemental phosphorus and iodine in carbon disulfide were stirred under argon at 0°C. Partial removal of solvent left orange gold crystals (P_2I_4) in 62% yield. The melting point of P_2I_4 was 123-125.5°C which is in accord with the reported values of 123-125°C[53] and 124°C[54]. The crystalline P_2I_4 is stable for several months under argon. The desired amount of reagent can be removed rapidly, and weighed without any difficulties and special precaution.

Overnight refluxing of diol **28-a** with two equivalents of P_2I_4 in dry pyridine at 80°C (oil bath temperature) afforded 2,4,6,8-tetracarbomethoxybarbaralane **18** (35%), 2,4,6,8-tetracarbo-methoxy-dihydrobarbaralane (2,4,6,8-tetracarbomethoxybicyclo[3.3.1]-nona-2,6-

diene) **30** (2%) and 2,4,6-tricarbomethoxybarbaralane **31-a** (3%), directly after column chromatography (hexane/ethyl acetate, 4:1) (see Scheme 1, p. 27) . Varying the amount of P_2I_4 (in ether solution) used resulted in changing the ratio of the products isolated, using less amount was easier in work-up than using too much excess of P_2I_4 which turned the reaction pretty dark. We also tried to run the reaction with P_2I_4 crystals instead of that in ether solution. Using P_2I_4 crystals was more convenient to handle, but, no better result was obtained. Several variations of reaction temperature and refluxing time were tried. In every attempt, compound **18** was isolated as a major product along with two additional products **30** and **31-a** in minor amount. Their structures were determined by variable temperature solution and solid-state NMR measurements, FT-IR studies, UV spectroscopy, GC/MS analysis, and variable temperature X-ray diffraction method.

The major desired product **18** forms colorless crystals (mp: 99-100°C) upon recrystallization from hexane. The ^{1}H and ^{13}C-NMR spectra of **18** reveal its fluxional character. These spectra derive, at room temperature in chloroform-d, from the average of two rapidly equilibrating structurally indistinguishable valency tautomers **18-a** and **18-b** (Figure 36). But, solid-state CP-MAS ^{13}C-NMR spectrum at room temperature corresponds to that of the single-structured, frozen molecule **18-a**.

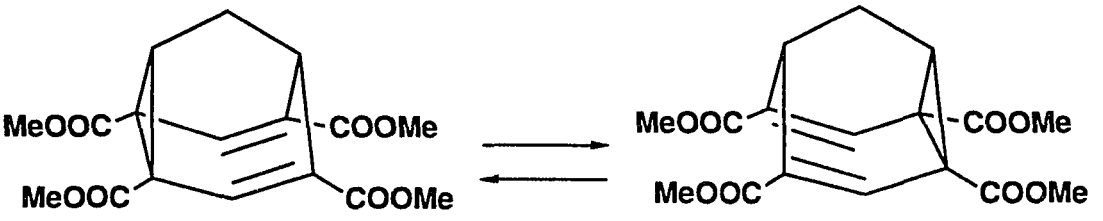

18-a 18-b

Figure 36: Valence Bond Isomerization of **18**

Independent evidence for the structure of **18** includes its UV spectrum in absolute ethanol at 295K which shows a single maximum at 238nm (ε =12808) with the characteristic shoulder at 250nm (Figure 37). Since the parent barbaralane **3** itself exhibits only end absorption (200nm),[55] the long-wavelength absorption of **18** must be considered as the extension of the conjugated system by the ester groups and may also be compared to that of 2,4,6,8-tetracarbomethoxybicyclo[3.3.1]nona-2,6-diene (2,4,6,8-tetracarbomethoxy-dihydrobarbaralane) **30** (λ_{max} 213nm in ethanol, ε = 8374) and ethyl 1-cyclohexene-1-carboxylate (λ_{max} 219nm).[56]

Structure 18 was also proved by single-crystal X-ray analyses at temperatures 295 and 110K. The structures from the two data sets at 295 and 110K are identical which show a C_2-C_8 bond of 1.611Å and the open end of the molecule C_4-C_6 = 2.40Å. Perspective drawing of a molecule of **18** at 110K is shown in Figure 38.

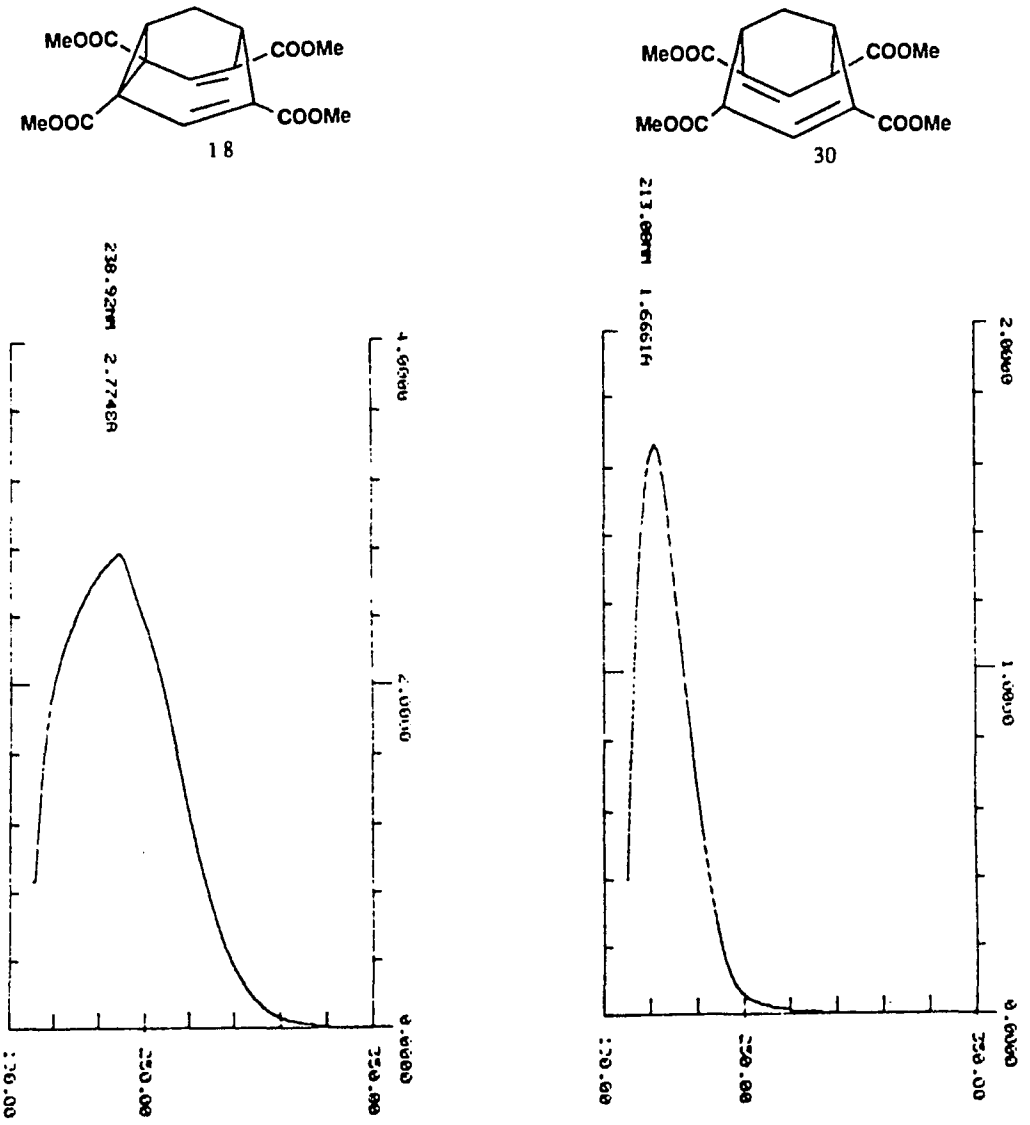

Figure 37: UV Spectra of **18** and **30**

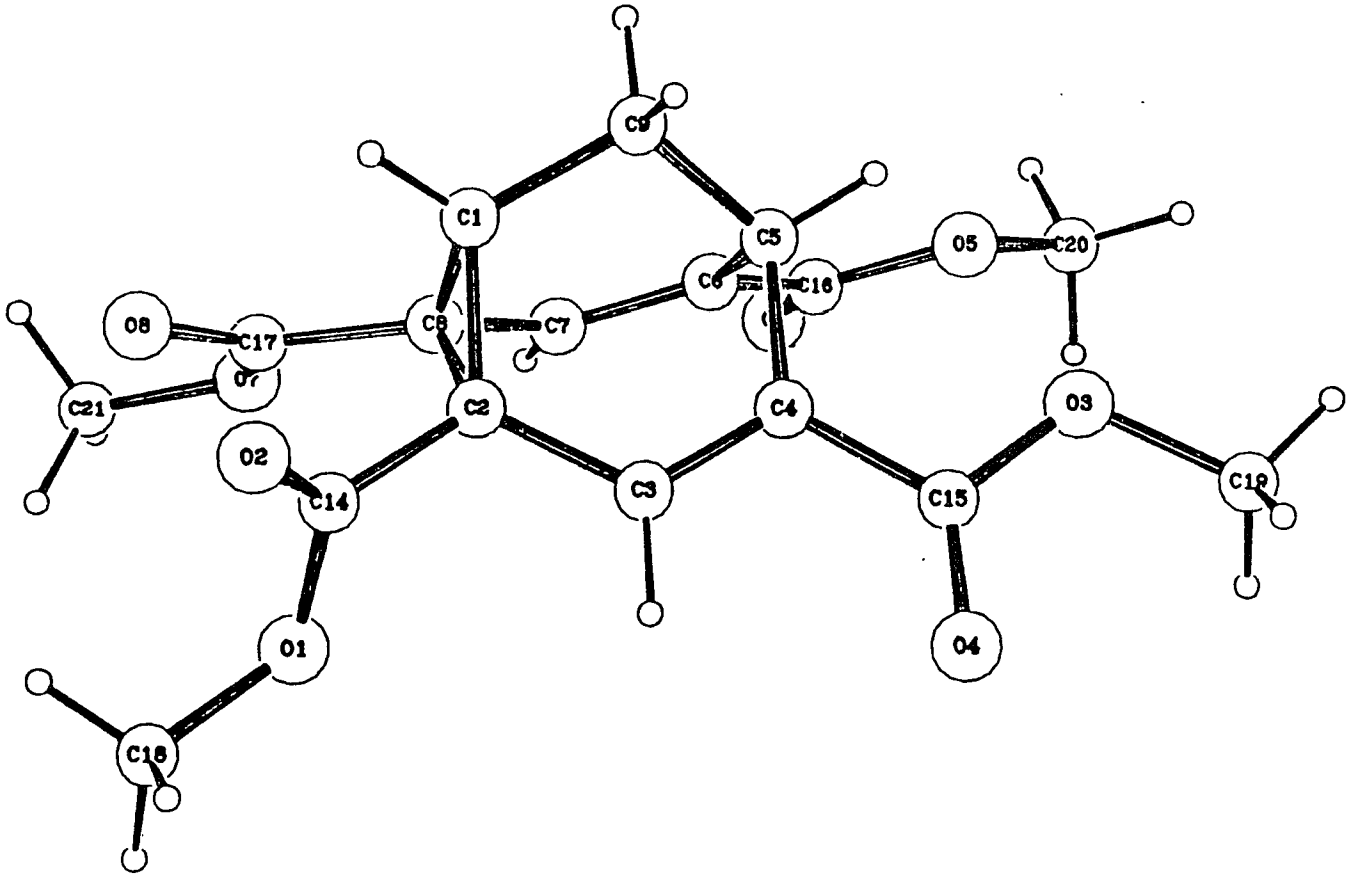

Figure 38: X-ray Crystal Structure of **18** at 110K

A detailed characterization of the X-ray structure analysis, IR studies, room temperature ^{1}H and ^{13}C-NMR measurements, variable temperatures solution and solid-state ^{13}C-NMR determination, and the calculation of the activation energy barrier for the exchange process of **18** at the coalescence temperature will be presented in Chapter 4 (p. 142).

One of the interesting side products from the P_2I_4 reaction is 2,4,6,8-tetracarbomethoxy-dihydrobarbaralane **30** (see Scheme 1, p. 27) which forms colorless needle shaped crystals, mp: 157-159°C. This side product **30** is most likely the result of a reductive cleavage of **18** by hydriodic acid formed in this reaction, followed by subsequent protonation (Figure 39).

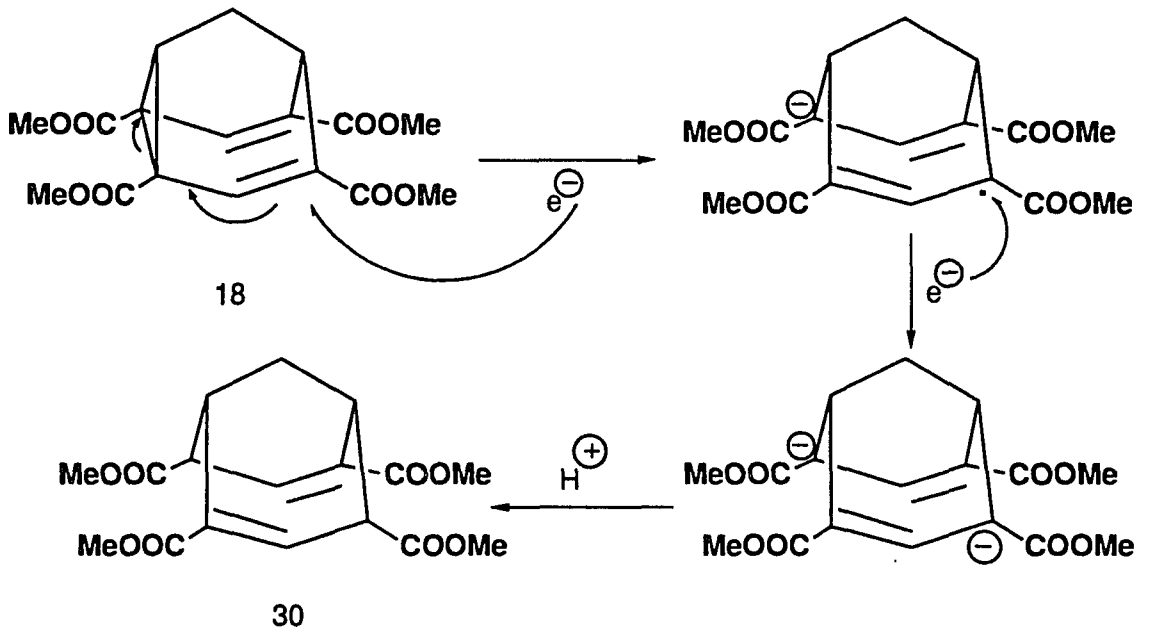

Figure 39: The Proposed Mechanism for the Formation of **30**

The proton and carbon NMR data for the compound **30** verified its structure and symmetry. The infrared spectrum of **30** in CCl_4 shows the carbonyl frequency of ν_{max} 1720 cm^{-1},which is similar to that of **18** in CCl_4.

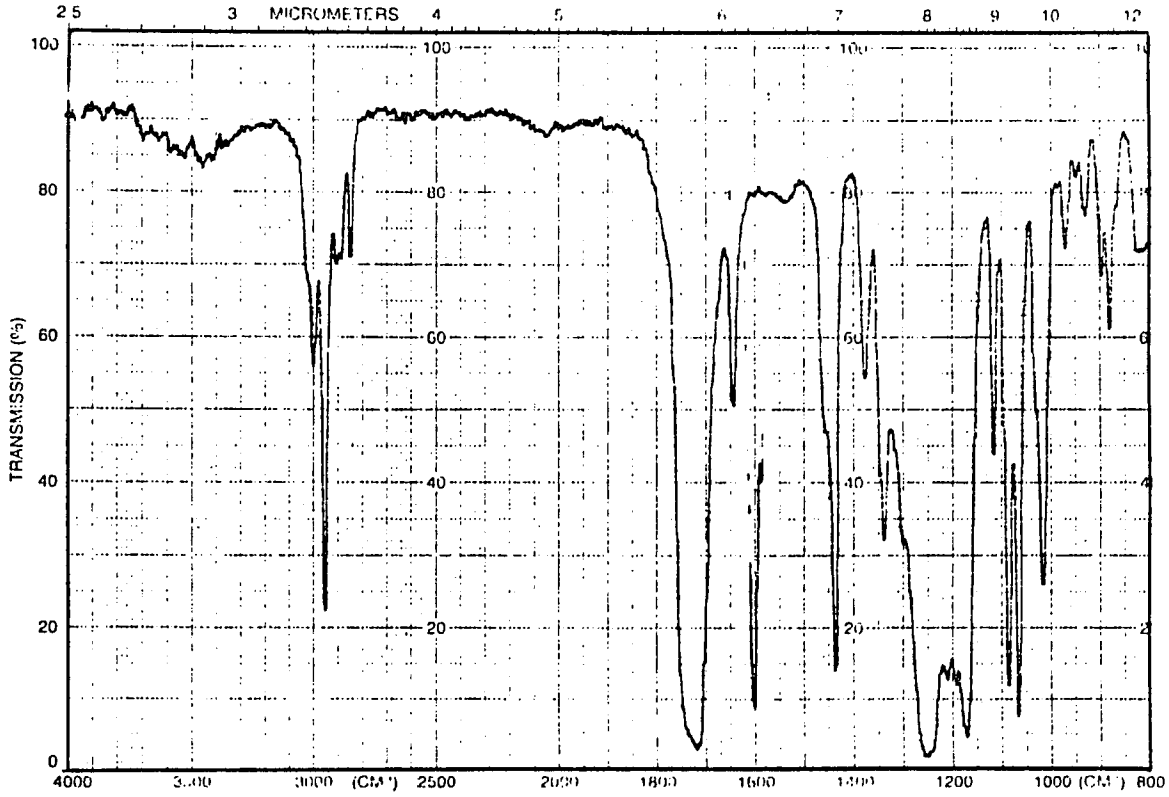

Figure 40: IR Spectrum of **30**

The structure of **30** has been determined by a single-crystal X-ray analysis. Half of the molecule is related to the other half by a crystallographic 2-fold rotation axis.

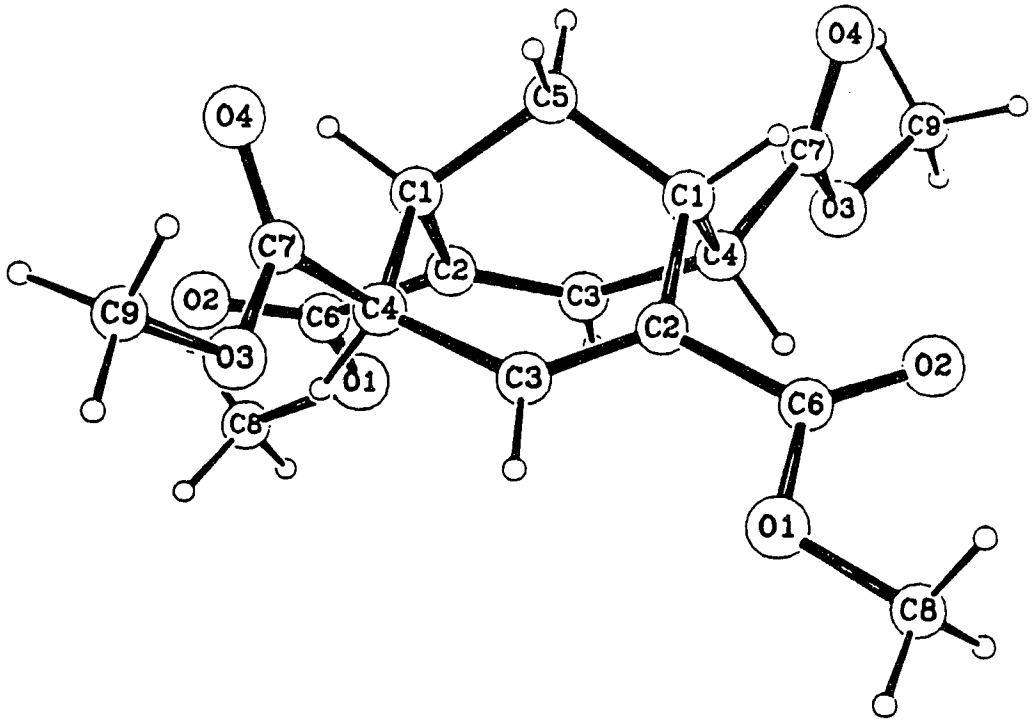

Figure 41: X-ray Crystal Structure of **30**

The second side product from the P_2I_4 reaction is 2,4,6-tricarbomethoxybarbaralane **31-a** (see Scheme 1, p. 27) which forms colorless crystals (mp: 105-107°C) upon recrystallization from methanol. The ^1H and ^{13}C NMR spectra of at room temperature exhibit its structure and the unsymmetry. Although there are two possible Cope isomers of tricarbomethoxybarbaralane, the one which in accord with the NMR spectra was tautomer **31-a**. A detailed discussion will be presented in the next section.

2.1.2. The Equilibrium Preference of 31

The ^{1}H-NMR spectrum of **31** at room temperature in chloroform-d consists of three carbomethoxy peaks at δ 3.76, 3.78, 3.82 ppm, a 2H AB quartet at δ 1.32 (two 9-H), a 1H multiplet at δ 3.06 (1-H), another 1H multiplet at δ 3.12 (8-H), a 1H broad singlet at δ 4.08 (5-H), a 1H doublet at δ 6.82 (J = 6.6 Hz) (7-H) and a 1H singlet at δ 7.41 ppm (3-H) (Figure 42). The ^{13}C NMR spectrum in chloroform-d which supports the unsymmetry of **31** shows the peaks at δ 17.6 (C_9), 27.3 (C_1), 28.3 (C_8), 34.7 (C_2), 34.9 (C_5), 51.7 (two $-OCH_3$), 52.5 ($-OCH_3$), 129.4 (C_6), 130.3 (C_7), 130.7 (C_3), 131.8 (C_4), 164.7 ($-COOCH_3$), 164.8 ($-COOCH_3$), and 170.4 ppm ($-COOCH_3$), respectively (Figure 43).

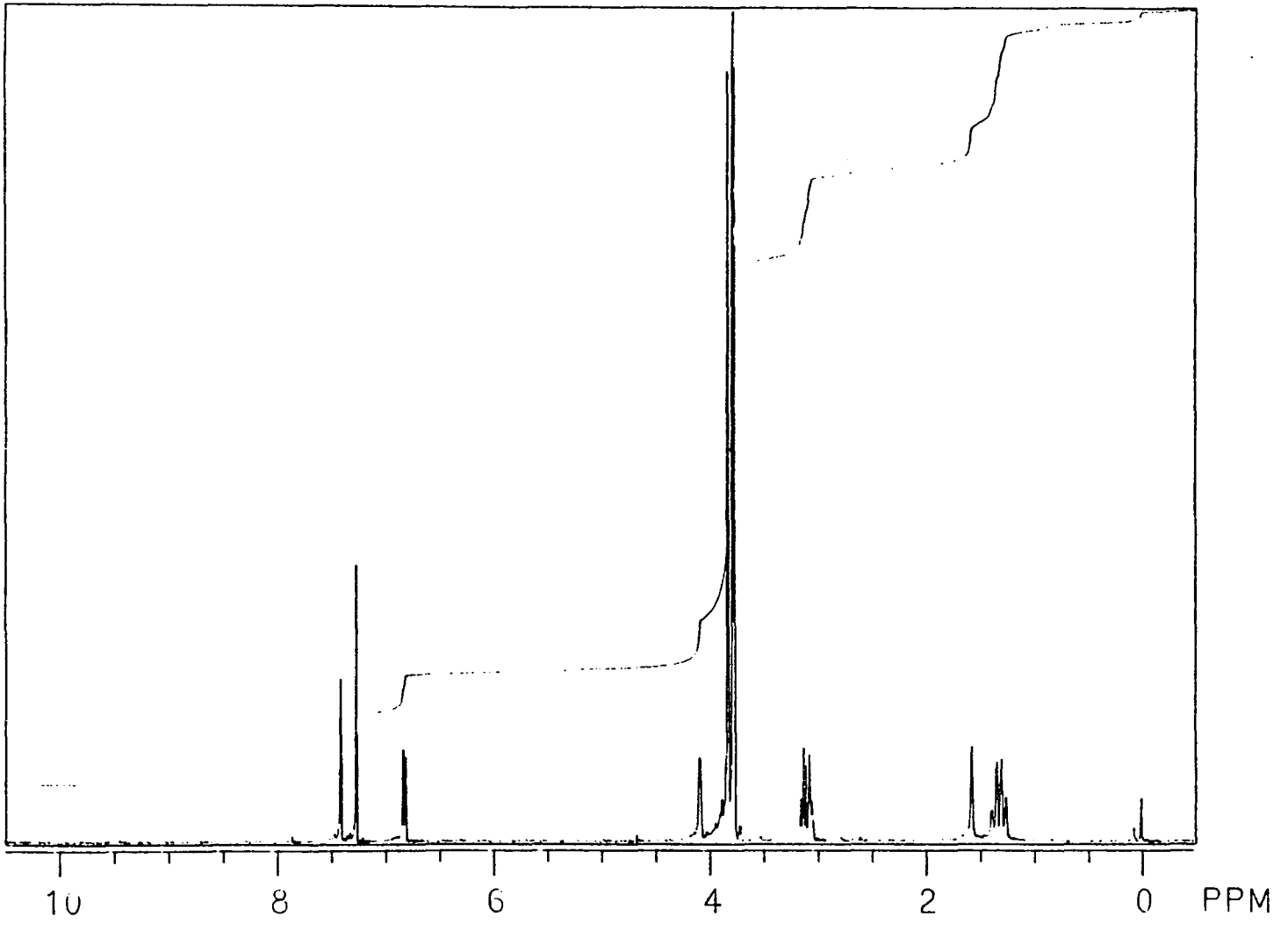

Figure 42: ^{1}H-NMR Spectrum of **31**

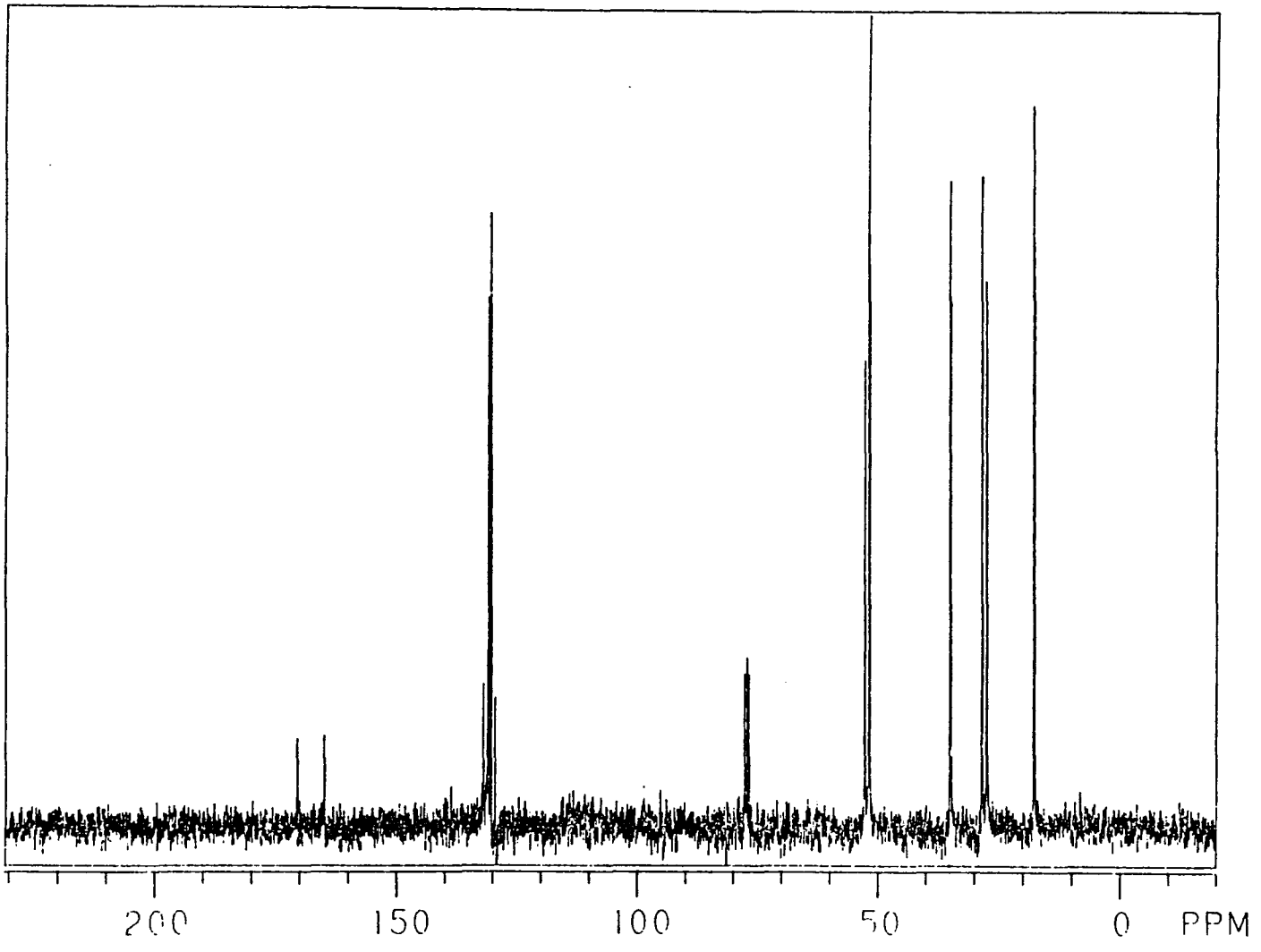

Figure 43: ^{13}C-NMR Spectrum of **31**

The ^{1}H and ^{13}C NMR data point toward **31-a** as the major tautomer of 2,4,6-tricarbomethoxybarbaralane.

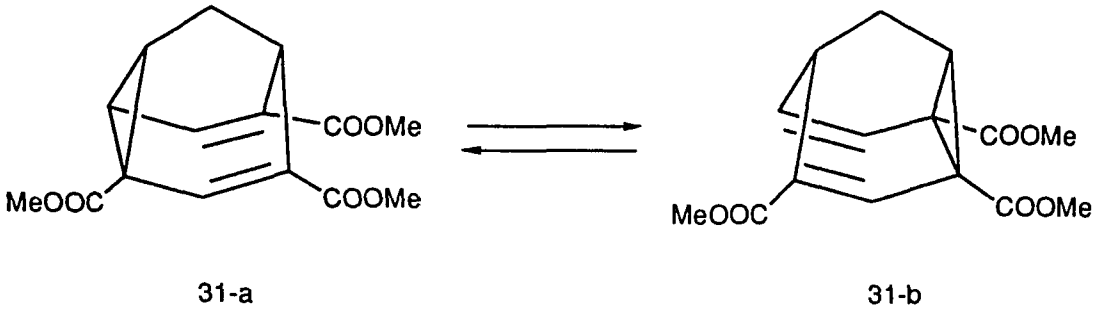

31-a 31-b

Figure 44: Two Cope Isomers of **31**

No detectable amount of **31-b** was observed. This result is based on the following data:

(a) the presence of two cyclopropyl protons at δ 3.06 and 3.12 ppm,
(b) the appearance of only two vinylic proton signals at δ 6.82 and 7.41 ppm, and
(c) the occurrence of two vinylic quarternary carbons at δ 129.4 and 131.8 ppm.

The substituent effects on a cyclopropane ring which influence the stability of ring bonds are important factors too. The pioneering work of Hoffmann et al.[15,57] showed the sensitivity of the 7-substituted norcaradiene – cycloheptatriene equilibrium to substituent effect. The Walsh orbitals of the cyclopropane interact in a π manner with π acceptors so as to strengthen the 1-6 bond in **48**, and with π donors so as to weaken the same bond. Therefore, π acceptors shift the Cope

equilibrium to the norcaradiene side **48**, π donors to the cycloheptatriene side **49** (Figure 45).

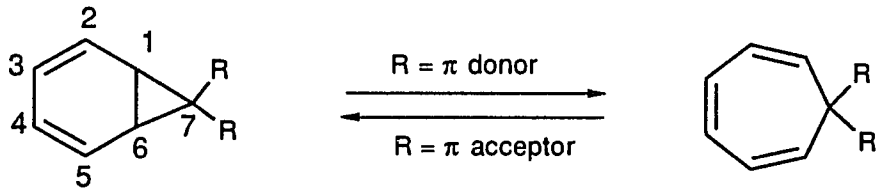

48 49

Figure 45: Norcaradiene-Cycloheptatriene Equilibrium

The above discovery can conceptually be related to the Cope rearrangement of substituted semibullvalene **50** to **51**.[15,58] If R is a π acceptor it will strengthen the 2-8 bond in **50** (The numbering system of semibullvalene is shown in Table 2, p. 5) and shift the equilibrium to **50**. Similarly if R is a π donor it will weaken the 2-8 bond in **50** and shift the equilibrium to **51**.

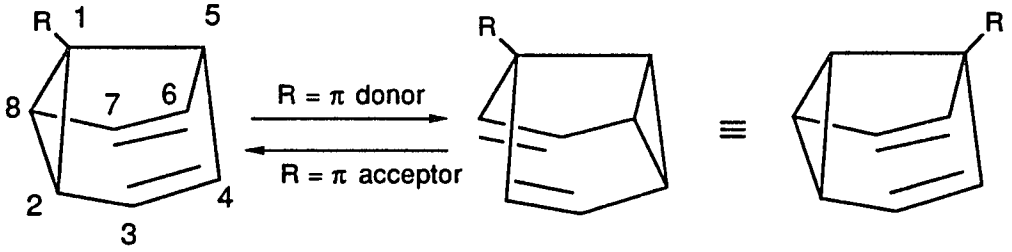

50 51

Figure 46: The Cope Equilibrium of Monosubstituted Semibullvalene

The same argument can be applied to disubstituted semibullvalene **52** and **53**. First, we need to consider the stability of mono- and disubstituted cyclopropane (**54** and **55**). In model **54**, monosubstituent (e.g., CN) will weaken the 1-2 and 1-3 bonds, and

strengthen the 2-3.[15] Since these effects should be additive in a disubstituted cyclopropane **55**, the 1-2 bond should be severely weakened. Another reason is that the bond-weakening effects of charge transfer to the acceptor reinforce each other in this 1-2 bond in **55**. Similarly, in the Cope rearrangement of disubstituted semibullvalene, **53** should be more stable than **52** whose severely weakened 2-8 bond will shift the Cope equilibrium to **53**.

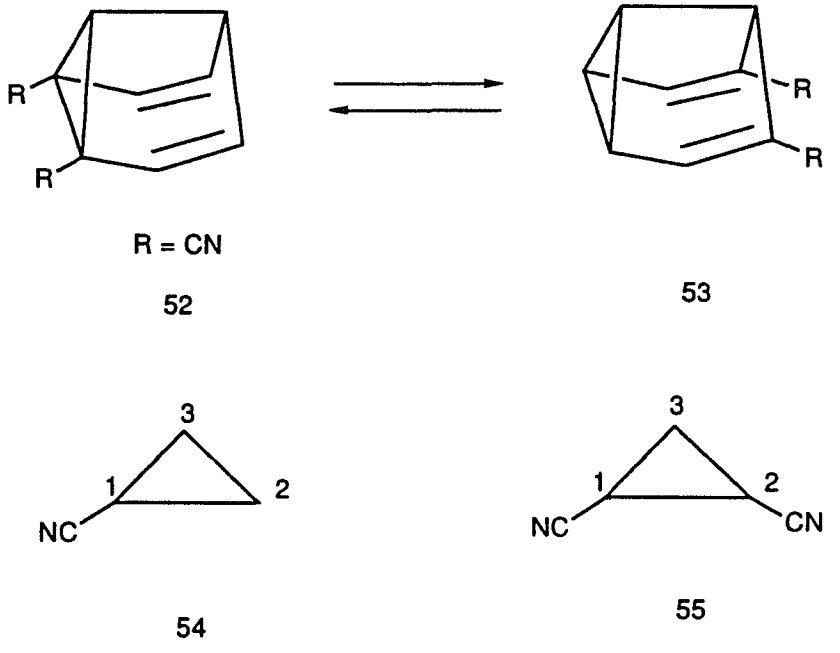

Figure 47: The Cope Equilibrium of Disubstituted Semibullvalene

Using the same concept, the mono-ester substituent on the cyclopropane of **31-a** weakens bonds 1-2 and 2-8, while it strengthens bond 1-8. However, the 2-8 bond of **31-b** suffers these effects twice due to disubstitution on the cyclopropane ring, and it thus should be destabilized. Based on this effect, we propose that 2,4,6-

tricarbomethoxybarbaralane **31-a** is the more stable and predominant structure from the Cope rearrangement of 2,4,6-tricarbomethoxybarbaralane.

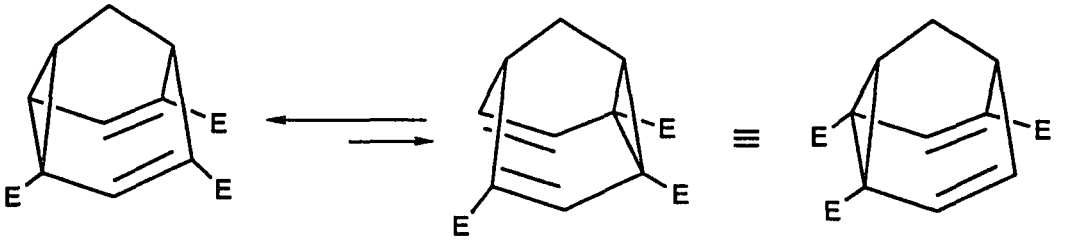

31-a 31-b

Figure 48: The Equilibrium Preference of **31**

The structure of **31-a** has in fact been proved by a single-crystal X-ray analysis (Figure 49). The distances C_2-C_8 and C_4-C_6 are 1.593Å and 2.405Å respectively, which are quite similar to those of 2,4,6,8-tetracarbomethoxybarbaralane **18** (C_2-C_8 = 1.611Å and C_4-C_6 = 2.40Å).

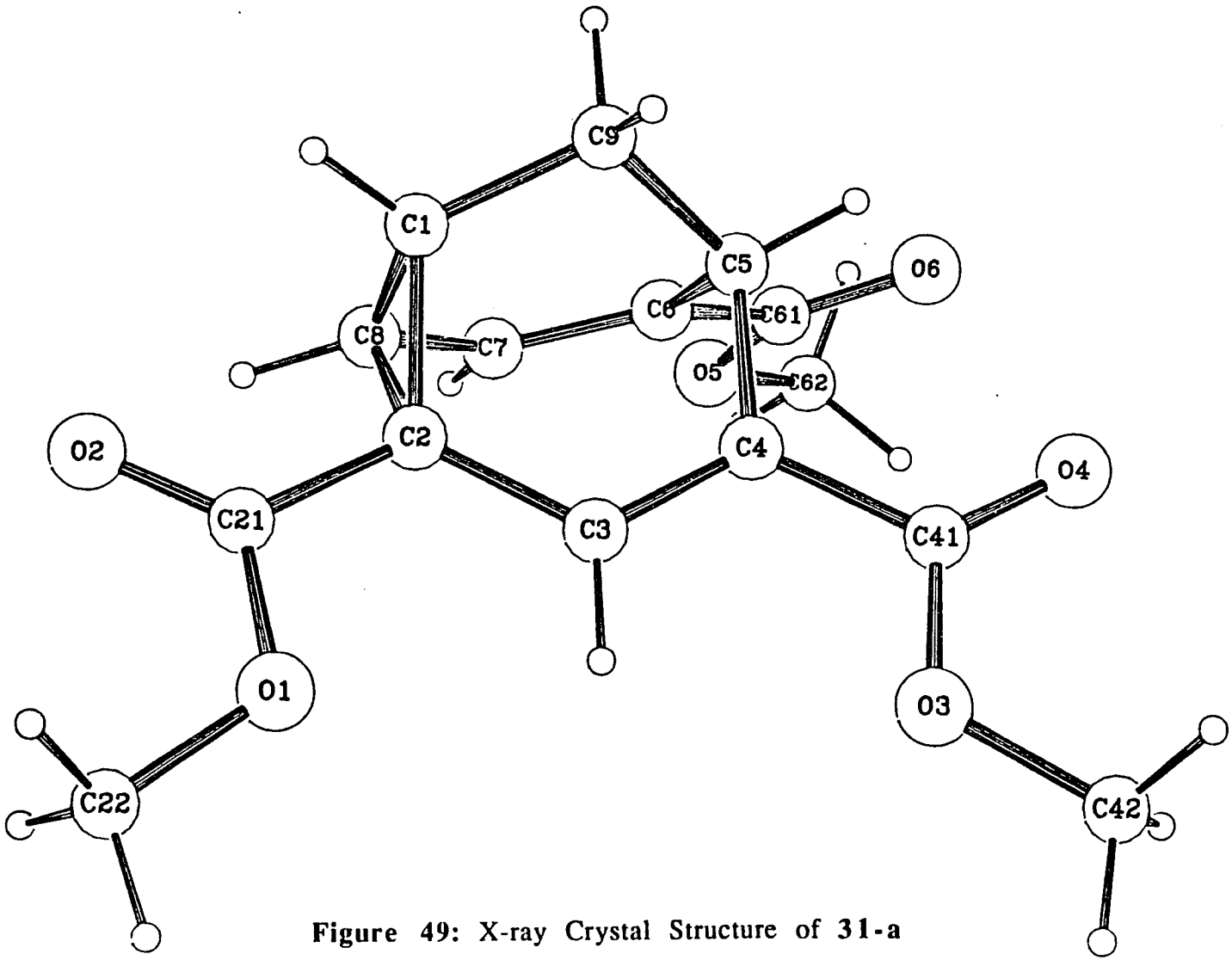

Figure 49: X-ray Crystal Structure of **31-a**

2.1.3. Selective Decarbomethoxylation of 18 toward 31-a

In order to prove the formation of compound **31-a** in the P_2I_4 reaction, we prepared it by selective decarbomethoxylation of compound **18** with NaI in pyridine under reflux (Figure 50). Pure crystalline of **31-a** was isolated in 51% yield after column chromatography (hexane/ethyl acetate, 4 :1). Its spectroscopic data are in accord with those of **31-a** from the P_2I_4 reaction.

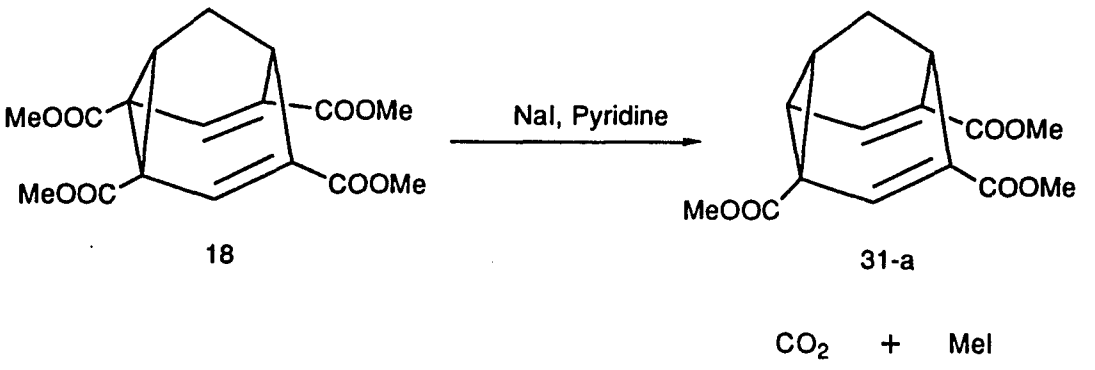

Figure 50: Selective Decarbomethoxylation of **18**

2.1.4. Interconversion between 18 and 30

During the P_2I_4 induced Grob-fragmentation, we obtained the minor products, **30** and **31-a**, as described in Scheme 1 (p. 27). The formation of **30** can be explained by a reductive bond cleavage of **18**. The reductive cleavage of the barbaralane with alkali metals is well known.[59] In order to confirm this proposed way of formation, reduction of **18** was done by using Na in liquid NH_3 which affords **30** in 29% yield.

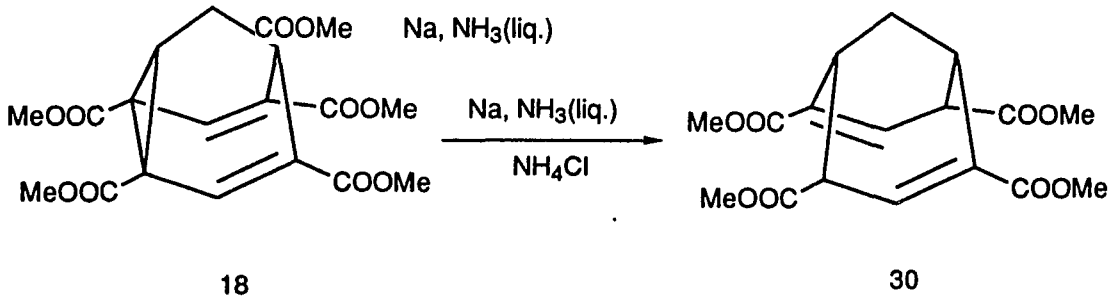

18 30

Figure 51: Conversion of 18 to **30**

Compound **30** can also be converted into **18** by using excess LDA and two equivalents of I_2. The pure compound **18** is isolated in 15% yield directly after chromatotron separation (hexane/ethyl acetate, 9 :1). The spectroscopic data from these reactions are identical to those from the P_2I_4 reaction.

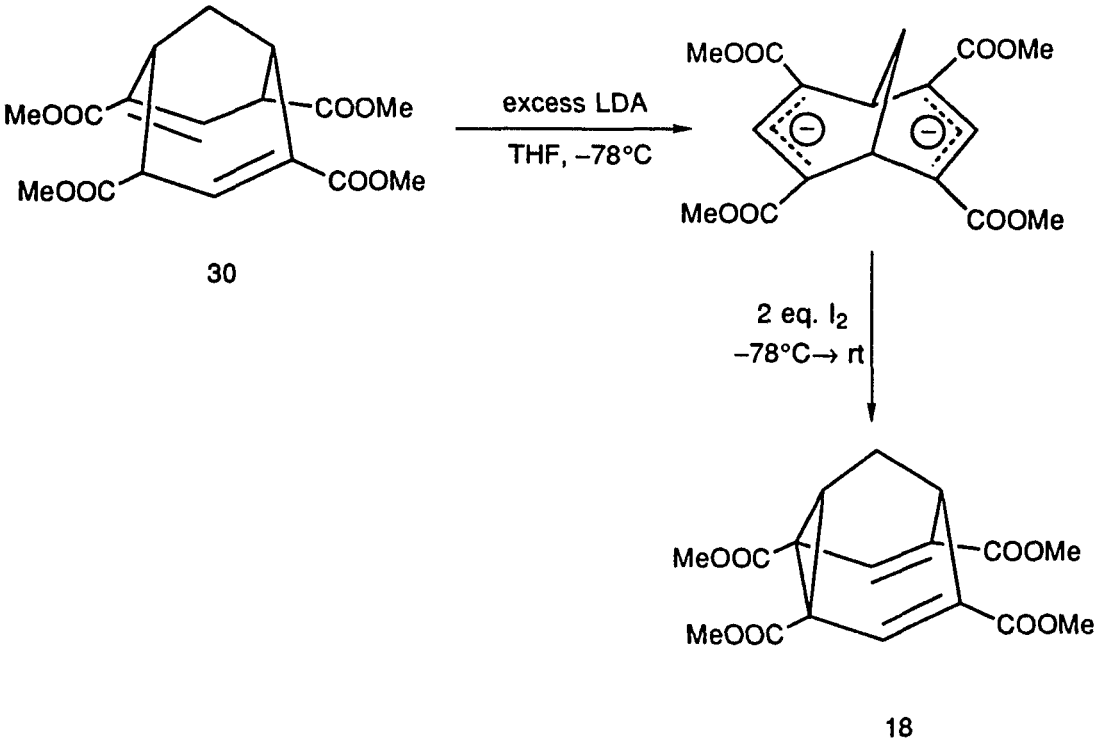

Figure 52: Conversion of **30** into **18**

2.2.1. Attempted Synthesis of 2,4,6,8-Tetracyanobarbaralane (19)

The X-ray crystal structure of **18** indicates clearly that one of the ester groups on cyclopropane is not in conjugation with the divinyl cyclopropane system. We, therefore, assumed that steric and/or electronic effects might influence the activation energy of **18**. It is quite clear that this effect will be absent in 2,4,6,8-tetracyanobarbaralane, due to the linearity and greater electron withdrawing ability of the cyano substituents. We attempted the four different synthetic routes to **19** outlined below.

In approach A (Figure 53), 2,4,6,8-tetracarbomethoxybarbaralane **18** is a precursor which will be transformed into tetracarboxamido analogue **56** followed by dehydration[60,61] to achieve our desired product, tetracyano analogue **19**.

In the second approach **B** (Figure 54), reduction[62] of **18** may provide tetraalcohol **59** which can be oxidized[63] into tetraaldehyde **60** by using a suitable oxidizing reagent. Tetraoxime analogue **61**, which can be prepared by using **60** and hydroxylamine,[64] can undergo dehydration [65] to afford tetranitrile **19**.

The starting material of approach C (Figure 55) will be tetracyclic diketo tetraester **27**, whose hydrolyzed product tetraacid analogue **62** is going to be converted into acid chloride **63.** The tetraamide analogue **64** is expected to result from the reaction of **63** and NH_3 (liquid), which

may then possibly provide tetracyclic diol **65** by the use of a suitable reducing agent. Dehydration of tetracarboxamido diol **65** should provide tetranitrile analogue **66**. The desired product tetranitrile **19** may be formed by using P_2I_4 induced Grob-fragmentation of diol **66**.

In approach **D** (Figure 56), tetraester dienol (Weiss product) **26** will be used as a starting material. Its diester analogue **67** can be formed via selective decarbomethoxylation. Our effective cyclization procedure, bromination and dehydrobromination, of **67** should afford tetracyclic diketo diester **68**. Reaction with suitable nucleophile (e.g. CuCN) may open up the doubly activated cyclopropane ring of **68** providing a diagonally symmetrical tetrasubstituted dienol **69**.[66] The efficient sequence of cyclization toward **70**, reduction toward **71**, P_2I_4 induced Grob-fragmentation toward **72** and dehydration of the corresponding diamide may yield tetranitrile **19**.

Although we attempted to synthesize **19** by using above approaches, none of the attempts could reach to our destination toward **19**. However, we have seen two interesting unexpected products from approach **A** and they will be discussed in the next section. Unfortunately, approaches **B** and **C** gave inconclusive results. In approach **D**, the tetracyclic diketo diester **68** is an important intermediate. After synthesizing **68**, we deviated from the route toward **19** and we concentrated in the following syntheses of 2,6-dicarbomethoxybarbaralane **23**, 2,6-dicyanobarbaralane **5-a** and barbaralane-2-carbomethoxy-6-carbonitrile **96-a** as discussed in sections 2.4.2 and 2.5.1.

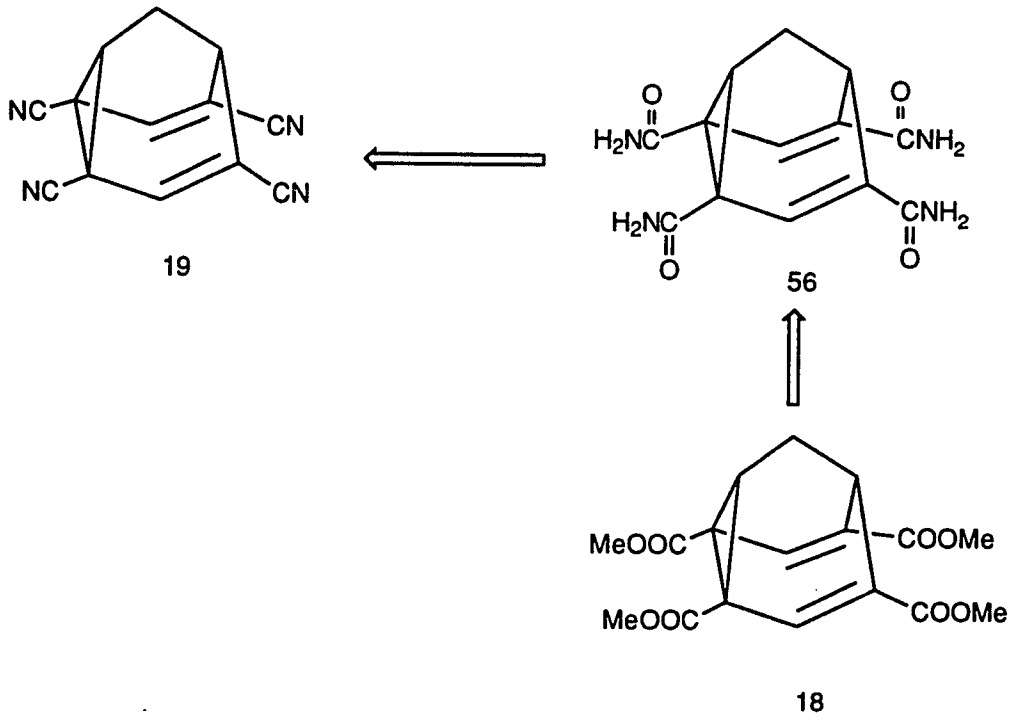

Figure 53: Approach A Toward **19**

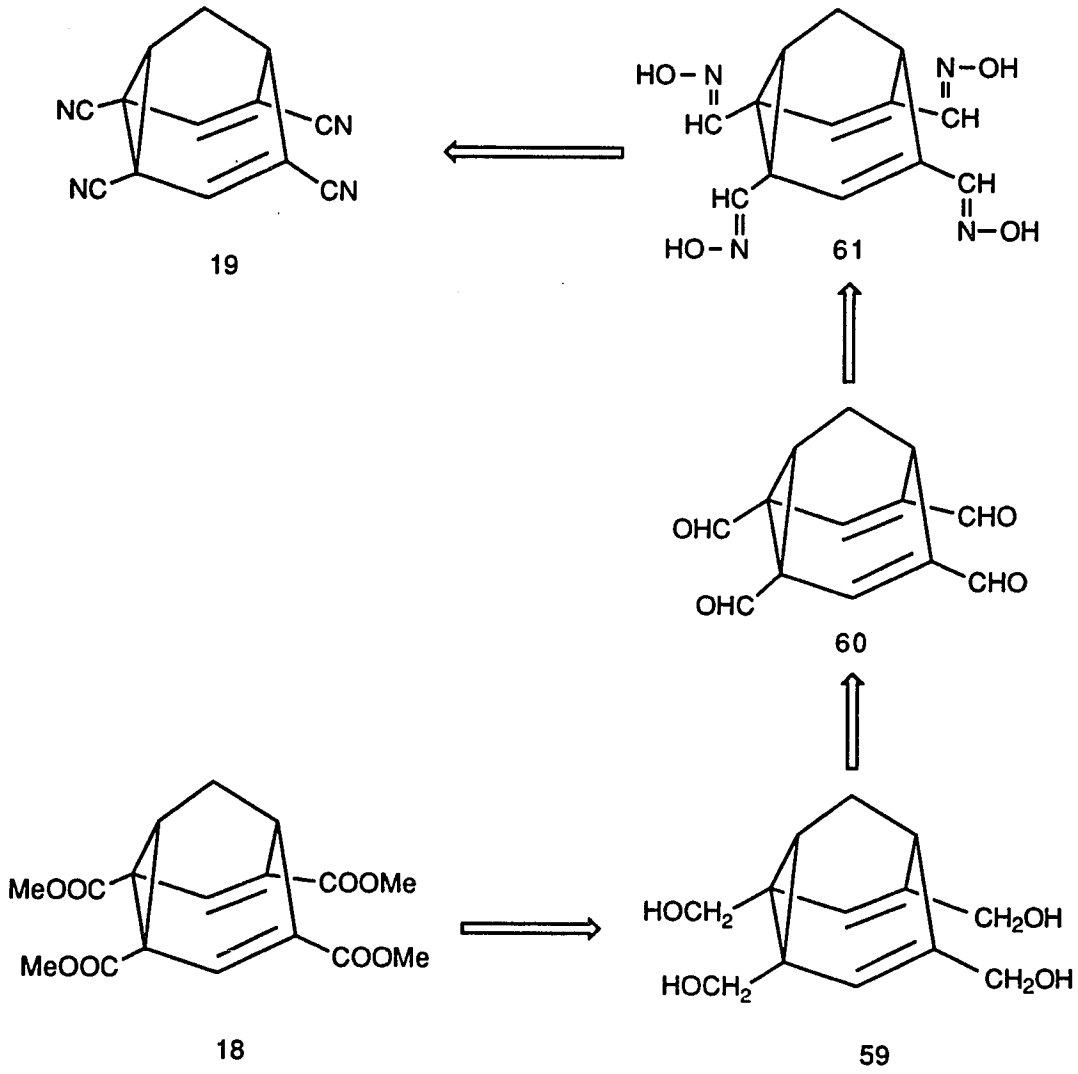

Figure 54: Approach **B** Toward **19**

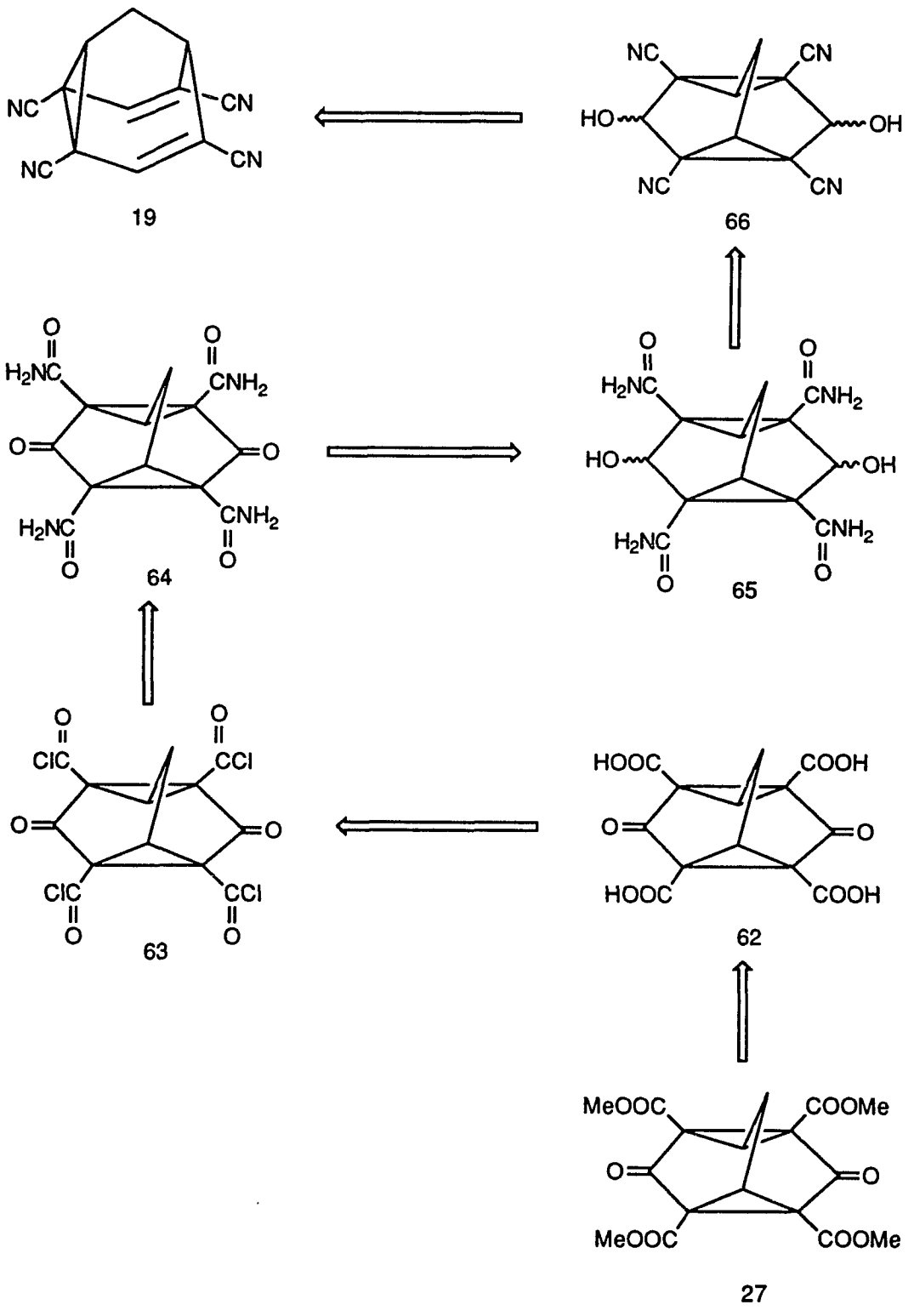

Figure 55: Approach C toward **19**

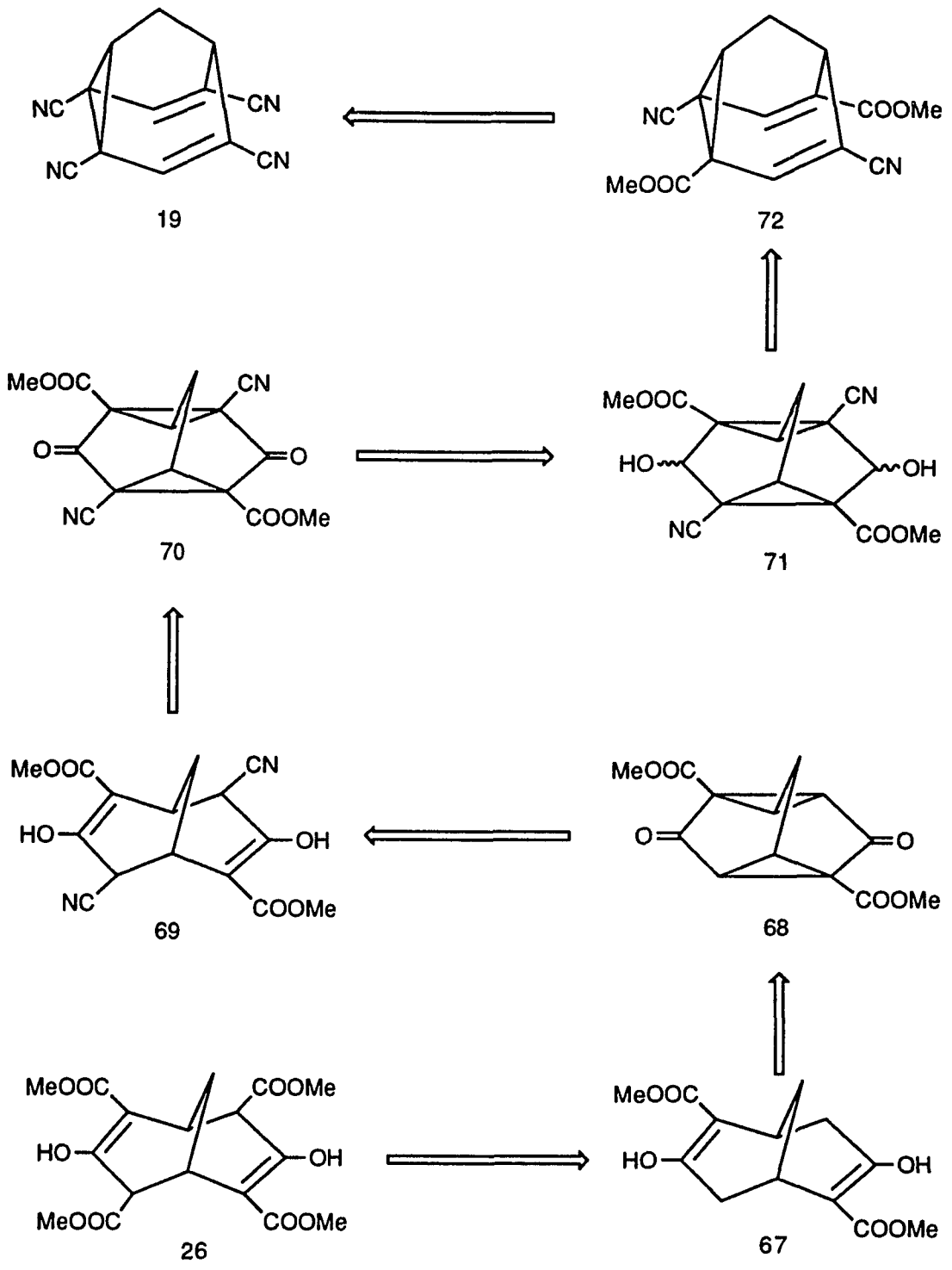

Figure 56: Approach **D** toward **19**

2.2.2. Attempted Synthesis of 2,4,6,8-tetracarboxamido-barbaralane (56)

Following route A (Figure 53), an attempt was made to convert **18** to **56** by using NH_3 in dry MeOH at 50°C (Figure 57). Instead of **56**, we isolated 4,6-dicarbomethoxy-barbaralane-2,8-dicarboximide **57** and 4,6-dicarboxamido-barbaralane-2,8-dicarboximide **58**. Fractional recrystallization afforded **57**: mp: 267-269°C, in 25% yield and **58**: mp: >300°C, in 6% yield. Formations of 2,8-dicarboximide analogues **57** and **58** are reasonable because of the steric proximity of the two ester groups at the C_2 and C_8 positions of the starting material **18**. This can be seen in the X-ray crystal structure of compound **18** (Figure 38), which shows a shorter C_2-C_8 bond (1.608Å) in contrast to a longer distance for the open end C_4-C_6 (2.404Å).

The structures of **57** and **58** are proved by their ^1H and ^{13}C-NMR structure analyses and IR studies.

^1H-NMR spectrum of **57** in DMSO-d_6 shows a 2H triplet at δ 1.38 (J= 2 Hz, two 9-H), a 6H singlet at δ 3.66 (two $-OCH_3$), a 1H doublet at δ 3.73 (J=1.92 Hz, 1-H), another 1H broad singlet at δ 3.98 (5-H), a 2H singlet at δ 6.96 (3-H and 7-H) and an imide proton broad singlet at δ 11.11 (Figure 58).

The ^{13}C-NMR spectrum of **57** in DMSO-d_6 shows peaks at 19.8 (C_9), 28.4 (C_2, C_8), 41.8 (C_5), 52.3 ($-OCH_3$), 127.9 (C_3, C_7), 129.5 (C_4, C_6), 164.3 ($-COOCH_3$), and 173.2 ppm (–CONHCO–)(Figure 59).

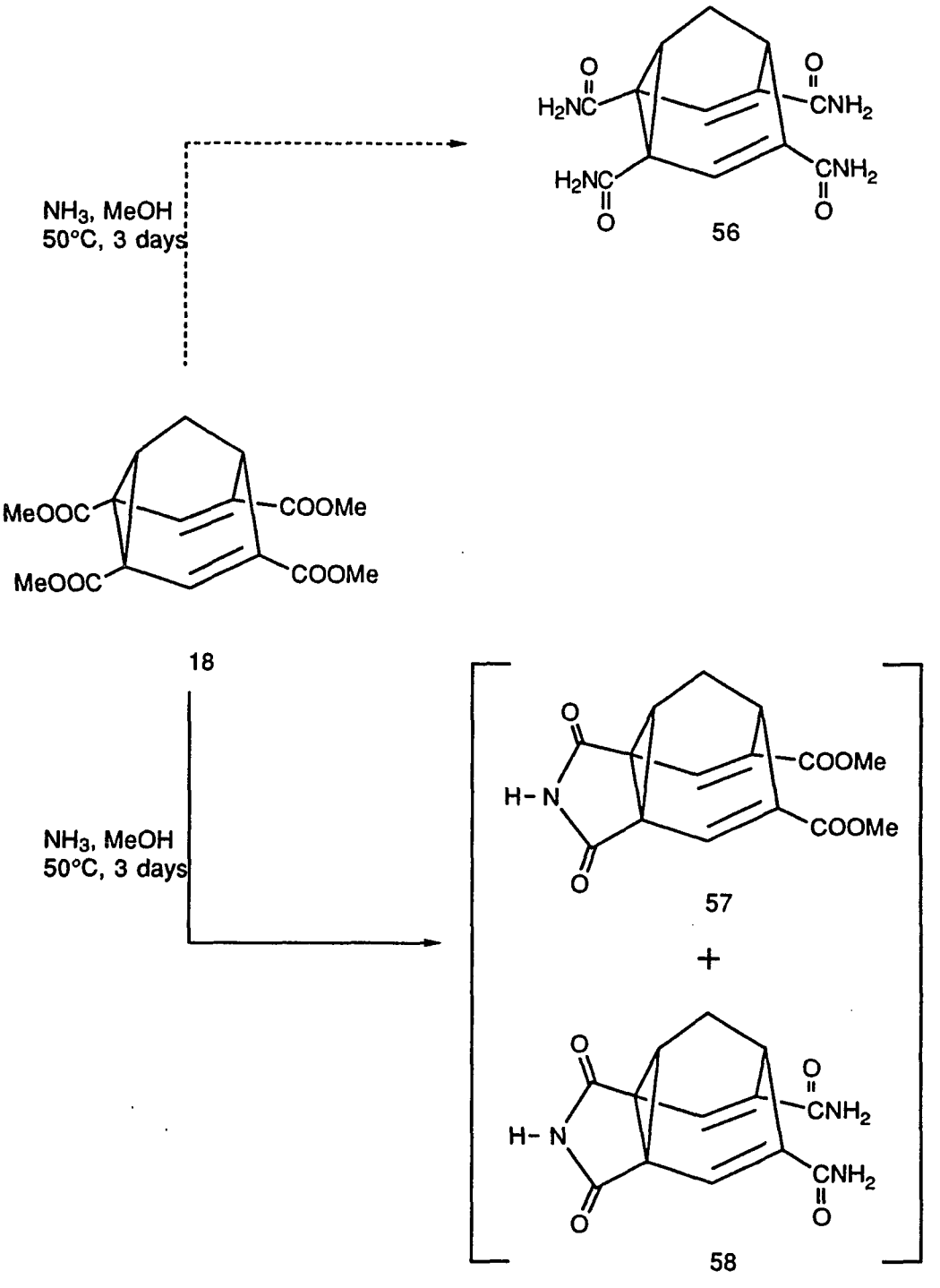

Figure 57: Attempted Synthesis of **56**

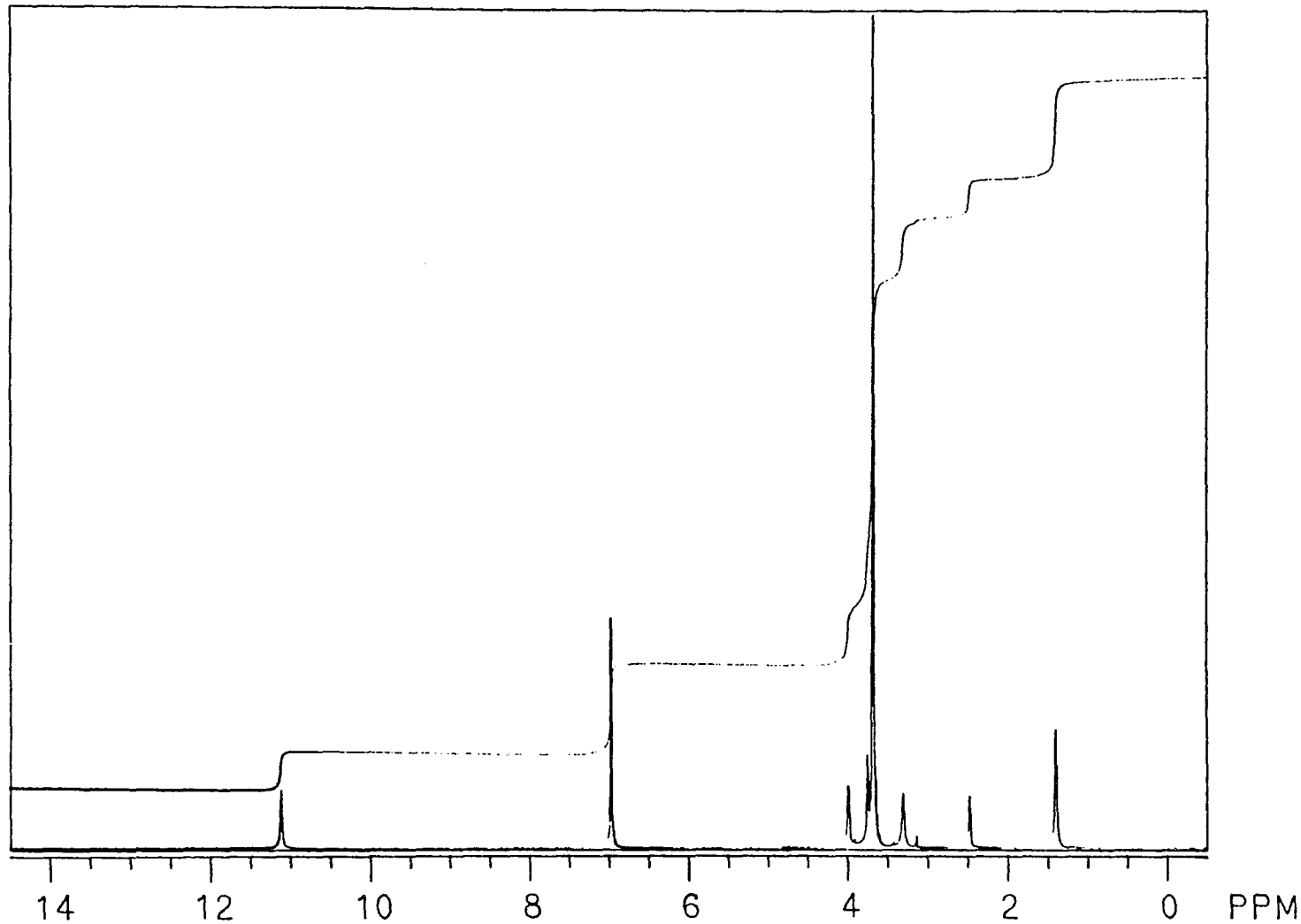

Figure 58: ^{1}H-NMR Spectrum of **57**

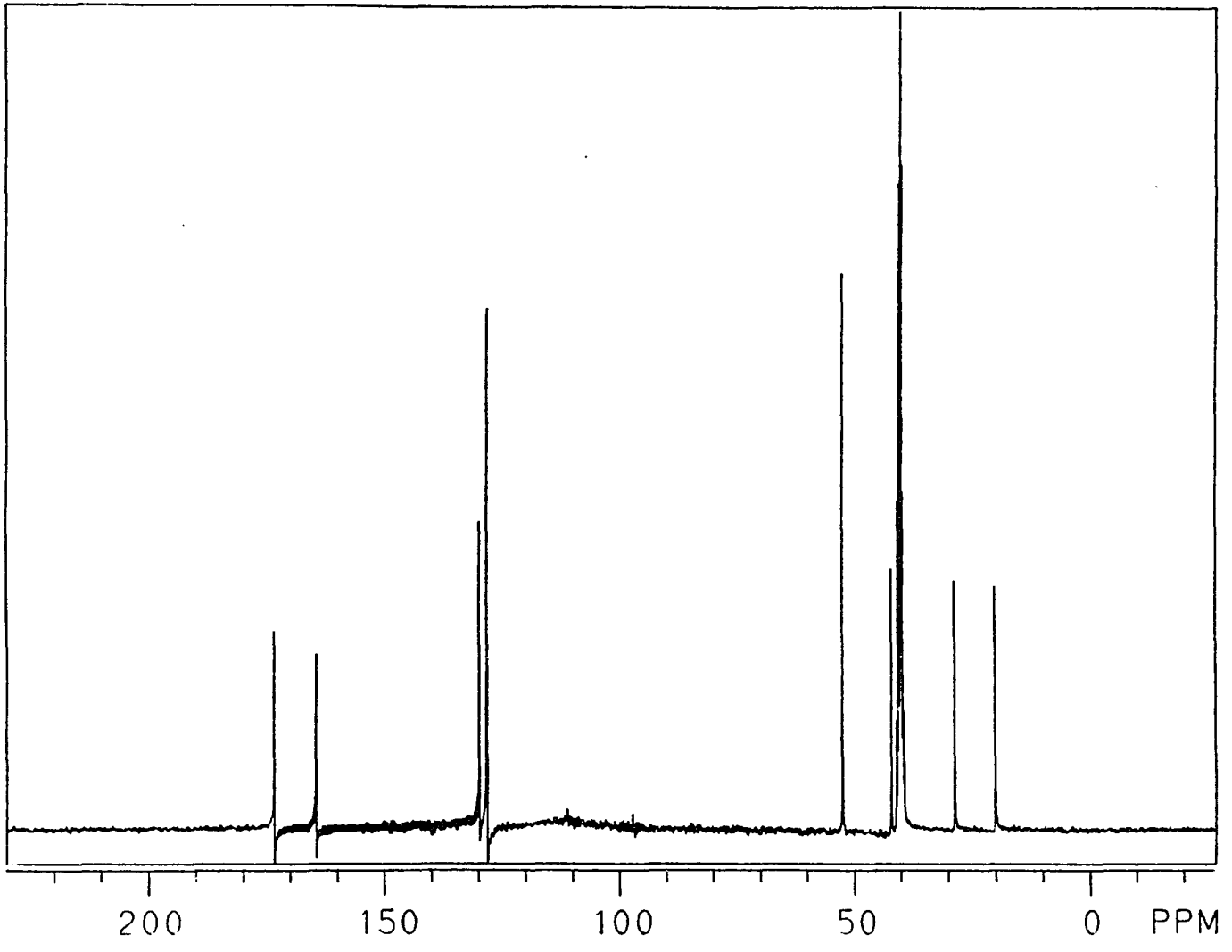

Figure 59: ^{13}C-NMR Spectrum of **57**

Single crystal X-ray analysis secured the formulation of **57** (Figure 60) The distances C_2-C_8 and C_4-C_6 are 1.558 and 2.468Å, respectively.

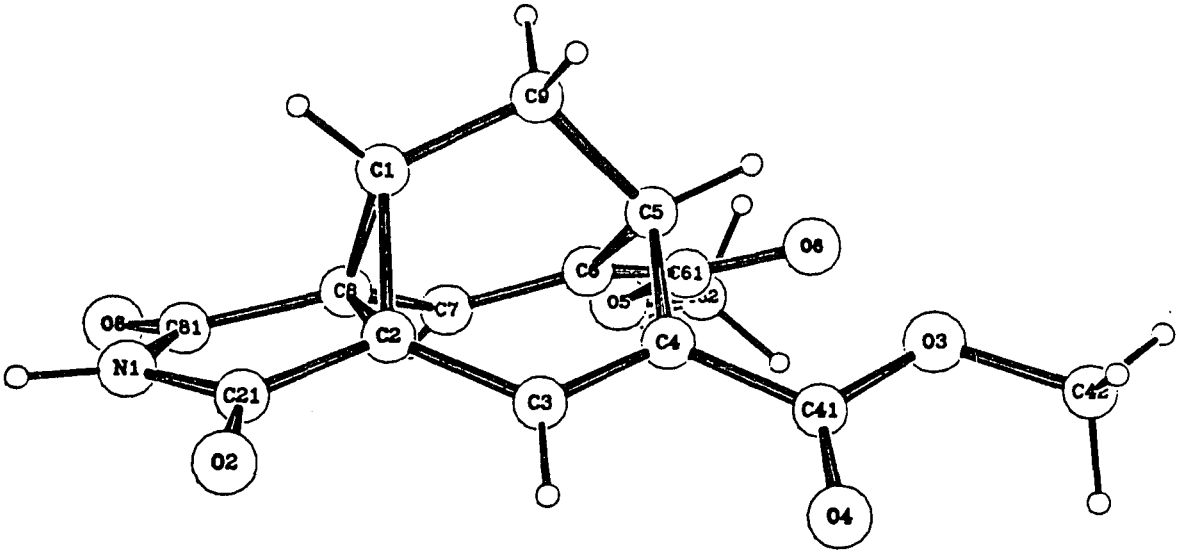

Figure 60 : X-ray Crystal Structure of **57**

The ^1H NMR data for compound **58** in DMSO-d_6 verified its structure by showing the peaks at δ 1.35 (t, 1.65 Hz, two 9-H), 3.63 (d, 1.83 Hz, 1-H), 3.67 (m, 5-H), 6.88 (s, 3-H and 7-H), 7.28 (bs, two amide protons), 8.13 (bs, two amide protons) and 11.05 (bs, –CONHCO–).

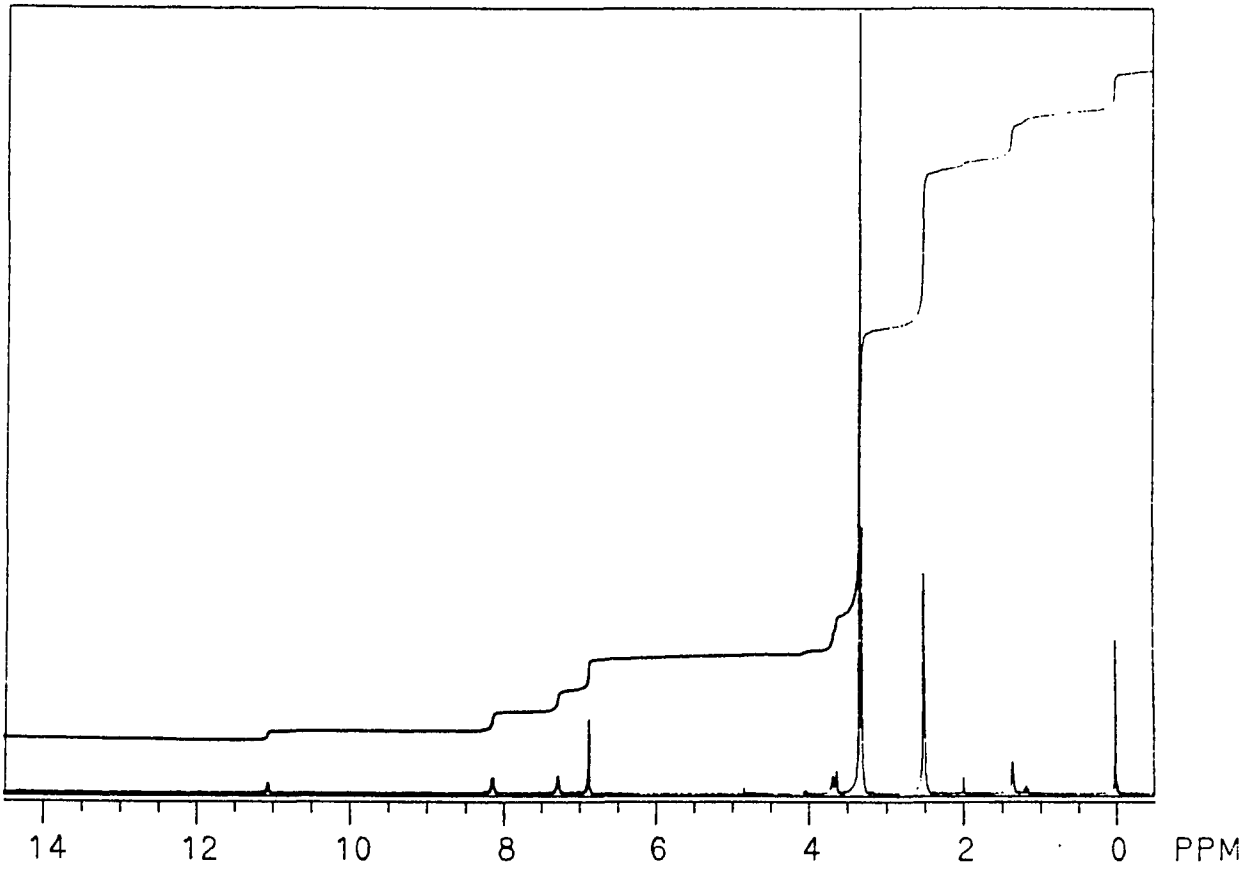

Figure 61: ^1H-NMR Spectrum of **58**

Since reaction of **18** and NH_3 in dry CH_3OH could not give tetracarboxamide **56**, we discontinued this approach.

2.2.3. Synthesis of 2,6-Dicarbomethoxy-triasterane-3,7-dione (68)

As shown in route **D** (Figure 56), 2,6-dicarbomethoxy-triasterane-3,7-dione (2,6-dicarbomethoxy-tetracyclo[3.3.1.$0^{2,8}$.$0^{4,6}$]nonane-3,7-dione) **68** is an important intermediate in the approach toward **19**. Outlined in Figure 62 are three different routes toward compound **68** via the Weiss product.

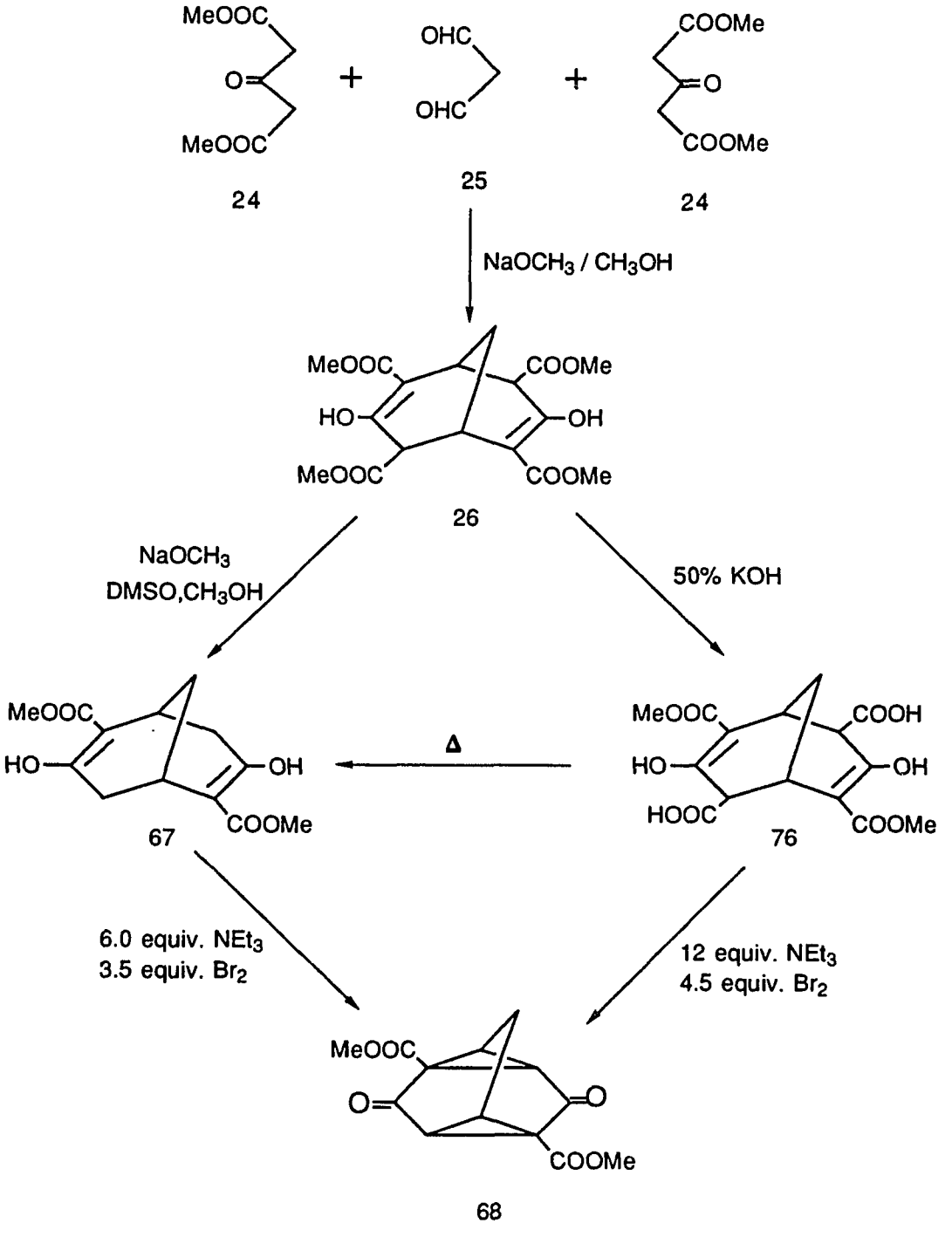

Figure 62: Synthesis of 2,6-Dicarbomethoxy-triasterane-3,7-dione **68**

2,4,6,8-Tetracarbomethoxy-bicyclo[3.3.1]nonane-3,7-dione (Weiss product) **26** was obtained in 64.7% yield by the reaction of dimethyl 1,3-acetonedicarboxylate **24** with malondialdehyde **25**. Selective decarbomethoxylation of **26** was done by following the procedure of Weiss et al.[67] where tetramethyl 3,7-dioxo-cis-bicyclo[3.3.0]octane-2,4,6,8-tetracarboxylate readily loses two of its carbomethoxyls on mild warming with 10 mol of NaOMe in Me_2SO/MeOH, giving exclusively the 2,6-diester in >90% yield. When compound **26** was treated with excess NaOMe in Me_2SO/MeOH, a diester was obtained in 41% yield: mp 149-152°C. There are three possible structures {**67**, **73** or **74**} for this diester (Figure 63).

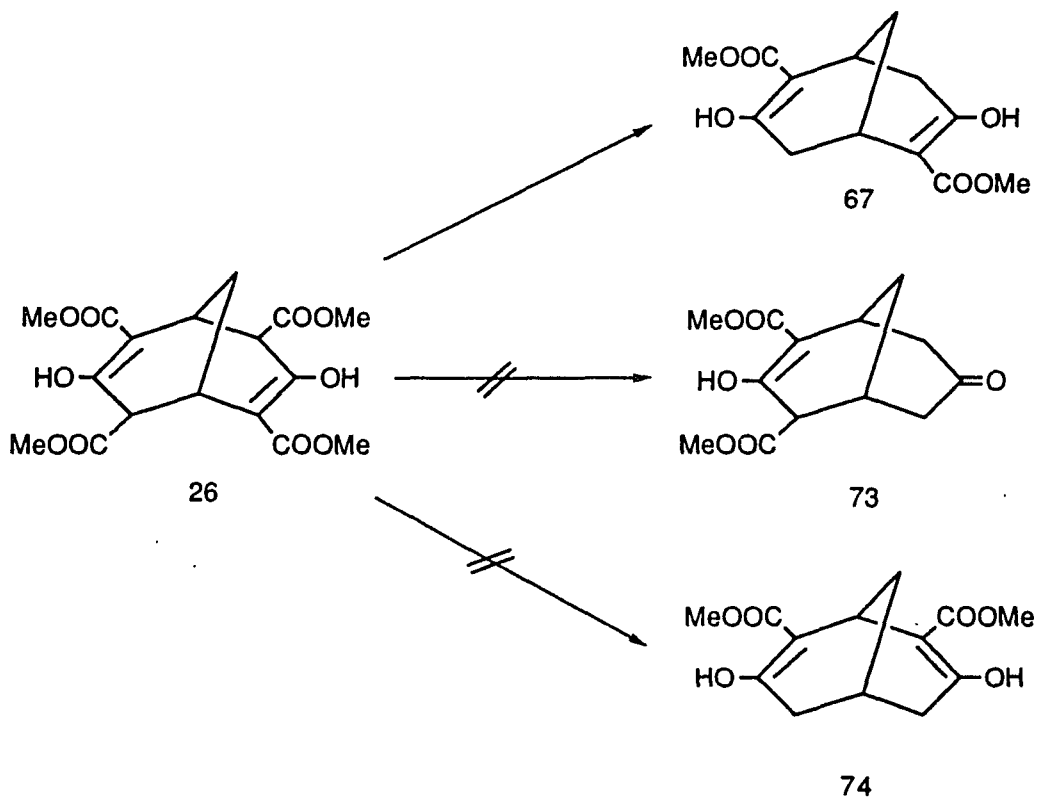

Figure 63: Three Possible Diesters

Of these three structures **73** is eliminated by the fact that the ^{13}C NMR spectrum (Figure 65) does not contain any signal from an isolated cyclohexanone carbonyl. If the diester were **74**, its ^{13}C should show 8 different peaks. Besides, one of the carbons of **74** is bisallylic which would undoubtedly give rise to very different signal. However, the ^{13}C NMR spectrum (Figure 65) showed only 7 carbon signals for the resulting diester. Therefore, the possibility of structure **74** was rejected.

Of the three possible structures, **67** was proved to be the correct one by its ^{1}H and ^{13}C NMR spectra. The ^{1}H-NMR of **67** in chloroform-d shows the peaks at δ 1.75 (t, 3.25 Hz, two 9-H), 2.41 (AB, two 4-H and two 8-H), 3.00 (m, 1-H and 5-H), 3.78 (s, two $-OCH_3$) and 12.25 (s, two enol protons, exchangeable with D_2O). The ^{13}C-NMR of **67** in chloroform-d shows the peaks at δ 26.0 (C_9), 29.2 (C_1, C_5), 36.2 (C_4, C_8), 51.5 ($-OCH_3$), 100.9 (C_2, C_6), 172.3 (C_3, C_7) and 172.4 ppm (two $-COOCH_3$).

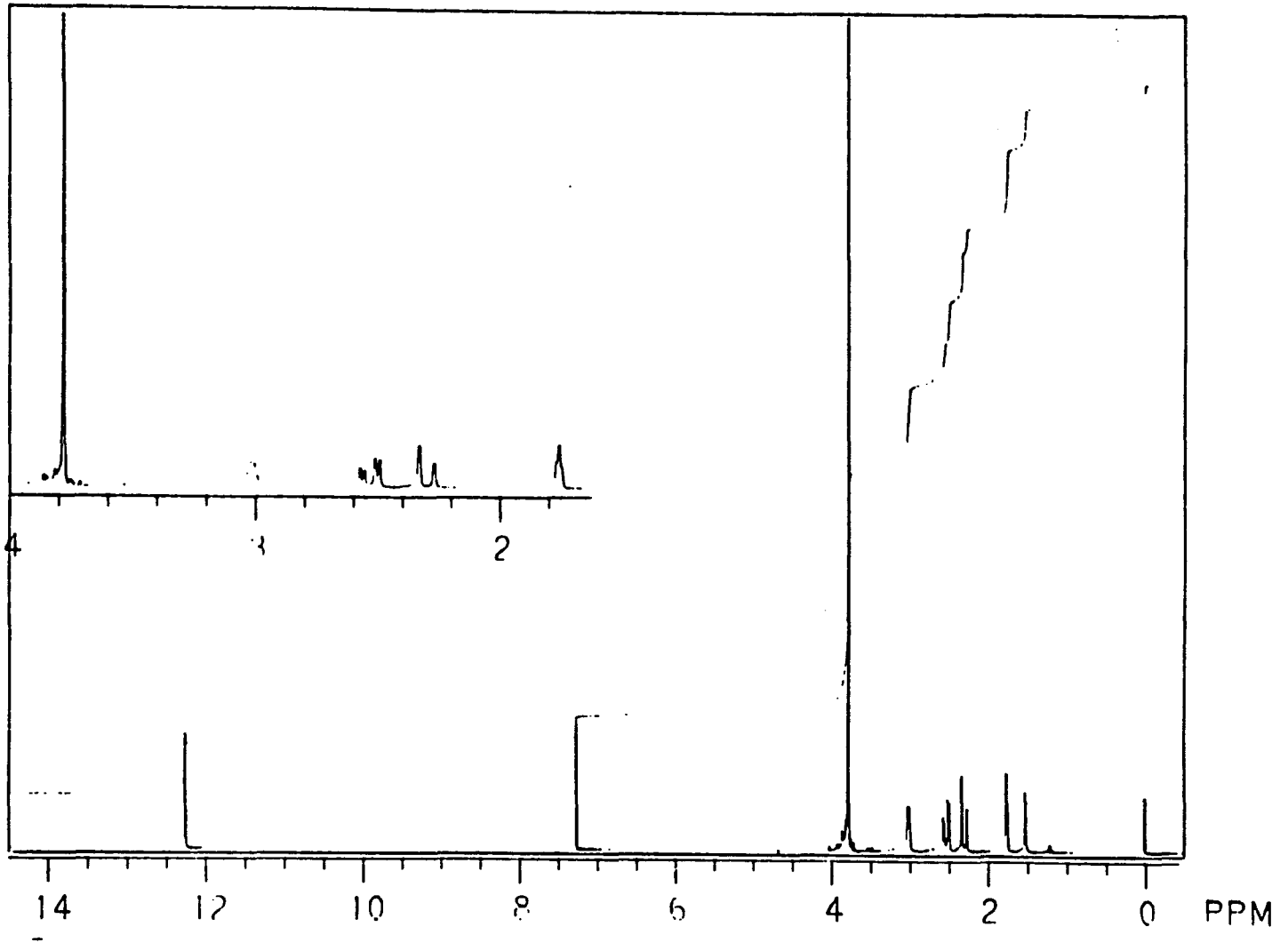

Figure 64: ^{1}H-NMR Spectrum of **67**

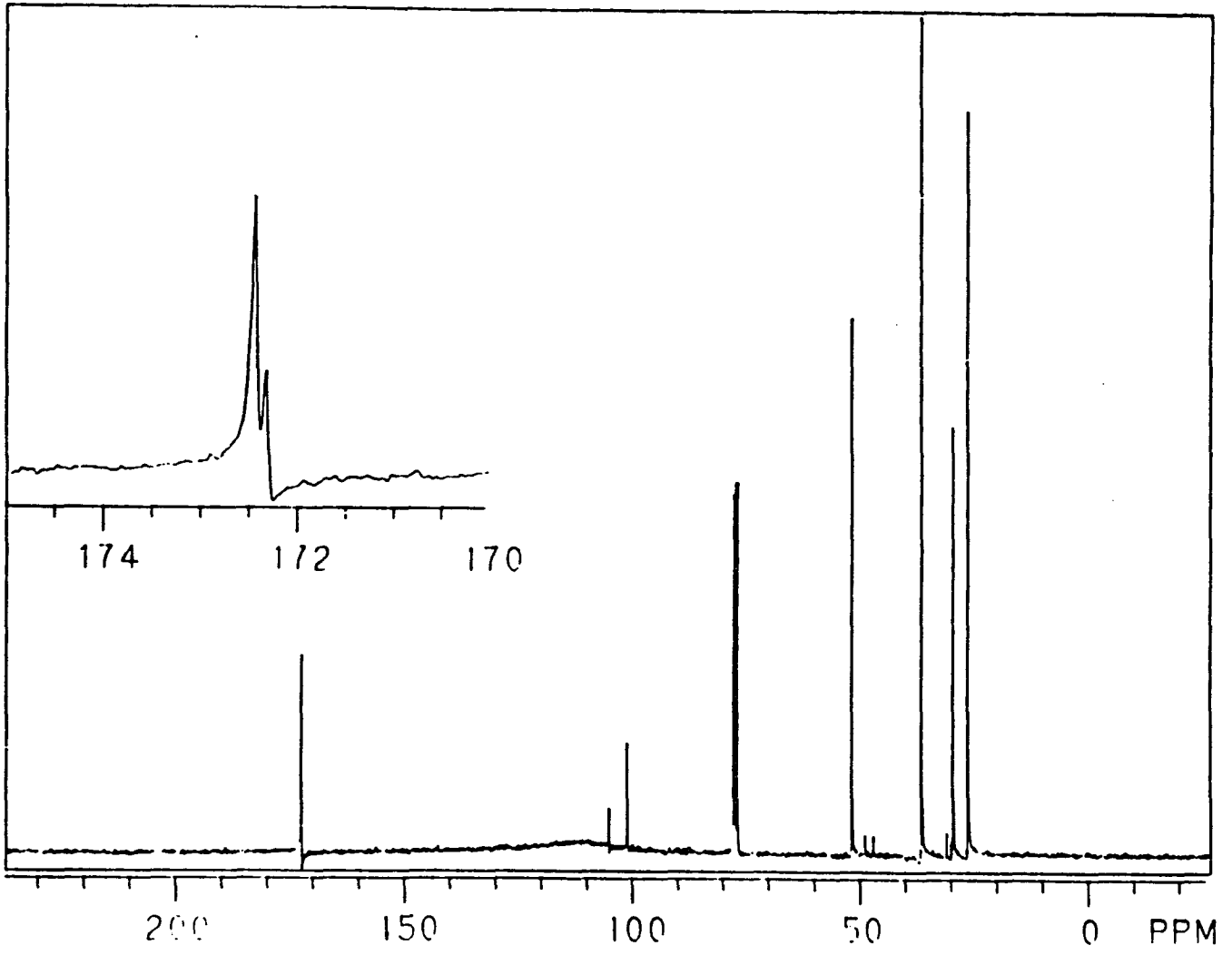

Figure 65: ^{13}C-NMR Spectrum of **67**

The removal of two carbomethoxy groups of **26** to give **67** proceeds most likely through loss of dimethyl carbonate as discussed by Weiss.[67] The formation of **67** can be explained by the mechanism shown in Figure 66.

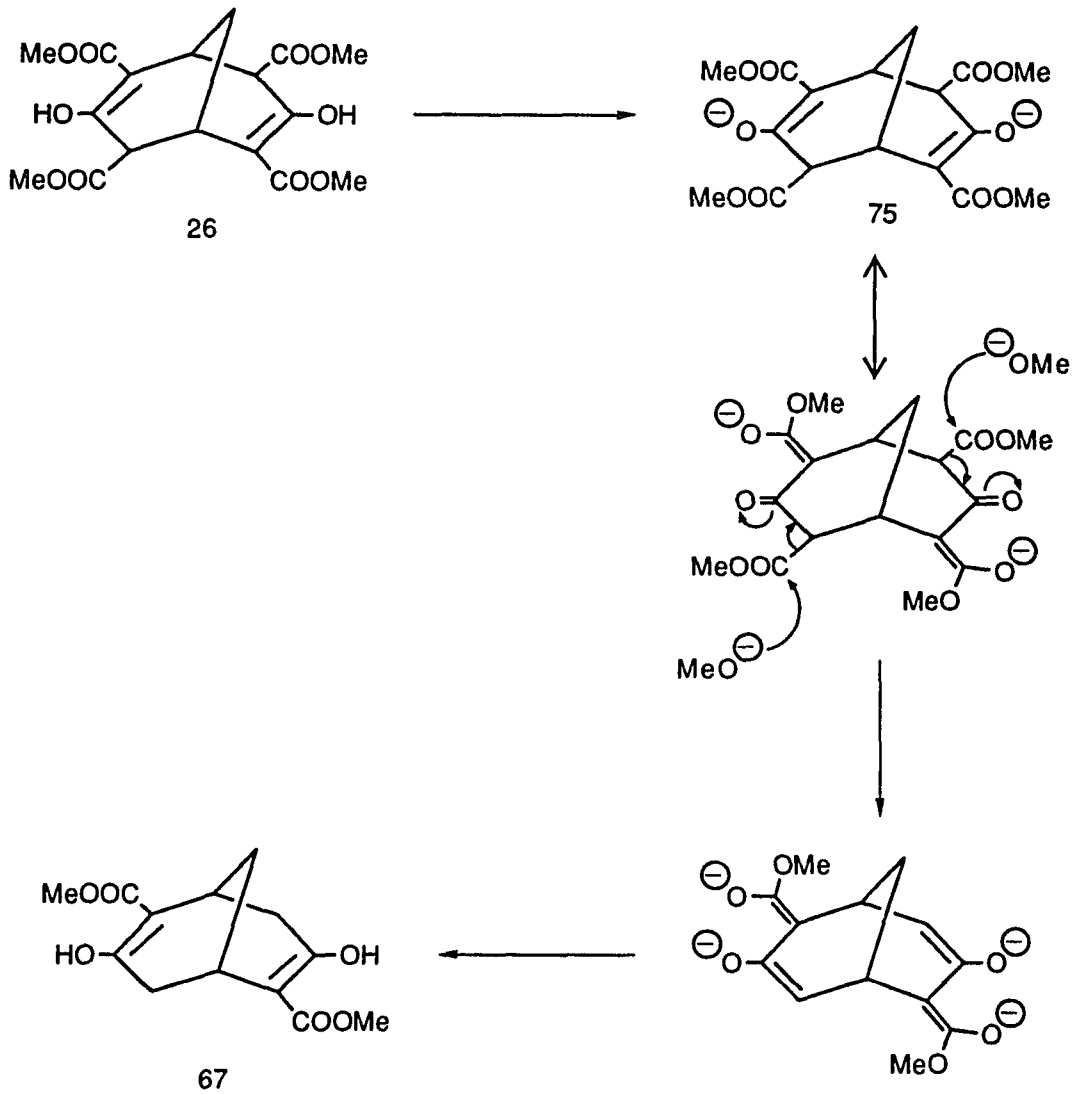

Figure 66: The mechanism of the formation of **67**

As shown in Figure 62, 2,6-diester **67** has also been synthesized by partial saponification of 2,4,6,8-tetracarbomethoxy-bicyclo[3.3.1]nonane-3,7-dione **26** to **76** followed by decarboxylation. The procedure used for the partial saponification of the tetraester **26** to the diagonally symmetrical diacid diester dienol **76** was developed by Findlay[68] in the synthesis of 2-carbomethoxytropinone **78** via the 2,4-dicarbomethoxytropinone **77** (Figure 67).

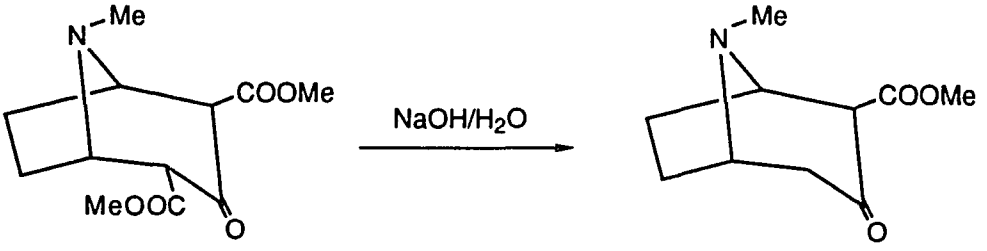

77 78

Figure 67: Selective Decarbomethoxylation of **77**

In his approach toward **78**, Findlay used equivalent amounts of compound **77** and sodium hydroxide, but in our procedure we used a large excess of 50% aqueous potassium hydroxide solution instead. The diacid diester **76** was characterized by its ^{1}H-NMR. Further transformation to the diester **67** was achieved by heating of **76** as the solid followed by addition of hot methanol. This process produced 92% of white colored shiny crystals **67**: mp 149-152°C.

A similar procedure was developed by Mercedes Connelly in our laboratory for the synthesis of 1,5-dimethyl-2,6-dicarbomethoxy-

bicyclo[3.3.0]octane-3,7-dione from the tetraester analogue leading to 1,5-dimethyl-2,6-dicarbomethoxysemibullvalene.[69]

Once compounds **67** and **76** were available, several attempts at brominative cyclization were investigated in order to convert those compounds to 2,6-dicarbomethoxy-triasterane-3,7-dione **68** (Figure 62, p. 75). Reaction of compounds **76** with 12 equivalents of NEt_3 and 4.5 equivalents of Br_2 afforded tetracyclic diketone **68** in 76% yield: mp 133-135°C. We improved the yield of **68** to 91% by using compound **67** with 6 equivalents of NEt_3 and 3.5 equivalents of Br_2.

Of the three approaches toward **68** (Figure 62, p. 75), the route **26**→**76**→**67**→**68** is the best one (41.86% overall yield) although the synthetic pathway is longer than the other two, **26**→**67**→**68** (24.01% overall yield) and **26**→**76**→**68** (37.66% overall yield).

The ^{1}H-NMR data for compound **68** verified its structure and symmetry by showing a 2H triplet at δ 2.49 (2.4 Hz, two 9-H), a 4H multiplet at δ 2.87 (1-H and 5-H, 4-H and 8-H) and a 6H singlet at δ 3.77 (two $-OCH_3$)(Figure 68).

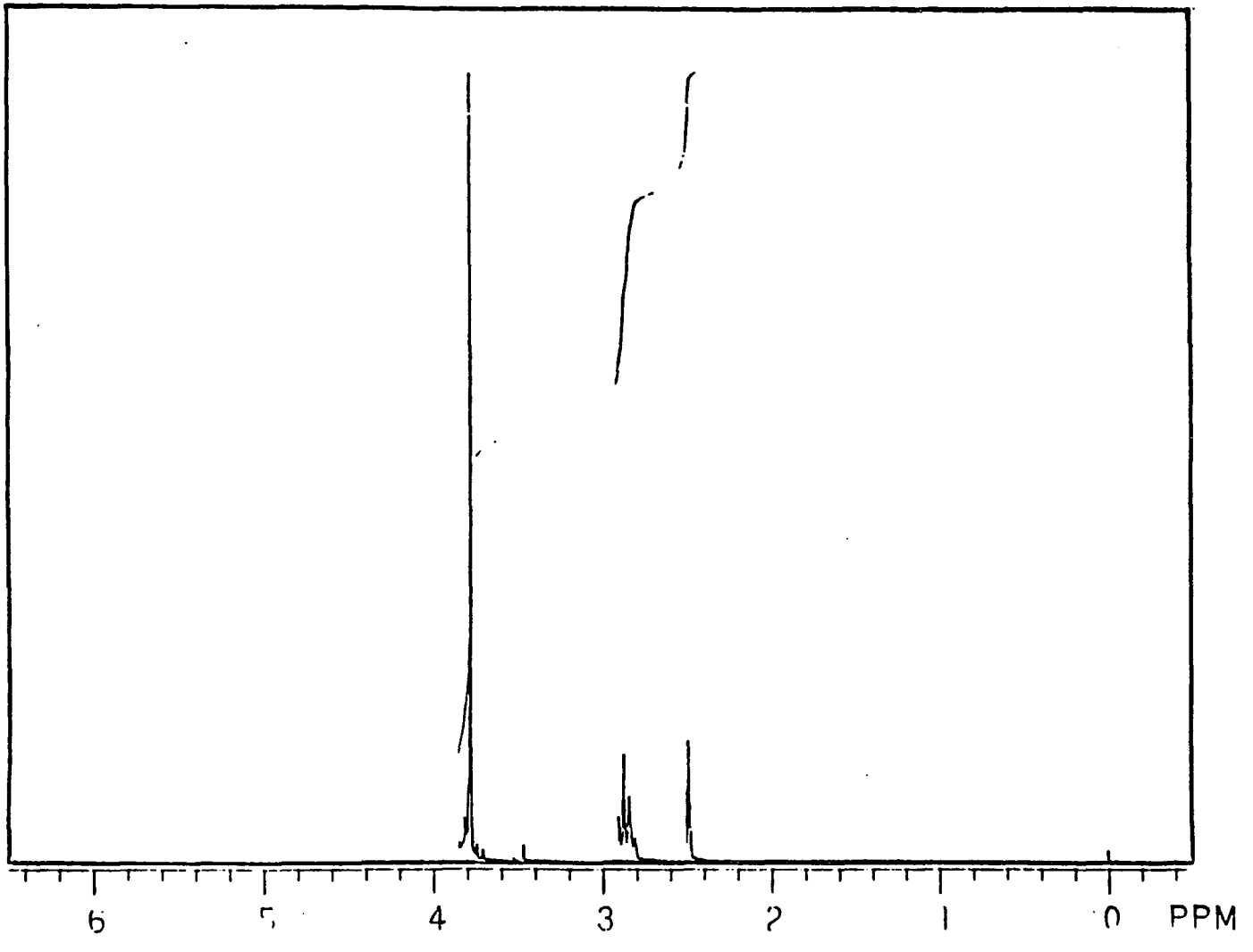

Figure 68: ^{1}H-NMR Spectrum of 68

The tetracyclic diketo diester **68** is an important intermediate for the syntheses of symmetrically tetrasubstituted barbaralanes, diagonally symmetrical tetrasubstituted barbaralanes, diagonally symmetrical disubstituted barbaralanes, and diagonally unsymmetrical disubstituted barbaralanes. It is expected that nucleophilic reagents such as CuCN and Ph_2CuLi could open the activated cyclopropane ring of **68**. By using CuCN and following multiple steps , we could hopefully obtain our desired tetracyanobarbaralane **19**. On the other hand , diagonally symmetrical tetrasubstituted barbaralane (e.g. 2,6-dicyano-4,8-diphenylbarbaralane **80**) could be synthesized by using Ph_2CuLi.

Diagonally symmetrical disubstituted barbaralanes such as 2,6-dicynobarbaralane and 2,6-diphenylbarbaralane were already synthesized by Quast and co-workers,[24,25] and their activation energies of the Cope rearrangement were reported as 5.78 kcal/mol and 5.16 kcal/mol respectively, each of them is lower than that of unsubstituted barbaralane (7.6 kcal/mol)[4]. The activation energies of these two diagonally symmetrical disubstituted barbaralanes prompted us to investigate the effect of diagonally symmetrical tetrasubstituted barbaralane such as 2,6-dicyano-4,8-diphenyl-barbaralane **80.**

We therefore put aside our attempt toward tetracyanobarbaralane **19** temporarily.

2.3.1. Attempted Cyclopropane Ring Opening Reaction with Ph_2CuLi

Once **68** was available, the cyclopropane ring openings were required to provide dienol **79** (Figure 69). Successful cuprate-induced cyclopropane openings that occur in the absence of a double bond and involve at least two activating groups on the same cyclopropyl carbon atom are known.[70]

Bertz and co-workers reported the set of experiments involving **82** and **83** to compare singly and doubly activated cyclopropanes[66] in which the remainder of the molecule is the same (Figure 70). In the synthesis of the modhephene, **82** and **83** were treated with Me_2CuLi in hope of stereo-specifically introducing a methyl group. While **82** could not be induced to react with Me_2CuLi, **83** was opened smoothly to **84** by Me_2CuLi. From their results, it appeared that two activating groups were necessary for cyclopropane ring opening.

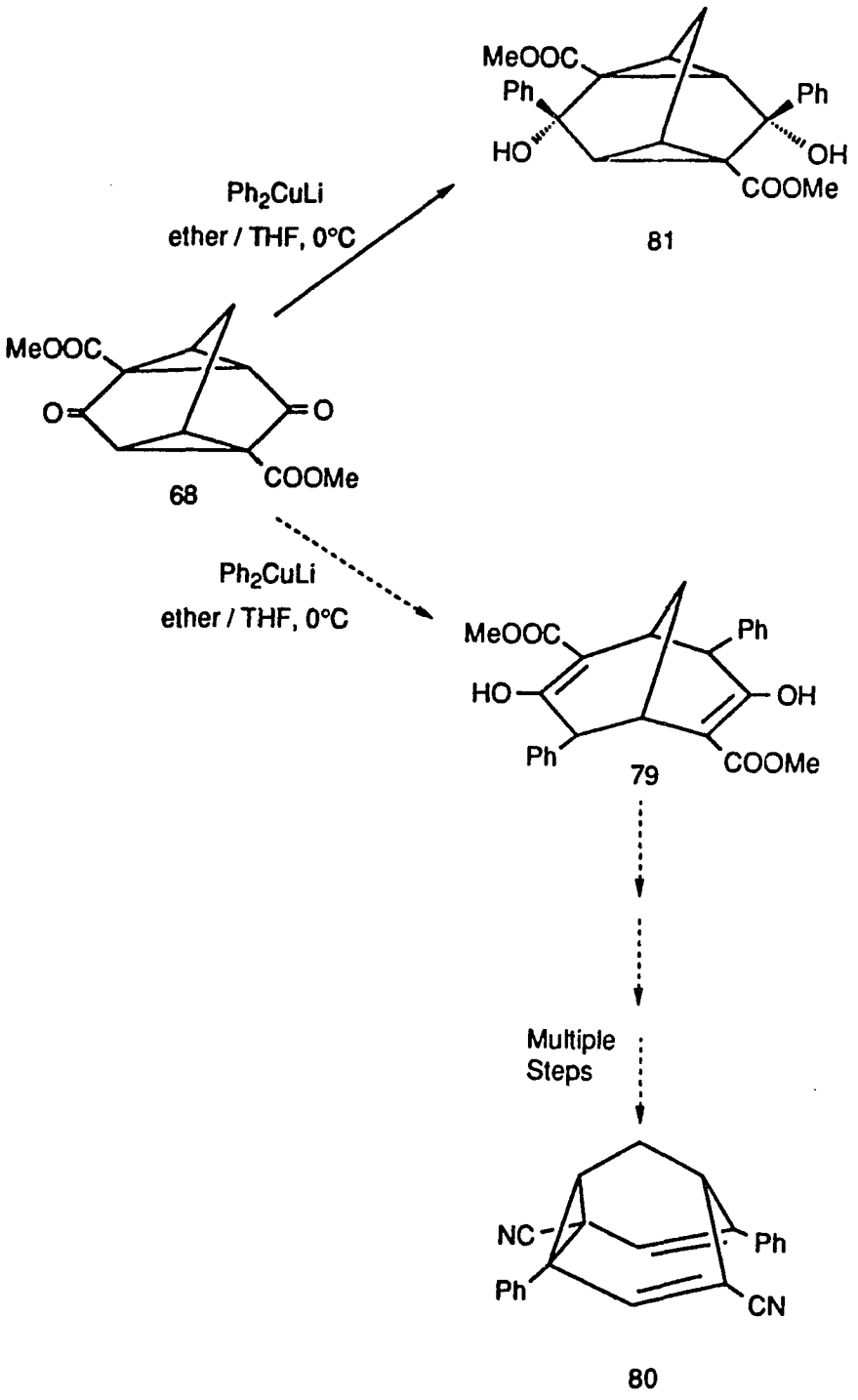

Figure 69: Attempted Cyclopropane Ring Opening Reaction with Ph_2CuLi

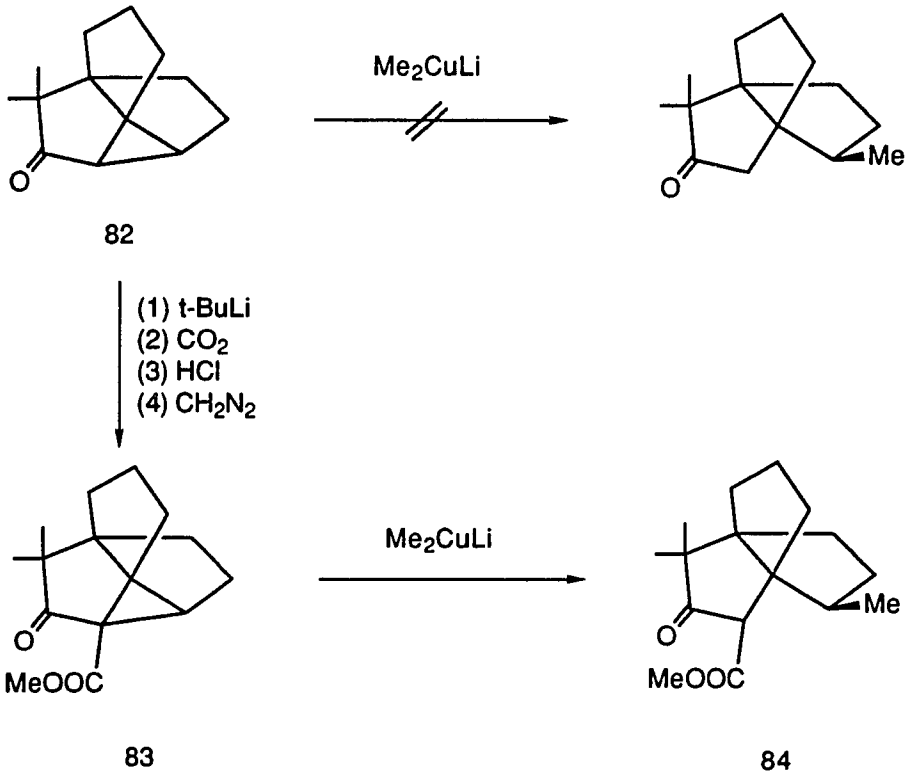

Figure 70: Reactions of Singly and Doubly Activated Cyclopropanes with Me_2CuLi[66]

Since the cyclopropanes of **68** have three different activating groups, we expected that cyclopropane ring opening would occur easily. Therefore, we treated **58** with Ph_2CuLi in ether-THF solvent mixture at 0°C (Figure 71).

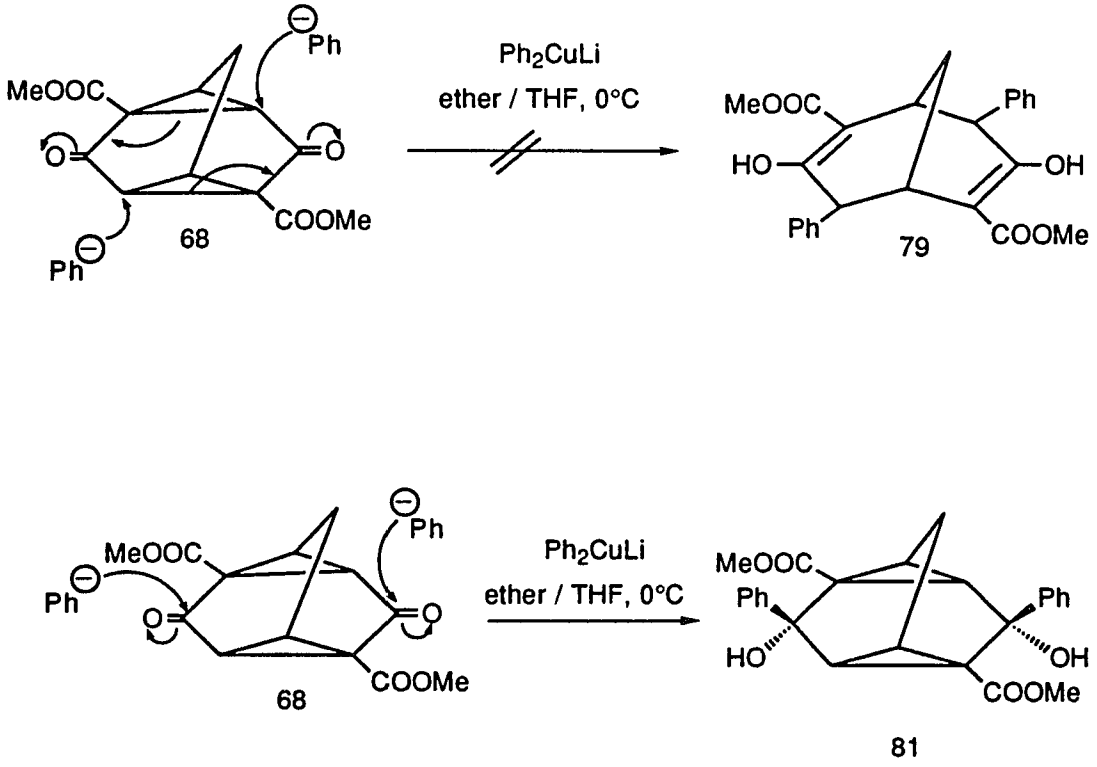

Figure 71: Reaction of **68** with Ph_2CuLi

The proposed transformation of **68** with Ph_2CuLi should have given the 1,4-addition product **79**. To our surprise, the carbinol (1,2-adduct) **81** was obtained in 29% yield. The ^{1}H-NMR spectrum of **81** shows the peaks at δ 2.13 (dd, 8.7 Hz and 0.7 Hz, 4-H and 8-H), 2.25 (dd, 8.7 Hz and 0.7 Hz, 1-H and 5-H), 2.41 (bs, two 9-H), 3.51 (s, $-OCH_3$), 5.05 (bs, –OH) and 7.30 – 7.53 (m, Ph–H).

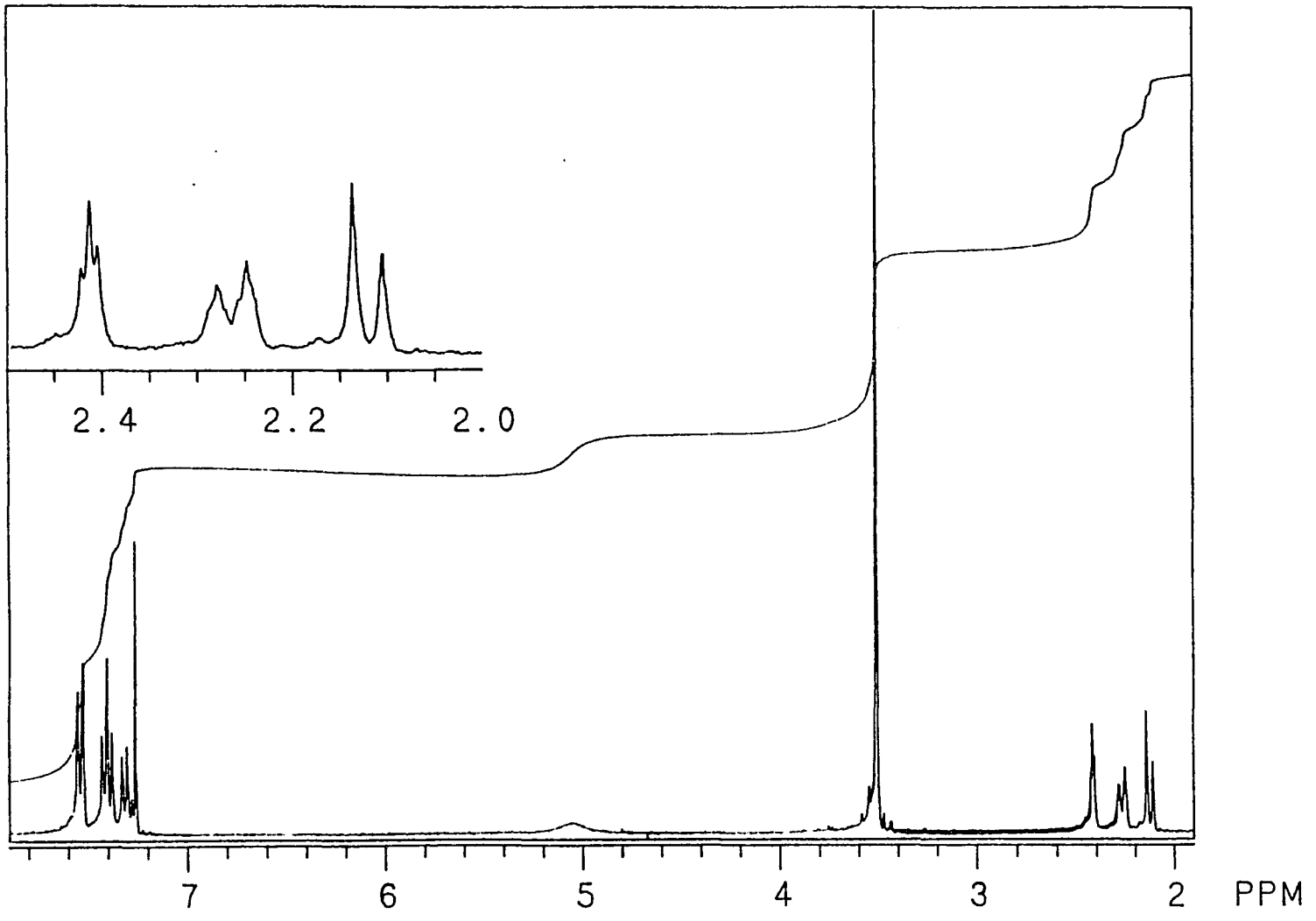

Figure 72: ^{1}H-NMR Spectrum of **81**

The structure of **81** has been confirmed by a single crystal X-ray analysis (Figure 73).

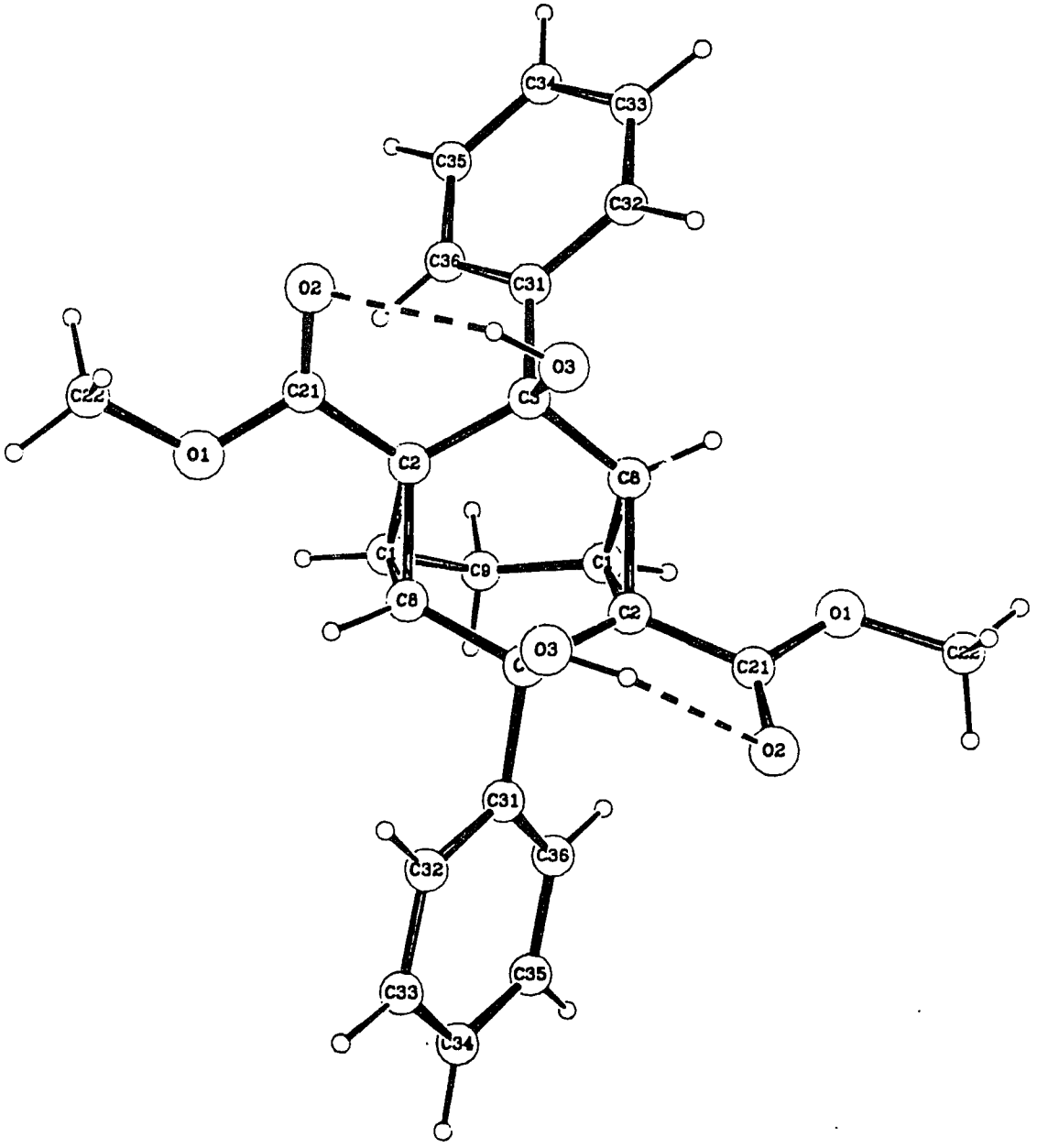

Figure 73: X-ray Crystal Structure of **81**

Formation of **81** caused to discontinue for now our attempts to synthesize 2,6-dicyano-4,8-diphenylbarbaralane **80**.

2.4.1. Diagonally Symmetrical Disubstituted Barbaralanes

The 2,6-disubstituted barbaralanes (**23** and **5-a**) are also of interest to us (Figure 74). After studying the results of the X-ray structure and the low temperature NMR spectra of the 2,4,6,8-tetracarbomethoxy-barbaralane **18** we felt that it would be interesting to compare the behavior of 2,6-dicarbomethoxybarbaralane **23** with the tetrasubstituted analogue **18** since only one ester group bisects the cyclopropane ring. The results of MNDO calculations on the semibullvalene also suggested that the presence of electron withdrawing groups in positions 2 and 6 should stabilize the delocalized structure in the Cope rearrangement.[16]

The 2,6-dicyanobarbaralane **5-a** also appeared to be an attractive entry into this area of disubstituted barbaralane chemistry since our attempts toward 2,4,6,8-tetracyanobarbaralane **19** via 2,4,6,8-tetracarbomethoxybarbaralane **18** were not successful.

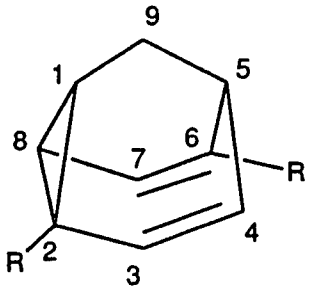

23: R = –$COOCH_3$

5-a: R = –CN

Figure 74: 2,6-Disubstituted Barbaralanes

2.4.2 Synthesis of 2,6-Dicarbomethoxybarbaralane (23)

Scheme 3

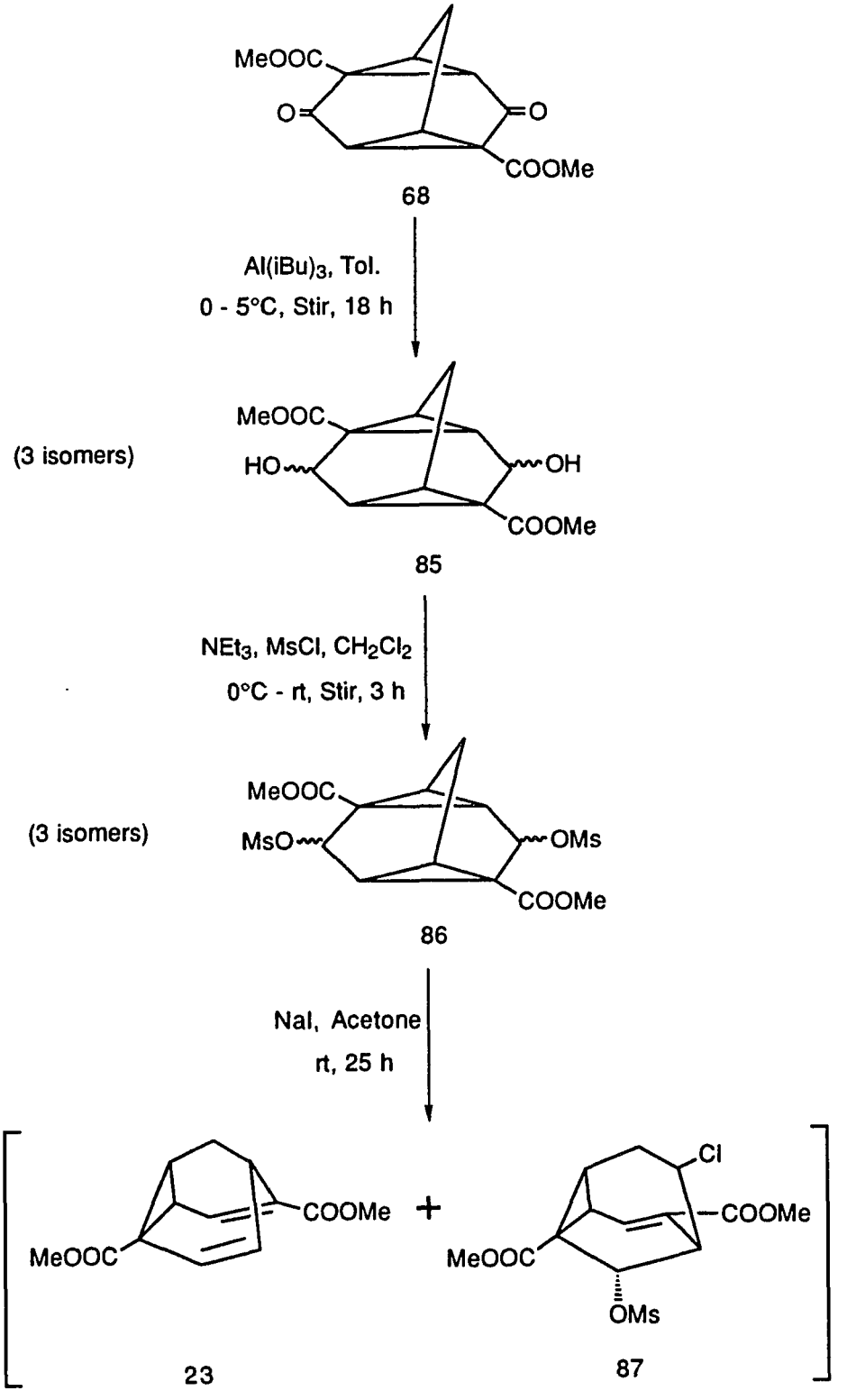

The starting material **68** used in Scheme 3 was prepared by the method shown in Figure 62 (p. 75) and was then treated with triisobutylaluminum in dry toluene to provide a mixture of three isomers, exo,exo-diol **85-a**, exo,endo-diol **85-b** and endo,endo-diol **85-c** in 81% (Figure 75).

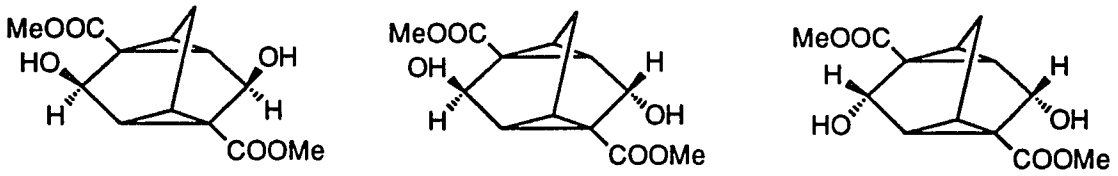

85-a 85-b 85-c

Figure 75: Formation of Three Diols

The endo,endo-diol **85-c** was isolated as white crystals upon recrystallization from dry ethyl acetate: mp 143-145°C. Compound **85-c** was characterized by its ^{1}H-NMR, and the structure of which was proven by X-ray crystallography (Figure 76).

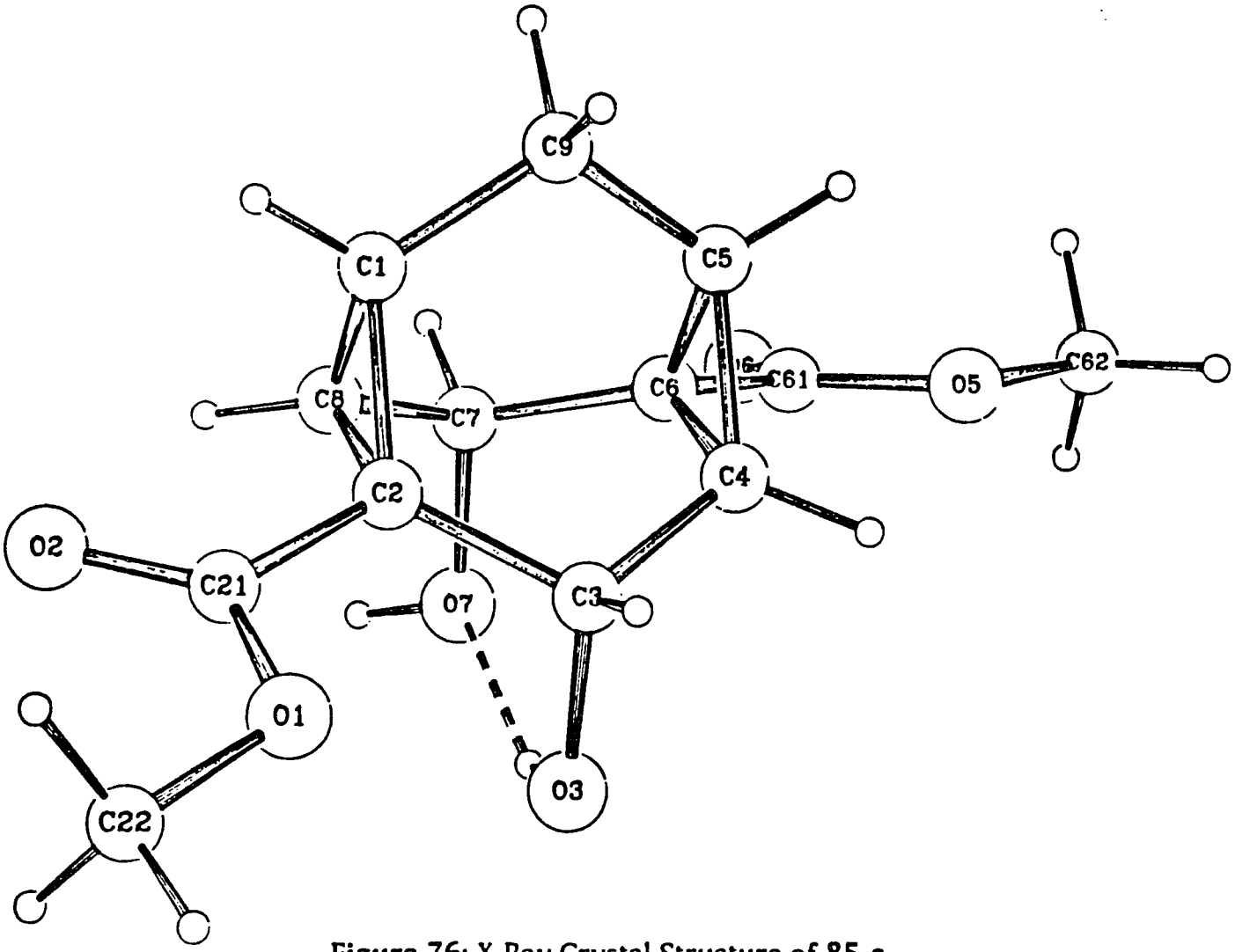

Figure 76: X-Ray Crystal Structure of 85-c

Once **85** was available, several attempts were made to mesylate it by using triethylamine and methanesulfonyl chloride (Figure 77).

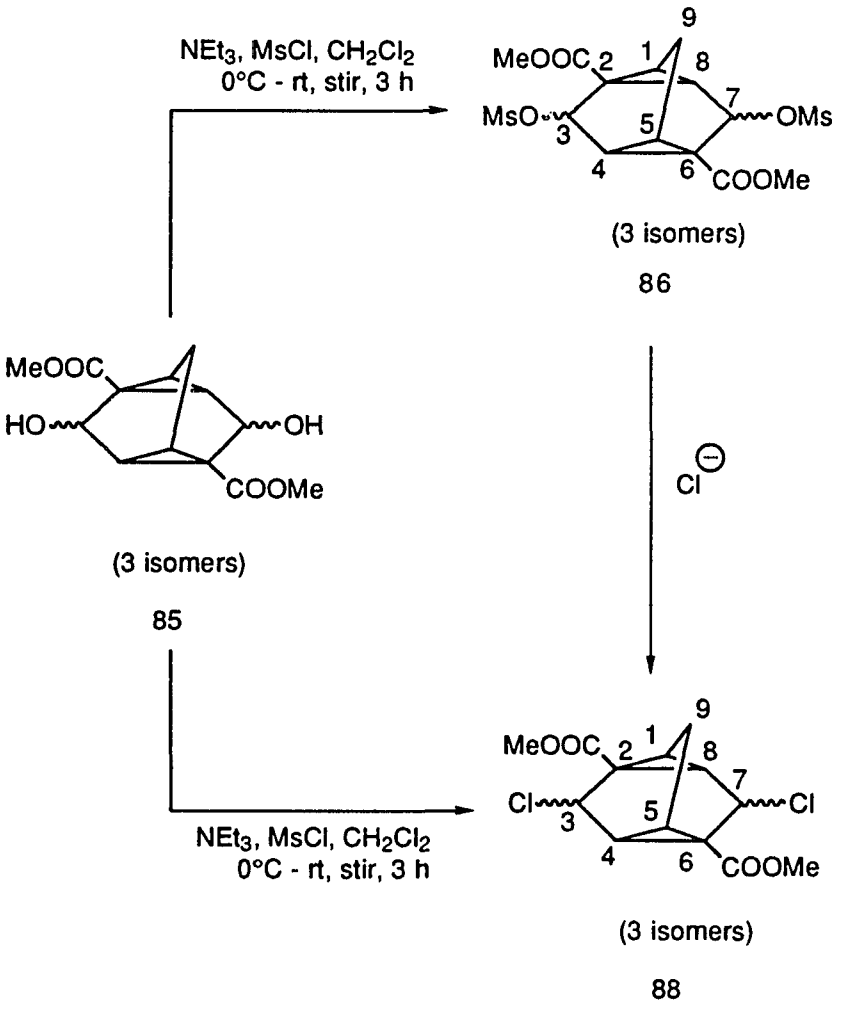

Figure 77: Formation of different products in mesylations

In one attempt, we obtained a red brown colored liquid product, a mixture of bismesylates **86**, in 77% yield. The presence of the CH_3SO_3-group was confirmed by its ^{1}H-NMR spectrum which showed peaks at 3.0-3.2 ppm. The peaks for protons at C_3 and C_7 have been assigned in the range between 4.3 and 6.2 ppm (Figure 78).

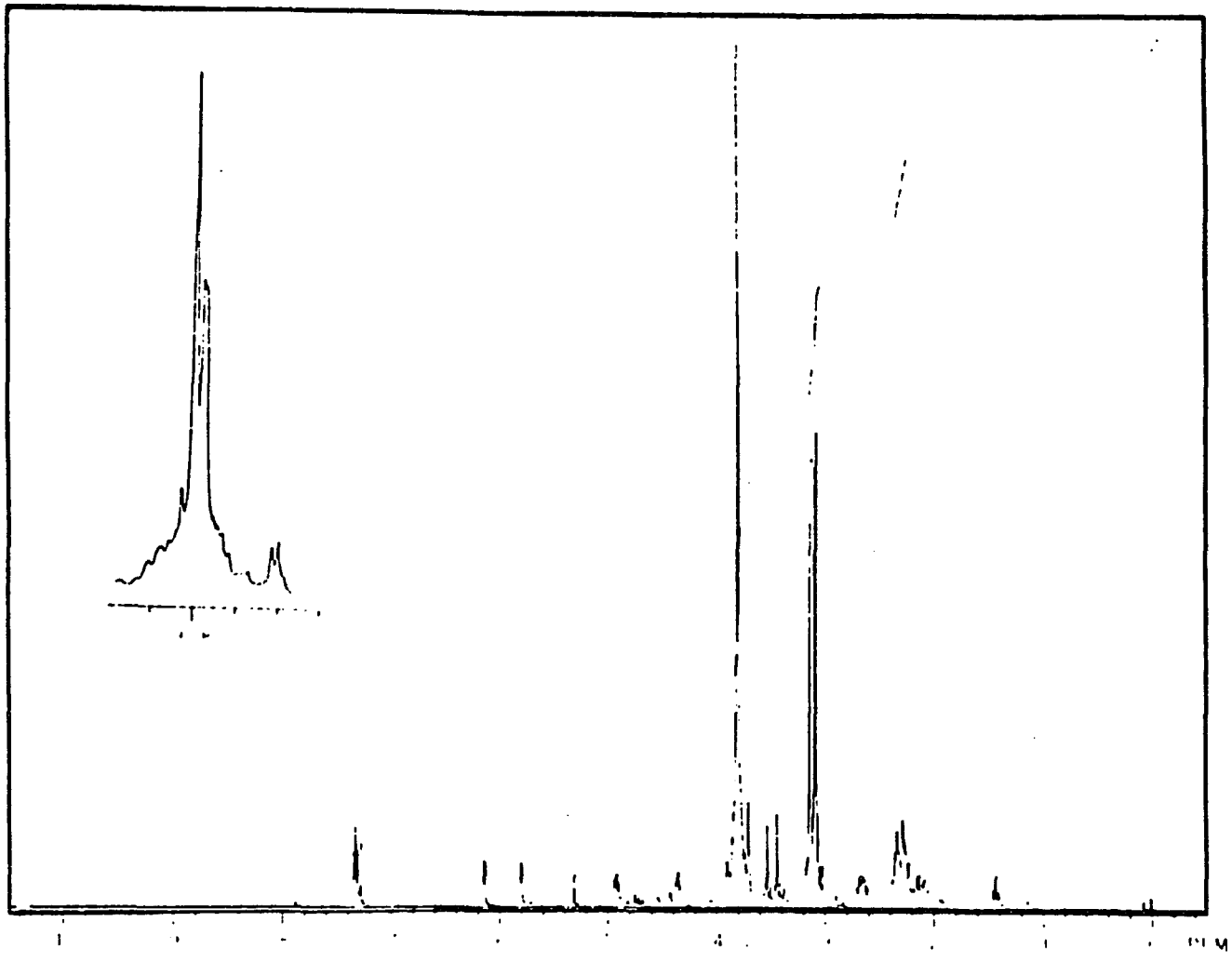

Figure 78: ^{1}H-NMR Spectrum of **86**

In contrast, although we used the same reactant ratio and similar reaction conditions in the later attempts at mesylation, we obtained a light yellow colored liquid product, a mixture of dichlorides **88**, in 86% yield.

The ^{1}H spectrum of **88** showed not only the absence of CH_3SO_3- groups but also the narrow range (5.2-5.4 ppm) of H_3 and H_7. So, we assumed that our compound could be a dichloride **88** instead of bismesylate **86** (Figure 79).

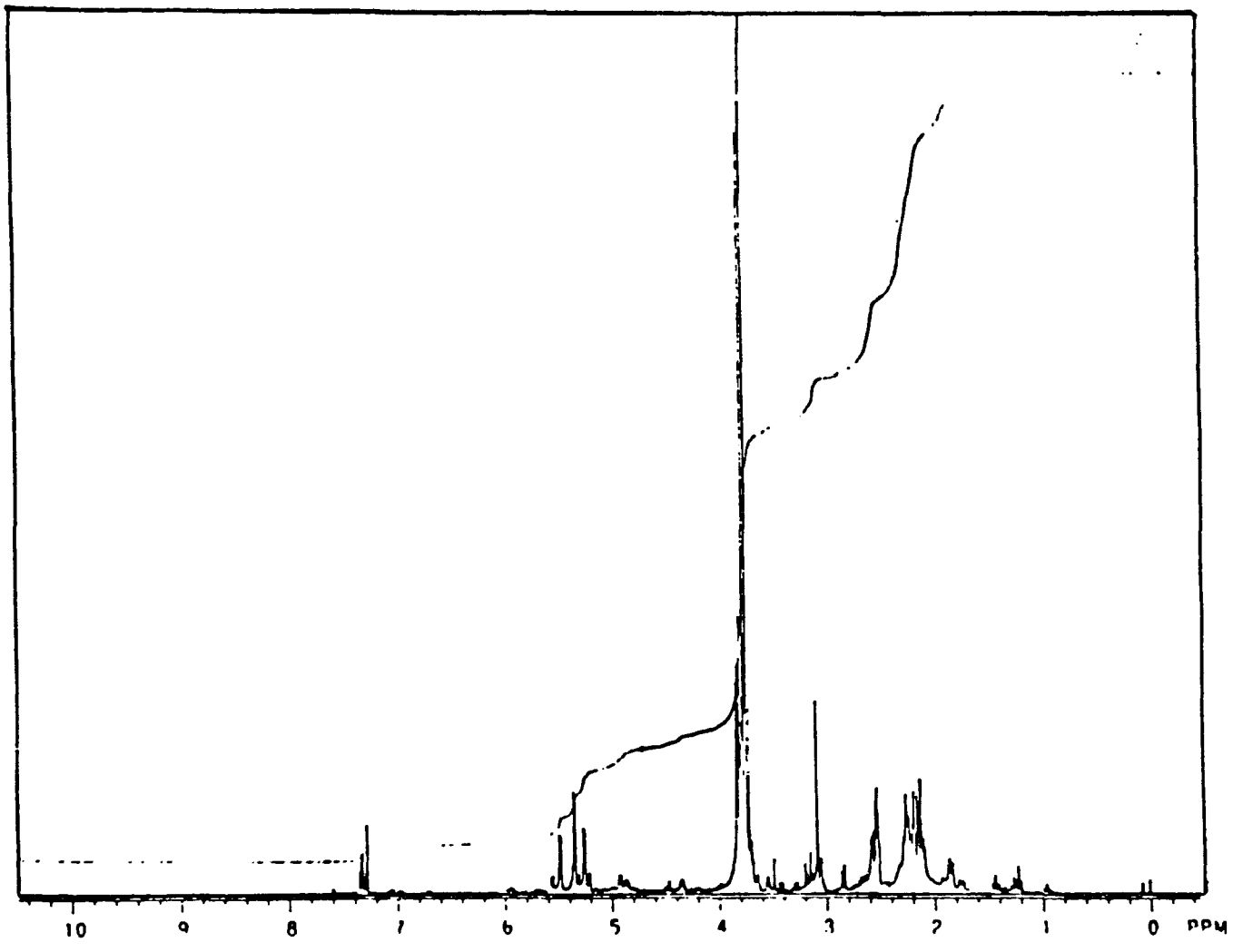

Figure 79: ^{1}H-NMR Spectrum of **88**

Both bismesylate **86** and dichloride **88** were individually utilized in the NaI in acetone induced Grob-fragmentation (Figure 80).

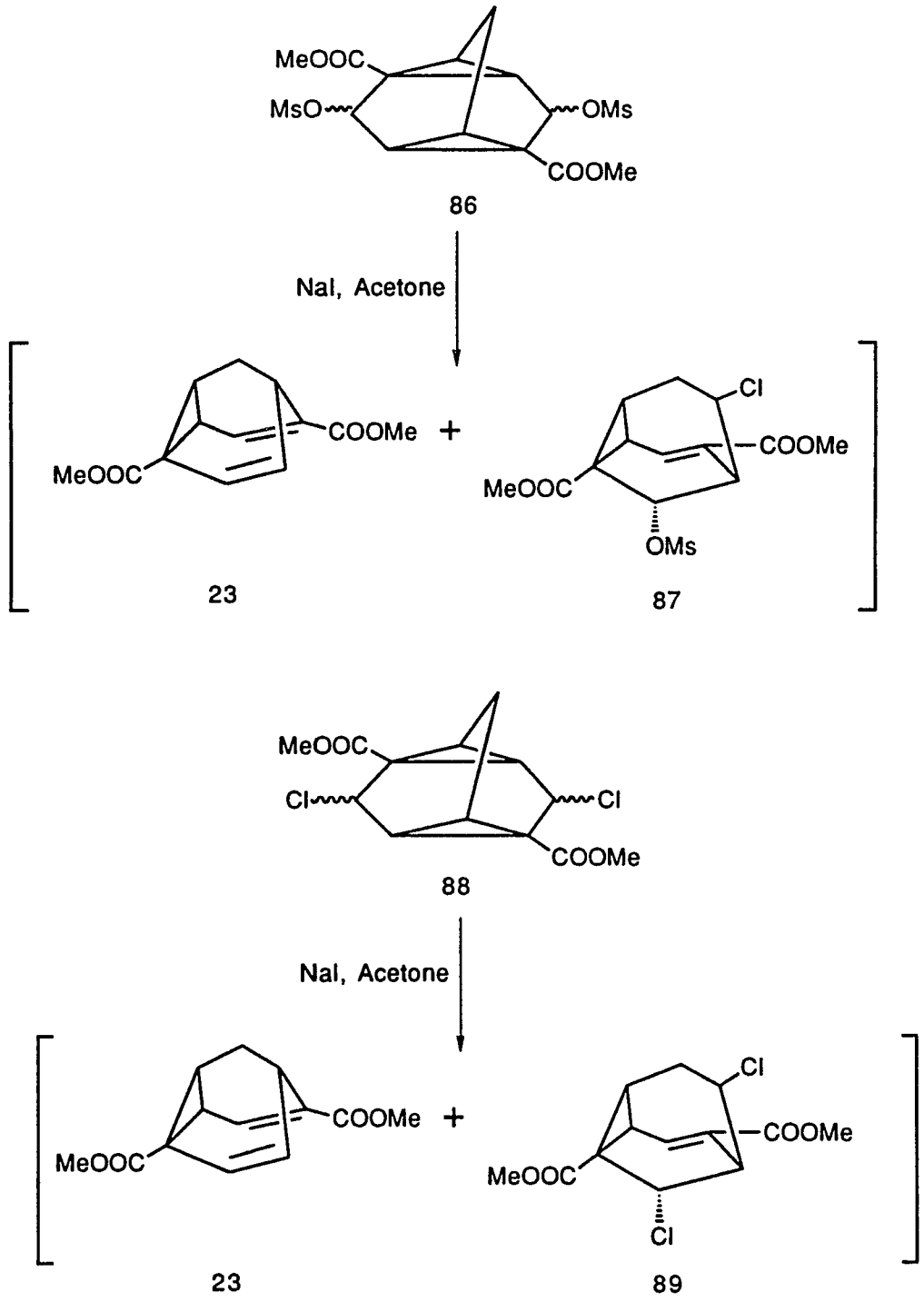

Figure 80: NaI in Acetone Induced Grob-Fragmentation

Stirring the bismesylate **86** in acetone with an excess of NaI produced a mixture of products. The TLC analysis showed two major spots (hexane/ethyl acetate, 2:1). After separating the components by column chromatography (hexane/ethyl acetate, 3:1), we obtained the 2,6-dicarbomethoxybarbaralane **23**, observed as a liquid product, in 28% yield, and an interesting side product **87**, seen as white crystals upon recrystallization from CH_3OH, in 31% yield.

When a similar reaction was performed with the mixture of dichlorides **88** under similar reaction conditions, two major products were seen on TLC again (hexane/ethyl acetate, 2:1). The components have been separated on a silica column using hexane/ethyl acetate, 2:1 as eluent. The 2,6-dicarbomethoxybarbaralane **23** eluted first and was obtained as an air sensitive cloudy liquid in 32% yield: mp ~20°C. The undesired product **89** was eluted next and crystallized as white solid in 8% yield.

The structure of **23** was verified by its ^{1}H and ^{13}C-NMR spectra. Based on the NMR data, **23** undergoes the rapid degenerate Cope rearrangement at room temperature by the following:

(a) a multiplet integrating for two protons (H_1 and H_5) at δ 3.22 ppm,

(b) the presence of an averaged quarternary carbons (C_2/C_6) signal at δ 83 ppm and an averaged methine carbons (C_4/C_8) signal at δ 80 ppm.

Room temperature ^{1}H and ^{13}C-NMR studies, variable temperatures solution ^{13}C-NMR analyses and the predicted energy barrier of **23** will be discussed in Chapter 4.

The properties of 2,6-dicarbomethoxybarbaralane **23** showed some striking differences in comparison to 2,4,6,8-tetracarbomethoxy-barbaralane **18**. While compound **18** is air-stable, compound **23** is air-sensitive. The light yellow clear liquid **23** turned to a cloudy liquid while standing in the air. The precipitate from the cloudy liquid, which is tentatively assigned as an oxygenated polymeric molecule **90**, is insoluble in almost all solvents (Figure 81). But, its ^{1}H spectrum in $CDCl_3$ shows the symmetry of the compound (Figure 82).

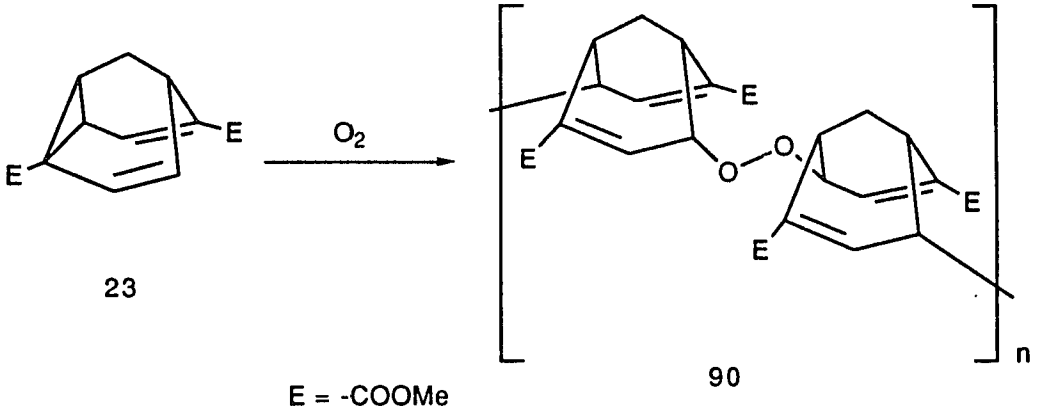

Figure 81: Oxygenated Polymeric Molecule **90**

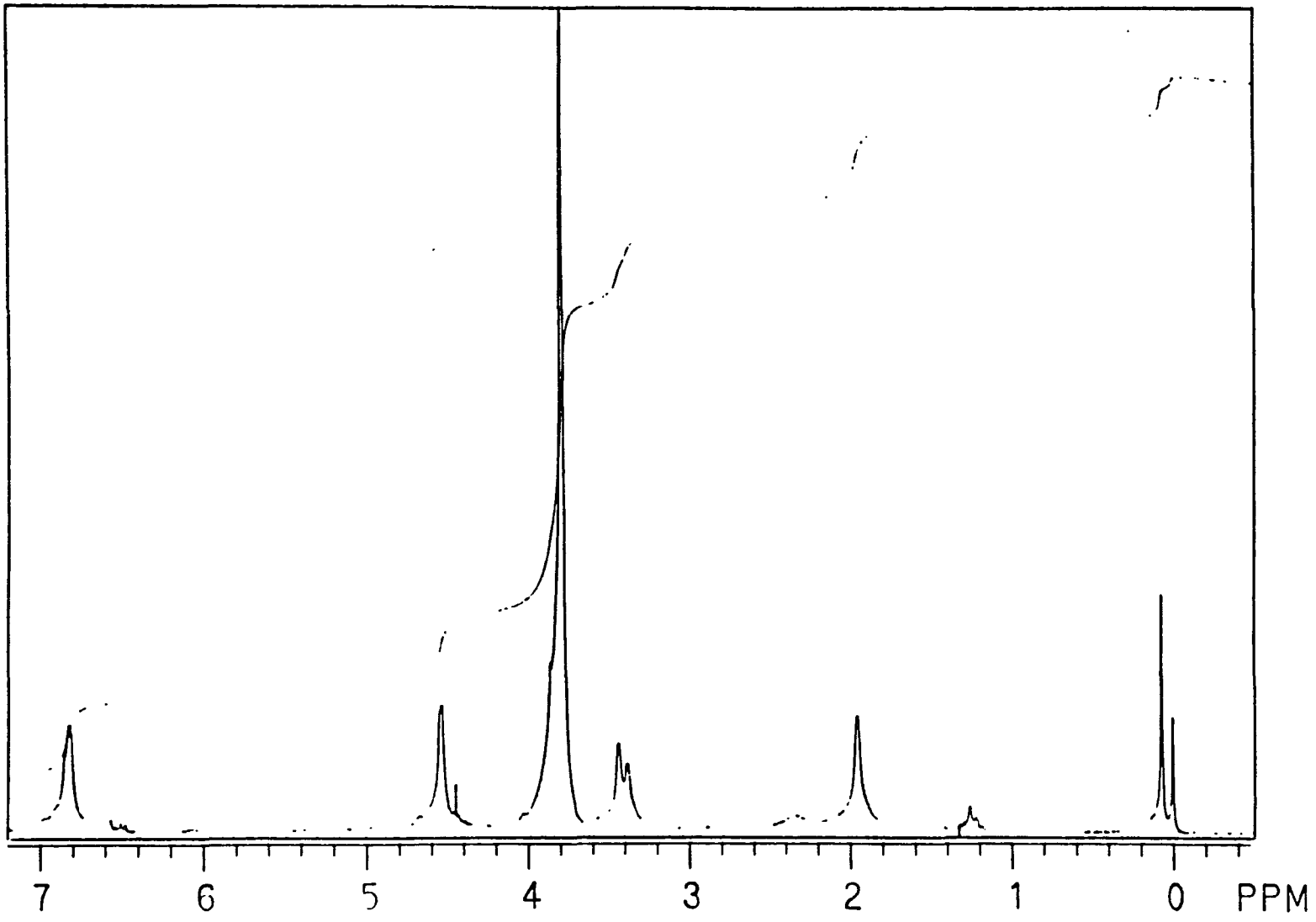

Figure 82: ^{1}H-NMR Spectrum of 90

2.4.3. Bromination of 23

The side products, **87** and **89**, obtained in the NaI in acetone induced Grob-fragmentation (Figure 80) have similar pattern of chemical shifts in their ^{1}H-NMR spectra. The structure verification of **87** and **89** was assisted by the bromination of 2,6-dicarbomethoxy-barbaralane **23** (Figure 83).

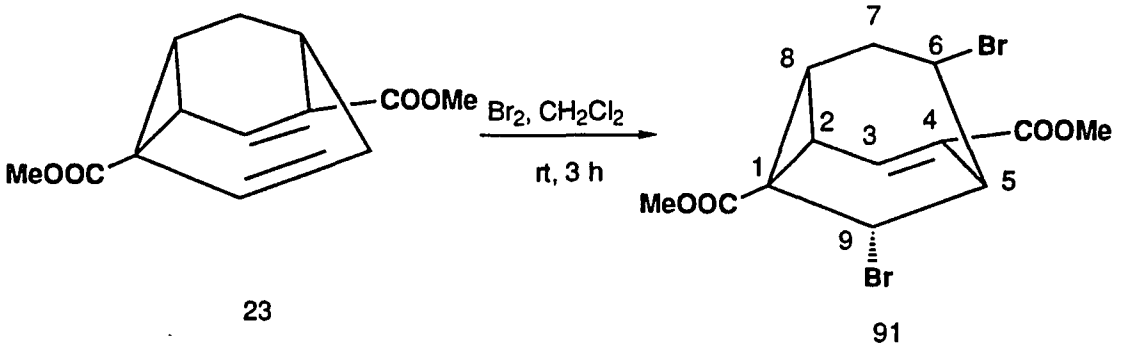

23 91

Figure 83: Bromination of **23**

When compound **23** was treated with bromine in methylene chloride solution at room temperature, there was obtained in 72% yield a crystalline 6,9-dibromo-1,4-dicarbomethoxy-tricyclo[3.3.1.$0^{2,8}$]nona-3-ene **91**, mp 117-120°C. The ^{1}H-NMR pattern of **91** was again similar to that of **87** and **89**. Since the 1D-^{1}H NMR spectrum (Figure 84) afforded little definitive stereochemical evidence, an X-ray crystal structure analysis was obtained (Figure 85).

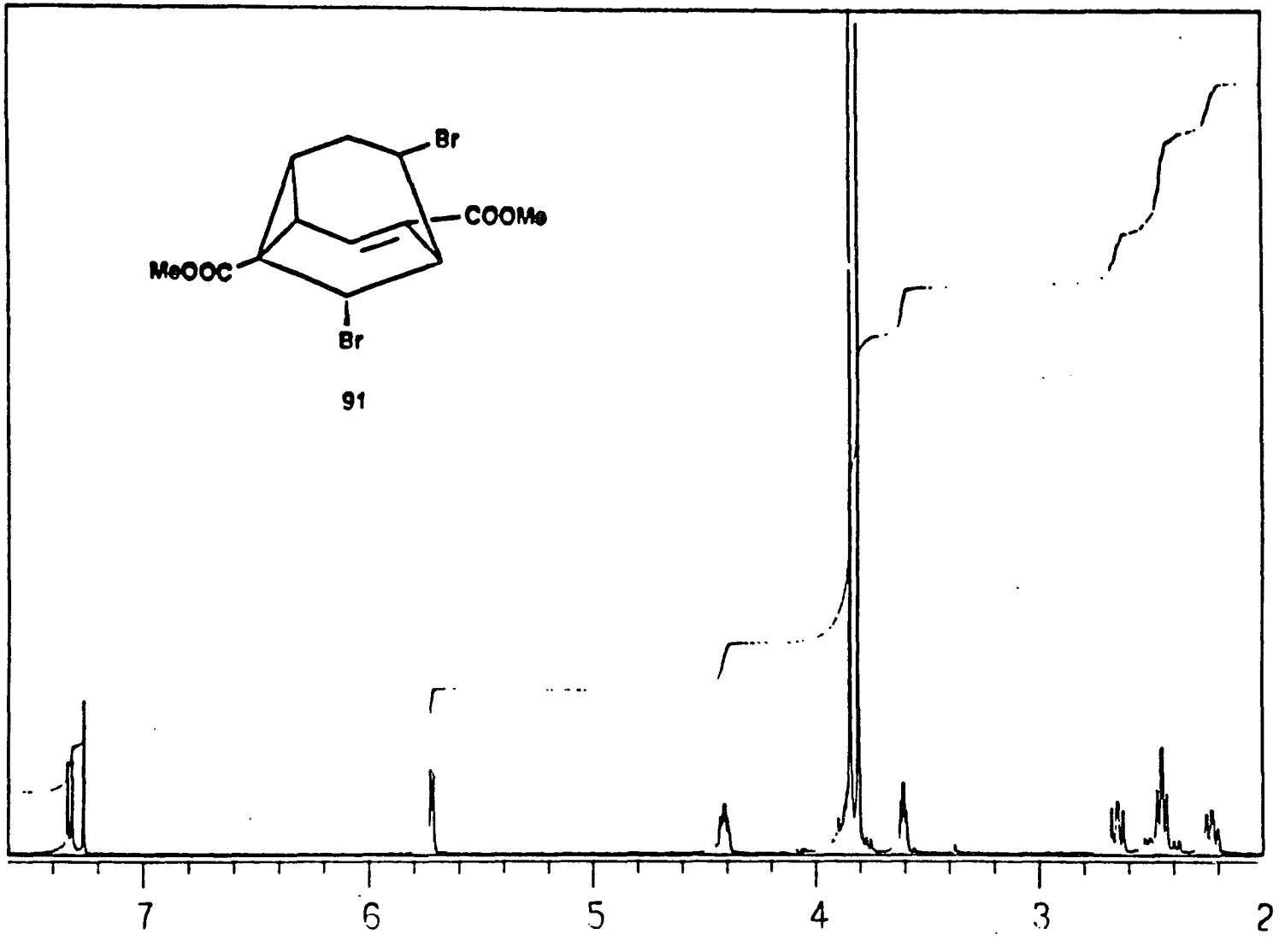

Figure 84: ^{1}H-NMR Spectrum of **91**

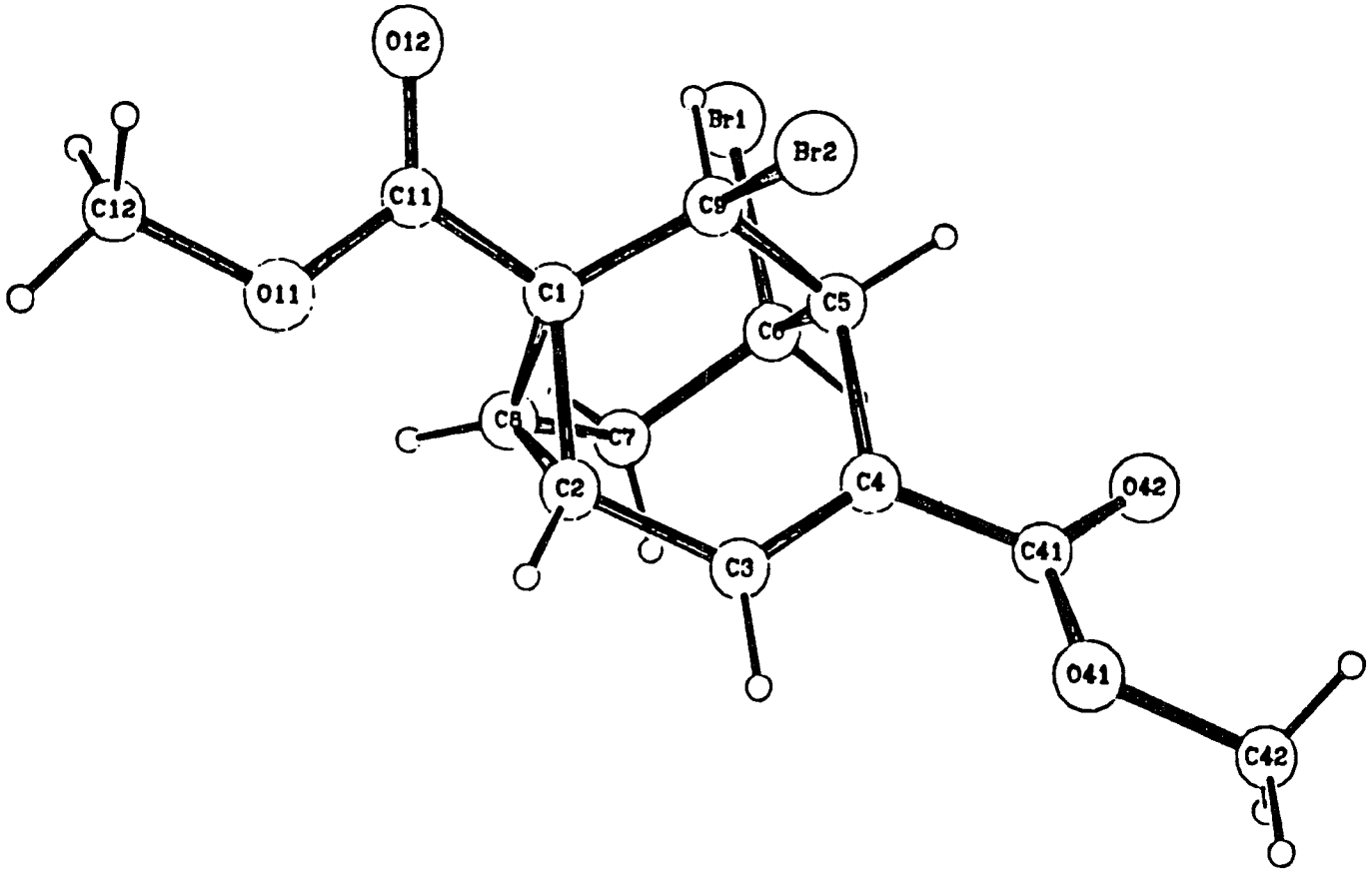

Figure 85: X-Ray Crystal Structure of **91**

From the X-ray structure of **91**, we assumed that initial cyclopropane formation together with endo attack by bromine on C_3 and subsequent cyclopropane ring opening by the attack of bromide ion on the C_5 must have occurred (Figure 86).

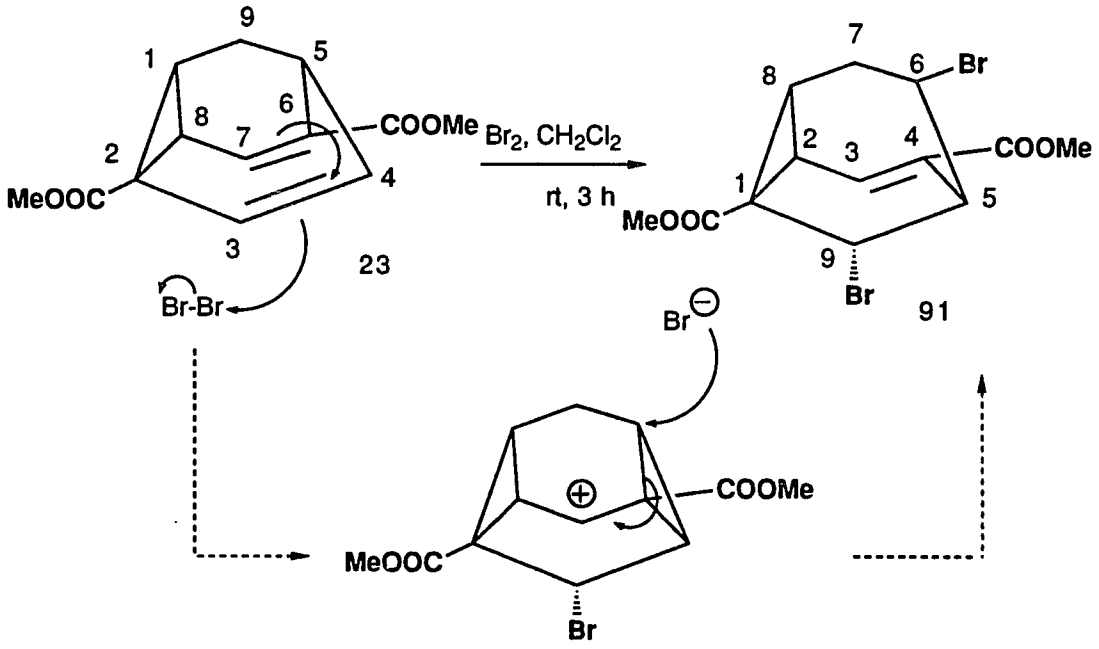

Figure 86: The proposed mechanism in the bromination of **23**

The dibromide **91** was also characterized by its 2-D ^{1}H-NMR spectrum (Figure 87). Once we assigned the C_3-vinylic proton at δ 7.37 ppm, the subsequent proton peaks for H_2 (2.7 ppm), H_8 (2.26 ppm), H_7 (2.5 ppm), H_6 (4.45 ppm), H_5 (3.63 ppm) and H_9 (5.76 ppm) were correlated easily.

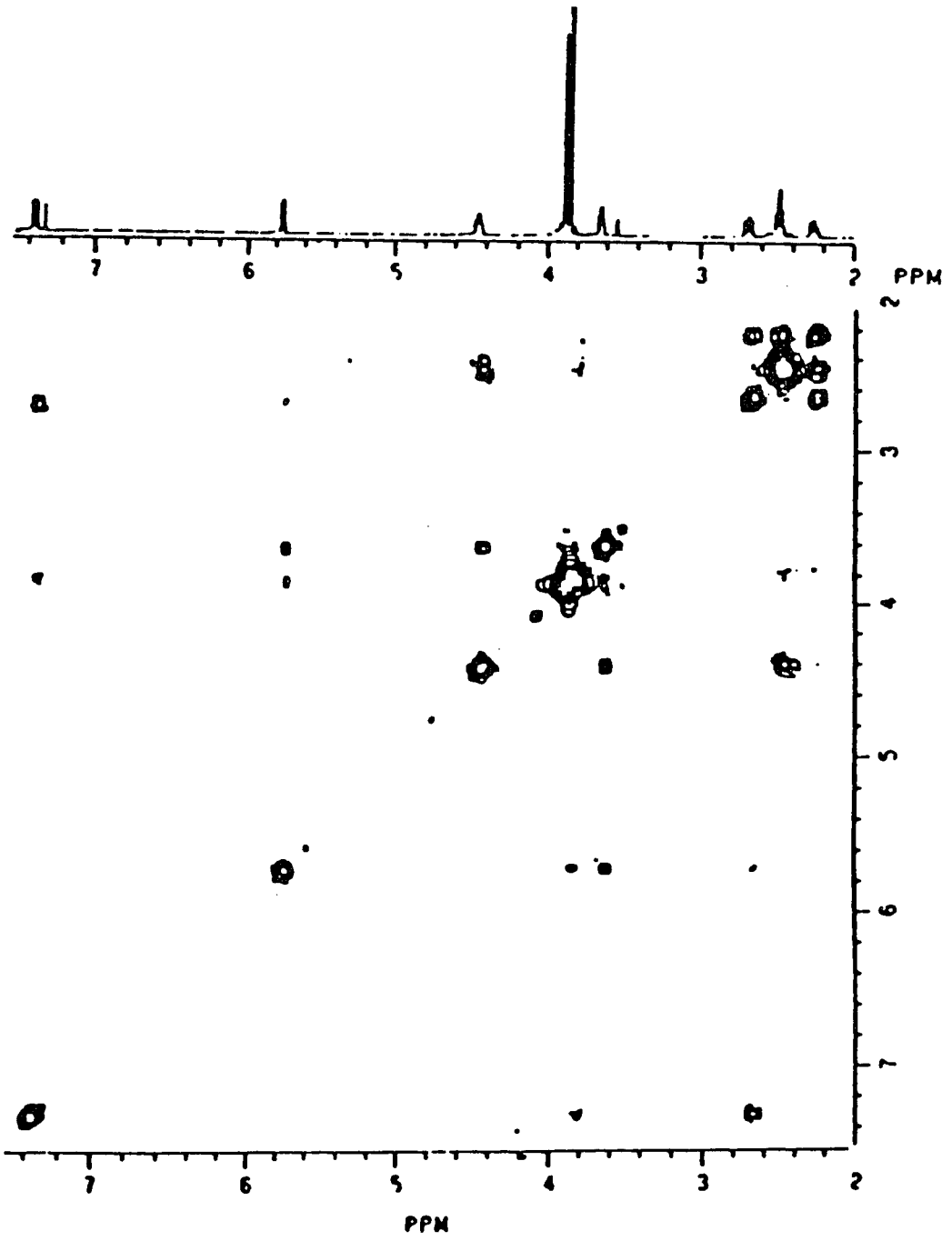

Figure 87: 2D-^{1}H NMR Spectrum of 91

After verifying **91**, the structures of **87** and **89** could be assigned promptly due to the similarity of the chemical shift patterns (Figure 88).

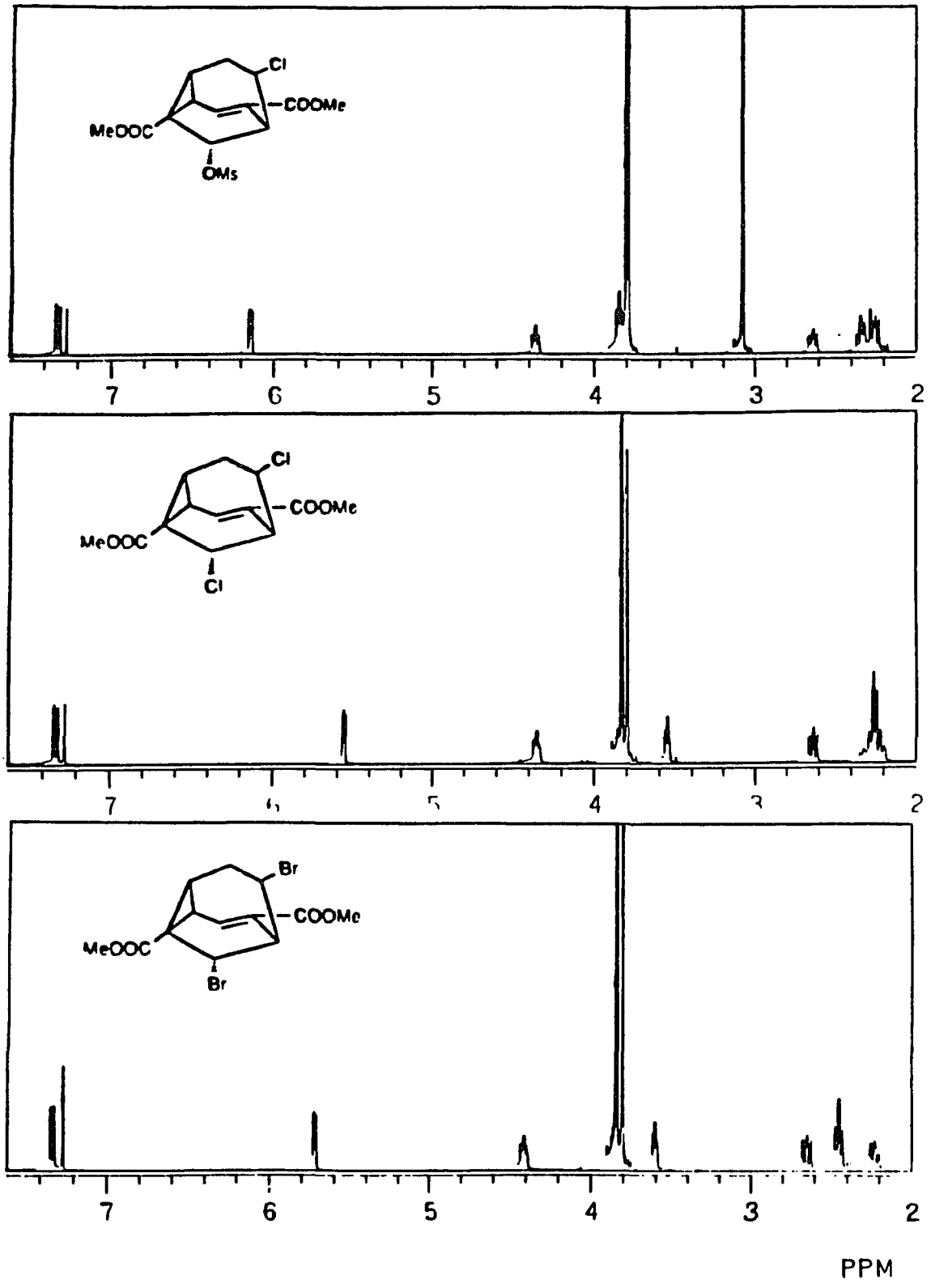

Figure 88: ^{1}H-NMR Spectra of 87, 89 and 91

In contrast to our result, bromination of semibullvalene **92** and 1,5-dimethylsemibullvalene **93** proceeded with stereoselective cis,exo-1,4-addition.[71,72](Figure 89)

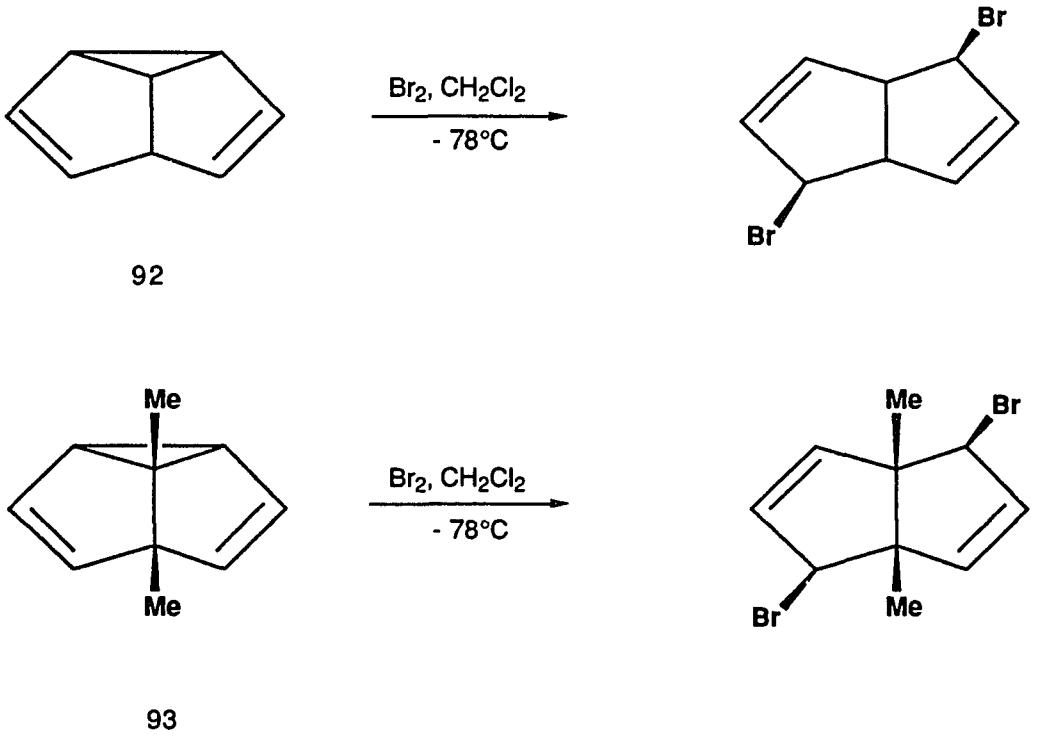

Figure 89: Stereoselective Bromination of Semibullvalene **92** and 1,5-Dimethylsemibullvalene **93**

2.5.1. Synthesis of 2,6-Dicyanobarbaralane (5-a)

Scheme 4

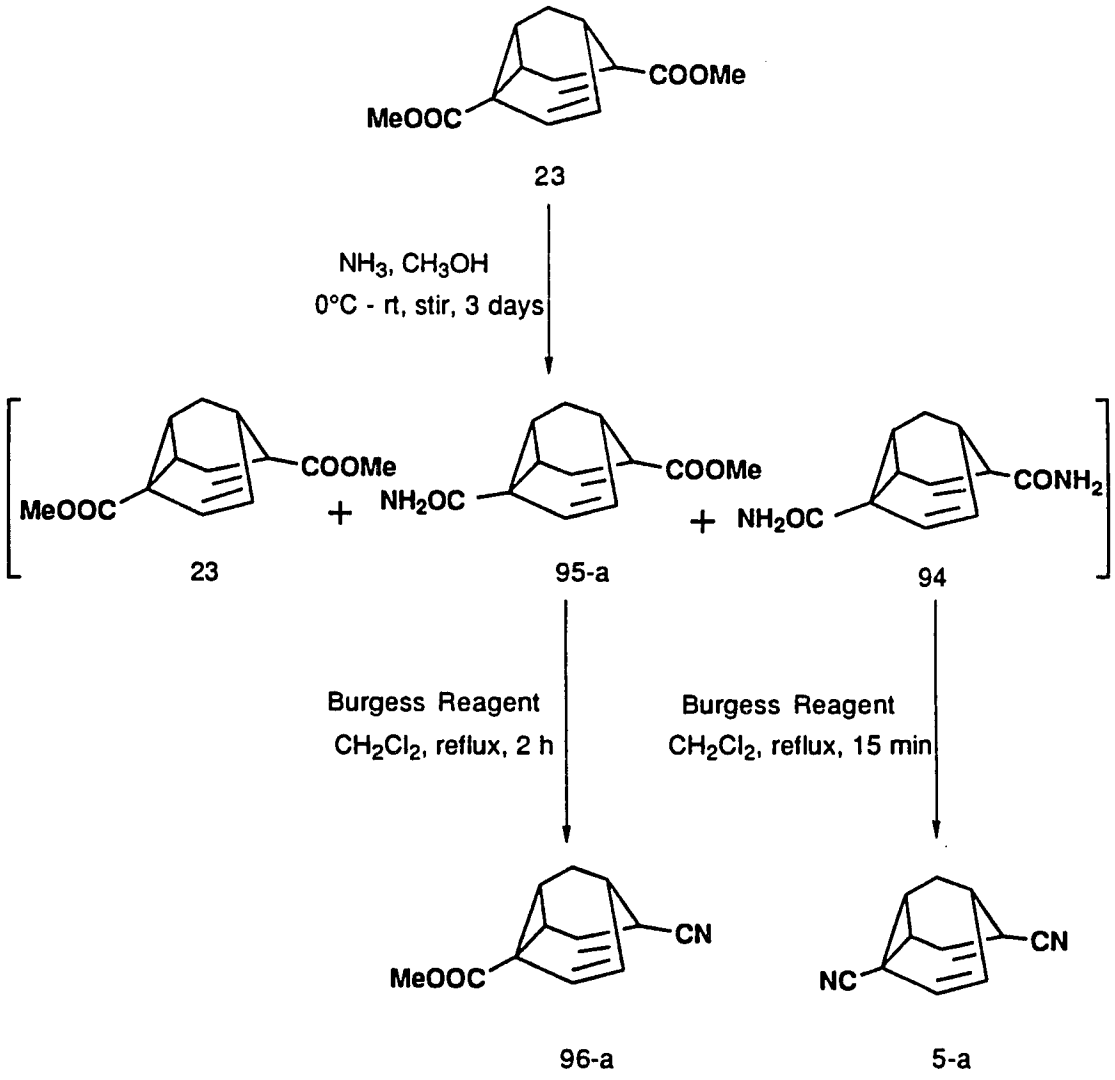

The synthesis of **5-a** starting from bicyclo[3.3.1]nonane-2,6-dione has been reported by Quast et al.[24,37] We have developed a different synthetic route toward **5-a** starting with 2,6-dicarbomethoxybarbaralane **23** via dicarboxamidobarbaralane **94**. The successful synthesis of 2,6-dicyanobarbaralane **5-a** lends support to our proposed transformation of 2,4,6,8-tetracarbomethoxybarbaralane **18** into 2,4,6,8-tetracyano-barbaralane **19**.

2,6-Dicarbomethoxybarbaralane **23** of this Scheme 4 was allowed to react with excess ammonia and a catalytic amount of 80% NaH in methanol for 3 days. Three spots were seen on TLC analysis (hexane/ethyl acetate, 1:3). The components were separated on a silica column using hexane/ethyl acetate, 1:3 as eluent. The unreacted 2,6-dicarbomethoxybarbaralane **23** was eluted first in 12% yield. Secondly, 2-carboxamido-6-carbomethoxybarbaralane **95-a** was eluted and crystallized as white solid in 51% yield: mp 165-166°C. The last spot with the lowest R_f value did not easily elute although we switched to 100% ethyl acetate. Eventually, when we used ethyl acetate/ethanol, 1:1 as eluent, the last spot, 2,6-dicarboxamido-barbaralane **94** was eluted in 34% yield as white crystals: mp >280°C.

The structure of compound **94** was confirmed by its room temperature ^{1}H-NMR spectrum in DMSO-d_6 which indicated the presence of a fast and reversible valence-bond isomerization (Figure 90).

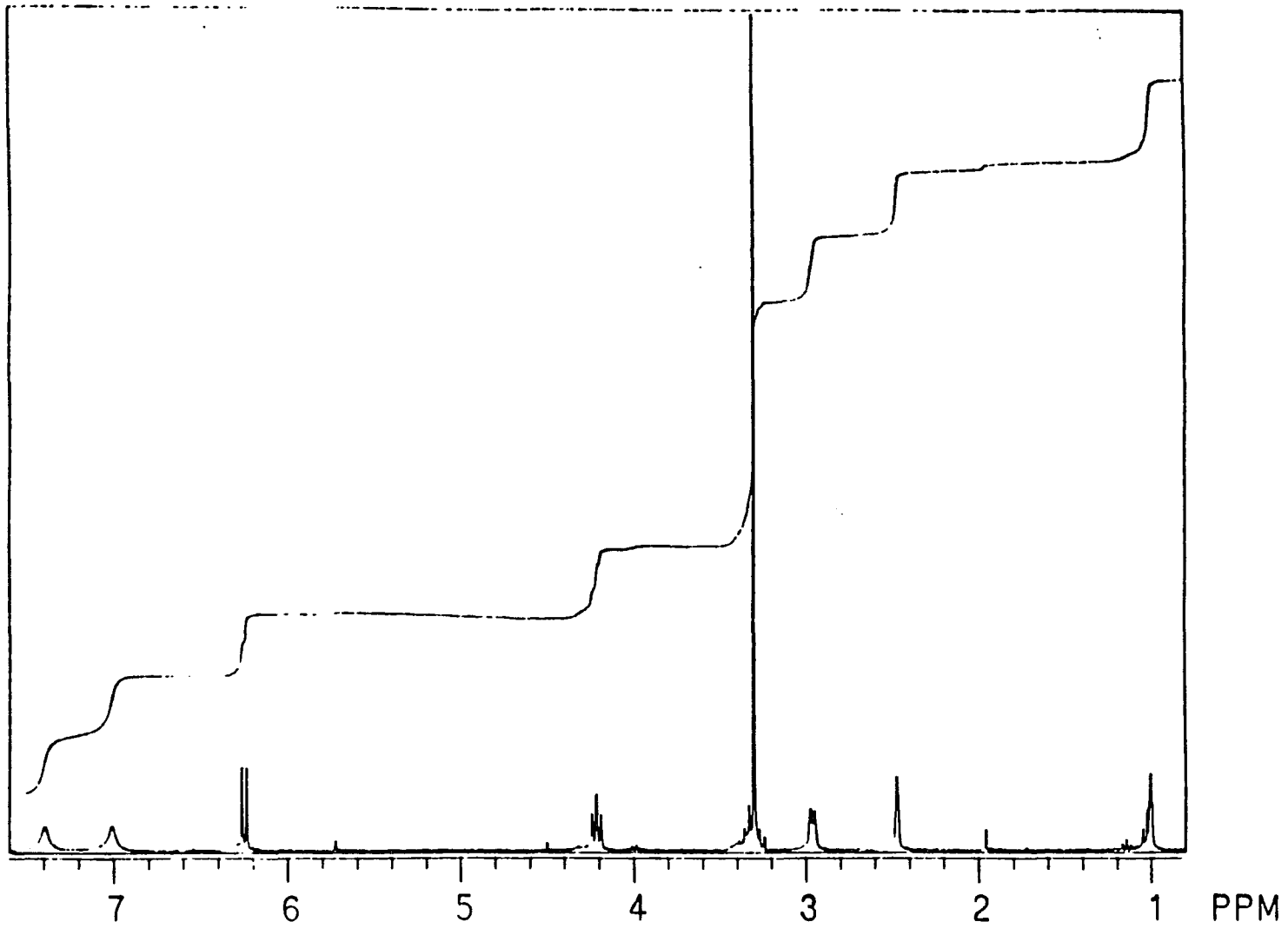

Figure 90: ^{1}H-NMR Spectrum of **94**

The ^1H chemical shifts of carboxamido-ester **95-a** (Figure 91) approximates the combination of the ^1H spectra of 2,6-dicarbomethoxy-barbaralane **23** (Figure 125) and 2,6-dicarboxamidobarbaralane **94** (Figure 90). The presence of the carbomethoxy and carboxamide groups of compound **95-a** were detected by the proton signals which appear at δ 3.66 ppm (for carbomethoxy group), and at 7.06 and 7.44 ppm (for the NH protons of the amide group which appear separately due to the partial π character of the N-CO bond). Both signals are exchangeable with D_2O. Although the dicarboxamido-ester **95-a** carries two different substituents, its proton NMR spectrum strongly supports its dynamic character. From this obvious evidence, we assumed that these two substituents, amide and carbomethoxy, have very similar cyclopropane C_2-C_8 σ bond weakening effect.

Relating to the substituents, a question is asked about where these two substituents are located on the barbaralane framework. To establish this point, we need to remember that substituents on a cyclopropane ring influence the stability of the ring bonds.[15] Normally, an electron withdrawing substituent on a cyclopropane ring will weaken the adjacent ring bonds and strengthen the opposite bond. Accordingly, the ring bond will be more severely weakened, when a stronger electron withdrawing group is attached. Thus, in **95-a** the substituent with less electron withdrawing ability should be on the cyclopropane side in terms of stability. The electron withdrawing ability of carboxamide substituent is slightly lower than that of carboxymethyl substituent (decrease of the Hammett-σ constants;[73] σ_p-$CONH_2$ = 0.627, σ_p-$COOCH_3$ = 0.636).

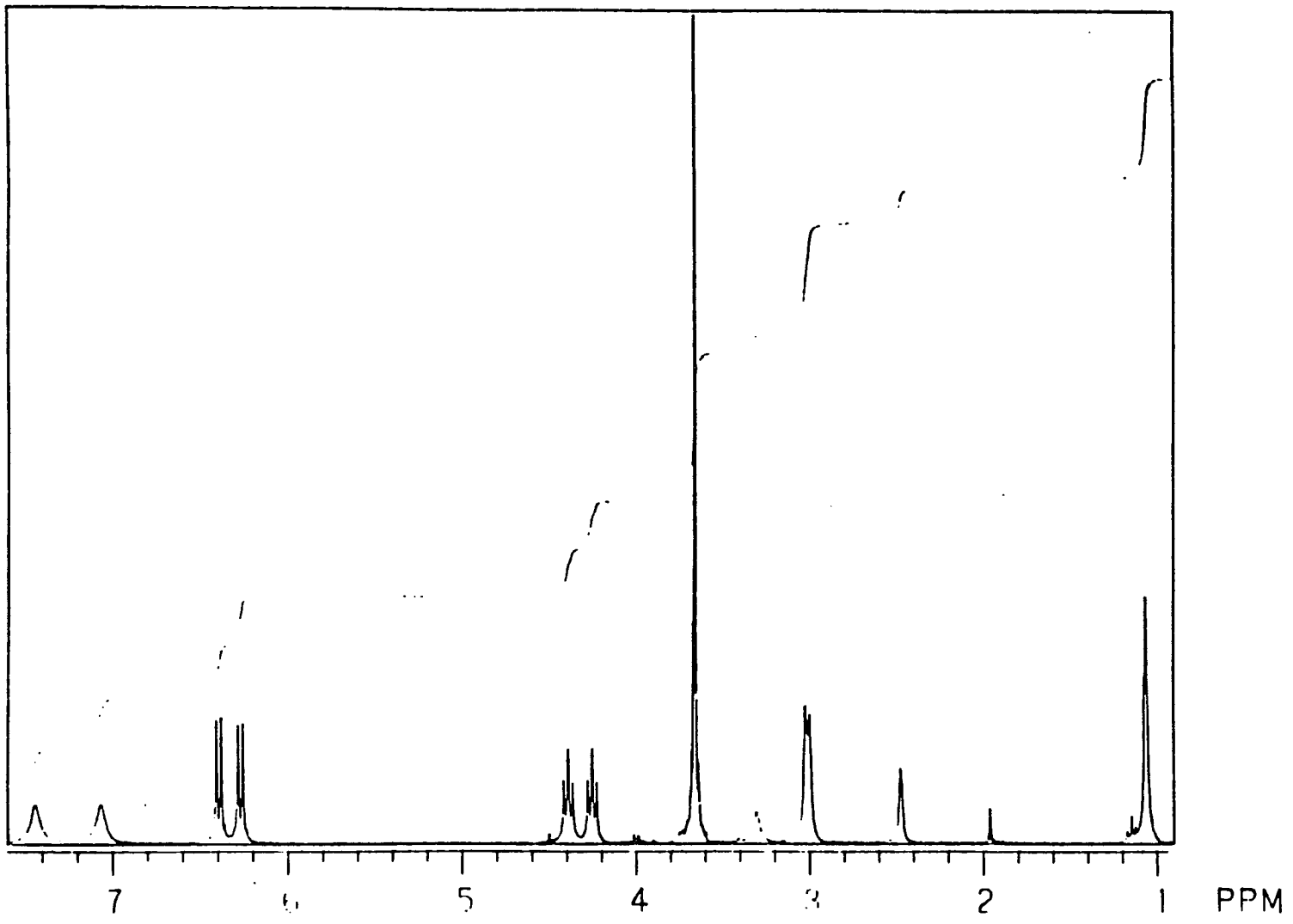

Figure 91: ^{1}H-NMR Spectrum of **95-a**

Eventually, we predicted that the carboxamide substituent would be on the cyclopropane ring and the carboxymethyl group would be on the olefinic carbon of the barbaralane skeleton. However, due to the ^{1}H spectrum (Figure 91), the Cope equilibrium of 2-carboxamido-6-carbomethoxybarbaralane is better drawn as shown in Figure 92.

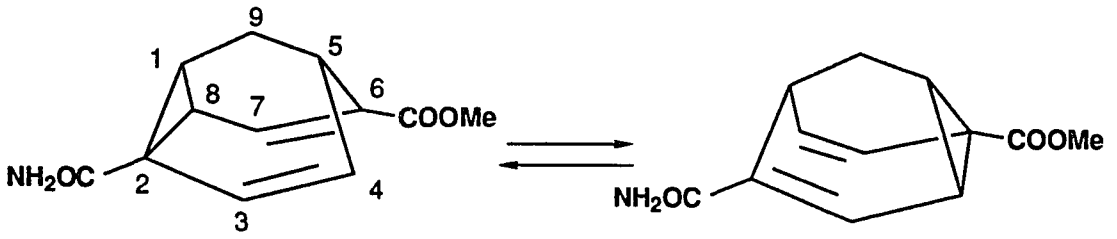

95-a 95-b

Figure 92: The Cope Equilibrium of **95**

The rapid degenerate Cope rearrangement of 2-carboxamido-6-carbomethoxybarbaralane **95** was confirmed by its room temperature ^{13}C spectrum which showed the C_2, C_4, C_6 and C_8 signals in the region between δ 75 and 90 ppm, the averaged region of cyclopropane carbons and olefinic carbons (Figure 93). Its variable temperature solution ^{13}C-NMR analysis will be discussed in Chapter 4.

X-ray structure determination has been performed on **95-a** and provides unequivocal proof of structure in the solid state (Figure 94).

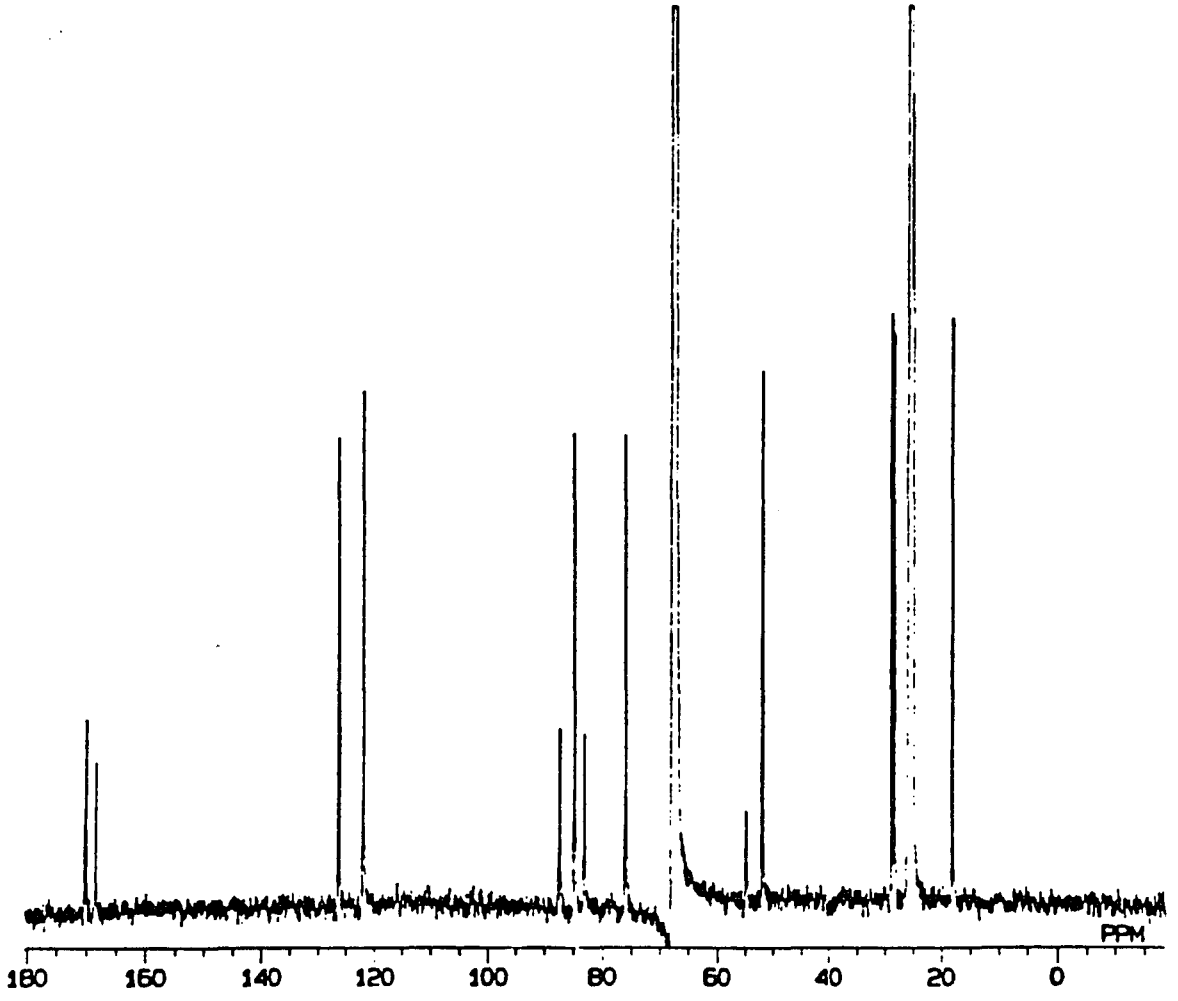

Figure 93: ^{13}C-NMR Spectrum of 95

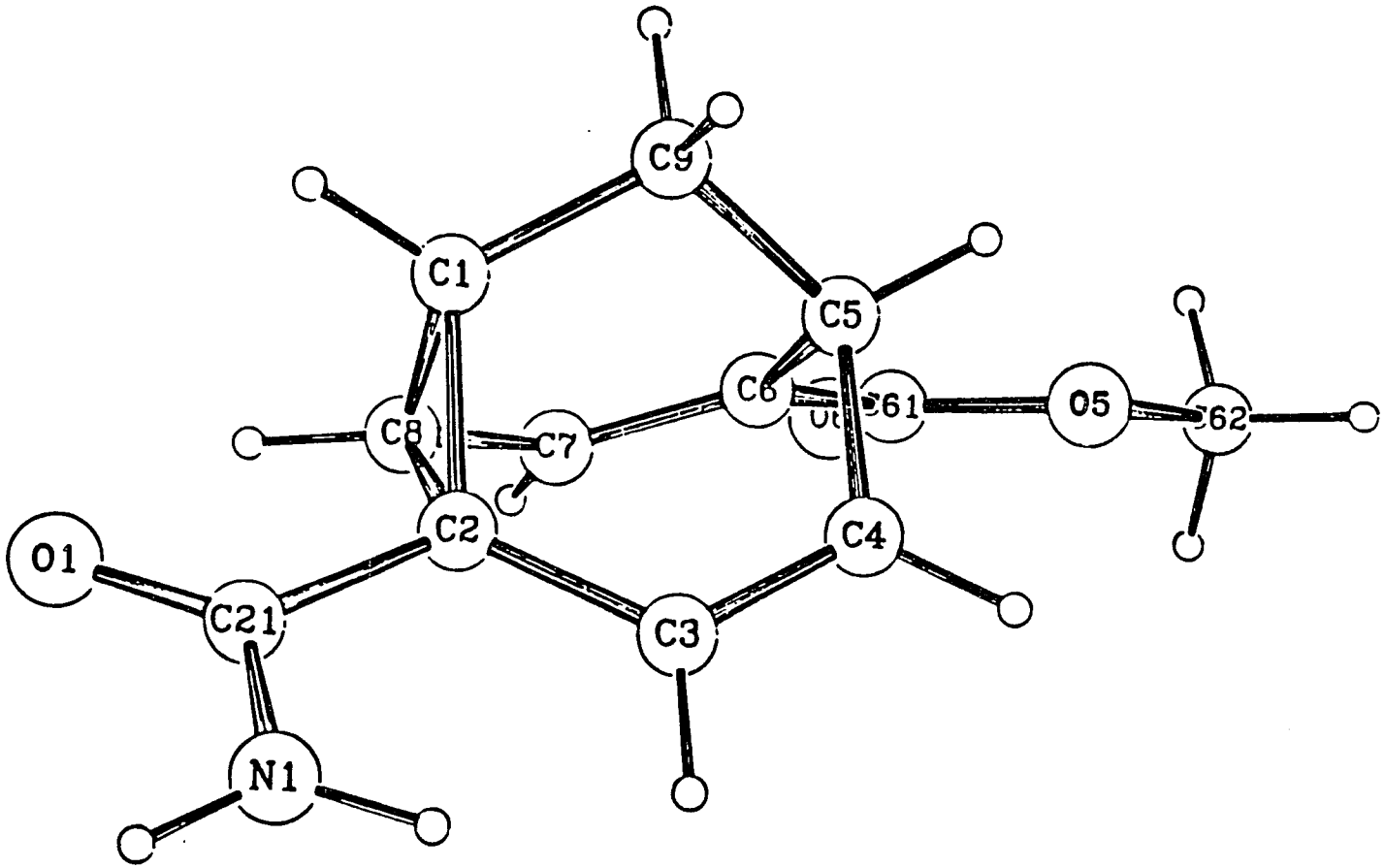

Figure 94: X-ray Crystal Structure of 95-a

Dehydration of a $-CONH_2$ substituted barbaralane to the $-C{\equiv}N$ analogue could be done by using many dehydrating agents, including $POCl_3$,[61] methyl (carboxysulfamoyl)triethylammonium hydroxide inner salt (Burgess reagent),[74] CCl_4-Ph_3P,[75] $TiCl_4$-base,[76] HMPT[77] and trimethylsilyl polyphosphate.[78] Among these reagents, $POCl_3$ was first used in the attempt to dehydrate dicarboxamide **94**. After refluxing **94** with a large excess of $POCl_3$ in dichloroethane for 8 h, one obtains dicarbonitrile **5-a** in 37% yield as a white solid, mp 100-102°C, after column chromatography (silica, hexane/ethyl acetate, 4:1). The low yield of **5-a** forced us to select a different dehydrating reagent.

An extremely efficient method for the preparation of nitriles from primary amides **94** and **95-a** utilizes methyl (carboxysulfamoyl)-triethylammonium hydroxide inner salt (Burgess reagent) as a very mild dehydrating reagent.[74]

The Burgess reagent **99**, which was originally discovered by Burgess to dehydrate alcohols, can be prepared by using the equivalent amount of chlorosulfonyl isocyanate **97** and anhydrous methanol in anhydrous benzene as solvent to afford 99% of methyl (chlorosulfonyl)carbamate **98**, followed by stirring with excess anhydrous triethylamine. Burgess reagent **99** was obtained as light tan colored, moisture sensitive crystals in 72% yield (Figure 95).

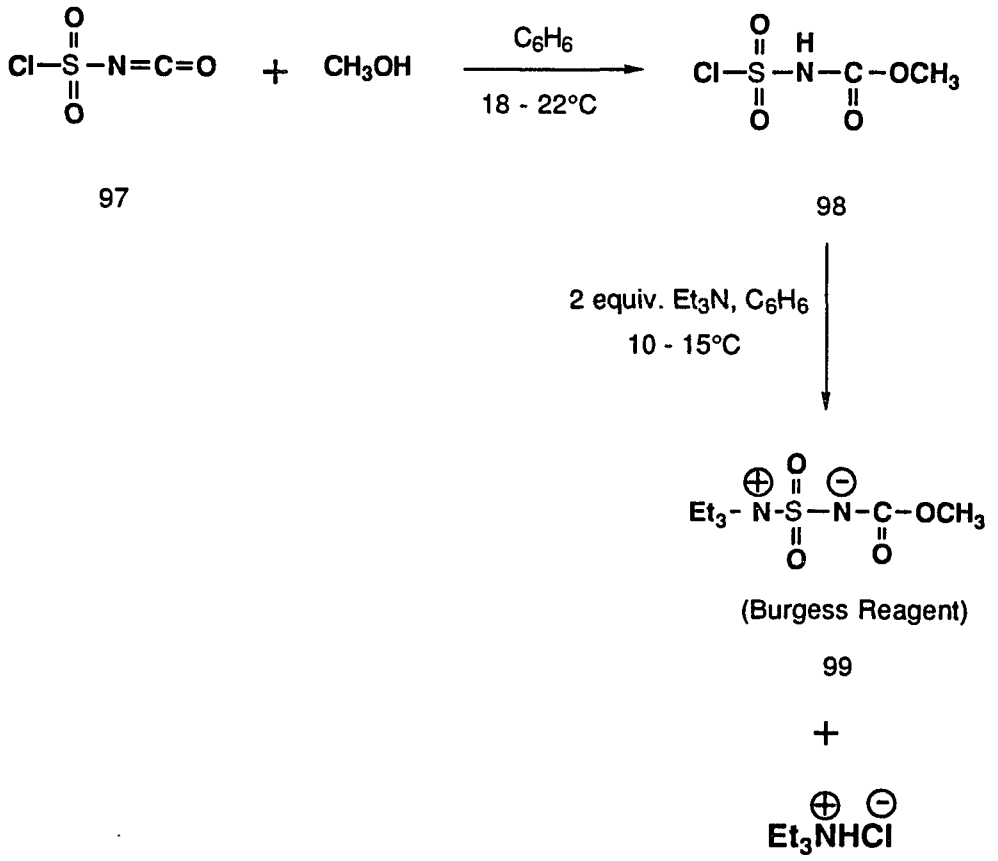

Figure 95: Preparation of Burgess Reagent **99**

After refluxing dicarboxamide **94** with ten equivalents of Burgess reagent **99** in dry dichloromethane under standard anhydrous conditions for 15 min (Scheme 4, p. 111), TLC analysis showed none of the starting material **94**. The crude compound was directly applied to a silica gel column. Flash chromatography (hexane/ethyl acetate, 1:1) gave dicarbonitrile **5-a** in 81% yield as a white crystalline solid: mp 100-102°C.

The dicarbonitrile **5-a** exhibits an averaged NMR spectrum at ambient temperature (p. 218) and its ^{1}H-NMR data are in agreement with those reported by Quast et al.[24]

The IR spectra of **5-a** display two nitrile bands in both solution and solid state at room temperature. We know from this then that the degenerate Cope rearrangement of **5-a** is slow at room temperature on the IR time scale, as stated by Quast et al.[24]

As in **94**, carboxamido-ester **95-a** reacted with five equivalents of Burgess reagent **99** in dry dichloromethane (Scheme 4). Reaction was complete within 2 hours as detected by TLC analysis. The crude compound was purified by column chromatography (silica, hexane/ethyl acetate, 1:3) affording 2-carbomethoxy-barbaralane-6-carbonitrile **96-a**, not 6-carbomethoxy-barbaralane-2-carbonitrile **96-b**, in 91% yield, white crystal, mp 107-108°C.

The positions of the nitrile and carbomethoxy substituents are predicted by their electron withdrawing abilities based on Hammett-σ constants,[73] σ_p-CN = 1.000; σ_p-$COOCH_3$ = 0.636. As the carbomethoxy substituent has less electron withdrawing ability, it should be on the cyclopropane side. The difference in electron withdrawing ability between carbomethoxy substituent and nitrile substituent is so big that the Cope equilibrium will certainly shift to **96-a** which is more stable than **96-b** (Figure 96).

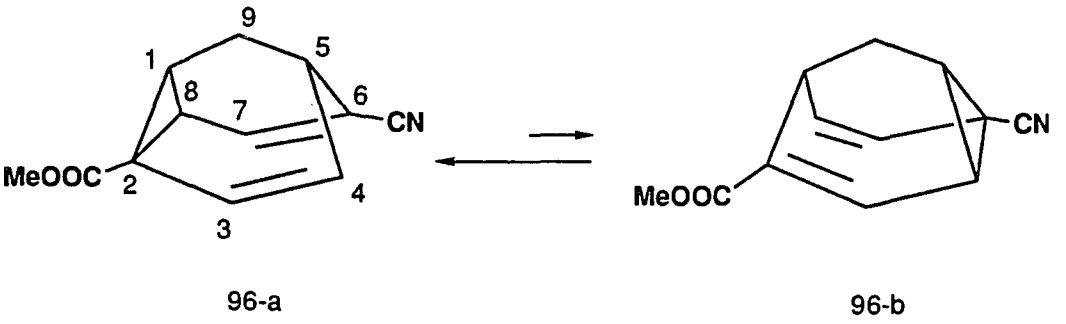

96-a 96-b

Figure 96: The Equilibrium Preference of **96**

Room temperature ^{1}H and ^{13}C-NMR spectra of **96-a** verified its structure and dissymmetry by showing the signals of every single proton and carbon. The 1D-^{1}H spectrum of **96-a** can be interpreted more accurately with the help of its 2D-^{1}H NMR spectrum. By knowing the H_7-vinylic proton at δ 6.41 ppm, all other protons can easily be assigned as follow: 3.21 ppm (t, 7.32 Hz, 8-H), 3.02 ppm (m, 1-H), 1.27 ppm (m, two 9-H), 2.93 ppm (m, 5-H), 5.78 ppm (dd, 9.30 Hz and 9.37 Hz, 4-H), 6.37 ppm (d, 9.37 Hz, 3-H) and 3.78 ppm (s, $-OCH_3$). (Figure 97)

Another significance was observed when we compared room temperature (25°C) and low temperature (−110°C) ^{13}C-NMR spectra of compound **96**.(Figure 98) The cyclopropane C_2, C_8 and vinylic C_4, C_6 signals of room temperature ^{13}C-NMR spectrum had been obviously changed when the ^{13}C spectrum was measured at −110°C. From this point, we felt that the equilibrium preference of compound 96 depends mainly on the temperature changes.

The FT-IR spectrum of the ester-nitrile **96-a** in CCl_4 shows only one C≡N frequency at 2213 cm^{-1} arising from the α,β-unsaturated nitrile group and two C=C frequencies at 1609 and 1611 cm^{-1} (Figure 99).

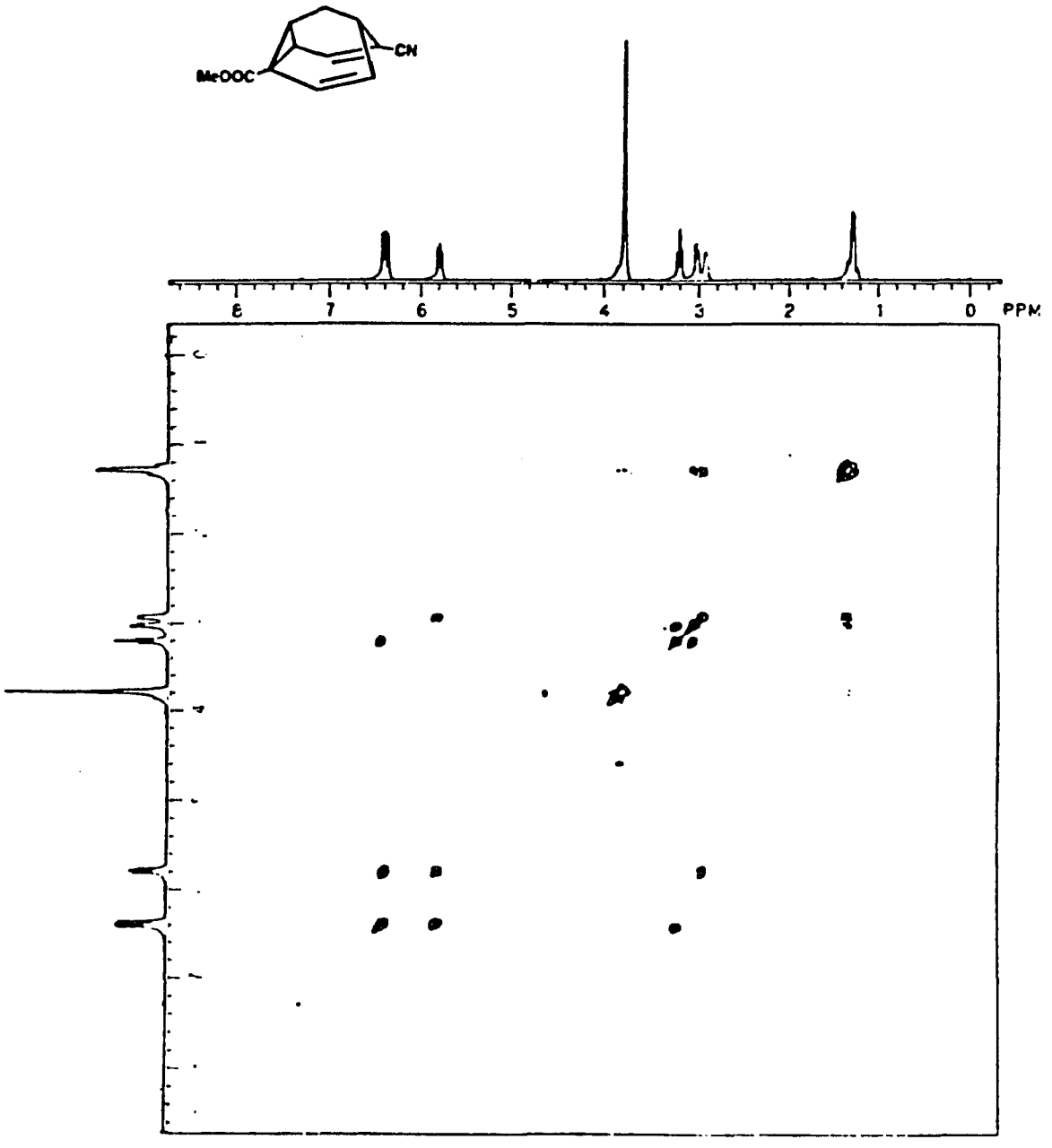

Figure 97: 2D-^{1}H NMR Spectrum of 96-a

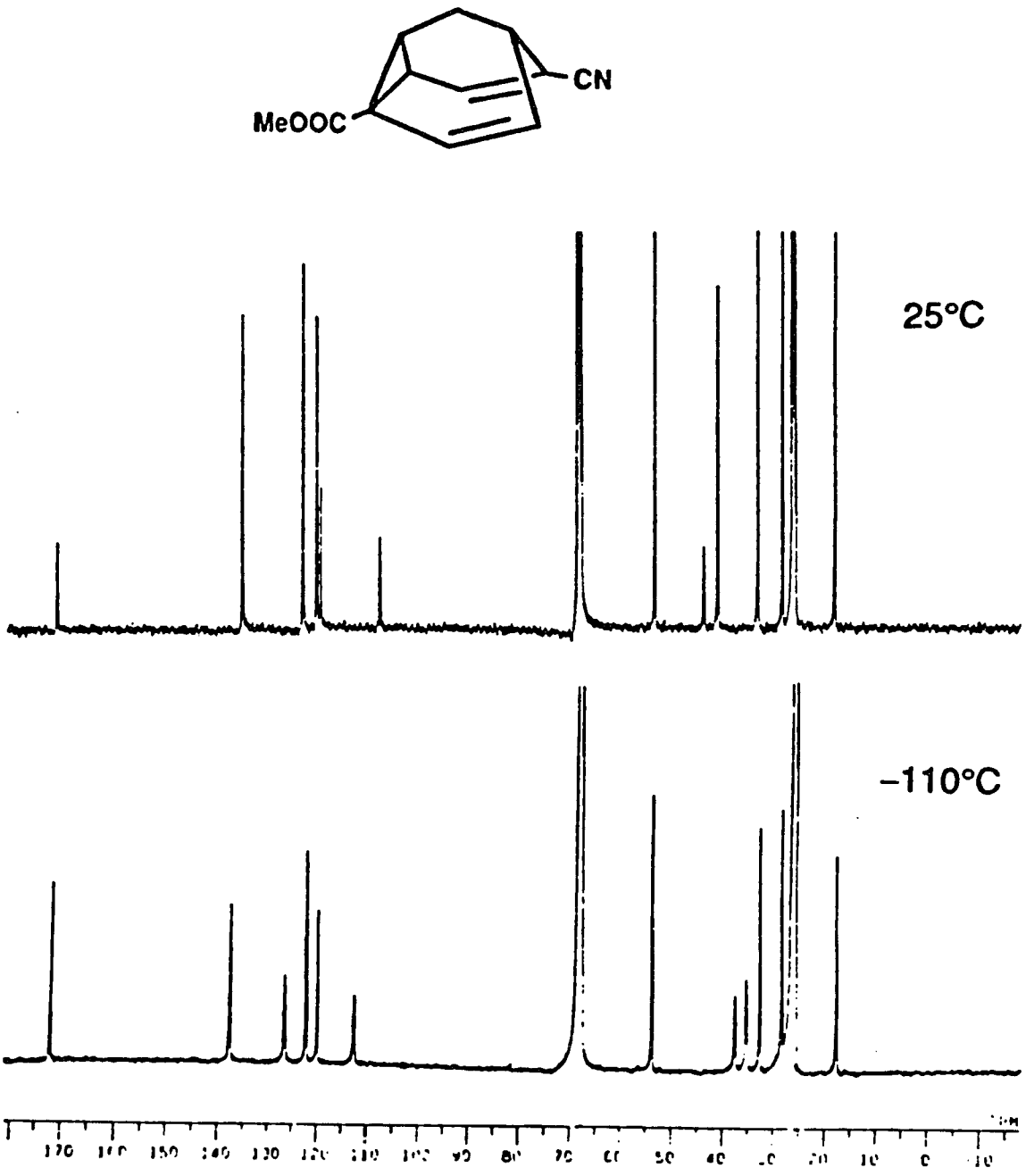

Figure 98: Variable Temperature Solution ^{13}C-NMR Spectra of 2-Carbomethoxy-barbaralane-6-carbonitrile (96-a)

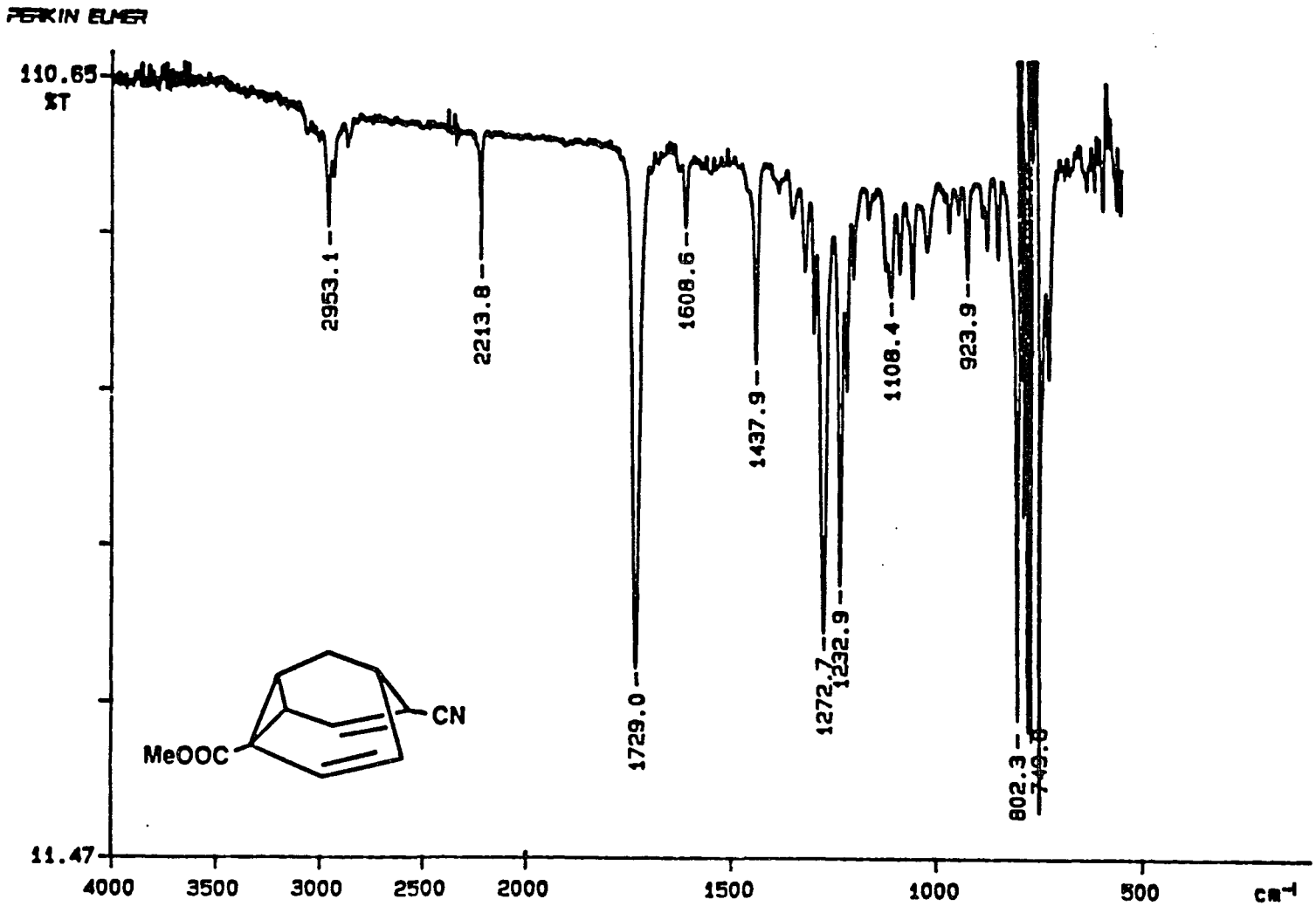

Figure 99: FT-IR Spectrum of 96-a in CCl_4 at Room Temperature

The structure of **96-a** was clearly established by X-ray structure determination in the solid state which is in agreement with our previous prediction, carbomethoxy substituent on the cyclopropane and nitrile substituent on the olefinic carbon (Figure 100).

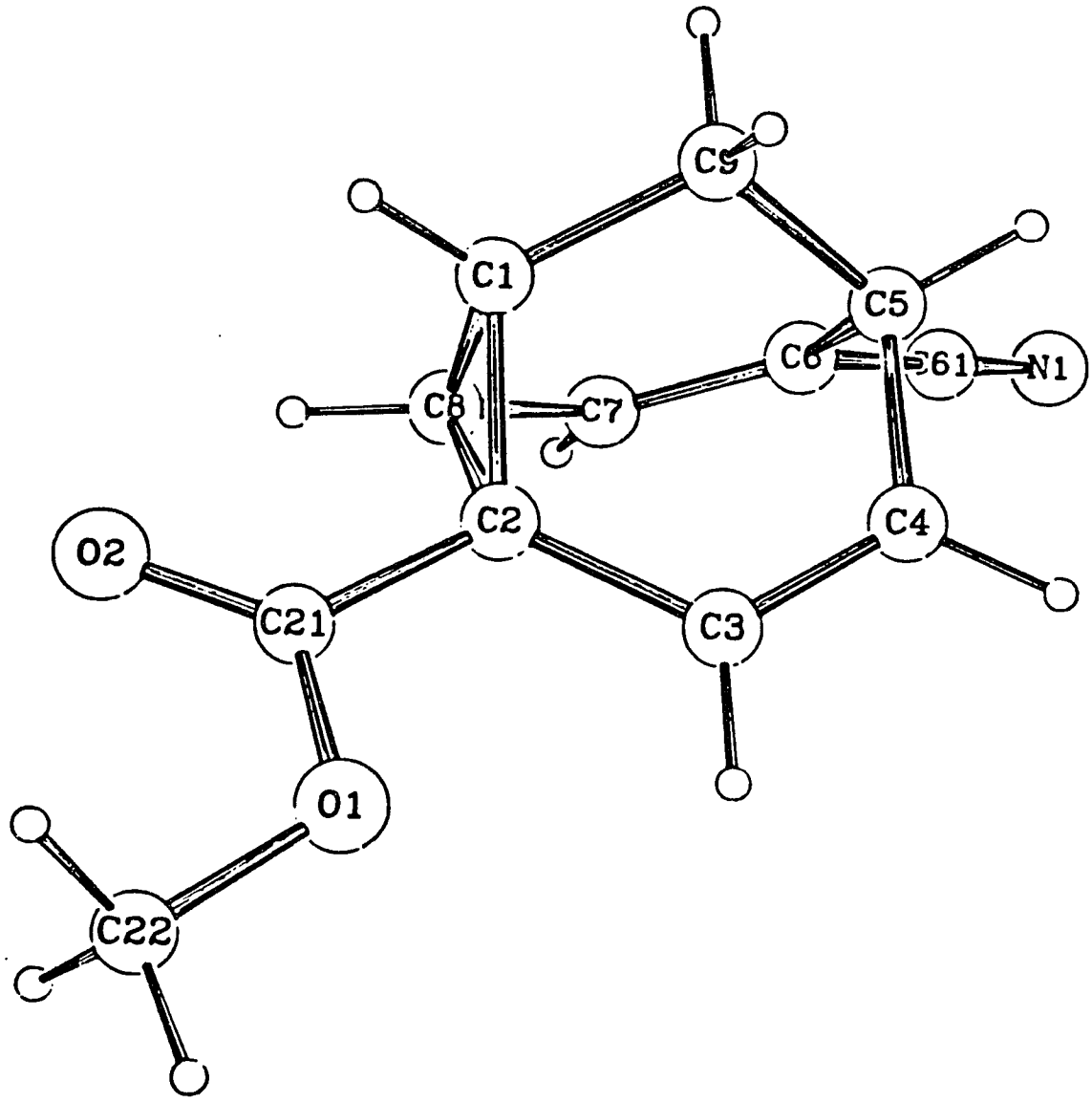

Figure 100: X-ray Crystal Structure of **96-a**

CHAPTER 3

3.0.0. UNSUCCESSFUL APPROACHES

In order to study the substituent effects on the activation energy of the Cope rearrangement with the goal of synthesizing the first neutral bishomoaromatic molecule, we attempted to synthesize a variety of electron-acceptor substituted barbaralanes and semibullvalene. Although a number of 2,6-disubstituted- and 2,4,6,8-tetrasubstituted barbaralanes have been synthesized whose substituent effects agree qualitatively with theoretical predictions, some attempted syntheses did not afford our desired products.

3.1.1.Attempted Syntheses of Electron Acceptor Substituted Barbaralanes

(a) 2,4,6,8-Tetracyanobarbaralane (19)

In an attempted synthesis of **19**, we first tried to transform tetraester barbaralane **18** into tetraalcohol **59** by LAH reduction (Figure 101). Since this step did not afford the desired product **59**, we terminated the attempt.

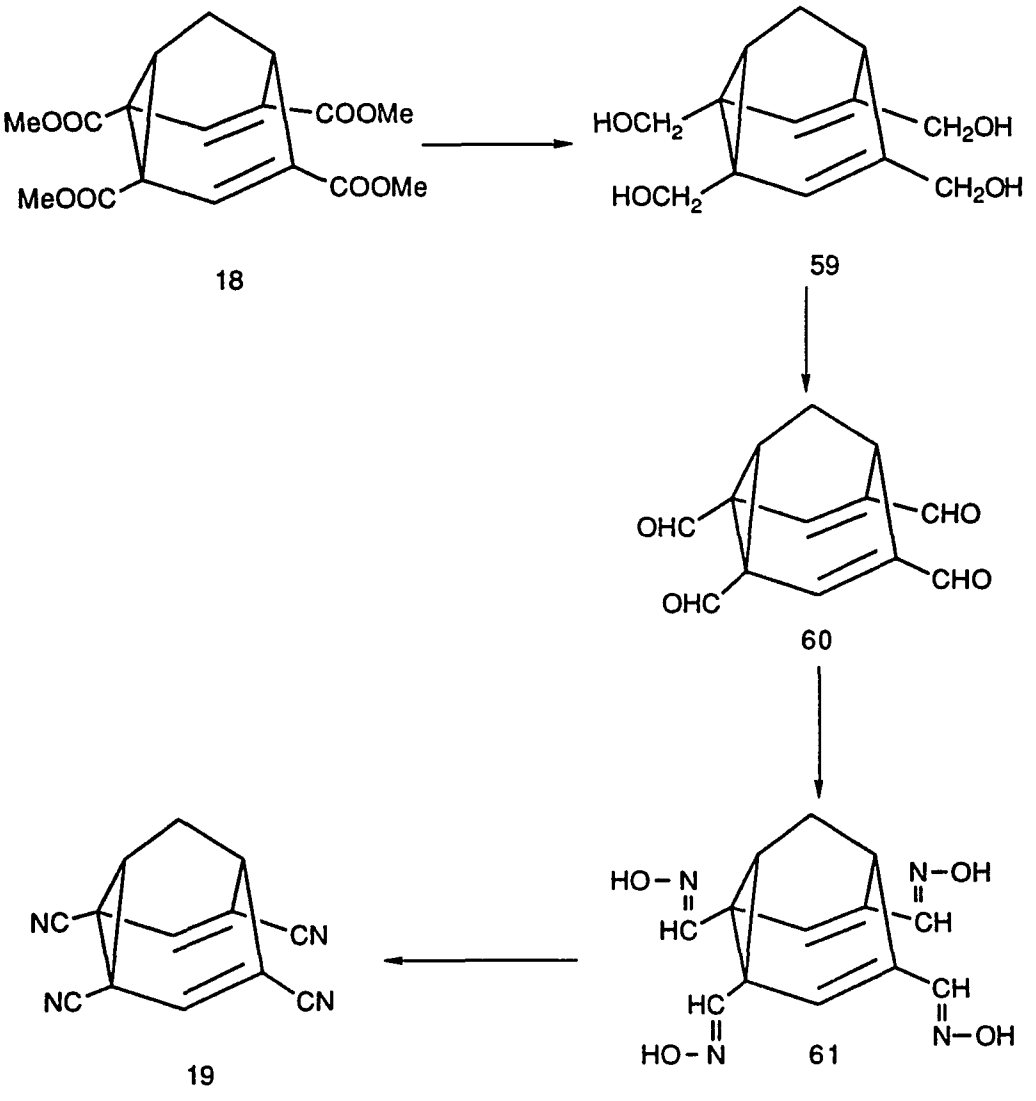

Figure 101: Attempted Synthesis of **19**

Alternatively, we attempted to synthesize compound **19** starting from tetracyclic diketo tetraester **27** (Figure 102). Hydrolysis of compound **27** with NaOH in methanol/water, 1:1 at 80°C provided tetraacid analogue **62** in 48% yield. The identification of **62** rests upon its ^{1}H-NMR spectrum. In the second step, compound **62** was treated with thionyl chloride at 66°C for two days in order to convert it into acid-chloride analogue **63**. Without purification, this intermediate was allowed to react with NH_3 in dry THF at 0°C for 2 hours. The result was inconclusive. We, therefore, discontinued our attempt toward **19**.

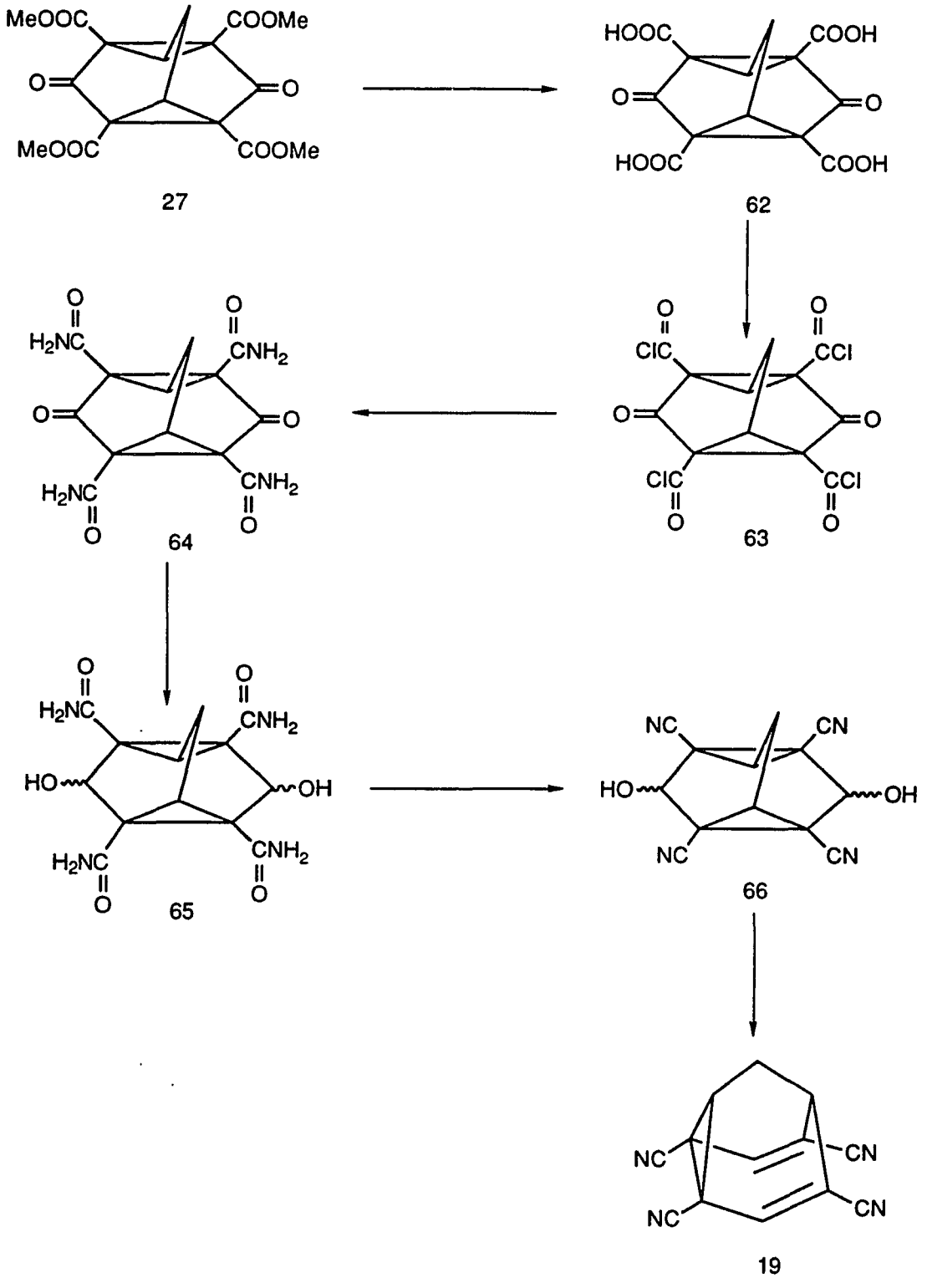

Figure 102: Attempted Synthesis of **19**

(b) 2,4,6,8-Tetraphenylbarbaralane (21)

The activation energies of 2,6-diphenylbarbaralane **5-b** (p. 13) and 3,7-diphenylbarbaralane **7** (p. 14) have been reported as 5.16 kcal/mol[25] and 9.3 kcal/mol[5] respectively. While a sizeable decrease of the Cope activation barrier is anticipated if the phenyl groups are attached to the termini of the allylic parts, the phenyl groups at the central carbons of the allylic parts exert only a minor, rate-retarding effect.[5] After studying the phenyl substituent effects at C_2, C_6 positions and C_3, C_7 positions respectively, we would have liked to study the effect in higher substituted system like 2,4,6,8-tetraphenylbarbaralane **21**. However, malondialdehyde **25** and 1,3-diphenyl-2-propanone **100** did not give compound **101**, and further study was terminated.(Figure 103)

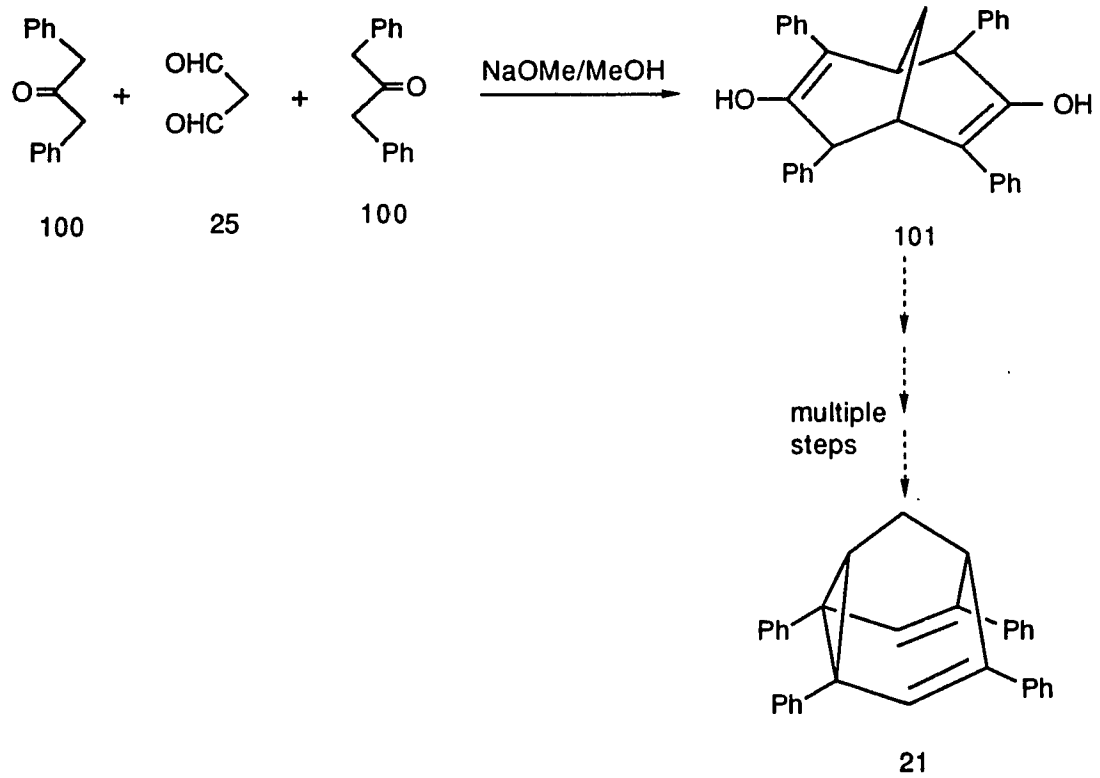

Figure 103: Attempted Synthesis of **21**

(c) 2,6-Dibromobarbaralane (107)

We also attempted to synthesize 2,6 Dibromobarbaralane **107**. As shown in Figure 104, tetraester dienol **26** was decarbomethoxylated to bicyclo[3.3.1]nonane-3,7-dione **102** in 49% yield following the method of Weiss et al.[67] The ^{1}H and ^{13}C spectra of **102** were consistent with the reference compound which was prepared by Bertz[41]. Bromination and dehydrobromination of **102** was attempted by the method of Dreiding et al..[79] Bromination of **102** with phenyltrimethylammonium tribromide in CH_2Cl_2 followed by dehydrobromination of the crude product mixture with triethylamine led to a mixture of 2,6-dibromo-triasterane-3,7-dione **104** and 2,4-dibromo-triasterane-3,7-dione **105** in a total yield of 92%. Recrystallization from benzene-hexane solvent mixture permitted the purification (17%) of only one isomer, which was 2,6-dibromo adduct **104**. The other isomer, 2,4-dibromo adduct **105** could not be obtained in pure form. However, it was identified in the mixture by its NMR signals. Dreiding et al. also found that bromination of compound **102** with 4.5 equivalents of phenyltrimethylammonium tribromide in CH_2Cl_2 followed by aqueous work-up led to a tetrabromosubstituted 1,3-dihydroxy-2-oxa-adamantane **103** in 23% yield along with 10% of 2,6-dibromo-triasterane-3,7-dione **104**.

The resulting pure isomer **104** was subjected to reduction by aluminum isopropoxide in isopropanol at reflux for one hour, followed by the distillation of isopropanol and acetone. Hydrolysis with dilute HCl afforded exo,exo diol **106** in 42% yield. The crude product was recrystallized from benzene-hexane, giving pure **106** in 8% yield. The

yield of the compound **106** was so low that the last step toward 2,6-dibromobarbaralane **107** could not be attempted.

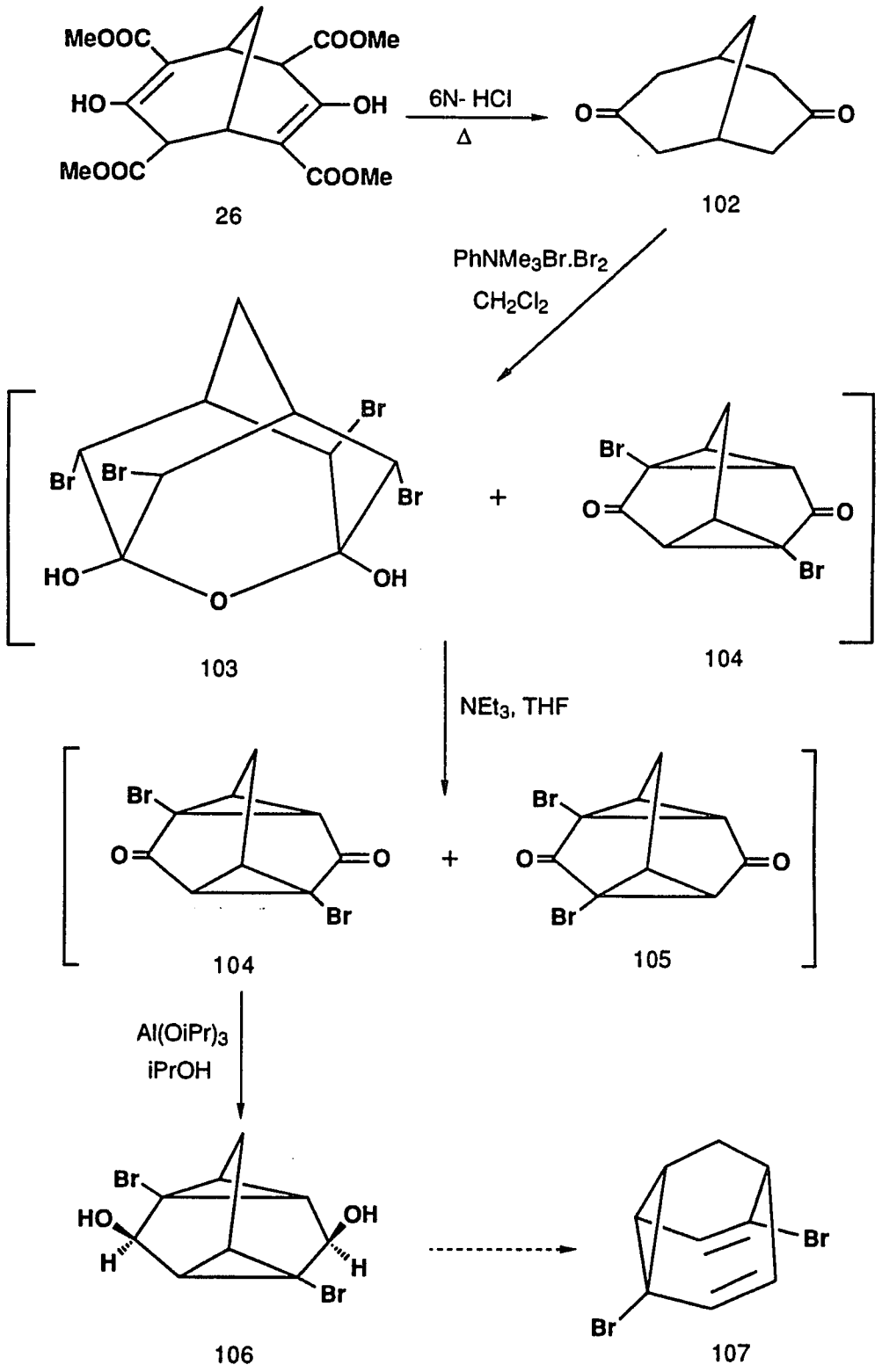

Figure 104: Attempted Synthesis of **107**

3.1.2. Attempted Syntheses of 2,8-4,6-Double Bridged Barbaralanes

(a) 2,8-4,6-N,N'-Bisbenzylimido-barbaralane (110)

In order to test Williams and Kurtz's theoretical prediction[39] that the activation energy of the Cope rearrangement would be lowered in 2,8-4,6 double bridged semibullvalenes, we attempted to synthesize 2,8-4,6-N,N'-bisbenzylimido-barbaralane **110**. We used the tetracyclic tetraester diol **28-a** and excess benzylamine **108**. After refluxing in methanol at 80°C for 6 days, we obtained 2,4,6,8-tetrabenzylamido-diol **111** instead of compound **109**. After digesting with ethanol, pure compound **111** was obtained as white solid, in 55% yield: mp 245-246°C (Figure 105).

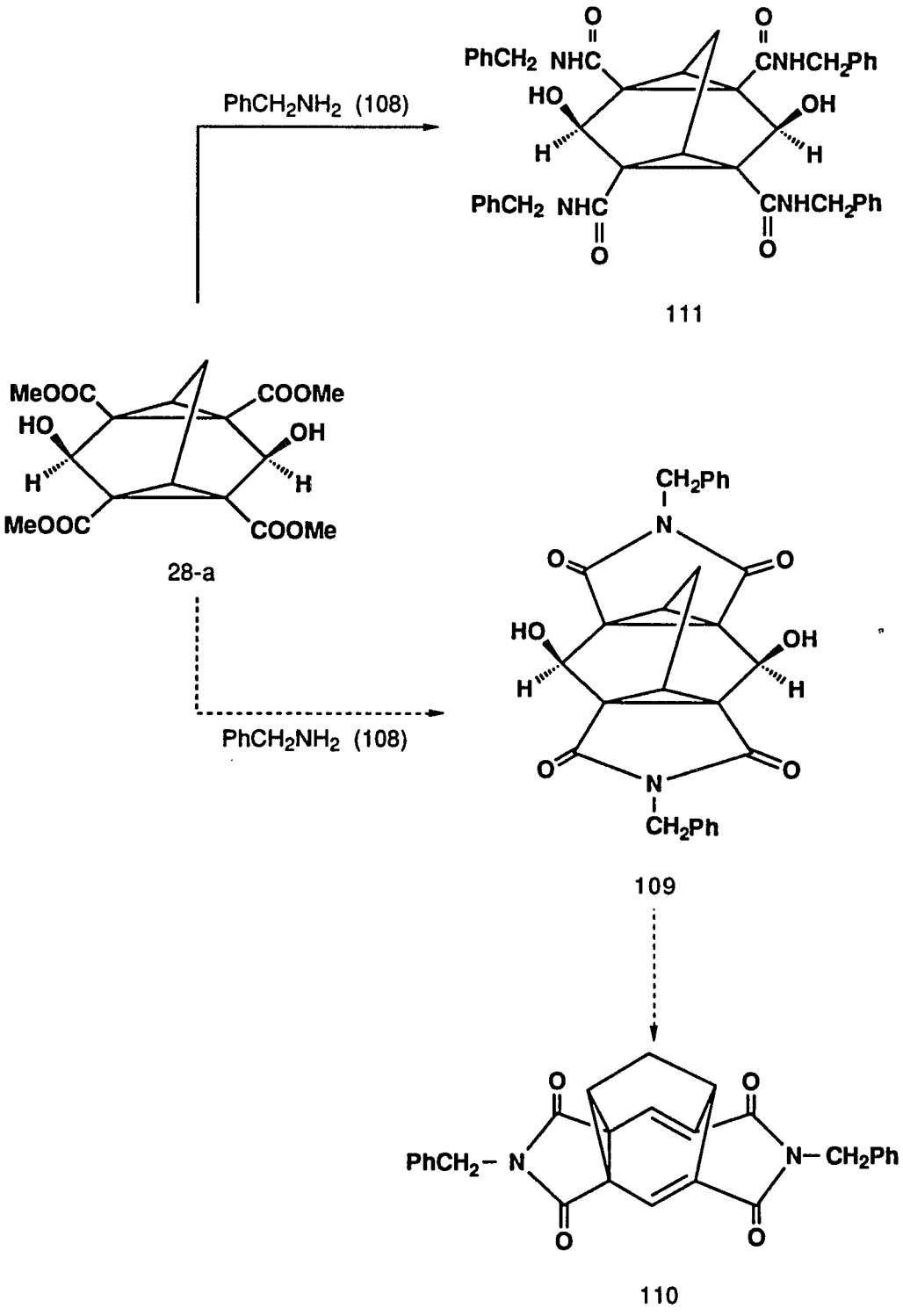

Figure 105: Attempted Synthesis of **110**

(b) 2,8-4,6-Bishydrazido-barbaralane (112)

As shown in Figure 106, an attempted preparation of 2,8-4,6-bishydrazido-barbaralane **112** from the known tetraester barbaralane **18** with hydrazine in methanol was carried out at reflux for 2 hours. The result was inconclusive.

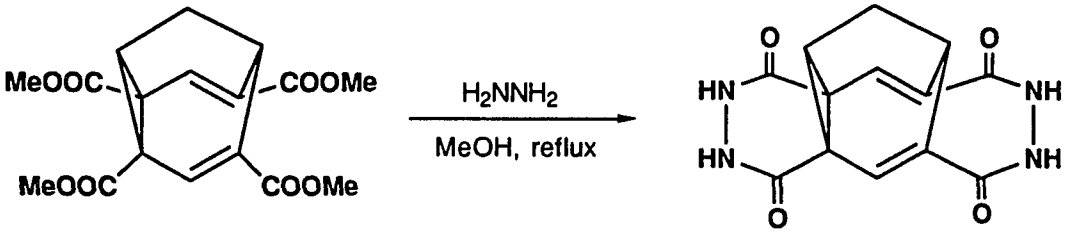

18 112

Figure 106: Attempted Synthesis of **112**

3.2.1. Attempted Synthesis of 1,5-Dibromosemibullvalene

The purpose of this study was the synthesis of 1,5-dibromosemibullvalene **116** which can lead to 1,5-dehydro-semibullvalene. The starting material in the synthesis of **116** is 1,2,4,5,6,8-hexacarbomethoxy-bicyclo[3.3.0]octane-3,7-dione **114**, obtained according to Weiss and Edwards[80] from acetone-dicarboxylic ester **24** and freshly prepared dimethyl diketosuccinate **113**.[81] The reaction yielded not only the desired product **114** in 6% yield: mp 210-213°C, but also the unexpected and interesting product 2-oxa-bicyclo[3.3.0]oct-7-ene-1, 4, 5, 6, 8-pentacarbomethoxy-3-carbomethoxy-methylene-3,7-diol **115** in 11% yield: mp 174-175°C, after fractional recrystallization (Figure 107). Regarding compound **115**, a similar observation is reported by Quast et al.[82]

The structures of **114** and **115** are consistent with their ^{1}H and ^{13}C-NMR spectra, and confirmed by X-ray structure analysis (Figure 108 and 109).

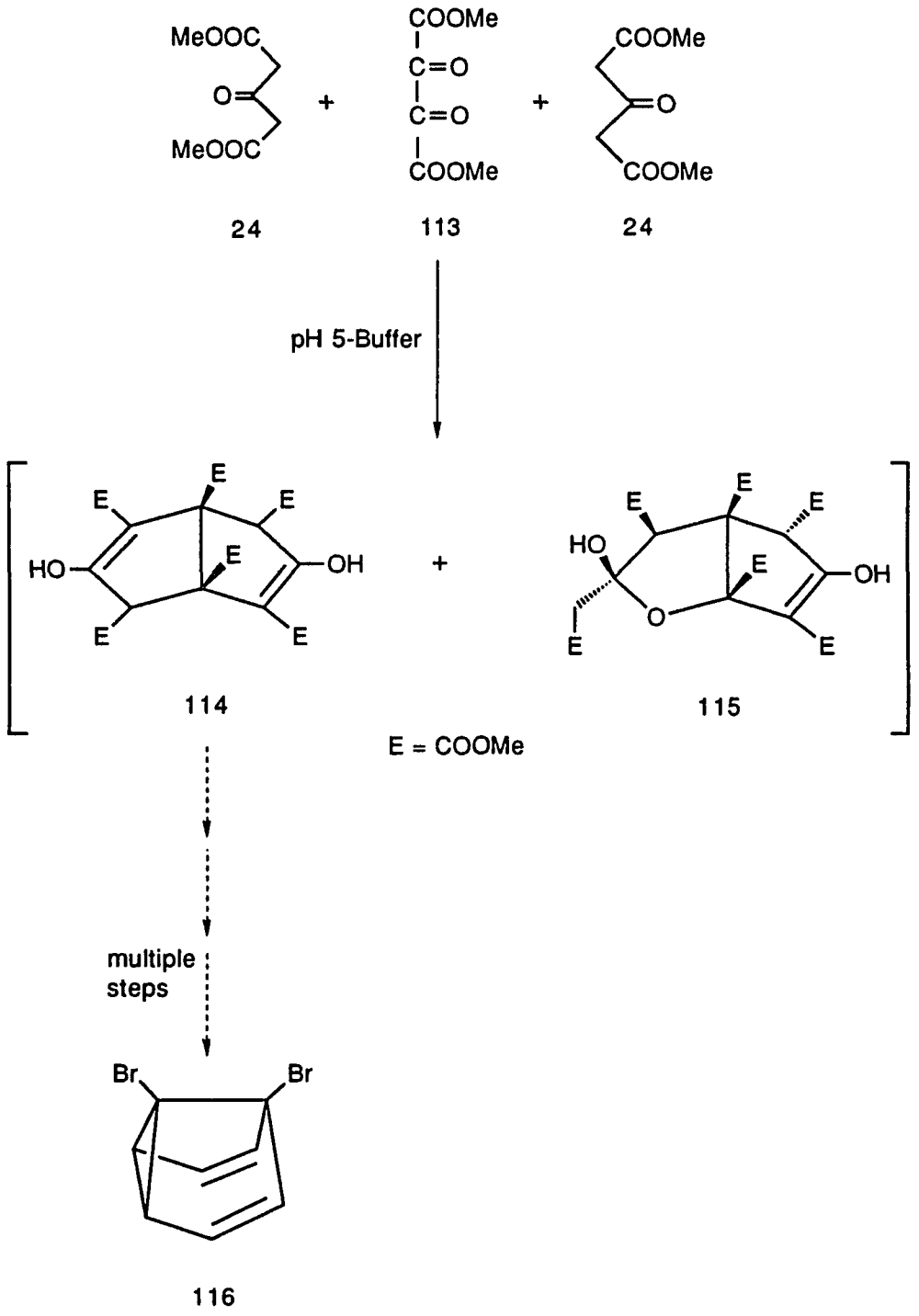

Figure 107: Attempted Synthesis of **116**

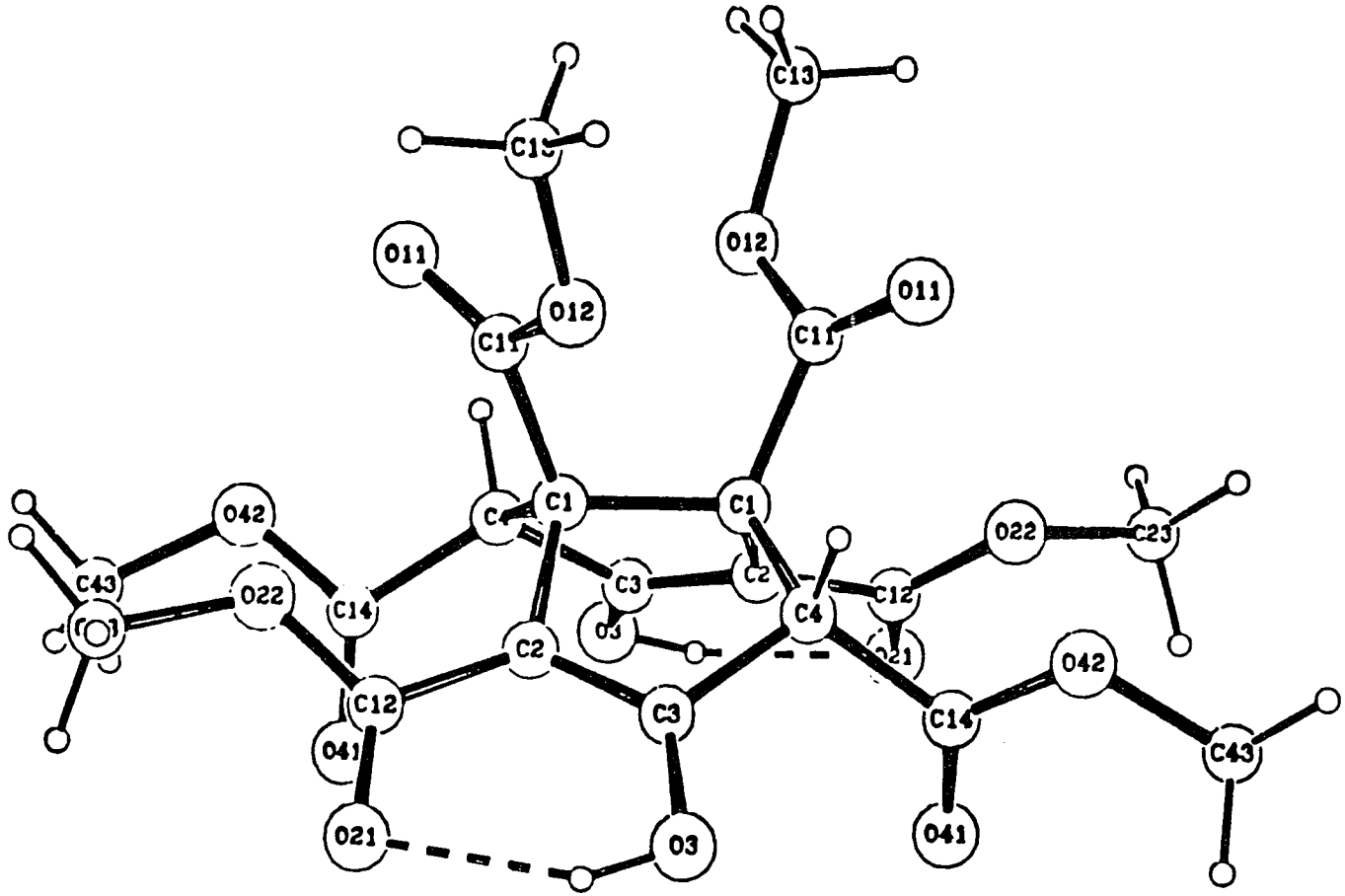

Figure 108: X-Ray Crystal Structure of 114

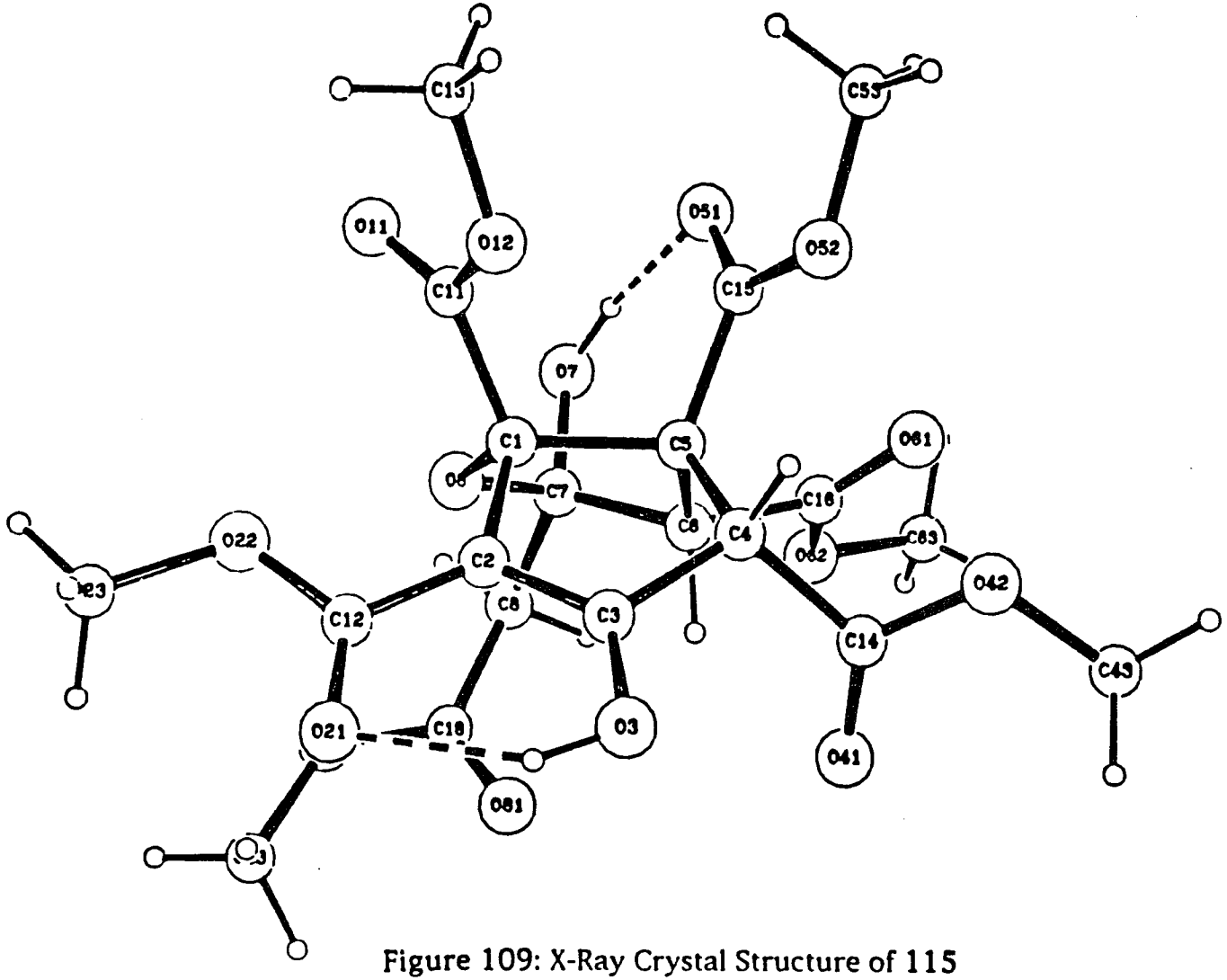

Figure 109: X-Ray Crystal Structure of 115

Once **114** is available, 1,5-dibromosemibullvalene **116** could be prepared in multiple steps, such as selective decarbomethoxylation at C_2, C_4, C_6 and C_8 positions, cyclization, reduction, P_2I_4 induced Grob-fragmentation, hydrolysis and Hunsdiecker reaction. However, the low yield of hexacarbomethoxy Weiss compound **114** led us to discontinue this investigation. Subsequently, we found the effective synthetic pathway toward **114** which was reported by Camps et al.[83]

CHAPTER 4

4.0.0. X-RAY STRUCTURE ANALYSIS, SPECTRAL CHARACTERISTICS AND DETERMINATION OF THE COPE ACTIVATION BARRIER

4.1.1. X-ray Diffraction Analysis of 2,4,6,8-Tetracarbomethoxybarbaralane (18)

The rapid degenerate Cope rearrangement renders barbaralane one of the fascinating members of the bullvalene series. After Hoffmann's[15] and Dewar's[19] predictions regarding the influence of substituents on the energy barrier to this rearrangement, substituted barbaralanes became the targets of numerous synthetic endeavors.[24,25,37] The predicted acceleration of the Cope rearrangement by electron-donating groups at the C_1 and C_5 positions and electron-withdrawing groups at the C_2, C_4, C_6 and C_8 positions of the molecule has been confirmed by Grohmann et al..[22,23,40] They reported a dramatic effect in 1,5-dimethyl-2,4,6,8-tetracarbomethoxysemibullvalene **4** and 1,5-annulated-2,4,6,8-tetracarbomethoxysemibullvalenes **117a-e** (Figure 110).

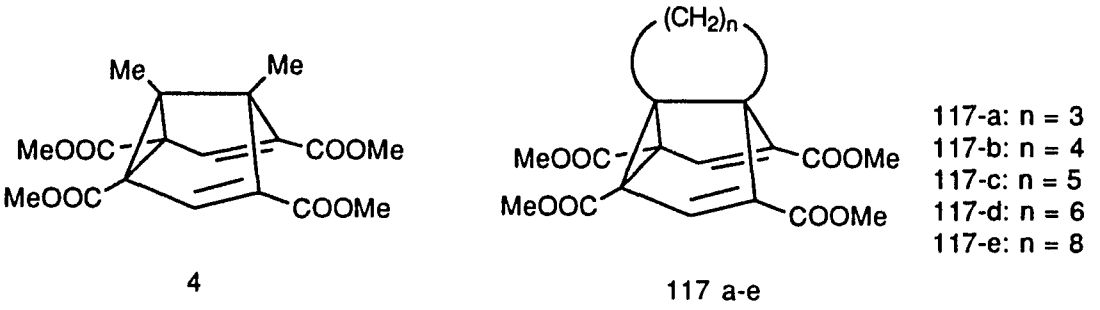

4 117 a-e

Figure 110: Derivatives of Semibullvalene

However, this existing series of semibullvalenes appeared less suitable for a systematic study involving X-ray structure analysis and ^{13}C-NMR spectroscopy because they rearrange readily to cyclooctatetraenes. Therefore, we have chosen to study the effect of substituents in barbaralane which also has the essential structure element of the homotropilidene system and is thermodynamically more stable compared to the semibullvalene system.

The solid-state structures of 2,4,6,8-tetracarbomethoxybarbaralane **18** were investigated by X-ray diffraction analyses at temperatures of 295 and 110 K. From the X-ray structures, we found out that the atomic distance C_2-C_8 in the cyclopropane ring and the distance C_4-C_6 at the open end of the molecule did not differ significantly at these temperatures. Experimental details and results of the X-ray diffraction analyses are compiled in Table 3. The numbering of the atoms is shown in Figure 111. The structures from the two data sets are almost identical. Atomic parameters are summarized in Table 4.

Table 3: Experimental details and results of the X-ray diffraction analyses of the 2,4,6,8-tetracarbomethoxybarbaralane **18** at 295 and 110K

Temperature (K)	295		110
Formula		$C_{17}H_{18}O_8$	
Formula weight		350.33	
Crystal size (mm)		0.10 × 0.36 × 0.50	
Crystal system		Monoclinic	
Space group		$P2_1/c$	
a(Å)	7.854(1)		7.757(1)
b(Å)	16.206(2)		16.101(5)
c(Å)	12.982(2)		12.866(3)
β(°)	90.64(1)		90.08(1)
Cell volume(Å^3)	1652.3		1606.9
Z		4	
d_{calc}(g cm^{-3})	1.408		1.448
μ(Cu Kα) (cm^{-1})	9.2		9.4

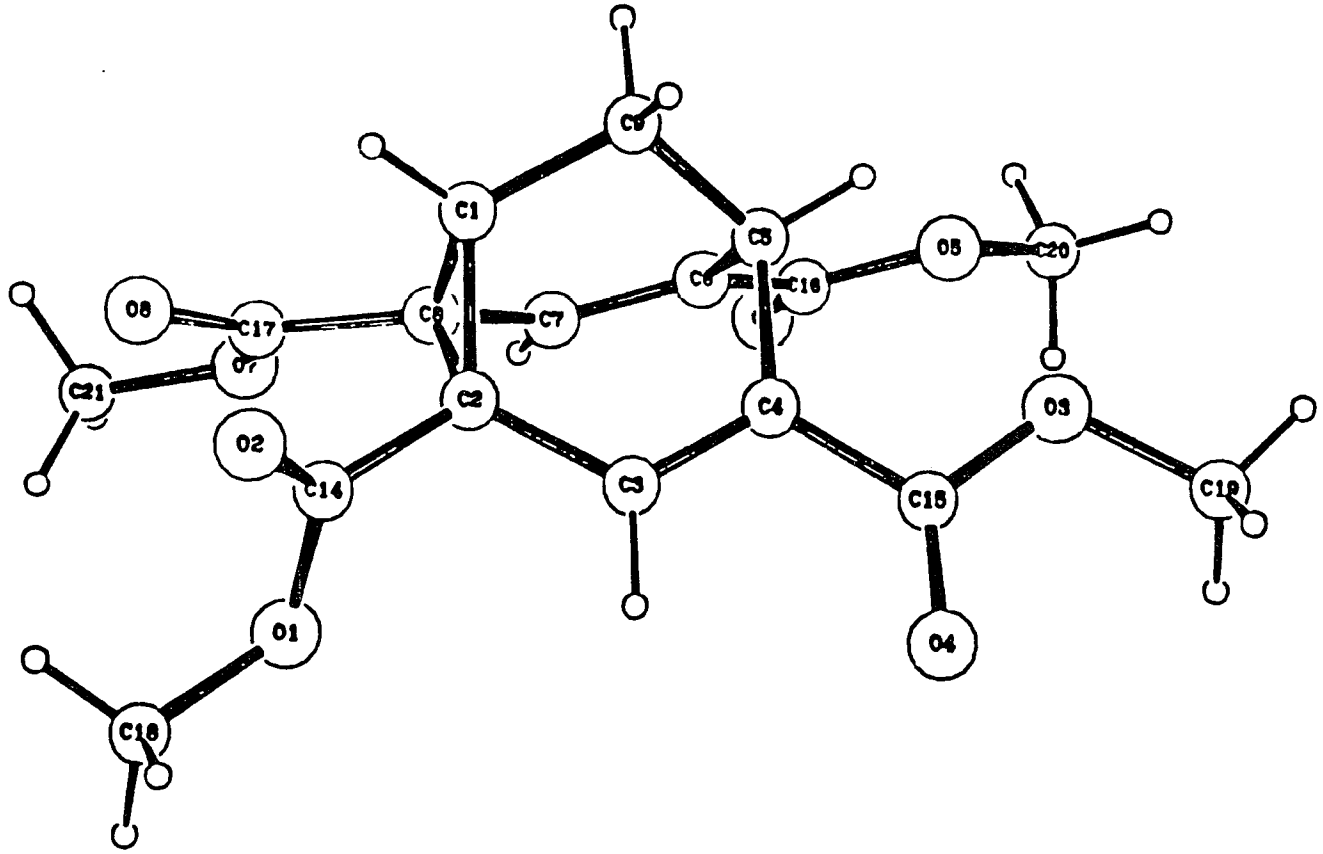

Figure 111: X-Ray Crystal Structure of **18** at 110K

Table 4: Selected Interatomic Distances and Bond Angles of 2,4,6,8-Tetracarbomethoxybarbaralane **18**

Distances (Å)

C_1-C_2	1.490	C_6-C_7	1.339	C_5-C_9	1.539
C_2-C_3	1.473	C_7-C_8	1.464	C_2-C_{14}	1.194
C_3-C_4	1.337	C_4-C_8	1.611	C_4-C_{15}	1.204
C_4-C_5	1.515	C_1-C_8	1.518	C_6-C_{16}	1.205
C_5-C_6	1.511	C_1-C_9	1.509	C_8-C_{17}	1.205
		C_4-C_6	2.40		

Bond Angles (°)

C_2-C_1-C_8	64.8	C_1-C_8-C_2	56.8	C_1-C_2-C_8	58.5
C_2-C_1-C_9	116.1	C_8-C_1-C_9	115.1	C_1-C_9-C_5	110.8
C_4-C_5-C_6	104.7	C_4-C_5-C_9	109.5	C_6-C_5-C_9	109.1
C_1-C_2-C_3	118.4	C_3-C_4-C_5	119.1	C_5-C_6-C_7	119.2
C_1-C_8-C_7	118.1	C_2-C_3-C_4	121.3		

Regarding four ester substituents, the X-ray crystal structure of compound **18** (Figure 111) reveals three different orientations. The two ester groups in conjugation with double bonds have the same orientation, pointing downwards, the carbonyl groups outwards, approximately parallel with the C_5-C_4 bond. The ester groups at C_2 and C_8 of the cyclopropane ring have two different orientations, one carbonyl group bisects the cyclopropane and the other one is more or less parallel, pointing outwards.

The X-ray crystal structure of compound **18** at 110 K (similar to that at 295 K) shows a somewhat longer C_2-C_8 bond of 1.611Å, while the C_1-C_2 bond is shortened (1.490Å). However, the C_1-C_8 bond (1.518Å) is a normal cyclopropane bond (1.51Å).[84] The bonds adjacent to the cyclopropane ring (C_2-C_3 = 1.473Å, C_7-C_8 = 1.464Å) are somewhat shorter than normal C_{sp2}-C_{sp2} bond (1.48Å). At the open end of the molecule, C_4-C_6 is 2.40Å.

Here, the question may be asked about how we can unequivocally characterize a neutral bishomoaromatic molecule. To understand this problem, we need to look at the model study of a bishomoaromatic semibullvalene/barbaralane, which predicts equal distances for C_2-C_8 = C_4-C_6 of 1.99Å and equal distances for the other bonds with a bond length similar to the one observed in benzene 1.39Å.[85]

From the X-ray structures and the atomic distances of **18** at 295 and 110 K, we clearly know that compound **18** possesses a static frozen structure in the solid-state.

In contrast, room temperature (295 K) X-ray data for 1,5-cyclo-octano-2,4,6,8-tetracarbomethoxysemibullvalene (Sb-8) **117-d** gave exactly the values expected for bishomoaromatic character (Table 5),[86] and furthermore, the room temperature solid state CP-MAS ^{13}C-NMR spectrum showed an average value for carbons 2, 4, 6 and 8 at δ = 104 ppm.[87] (Figure 112)

Table 5: X-ray Data of Sb-8 (**117-d**) at temperatures between 20 and 355 K

	Temp: (K)	C_2-C_8 (Å)	C_4-C_6 (Å)
1	20	1.675	2.296
2	115	1.722	2.244
3	115	1.741	2.231
4	127	1.772	2.199
5	140	1.798	2.173
6	153	1.825	2.145
7	181	1.875	2.098
8	208	1.918	2.064
9	236	1.949	2.034
10	265	1.967	2.013
11	279	1.978	2.002
12	294	1.990	1.987
13	295	1.990	1.992
14	335	2.001	1.973
15	360	2.017	1.974

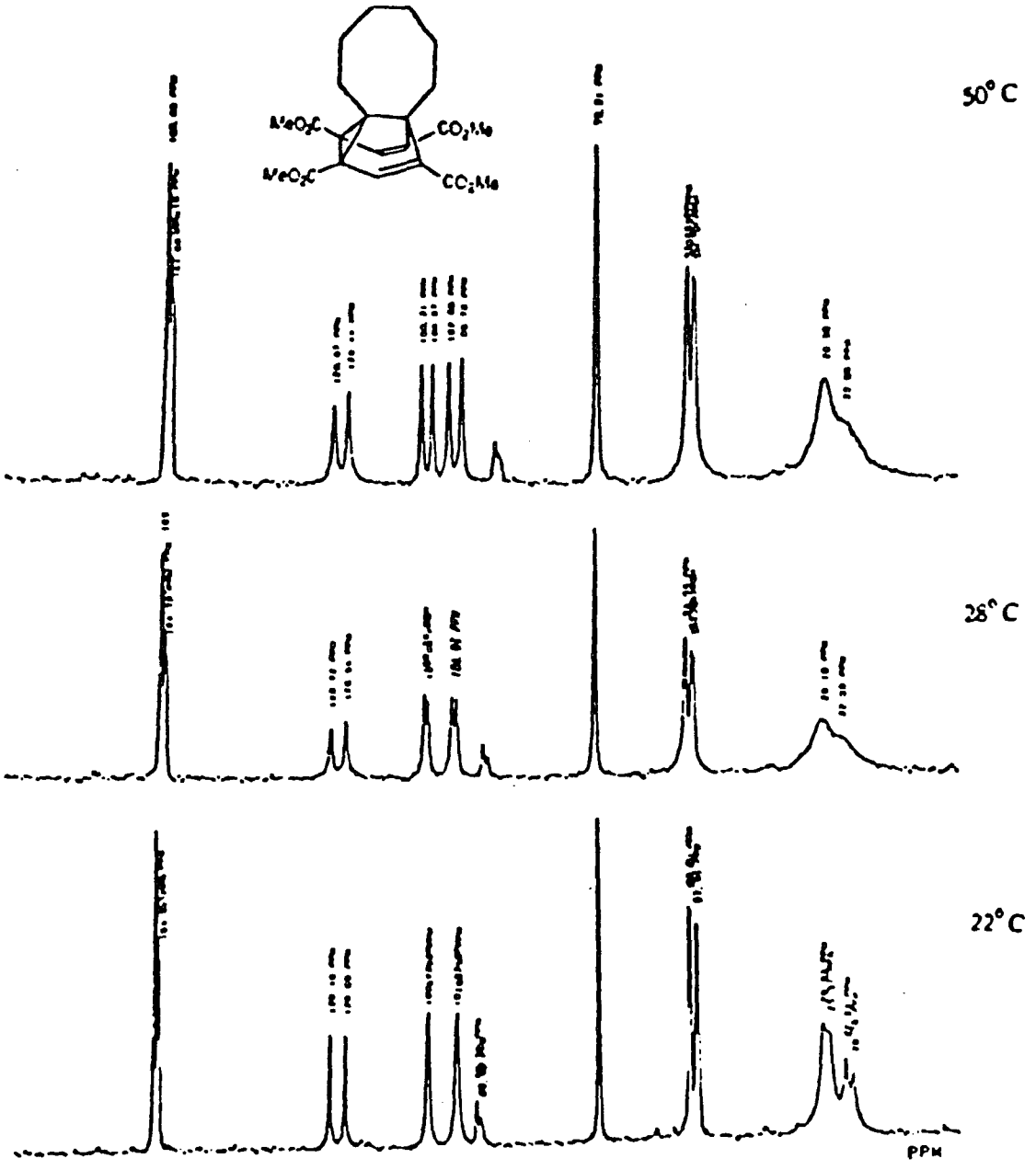

Figure 112: CP-MAS Solid-state ^{13}C -NMR Spectra of Sb-8 (117-d)

High-resolution variable temperature X-ray data between 20 and 355 K (Table 5) and variable temperature solid state NMR studies (Figure 112) of **117-d** revealed a non-degenerate Cope rearrangement between two energetically non-equivalent molecules in the solid state.[14,88] At room temperature, the ratio between the two non-equivalent forms was 1:1 thus explaining the observed deceptive solid state NMR results and the X-ray data.

4.1.2. Variable Temperature Vibrational Analyses of Thermal Ellipsoids of C_2 for 18 and 117-d

In order to learn more about the static character of 2,4,6,8-tetracarbomethoxybarbaralane **18** and the dynamic character of Sb-8 (**117-d**) in the solid-state, variable temperature, vibrational analyses of the thermal ellipsoids of C_2 were performed on both compounds in the temperature range of 110-340 K. (Figures 113 and 114) The vibrational analysis (ellipsoid motion) is measured by the root mean square (RMS) method.[86] The stronger the vibration, the bigger the RMS value. While the C_2 ellipsoid of compound **18** denotes a moderate increase in vibration with increasing temperature, that of Sb-8 **117-d** shows a drastic increase. This strongly supports the static nature of compound **18** and the dynamic nature of **117-d** in the solid-state.

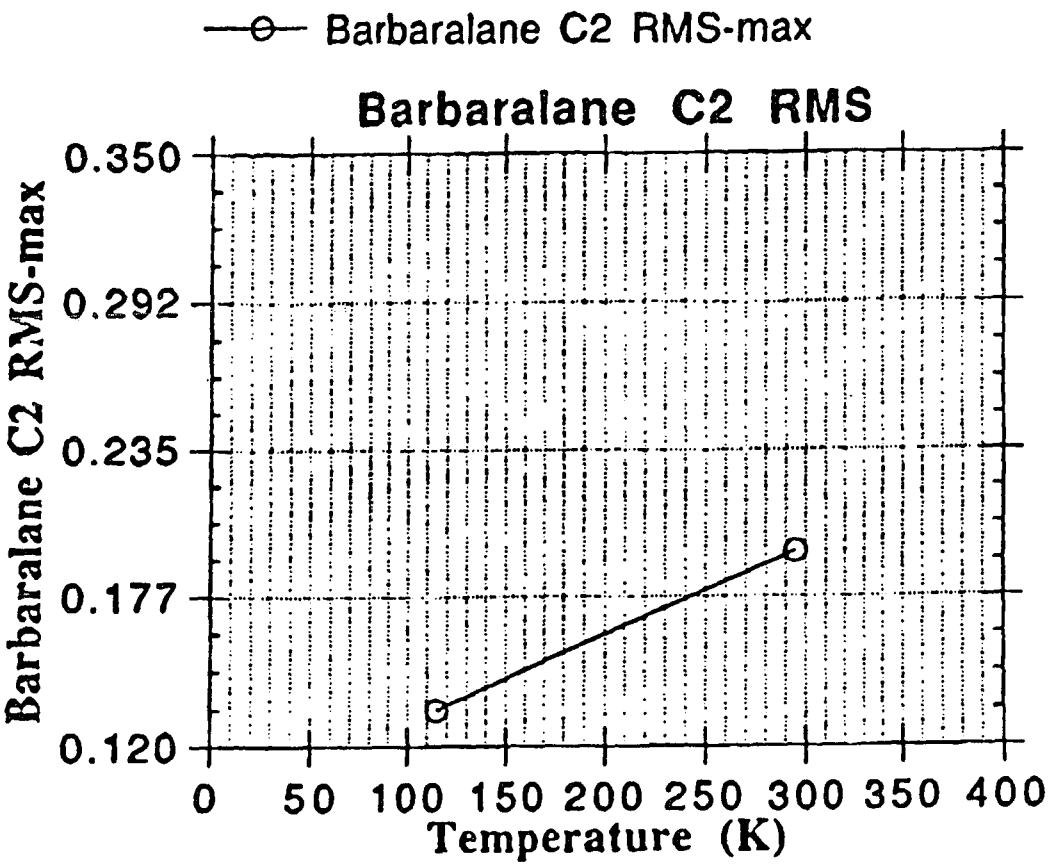

Figure 113: Temperature Dependence of Vibrational Analysis of C_2 Ellipsoid in 18

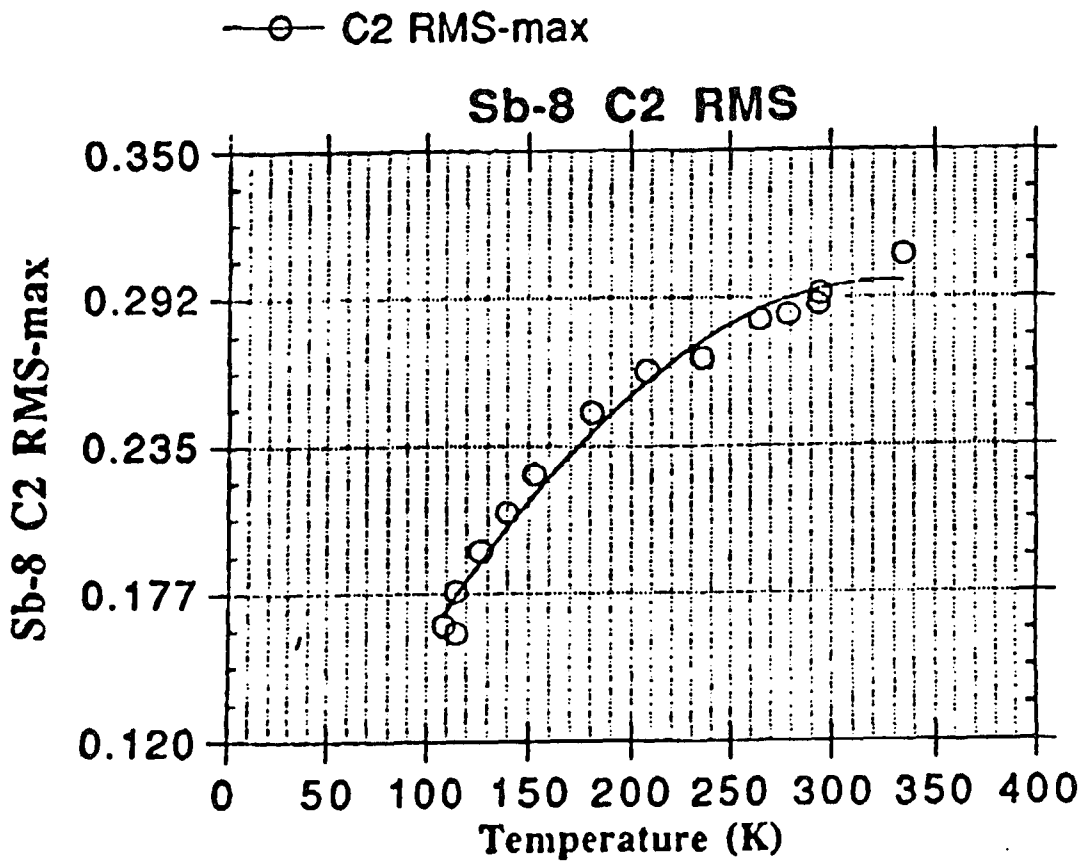

Figure 114: Temperature Dependence of Vibrational Analysis of C_2 Ellipsoid in **117-d**

4.2.1. Solution and Solid-state IR Studies for 18

The structure of **18** was also inspected by infrared radiation. The appearance of C=O stretching vibrations for ester groups is strikingly different in solution (CCl_4) and in the solid-state (KBr). In solution, compound **18** undergoes degenerate Cope rearrangement so rapidly that an averaged C=O stretching vibration for four ester substituents appeared at 1725 cm^{-1} (Figure 115).

But, infrared spectroscopy of a KBr pellet of the compound **18** shows two C=O (1710, 1740 cm^{-1}) stretching vibrations indicating the presence of cyclopropane ester and olefinic ester (Figure 116). Furthermore, the high resolution FT KBr pellet IR spectrum of **18** exhibited four overlapping carbonyl bands indicating the presence of four different carbonyl groups in the solid-state (Figure 117). Indeed, IR studies lend great support to confirming our previous results of room temperature ^{1}H and ^{13}C-NMR spectra, solid-state ^{13}C-NMR spectra and high resolution variable temperature X-ray analysis showing a dynamic molecule in solution which is static in the solid-state.

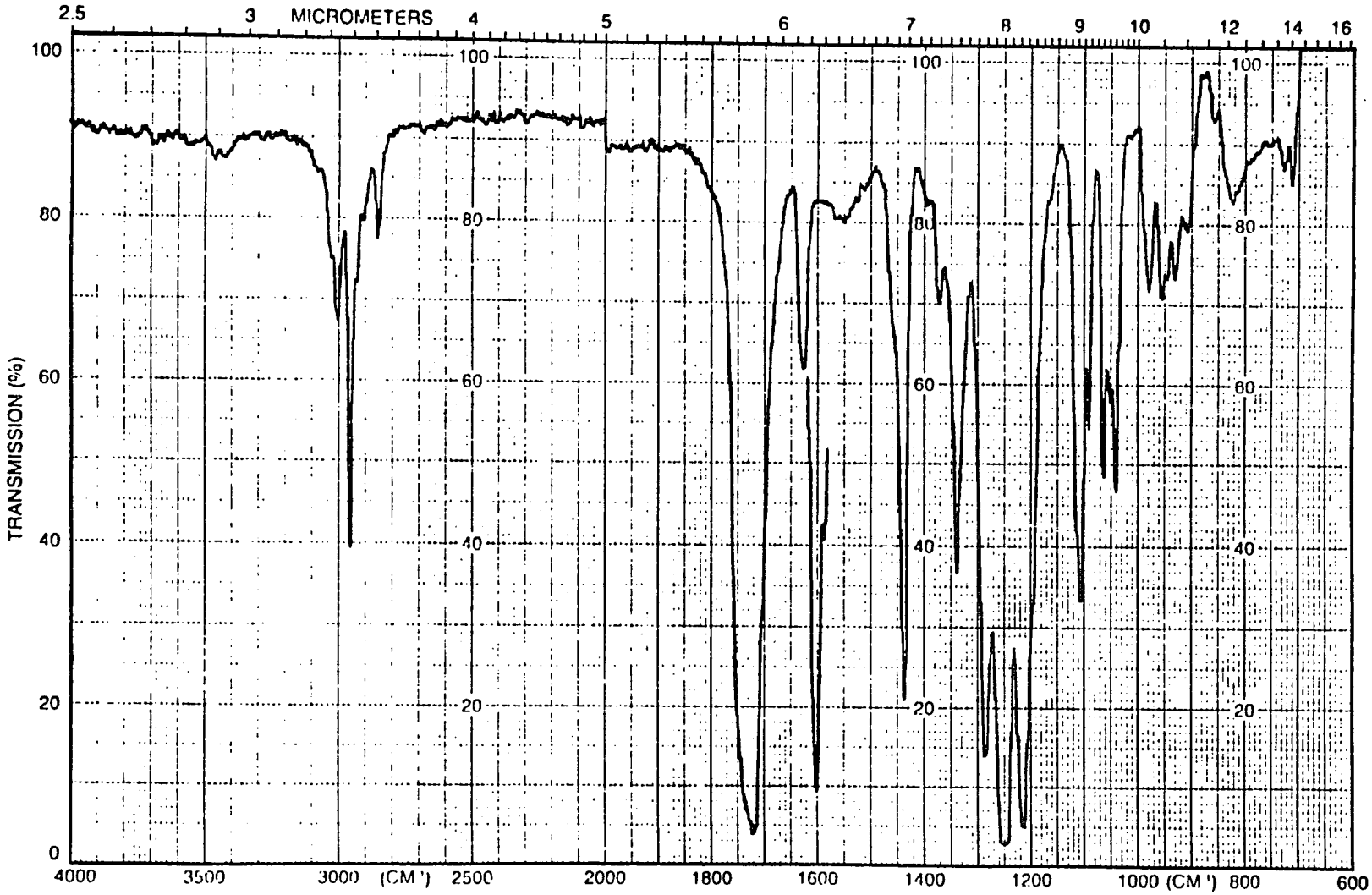

Figure 115: IR Spectrum of **18** in CCl_4 at Room Temperature

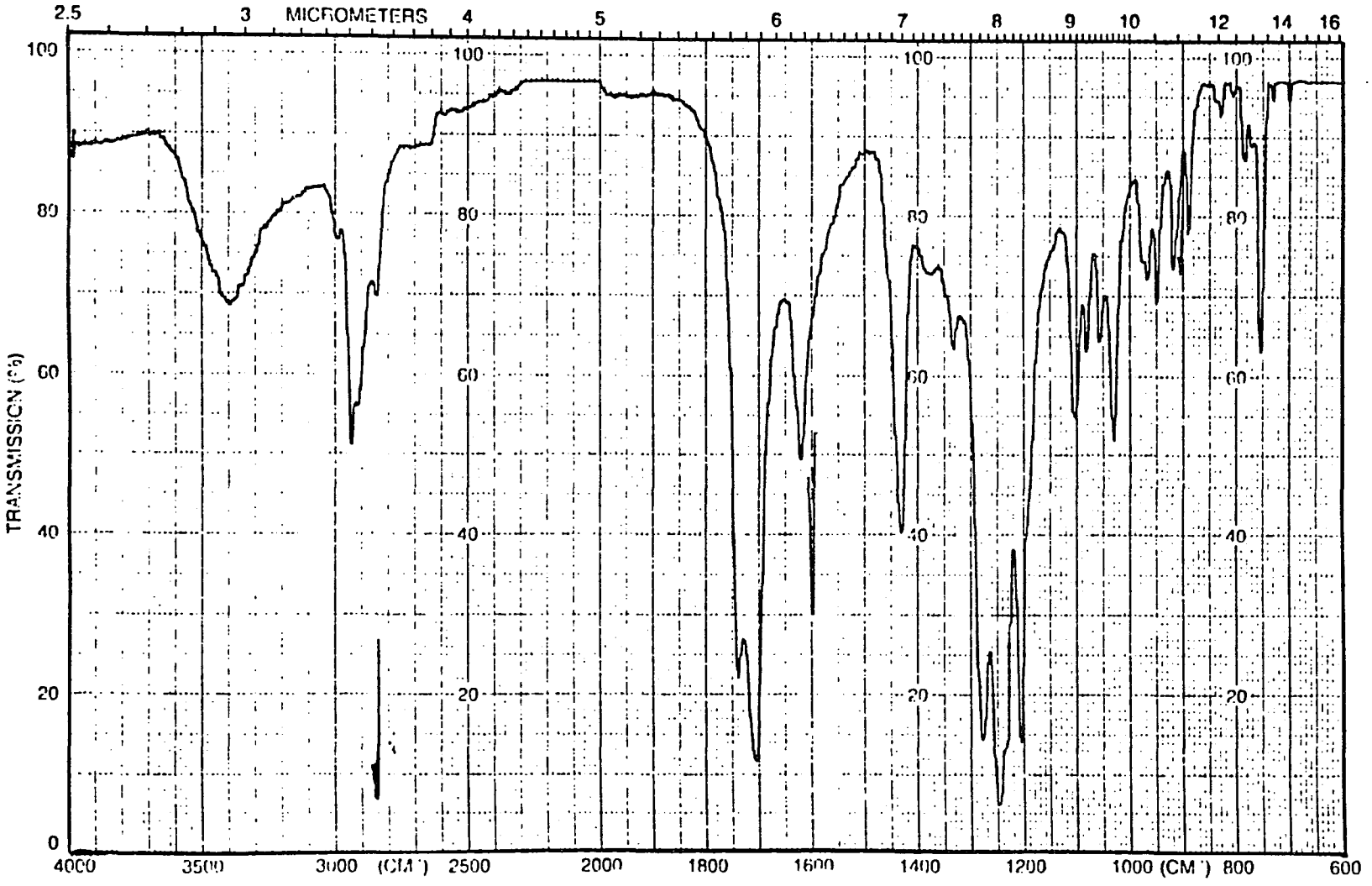

Figure 116: Solid-State IR Spectrum of **18** at Room Temperature

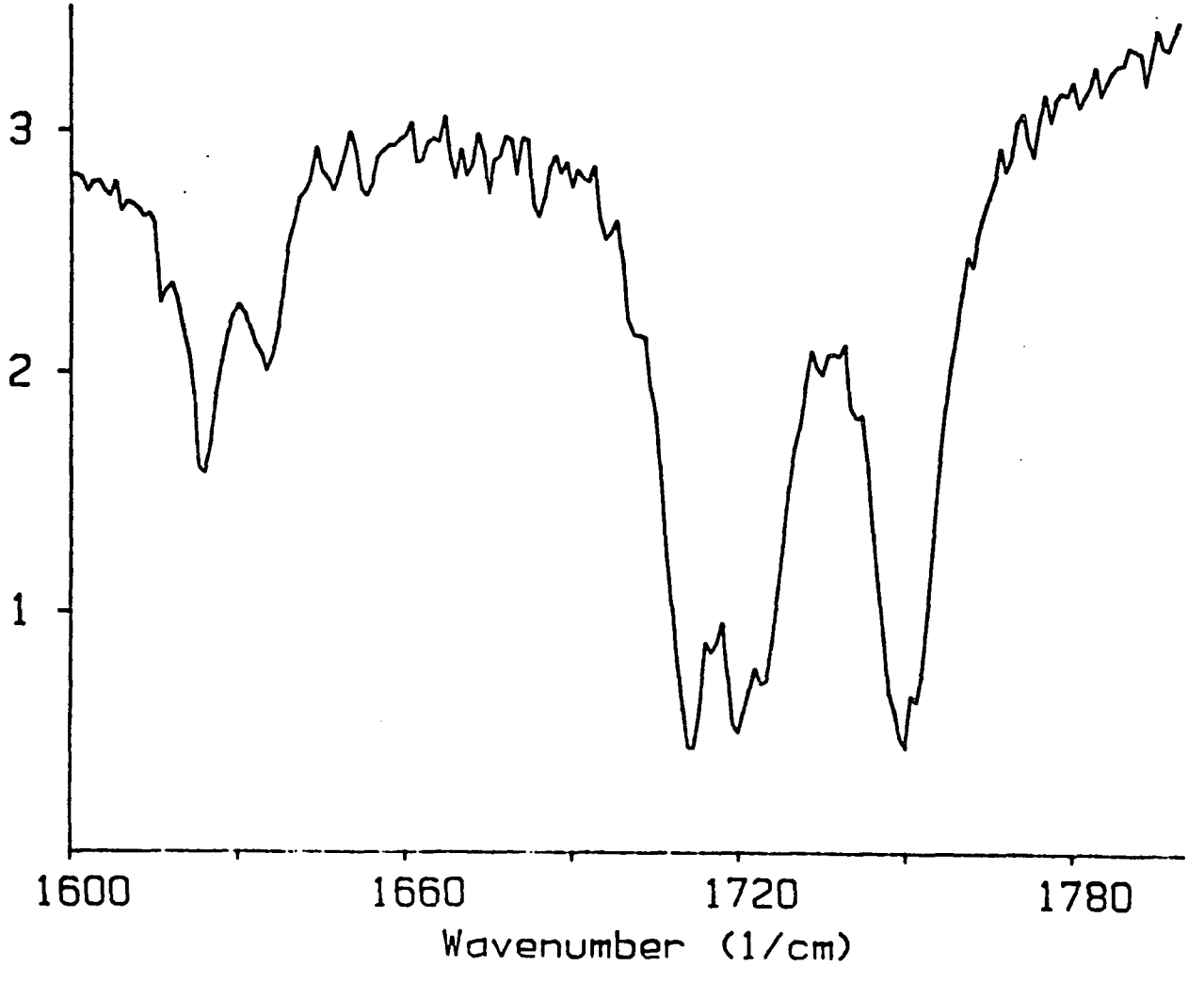

Figure 117: Solid-State FT-IR Spectrum of **18** at Room Temperature

For Sb-8 **117-d**, the solid-state FT-IR spectrum shows at least four different ester IR bands which upon warming merge into one band (Figure 118). This process is completely reversible indicating a dynamic process in the solid-state on the IR time scale.

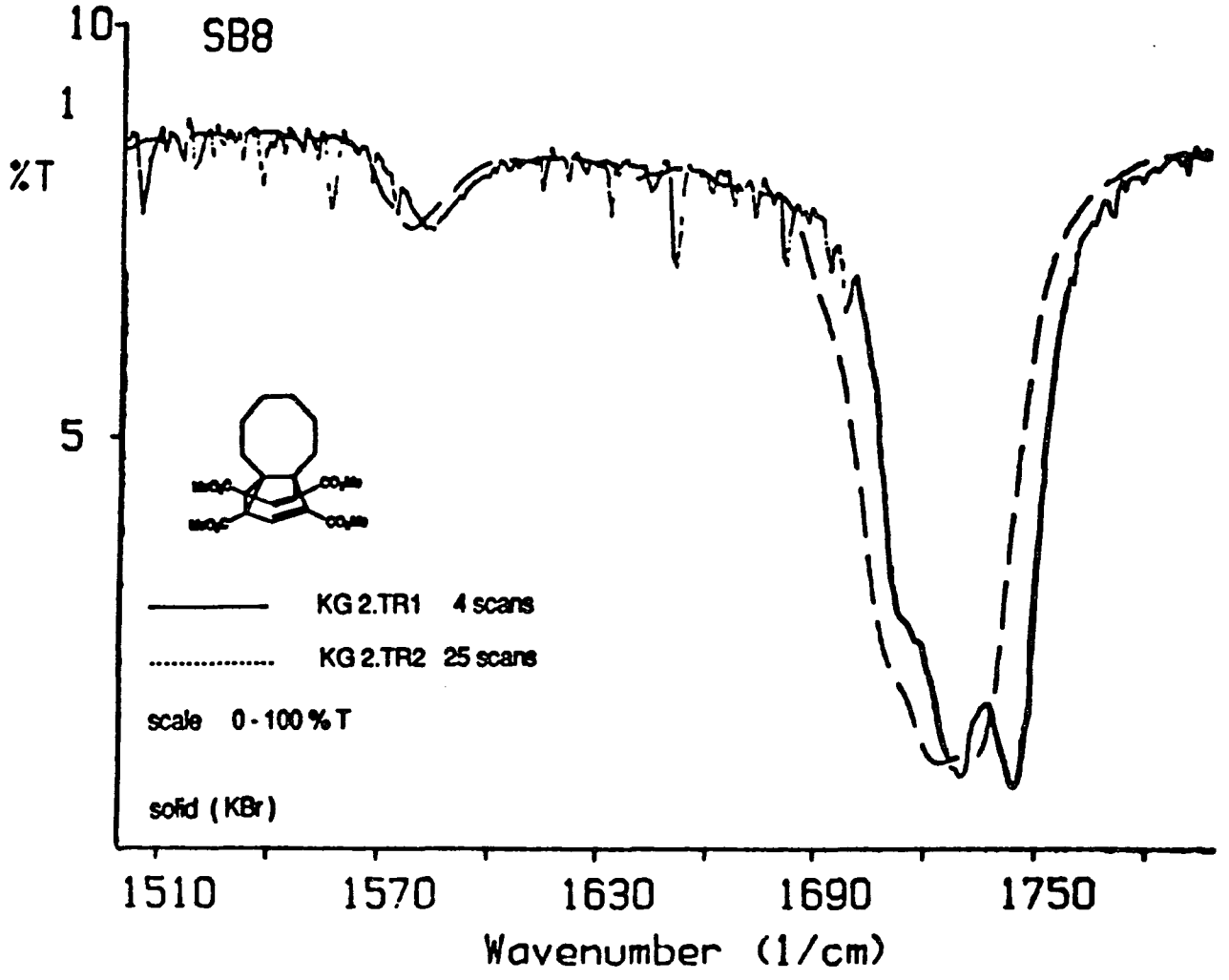

Figure 118: Solid-State IR Spectrum of 117-d

4.2.2. Room Temperature ^{1}H and ^{13}C-NMR Studies on 18

Nuclear Magnetic Resonance (NMR) has proved to be a powerful tool for the determination of barriers in molecules with fluctuating bonds. Before attempting an analysis of the low temperature ^{13}C-NMR spectra, an interpretation of the room temperature proton and carbon NMR data is necessary.

The 300 MHz ^{1}H and ^{13}C-NMR spectra of compound **18** recorded at room temperature are shown in Figures 119 and 120. The proton spectrum shows four averaged resonances at δ 1.33, 3.79, 3.82 and 7.07 ppm, which have been assigned to $2(H_9)$, $4(-OCH_3)$, (H_1, H_5) and (H_3, H_7) respectively. Among them, (H_1, H_5) which appears at 3.82 ppm provides much information regarding this rearrangement. Although H_1 is a cyclopropyl proton and H_5 is a diallylic proton, both H_1 and H_5 appear together at δ 3.82 ppm which derives from the average of two rapidly equilibrating, structurally indistinguishable valence tautomers.

The ^{13}C spectrum of compound **18** at room temperature has been determined and consists of six resonances at δ 16.2, 27.9, 52.6, 87.9, 129.2 and 166.7 ppm assigned to the carbons C_9, $C_{1,5}$, $4(-OCH_3)$, $C_{2,4,6,8}$, $C_{3,7}$ and 4(C=O) respectively. The ^{13}C result of compound **18** indicates that $C_{1,5}$ and $C_{2,4,6,8}$ resonances are averaged between the cyclopropyl and vinyl resonances expected for the static structure.

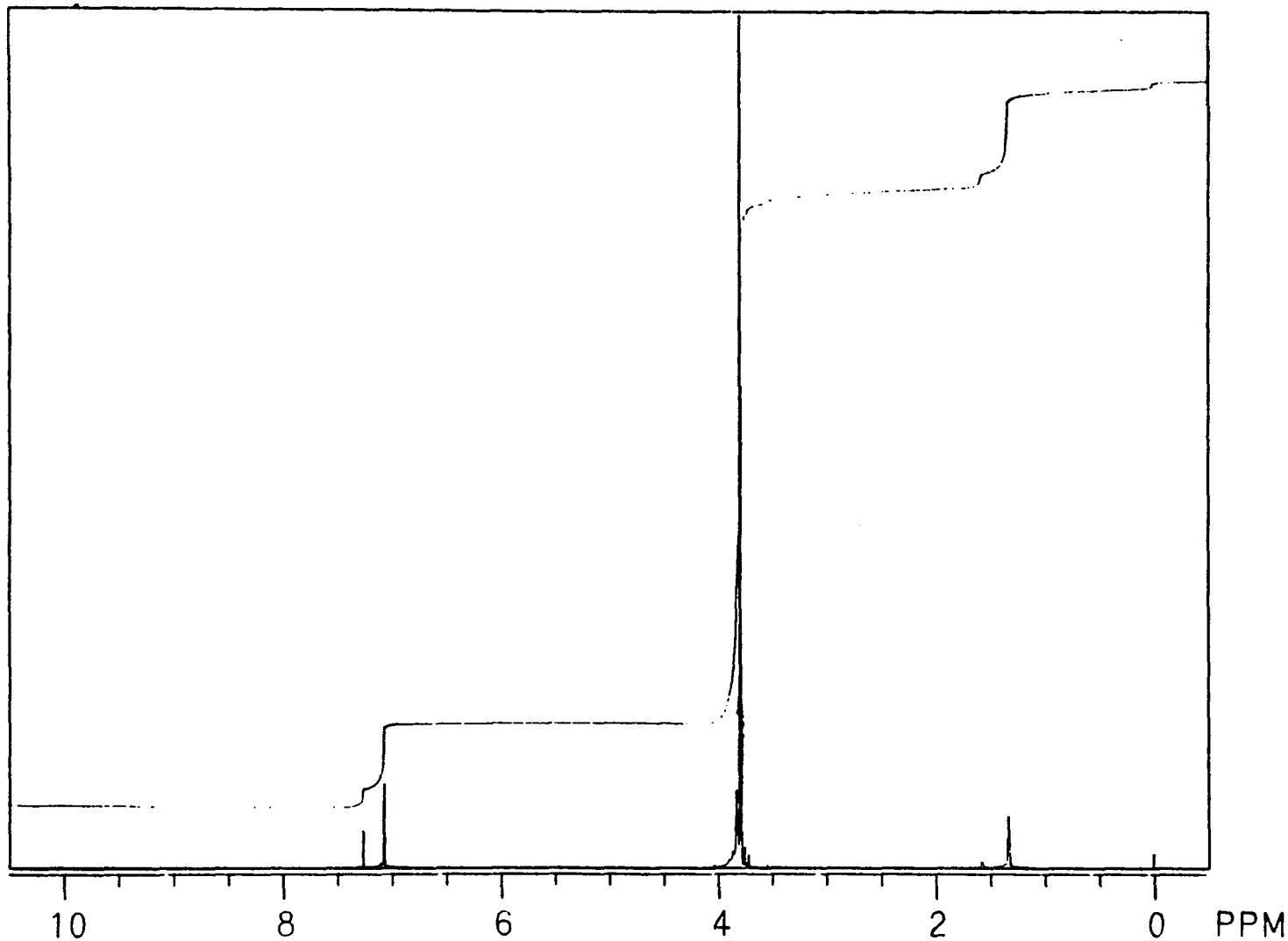

Figure 119: ^{1}H-NMR Spectrum of **18**

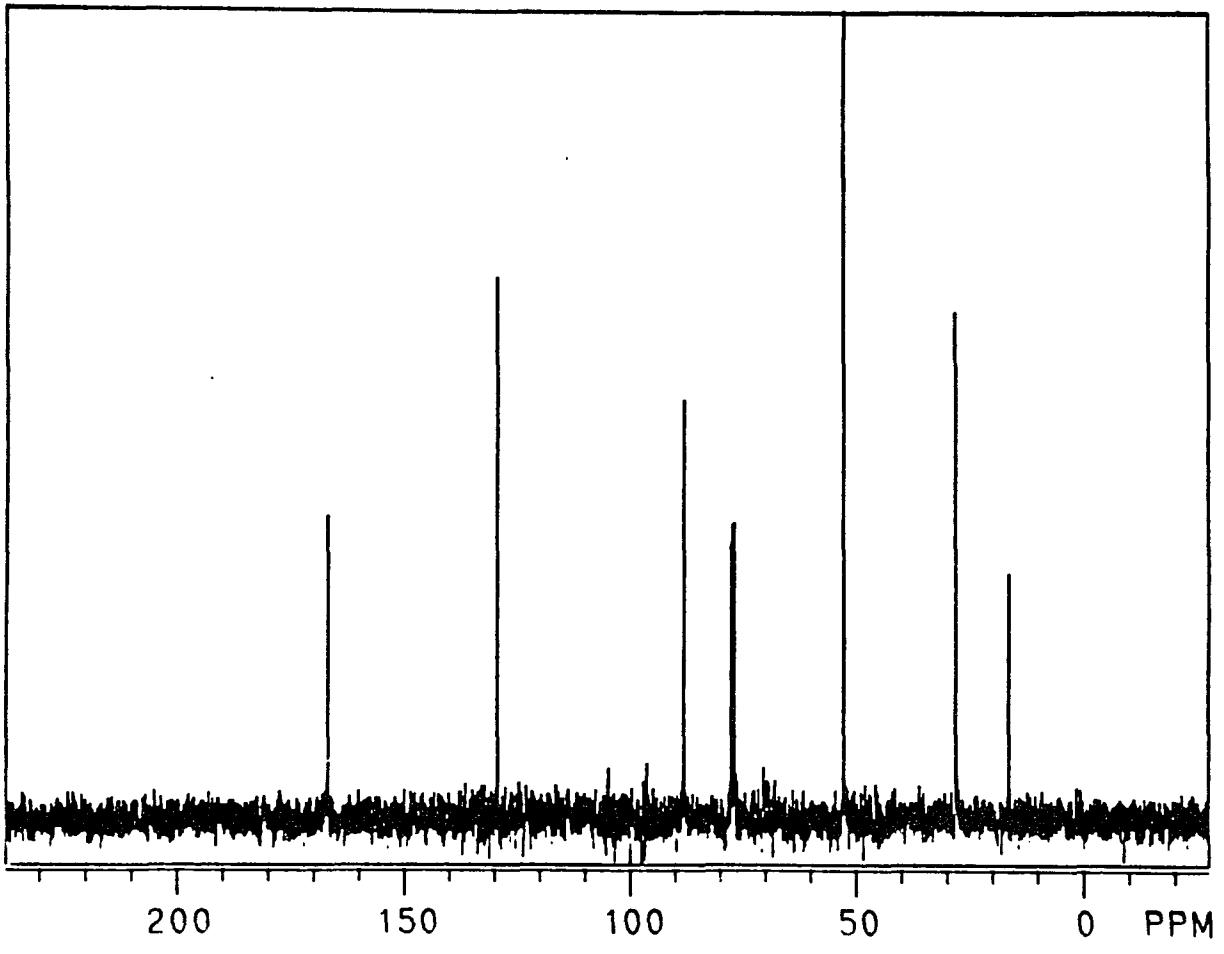

Figure 120: ^{13}C-NMR Spectrum of **18**

4.3.1. Determination of the Fluxional Barrier of 18

The assignment of the activation energy ($\Delta G^{\neq}$) in this system is based on the assumption of a transition state resembling a neutral bishomoaromatic structure (Figure 121).

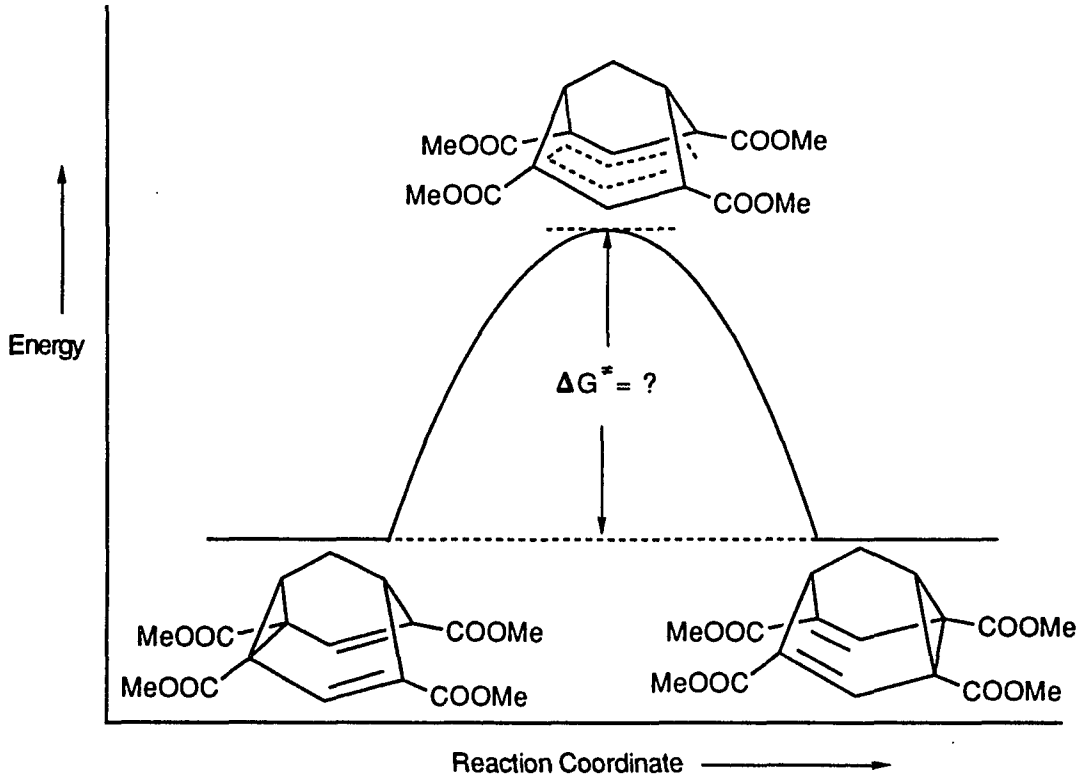

Figure 121: Degenerate Cope Rearrangement of **18**

The chemical equilibrium in this process depends on the rate constant k_r. The bigger the k_r, the faster the reaction. The rate constant k_r of isomerization is given by the Eyring equation {1}.[89,90]

$$k_r = \frac{kT}{h} e^{-\Delta G^{\neq}/RT} \quad \text{---------- \{1\}}$$

Equation {1} arises from the absolute rate theory and can be expressed in the following logarithmic form, using the numeric values of the Boltzmann constant k, the gas constant R, the Planck constant h and log e.[91]

$$\Delta G^{\neq} = 4.57T_c(10.32 + \log \frac{T_c}{k_r}) \text{ cal/mol} \quad \text{---------- \{2\}}$$

To calculate $\Delta G^{\neq}$ as shown in eq. {2}, we need to know two unknowns, T_c (coalescence temperature) and k_r (rate constant). T_c and k_r can be obtained from low temperature solution ^{13}C-NMR and solid-state CP-MAS ^{13}C-NMR spectra.

If two nuclei have different chemical environments (A is different from B) or if they are interconverting so slowly that the rate constant (k_r) is very small relative to the chemical shift difference, then two separate signals for the nuclei A and B will be observed in the NMR spectrum. (We are assuming uncoupled signals whose intensities are equal.) In an equilibrating system, the rate constant (k_r) is a function of temperature and the NMR spectra of such systems are temperature dependent. This is shown schematically in Figure 122.

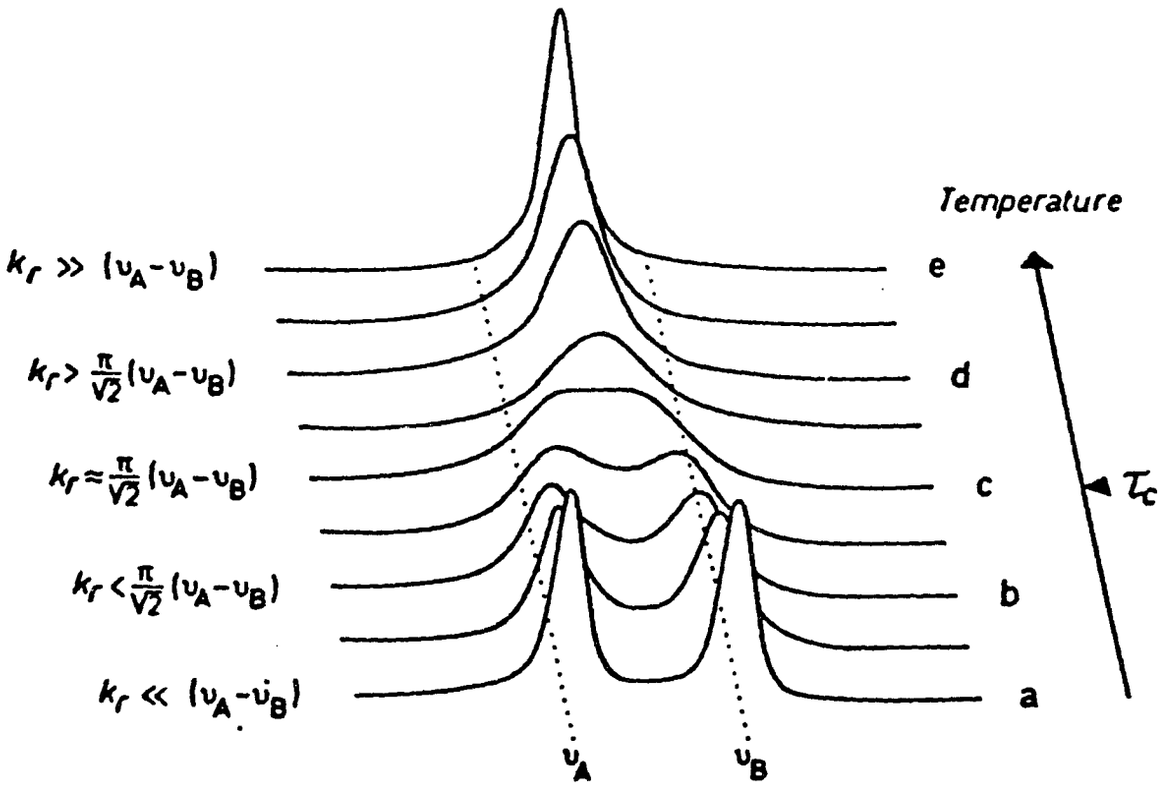

Figure 122: Temperature dependence of chemical shifts and line shapes due to intramolecular mobility[90]

In this illustration, it is seen that at low temperature k_r is very small (only a small percentage of the molecules are interconverting) and the rearrangement is said to be slow on the NMR time scale. Two sharp peaks are seen separated by $\Delta\upsilon = \upsilon_A - \upsilon_B$. As the temperature is increased, k_r increases and the signals first broaden and approach each other (b in Figure 122). At the coalescence temperature (T_c), the signals have merged into one very broad peak (c in Figure 122) which is almost indistinguishable from the baseline. At the coalescence temperature, the rate constant is related to the chemical shift difference for A and B by eq.{3}.

$$k_r = \frac{\pi}{\sqrt{2}}(\nu_A - \nu_B) \quad \text{---------- } \{3\}$$

The rate increases with increasing temperature until the signals for A and B have become one sharp peak whose chemical shift is $1/2(\upsilon_A+\upsilon_B)$ (e in Figure 122). If the coalescence temperature is known, k_r can be calculated using eq. {3}.

If T_c is not known, the rate constant can be estimated by measuring the line widths of the signals at half height near T_c, $\Delta\upsilon_{1/2}$ (T_c), and using eq. {4}.

$$k_r \equiv 2.2\Delta\nu_{1/2(T_c)} \quad \text{---------- } \{4\}$$

Once the value for k_r is determined, $\Delta G^{\ddagger}$ can be calculated for the equilibrium using eq. {2}.

The variable temperature solution ^{13}C-NMR spectrum of **18** is shown in Figure 123.

As the temperature is decreased, the signals for $C_{2,4,6,8}$ should broaden first. We would expect the largest chemical shift difference in the static state between $C_{2,8}$ and $C_{4,6}$, as one set of carbons will be part of a cyclopropyl ring and the other set will be vinylic. Carbons 3 and 7 should be equivalent in both equilibrating structures and should not show broadening due to changes in the rate of Cope rearrangement.

The ^{13}C spectrum at 100 MHz of compound **18** was examined as a function of temperature. Below −80°C, there is clear evidence of line broadening due to the slowing of the degenerate Cope rearrangement. Even at −103°C, the lowest temperature achievable with the spectrometer available to us, the $C_{2,4,6,8}$ signal had not yet coalescenced. The resonances for the methoxy and carbonyl carbons are still sharp, as are the resonances for carbons 1 and 5.

In our studies, coalescence of the signals for carbons 2, 4, 6. and 8 has not been reached at −103°C. We can therefore only estimate an upper limit for $\Delta G^{\ddagger}$ of the Cope rearrangement at an approximate coalescence temperature of −110°C.

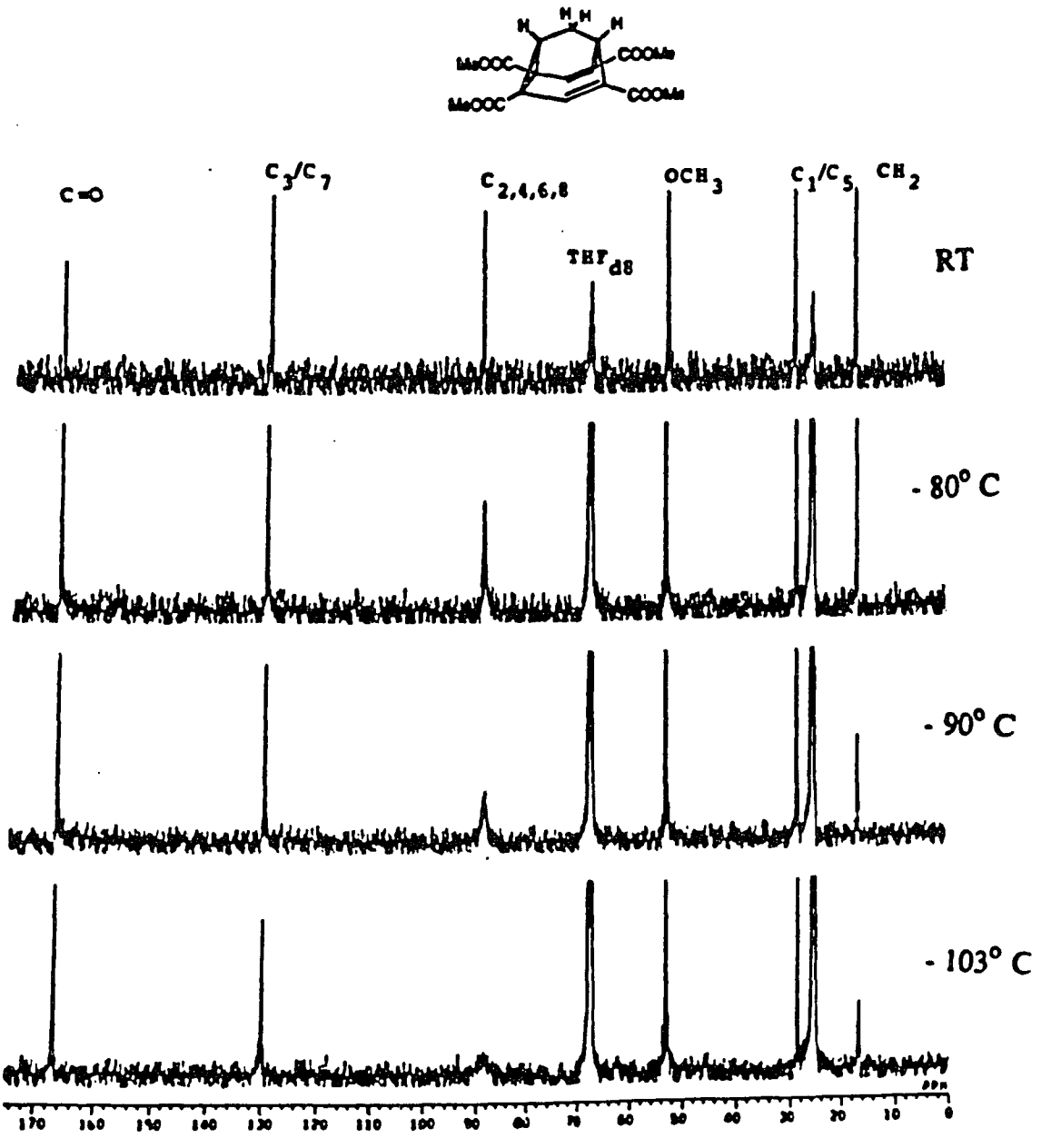

Figure 123: Variable Temperature Solution ^{13}C-NMR Spectra of 18 in THF-d_8

Therefore the chemical shift differences between C_2/C_8 (cyclopropyl carbons) and C_4/C_6 (olefinic carbons) of static **18** are required and were obtained from variable temperatures solid-state CP-MAS ^{13}C-NMR spectra. They were measured at 22°C and −20°C respectively (Figure 124). It confirmed the results of the X-ray analysis that 2,4,6,8-tetracarbomethoxybarbaralane **18** in the solid-state is a static molecule with no detectable Cope rearrangement. The chemical shift values for the cyclopropyl carbons C_2/C_8 (δ = 47.8 and 40.2 ppm) and for the olefinic carbons C_4/C_8 (δ = 128.09 ppm) from the solid-state spectrum allowed us to calculate the activation energy for the Cope rearrangement of **18** at the estimated coalescence temperature (T_c = −110°C). The resulting value of 6.24 kcal/mol is ca 1.20 kcal/mol lower than the value for barbaralane itself ($\Delta G^{\neq}_{163}$ = 7.44 kcal/mol)*.[4] The four carbomethoxy groups therefore lower the activation energy for the Cope rearrangement in barbaralane by 1.20 kcal/mol. While this value qualitatively agrees with the theoretical predictions, it nevertheless is smaller than expected.

---

* $\Delta G^{\neq}_{163}$ was calculated by using the equation: $\Delta G^{\neq} = \Delta H^{\neq} - T\Delta S^{\neq}$, where $\Delta H^{\neq}$ = 7.32 kcal/mol, $\Delta S^{\neq}$ = −0.73 eu and T = 163K.[4]

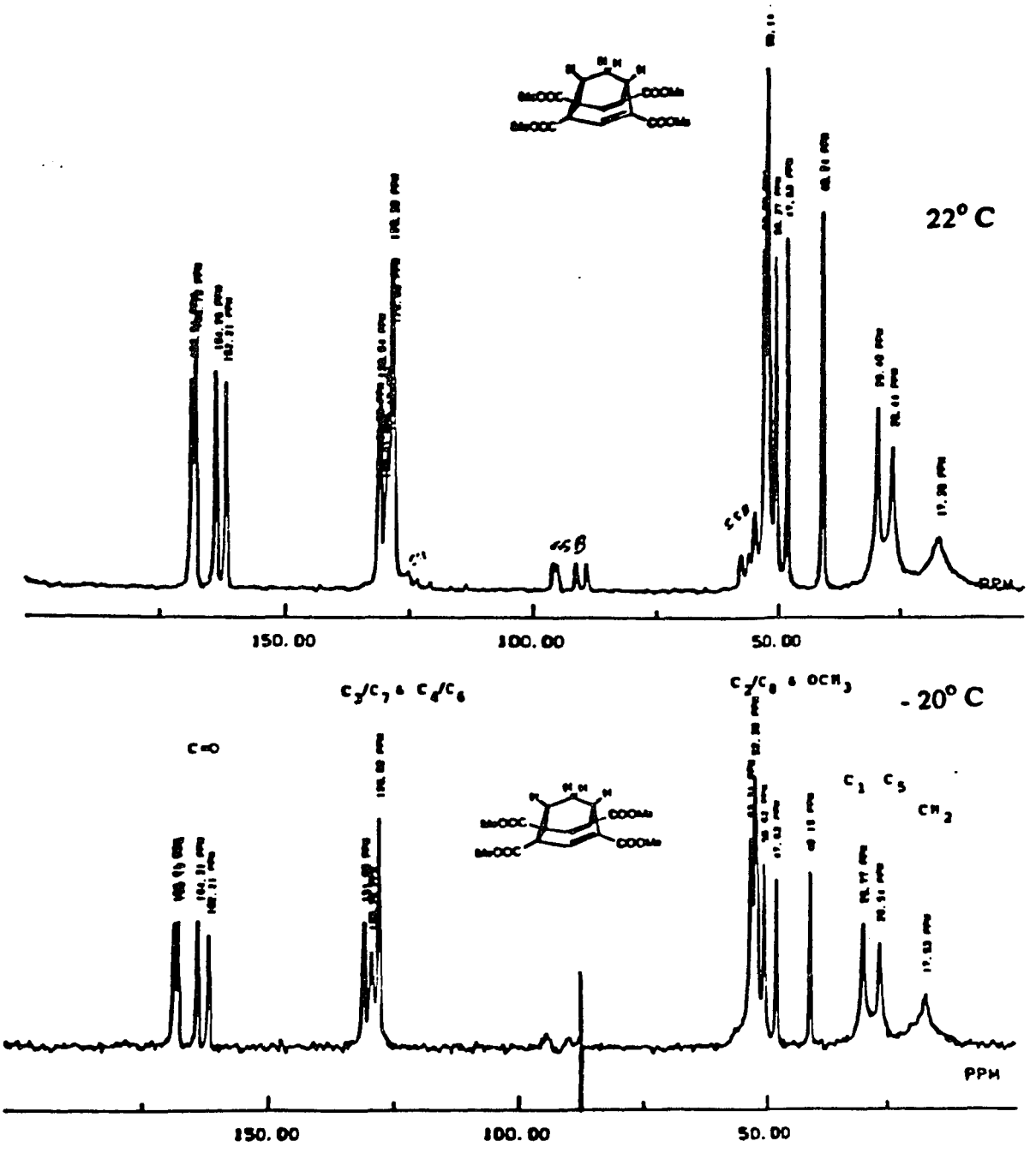

Figure 124: Variable Temperature Solid-state CP-MAS ^{13}C-NMR Spectra of 18

4.3.2. Determination of the Fluxional Barrier of 23

After confirming the predicted acceleration of the Cope rearrangement by four carbomethoxy groups (electron-withdrawing groups) at the $C_{2,4,6,8}$ positions of the barbaralane (**18**), we investigated the effect of 2,6-disubstitution in barbaralane (**23**). Like **18**, the fluxionality of **23** was detected by room temperature ^{1}H and ^{13}C-NMR analyses (Figures 125 and 126).

The room temperature ^{1}H and ^{13}C spectra showed an averaged structure of compound **23** based on:

(a) a multiplet integrating for two protons (H_1/H_5) at δ 3.22 ppm, and
(b) an averaged quarternary carbons (C_2/C_6) signal at δ 83 ppm and an averaged methine carbons (C_4/C_8) signal at δ 80 ppm.

In solution at ambient temperature, the degenerate Cope rearrangement of **23** is fast on the ^{1}H and ^{13}C-NMR time scales. Lowering the temperature will result in line broadening, coalescence phenomena and eventually separation into signals resulting from the ^{13}C atoms of the non-rearranging valence tautomers.

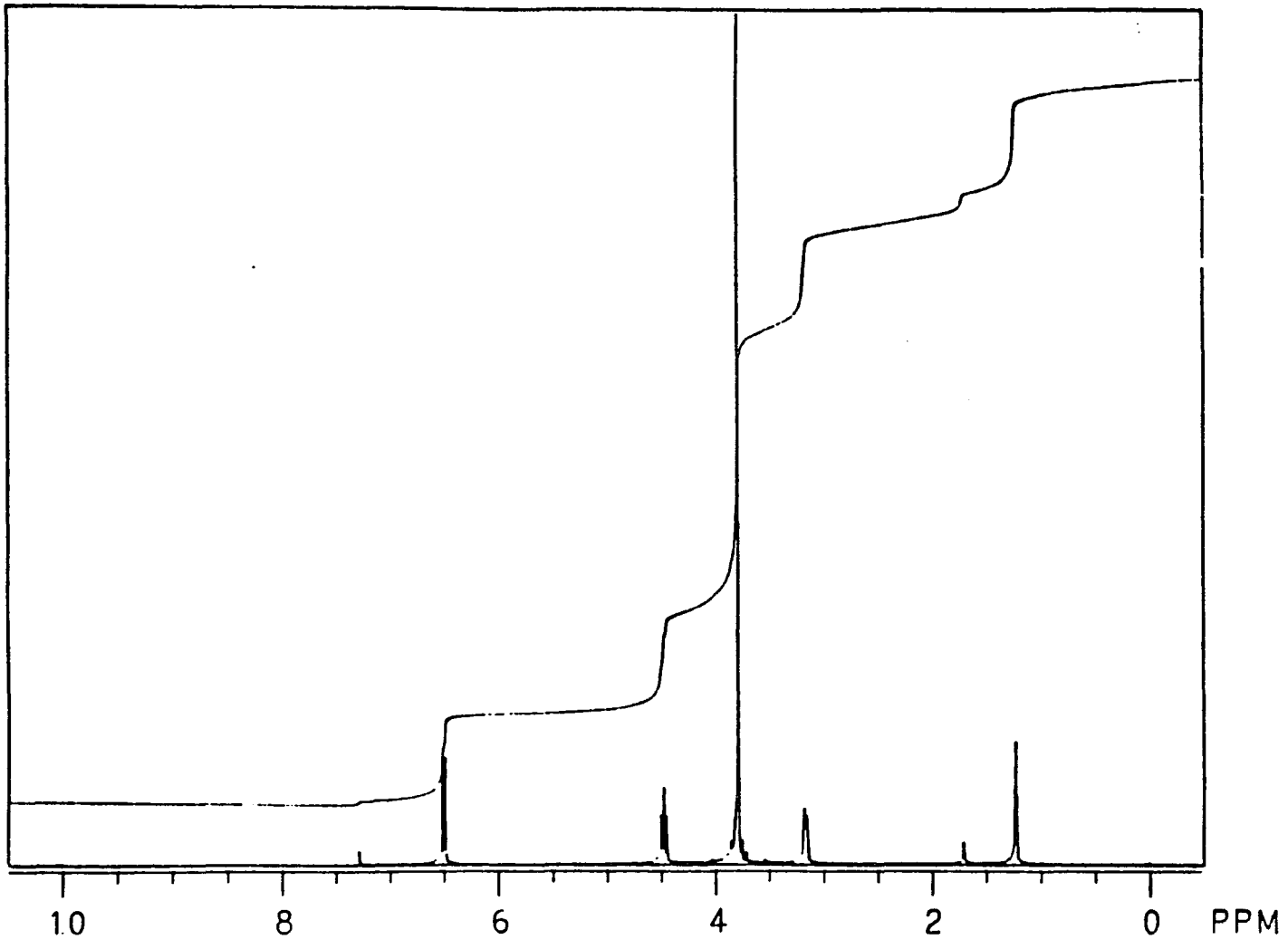

Figure 125: Room Temperature ^{1}H-NMR Spectrum of **23**

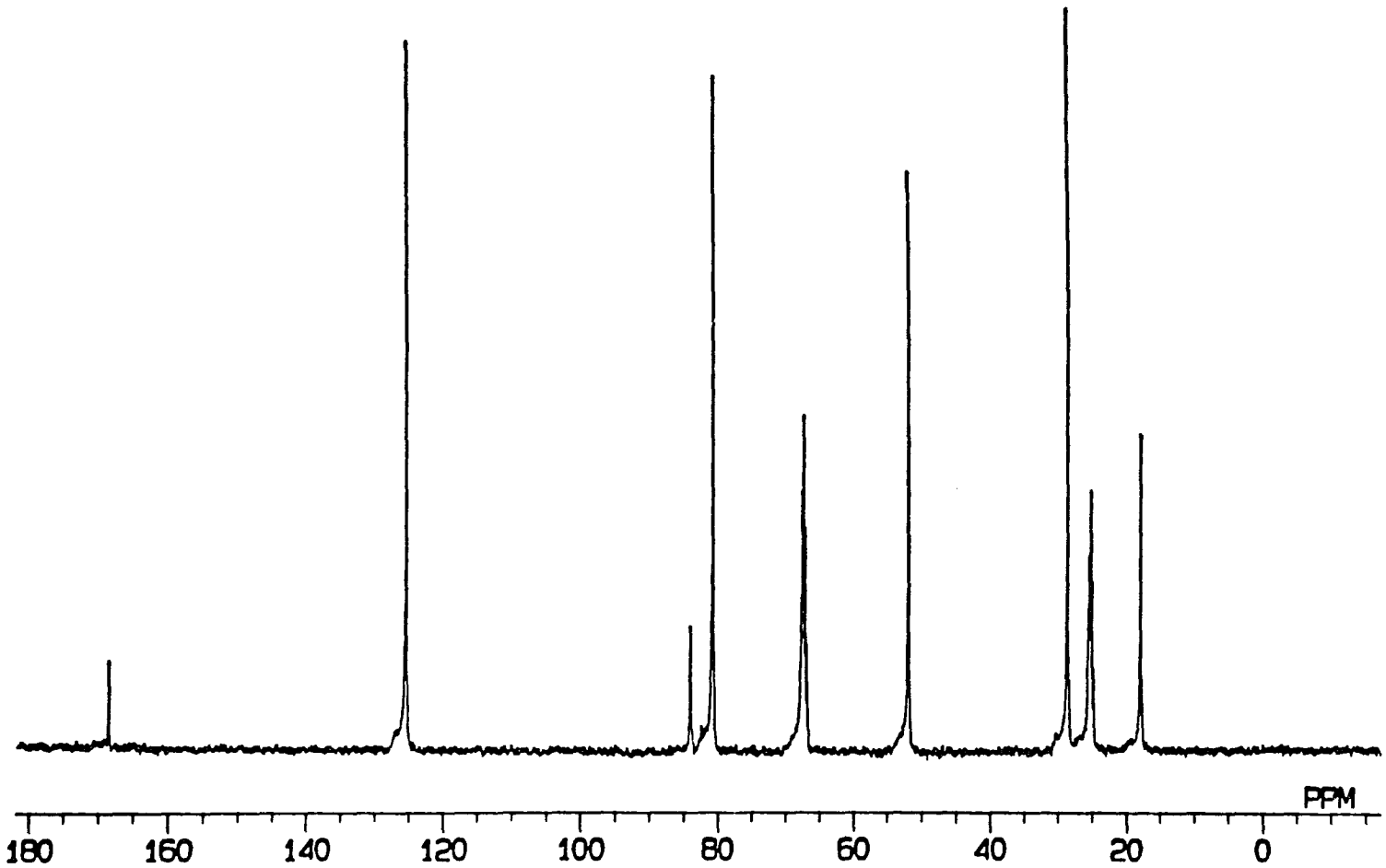

Figure 126: Room Temperature ^{13}C-NMR Spectrum of 23

Variable temperatures solution ^{13}C-NMR spectra of **23** in tetrahydrofuran-d_8 were measured with a ^{13}C frequency of 100 MHz instrument (Figure 127). The signal of C_2/C_6 as well as that of C_4/C_8 begins to broaden at −81°C. At −110.6°C, the lowest temperature attainable with the spectrometer available to us, coalescence of the signals (C_2/C_6 and C_4/C_8) has been reached. Further measurements below −110.6°C were not possible with this instrument to determine the chemical shift data for the non-exchanging valence tautomer. Since compound **23** is a liquid, the technique of solid-state CP-MAS ^{13}C-NMR studies for getting the chemical shift values was not possible. Thus, in order to extract the rates of the exchange process, it was necessary to obtain estimates for the chemical shifts at the low temperature limit. At this point, we felt confident that we could use the ^{13}C-NMR spectrum of 2,4,6-tricarbomethoxybarbaralane **31-a** (Figure 43) as a model for the non-rearranging valence tautomer because it existed as single valence tautomer (see section 2.1.2, p. 51)

That the shifts of C_2 and C_6 for the 2,4,6-tricarbomethoxy-barbaralane **31-a** are indeed appropriate for the analogous nuclei in 2,6-dicarbomethoxybarbaralane **23** itself is confirmed by agreement between the observed shift (δ = 83.5 ppm) for C_2/C_6 in **23** and the averaged (δ=82.05 ppm) of the two shifts in the model **31-a**. A value of chemical shift difference ($\upsilon_A - \upsilon_B$) = 94.62 ppm, corresponding to 9462 Hz with 100 MHz instrument at −110°C, was used in the calculation of rate constant for diesterbarbaralane **23**.

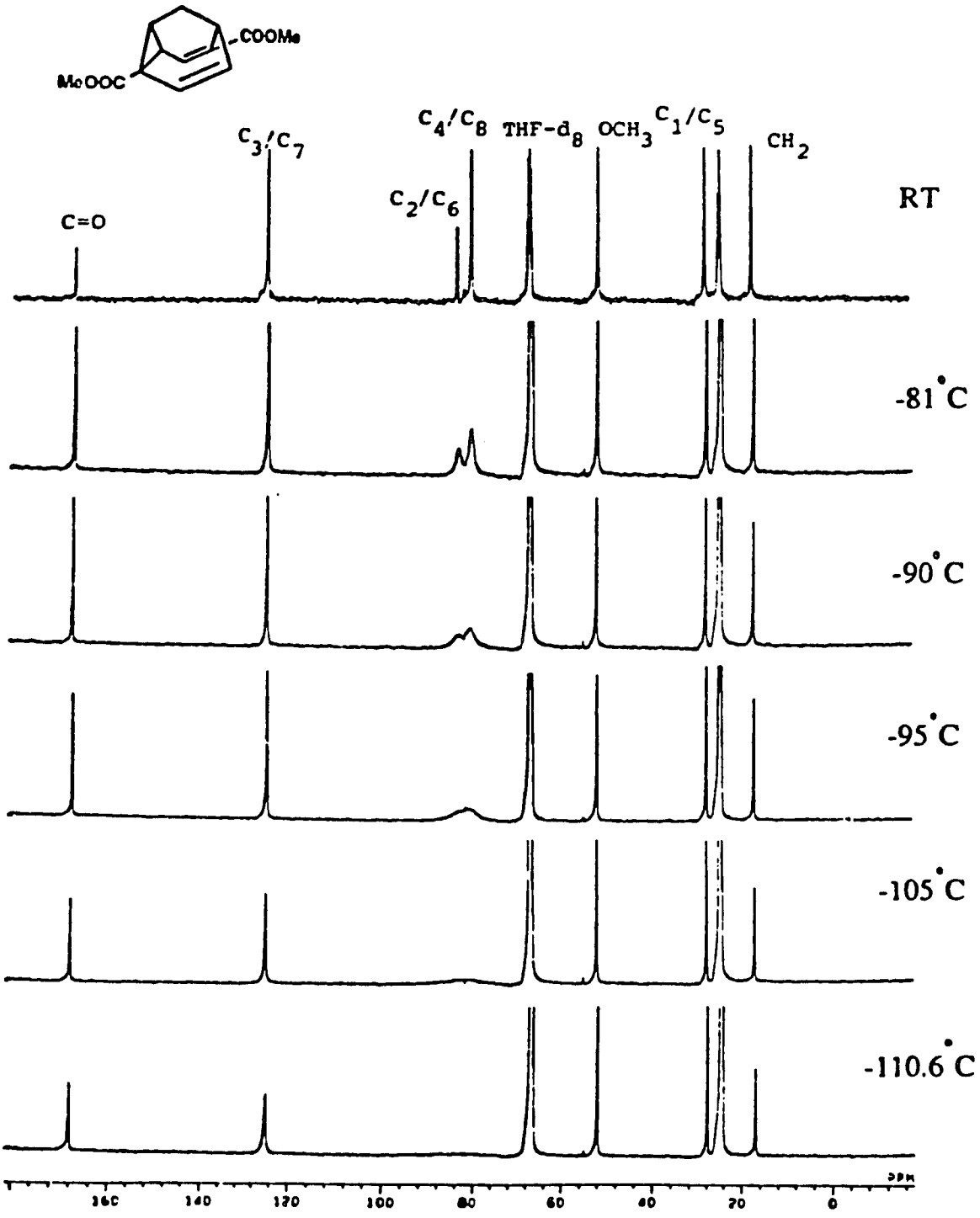

Figure 127: Variable Temperatures Solution ^{13}C-NMR Spectra of 23 in THF-d_8

The fluxional barrier of **23** in THF-d_8 was thereby estimated to be $\Delta G^{\ddagger}_{163}$ = 6.11 kcal/mol, which is ca 1.33 kcal/mol lower than the value for unsubstituted barbaralane itself ($\Delta G^{\ddagger}_{163}$ = 7.44 kcal/mol)*.[4]

A similar lowering of the barrier by carboxymethyl groups is found for 2,4,6,8-tetracarbomethoxybarbaralane 18 ($\Delta G^{\ddagger}$ = 6.24 kcal/mol) (see section 4.3.1, p. 165). It is remarkable that the fluxional barraier of 2,6-dicarbomethoxybarbaralane **23** is slightly lower than that of 2,4,6,8-tetracarbomethoxybarbaralane **18** which is due possibly to the orientation of four ester groups in **18**.

---

* $\Delta G^{\ddagger}_{163}$ was calculated by using the equation: $\Delta G^{\ddagger} = \Delta H^{\ddagger} - T\Delta S^{\ddagger}$, where $\Delta H^{\ddagger}$ = 7.32 kcal/mol, $\Delta S^{\ddagger}$ = –0.73 eu and T = 163K.[4]

4.3.3. 2-Carboxamido-6-carbomethoxybarbaralane 95-a: A Fluxional Molecule!

So far, we have observed fluxional characters only in the symmetrically substituted barbaralanes such as 2,4,6,8-tetracarbomethoxybarbaralane **18** and diesterbarbaralane **23**. The ^{1}H and ^{13}C spectra of diagonally unsymmetrical disubstituted barbaralane, 2-carboxamido-6-carbomethoxybarbaralane **95-a**, at room temperature also describe its dynamic character (Figures 128 and 129). Due to the electron-withdrawing abilities of $-COOCH_3$ and $-CONH_2$ substituents (having very similar Hammett-σ constants,[73] σ_p-$COOCH_3$ = 0.636 and σ_p-$CONH_2$ = 0.627, respectively), compound **95-a** exhibits fluxional character.

The presence of fluxional character in **95-a** is known from its room temperature ^{1}H and ^{13}C-NMR spectra by showing:

(a) a symmetric ^{1}H-NMR pattern and
(b) the carbon chemical shifts of C_2, C_4, C_6 and C_8 which appeared in a region of averaged cyclopropyl and olefinic carbons.

Similar to previous fluxional molecules **18** and **23**, we measured variable temperature solution ^{13}C-NMR spectra of **95-a** in tetrahydrofuran-d_8 with a ^{13}C frequency of 100 MHz instrument (Figure 130).

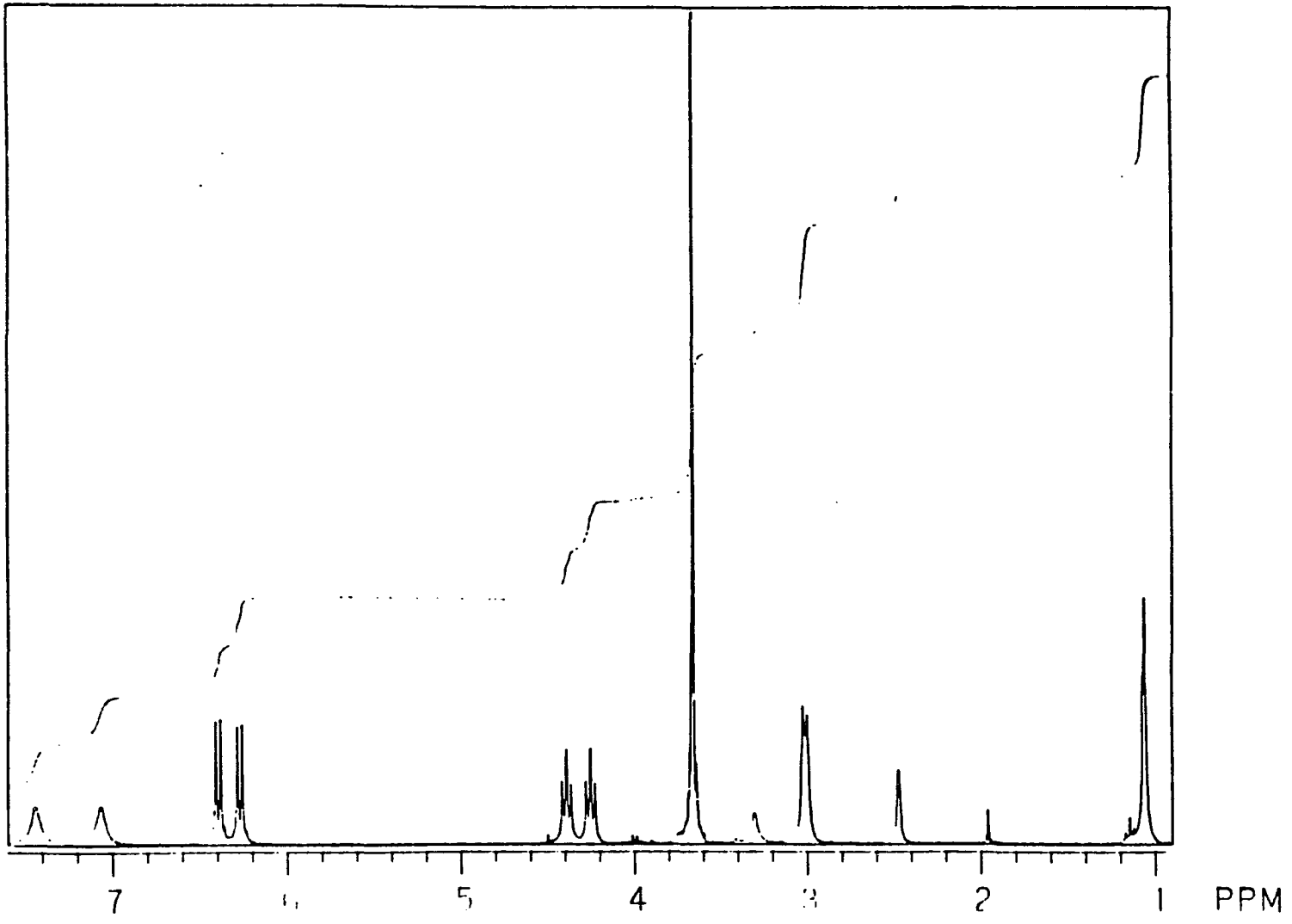

Figure 128: Room Temperature ^{1}H-NMR Spectrum of **95-a**

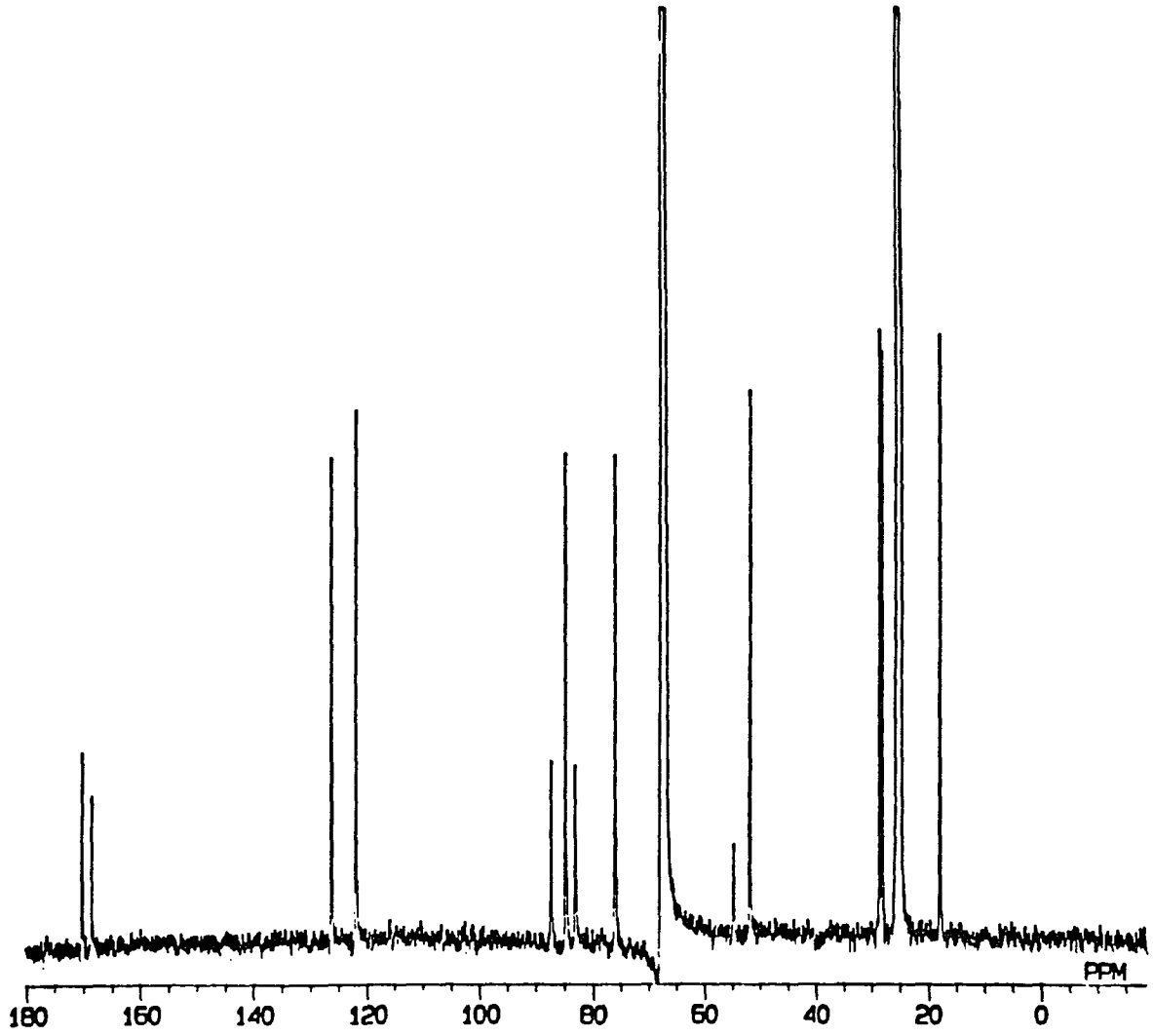

Figure 129: Room Temperature ^{13}C-NMR Spectrum of 95-a

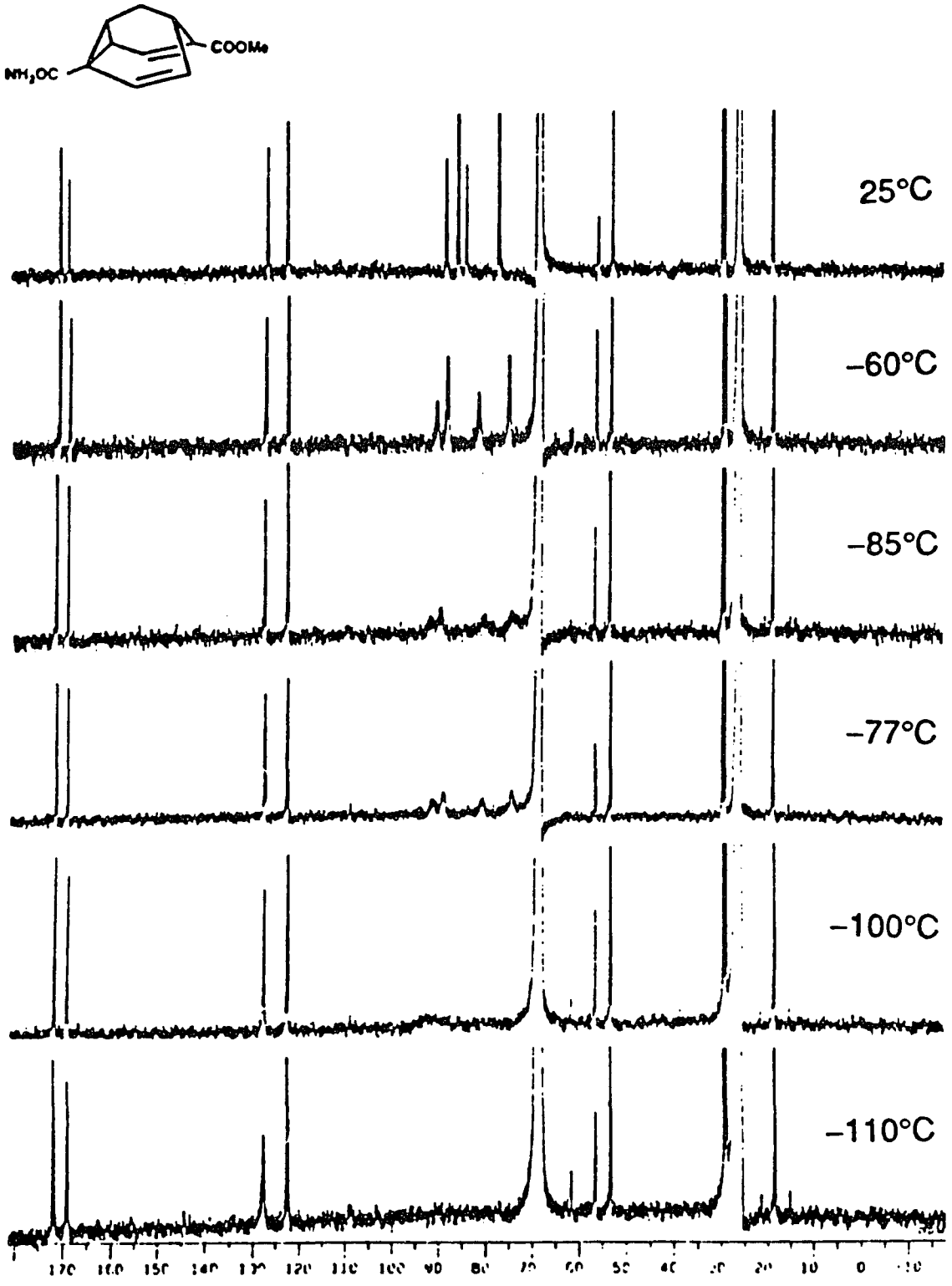

Figure 130: Variable Temperature Solution ^{13}C-NMR Spectra of 95-a in THF-d_8

The signals of C_2, C_4, C_6 and C_8 which appear between δ 76-89 ppm begin to broaden at −60°C. At −110°C, the lowest temperature attainable with the spectrometer available to us, coalescence of the signals for C_2, C_4, C_6 and C_8 has been reached. This temperature limit has frustrated our attempts to determine coalescence temperatures unambiguously.

So far, we have performed variable temperature solution ^{13}C-NMR experiments for 2,4,6,8-tetracarbomethoxybarbaralane **18**, 2,6-dicarbomethoxybarbaralane **23** and 2-carboxamido-6-carbomethoxy-barbaralane **95-a**. Coincidentally, all three compounds exhibit identical coalescence temperatures of ca −110°C. Although NMR line shape analysis could not be pursued to temperatures lower than −110°C with our instrument, the upper limit of the Cope energy barrier of **18** has been calculated with the help of variable temperatures solid-state CP-MAS ^{13}C-NMR studies (Section 4.3.1, p. 165). On the other hand, that of **23** has been estimated with the assistance of model 2,4,6-tricarbomethoxybarbaralane **31-a** (Section 4.3.2, p. 173). We have noticed from both determinations that there is no pronounced differences in substituent effects between tetraester and diester substitution (6.24 kcal/mol vs. 6.11 kcal/mol). With this knowledge and similar coalescence temperatures of all three compounds in hand, we would like to predict that the upper limit of compound **95-a** will be very similar to that of compounds **18** and **23**. Finally, since the Hammett-σ constants of $-CONH_2$ and $-COOCH_3$ are very similar, 0.627 and 0.636 respectively,[73] it is expected that **95-a** will have a fluxional barrier quite similar to that of diester **23**.

5.1. CONCLUSION

In order to lend great support to confirming Hoffmann's[15] and Dewar's[19] theoretical investigations of the effects of substituents on the Cope rearrangement in molecules of type **118**, we have investigated a number of electron acceptor substituted barbaralanes as shown in Figure 131.

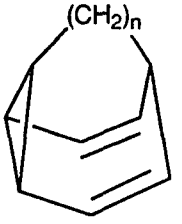

n = 0, 1, 2

118

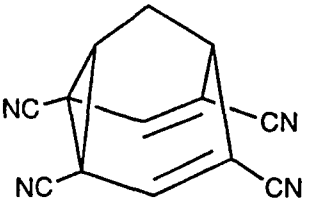

19

A new four-step sequence to 2,4,6,8-tetracarbomethoxybarbaralane **V** starting from the readily available 2,4,6,8-tetracarbomethoxybicyclo-[3.3.1]nonane-3,7-dione and utilizing the P_2I_4 induced Grob-fragmentation has been developed. Room temperature ^1H and ^{13}C-NMR studies in chloroform-d and IR investigation in CCl_4 of compound **V** reveal its fluxional character. However, room temperature solid-state CP-MAS ^{13}C-NMR studies, room temperature solid state FT-IR studies, high-resolution X-ray crystal structure analysis, and variable temperature vibrational analysis of the thermal ellipsoid of C_2 for compound **V** correspond to a static structure in the solid state.

Variable temperature solution ^{13}C-NMR studies and solid-state CP-MAS ^{13}C-NMR investigation allowed us to calculate the Cope activation

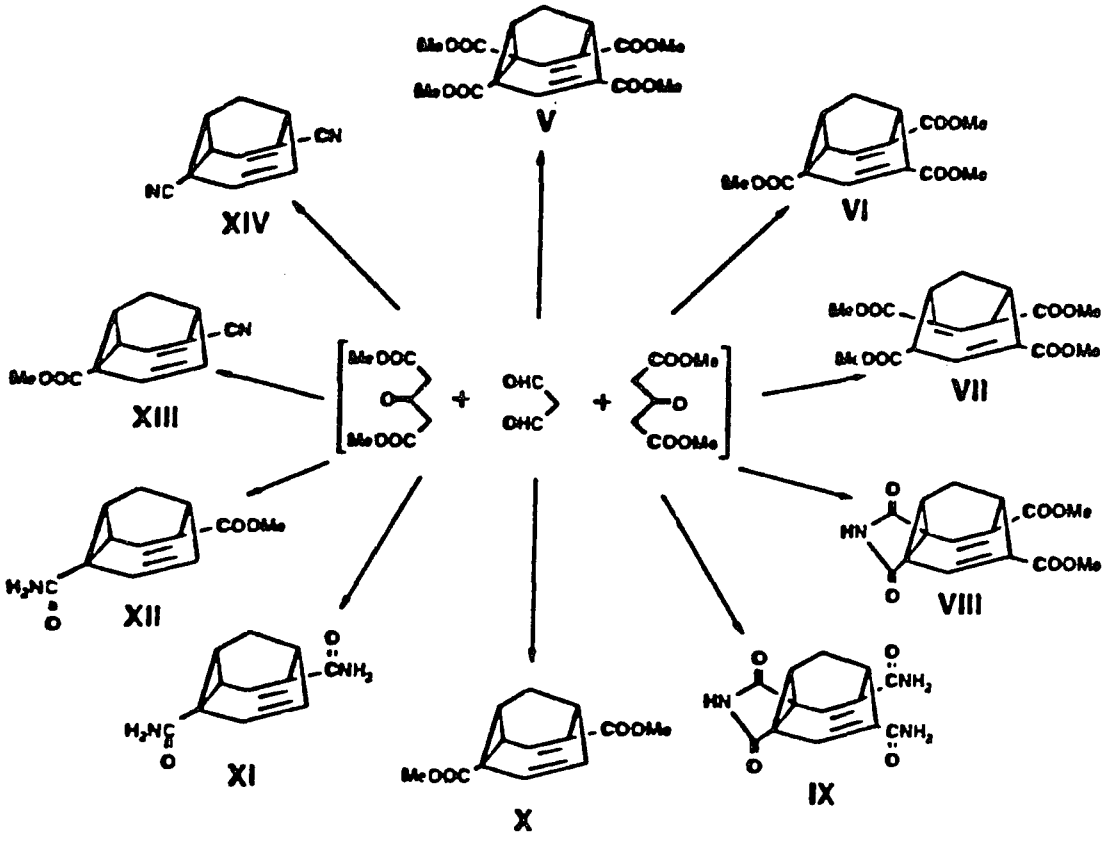

Figure 131: Electron Acceptor Substituted Barbaralanes Synthesized via the Weiss Reaction

barrier of V at 163 K. The resulting value of 6.24 kcal/mol is ca 1.24 kcal/mol lower than the value for barbaralane itself ($\Delta G^{\neq}$ = 7.44 kcal/mol).[4]

In the synthesis of compound V, two side products were identified as 2,4,6-tricarbomethoxybarbaralane VI and 2,4,6,8-tetracarbomethoxy dihydrobarbaralane VII. The ^{1}H and ^{13}C-NMR spectra highlighted

compound **VI** as the energetically favored tautomer in the Cope equilibrium.

In the attempted synthesis of 2,4,6,8-tetracyanobarbaralane **19**, barbaralane-4,6-dicarbomethoxy-2,8-dicarboximide **VIII** and barbaralane-4,6-dicarboxamido-2,8-dicarboximide **IX** were obtained as the sole products. ^{1}H and ^{13}C-NMR studies and X-ray crystal structure analysis strongly suggested their static behavior. The synthesis of compound **19** could be possible by reacting compound **IX** with sodium amide in liquid ammonia, followed by dehydration. Also debenzylation of compound **111** (Figure 105, p. 137) and further manipulation could possibly afford compound **19**.

Selective decarbomethoxylation, or hydrolysis and decarboxylation of 2,4,6,8-tetracarbomethoxy-Weiss compound led to the synthesis of 2,6-dicarbomethoxybarbaralane **X**. The fluxionality of compound **X** was detected by room temperature ^{1}H and ^{13}C-NMR analyses. From the variable temperature solution ^{13}C-NMR studies, a coalescence temperature of 163 K was found for compound **X**. Since the compound **X** is a liquid, the chemical shift difference between C_2 and C_6 could not be obtained from the solid-state CP-MAS ^{13}C-NMR technique. But, the rate of the exchange process of compound **X** has been calculated to be 6.11 kcal/mol, with the use of the ^{13}C-NMR spectrum of compound **VI** as a model. The fluxional barrier of **X** was predicted to be 1.33 kcal/mol lower than the value for unsubstituted barbaralane itself ($\Delta G^{\ddagger}_{163}$ = 7.44 kcal/mol).[4]

When compound **X** was treated with ammonia in methanol, 2,6-dicarboxamidobarbaralane **XI** and 2-carboxamido-6-carbomethoxy-barbaralane **XII** were obtained. The room temperature ^{1}H spectrum of compound **XI** shows its dynamic character. The Cope activation barrier of **XI** has not been calculated yet.

Although the compound **XII** is substituted by two different substituents, their Hammett-σ constants are very similar, and as expected, room temperature ^{1}H and ^{13}C spectra of **XII** illustrate its fluxional character. Variable temperature solution ^{13}C-NMR studies of **XII** provided us a coalescence temperature of 163 K. Attempts to measure NMR spectra below 163 K were unsuccessful. Since the coalescence temperatures of **V**, **X** and **XII** are so close (163 K) and the Cope activation barriers of **V** and **X** are so similar (6.24 vs 6.11 kcal/mol), the $\Delta G^{\neq}$ of **XII** is expected to show a striking resemblance to those of **V** and **X** as an upper limit. The position of two different substituents on **XII** has been predicted by their slight difference of Hammett-σ constants, and the agreement was obtained by its X-ray crystal structure.

When dehydration of compound **XI** was effected using the Burgess reagent as a very mild dehydrating agent, we obtained 2,6-dicyano-barbaralane **XIV** in 81% yield. Our result illustrates the value and the feasability of converting $-CONH_2$ into $-CN$ as ultimately proposed for transformation of 2,4,6,8-tetracarbomethoxybarbaralane **18** into 2,4,6,8-tetracyanobarbaralane **19**.

2-Carbomethoxy-barbaralane-6-carbonitrile **XIII** was obtained in 91% yield by dehydration of **XII** by using the Burgess reagent. Its equilibrium preference was predicted by the difference in Hammett-σ constants of two substituents. X-ray crystal structure analysis confirmed our prediction.

When we evaluate our results, we noted the strong equilibrium preferences for **VI, VIII, IX** and **XIII**. Regarding the dynamic barbaralanes (**V, X, XI, XII** and **XIV**), some fragmentary evidence which suggests the qualitative correctness of the predicted substituent effect has been found. The truly definitive example which will allow to provide the quantitatitve evaluation of the effect is in under way.

5.2. Outline of Further Studies

5.2.1.Synthetic Possibilities Toward 19

Hoffmann's[15] theoretically predicted homoaromatic molecule, 2,4,6,8-tetracyanobarbaralane **19**, is only two steps away from 4,6-dicarboxamido-barbaralane-2,8-dicarboximide **58**. Reaction of **58** with sodium amide in liquid ammonia may provide 2,4,6,8-tetracarboxamido analogue **56**. Once **56** is available, Burgess reagent should effectively dehydrate **56** into tetranitrile analogue **19** (Figure 132).

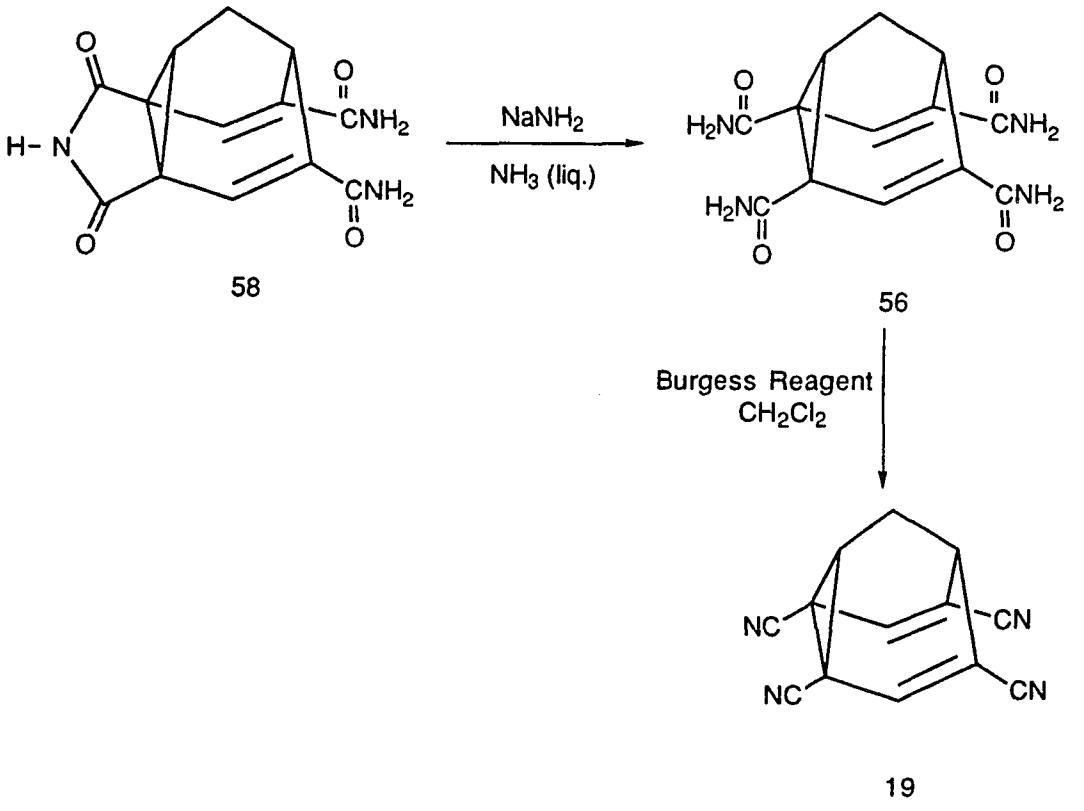

Figure 132: Synthetic Possibility Toward **19** Via **58**

Alternatively, compound **19** could be synthesized starting from compound **111** (Figure 133). Debenzylation to **65**, dehydration to **66** and P_2I_4 induced Grob-fragmentation may afford compound **19**. Another possible pathway toward **19** is debenzylation to **65**, P_2I_4 induced Grob-fragmentation to **56** and subsequent dehydration.

Compound **19** could also be prepared by using 2,6-dicarbomethoxy-triasterane-3,7-dione **68** as a precursor (Figure 56). Reaction with CuCN may open up the doubly activated cyclopropane ring of **68** providing diagonally symmetrical tetrasubstituted dienol **69**.

The efficient sequence of cyclization to **70**, reduction to **71**, P_2I_4 induced Grob-fragmentation to **72** and dehydration may yield compound **19**.

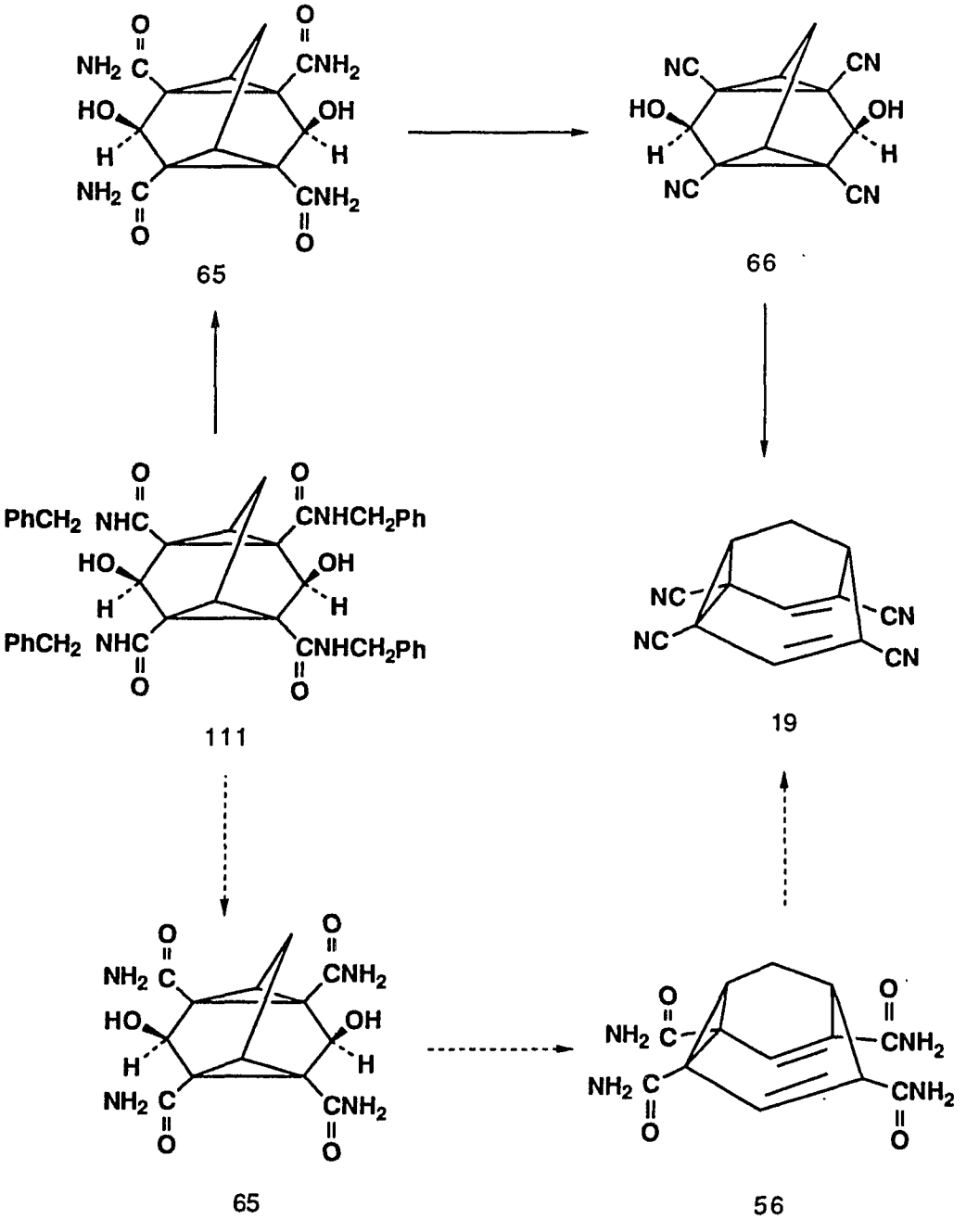

Figure 133: Synthetic Possibility Toward **19** Via **111**

5.2.2. Suggestion for the Extraction of Cope Energy Barrier ($\Delta G^{\neq}$) From FT-IR Studies

The solid-state FT-IR spectrum of Sb-8 **117-d** shows at least four different ester bands which upon warming merge into one band (Figure 117). This process is completely reversible indicating a dynamic process in the solid-state on the IR time-scale. Since the IR time-scale is much shorter than NMR time-scale, extraction of much lower activation energy of the degenerate Cope rearrangement from the dynamic IR spectra is strongly encouraged.

5.2.3. Suggestion for the NMR Line Shape Analysis

NMR line shape analysis could be done only down to −110°C for all dynamic compounds that we synthesized in this project. If we can obtain a better NMR facility with a very high resolution NMR instrument and measure down to −170°C, more accurate $\Delta G^{\neq}$ values can be calculated.

CHAPTER 6

6.1.0. EXPERIMENTAL SECTION

6.1.1. Spectroscopy

Pulsed Fourier transform 300 MHz ^{1}H and 75 MHz ^{13}C spectra were obtained with chloroform-d solutions (99.8% D, 0.03% v/v TMS, Aldrich) using a General Electric QE-300 spectrometer. Chemical shifts are in δ or ppm units downfield from Me_4Si as internal reference. Resonance splitting are described as s=singlet, d=doublet, t=triplet, m=multiplet, b=broad and AB=AB quartet. Coupling constants are reported in Hertz units (J value). Labile protons were exchanged using deuterium oxide (99.8% D, Aldrich, Gold Label). The assignment of the ^{13}C was confirmed by single frequency off resonance decoupled or proton coupled spectra.

The variable temperatures solution ^{13}C spectra were measured on the JEOL 400 spectrometer.

Infrared spectra were measured with a Perkin-Elmer 1310 IR spectrophotometer, during 12 minute scans, and calibrated against the 1601 cm^{-1} band of a polystyrene film. Liquid samples were examined as thin films deposited between sodium chloride cells (23 × 4 mm). Solid samples were examined as melts, or in solutions using sodium chloride cells and carbon tetrachloride or chloroform as the solvent, or as KBr pellets.

High resolution infrared spectra were recorded on a Beckman 4042 spectrophotometer. FT-IR spectra were obtained by using Perkin-Elmer spectrophotometer.

Ultraviolet spectra were measured with a Beckman DU-8 spectrophotometer, between 340 and 200 nm using absolute ethanol as the solvent. UV bands are reported by the maximum wavelength and the absorbance intensity.

6.1.2. Chromatography

(a) Column Chromatography. All regular and flash[92] column chromatography separations were performed using grade 60 silica gel available from Aldrich Chem. Co.. A separation by a R_f difference of ~0.1 units required 40-55g of gel per gram of residue to be purified. A bigger difference usually required ~30g of gel.

(b) Radial Thin-layer Chromatography. A mixture of compounds with a mass of 0.5g or less, was purified on a chromatotron model 7924T made by Harrison Research. The chromatotron plates were coated with silica gel 60 PF-254 containing calcium sulfate, available from EM Science or VWR Scientific, according to a recipe supplied by Harrison.[93] The sample was introduced using the minimum amount of a good solvent (i.e. methylene chloride), dried and eluted with hexane. The polarity of the eluent was increased only after a good separation was observed. These polarity changes were accomplished by adding 2.5%

increments of ethyl acetate (v/v). The plates were observed using the UV light described for TLC.

(c) Thin Layer Chromatography. TLC analysis were done on Polygram Sil G/UV plates available from Macherey-Nagel, and visualized using (a) a UVS-54 short wave ultraviolet lamp from Ultraviolet Products Inc., and (b) by exposure to iodine. Ratio to front values (R_f) were measured from the center of the respective spot to its initial position divided by the distance traveled by the solvent front.

(d) Eluents. Hexane and ethyl acetate were distilled prior to use.

6.1.3. Melting Points

The melting points were determined in capillary tubes (1.5×9 0 mm, Kimax) using a Dr. Tottoli melting point apparatus made by Büchi and were uncorrected.

6.1.4. Solvents and Reagents

Solvents were available from either Fischer or Aldrich Chemicals. Commercially available reagents were obtained from Aldrich Chemicals Co..

Anhydrous diethyl ether and ethanol were used as obtained from the suppliers.

All solvents and bases listed below were refluxed until dried[94] prior to distillation under a blanket of either anhydrous nitrogen or argon.

SOLVENT	DRIED OVER
Acetone	Calcium chloride
Acetonitrile	Phosphorus pentoxide
Benzene	Calcium hydride
Carbon tetrachloride	Phosphorus pentoxide
Chloroform	Phosphorus pentoxide
1,2-Dichloroethane	Calcium hydride
Diisopropylamine	Sodium metal
Ethyl acetate	Calcium hydride
Hexane	Calcium hydride
Liquid ammonia	Sodium metal
Methanol	Magnesium metal
Methylene chloride	Calcium hydride
Methyl sulfoxide	Calcium hydride
Pyridine	Calcium hydride
Toluene	Calcium hydride
Triethylamine	Calcium hydride
Tetrahydrofuran	Potassium metal

Triisobutylaluminum was supplied in a metal cylinder and was transferred by syringe technique.[95]

All other solvents and reagents were distilled prior to use. Sodium iodide, potassium iodide and copper(I) cyanide were kept in an oven (110°C) until needed.

6.1.5. Reaction Conditions

All nonaqueous reactions were run under a blanket of either anhydrous nitrogen or argon. Glassware was either oven-dried overnight or flame dried under vacuum and flushed with a stream of anhydrous nitrogen. Usually, a three-necked round-bottomed flask equipped with a pressure-equalizing dropping funnel, a magnetic stirrer, a rubber septum, and a reflux condenser was used. The top of the condenser was connected to a three-way stopcock with one branch connected to the nitrogen source and the other to a drying tube. Drying tubes were filled with anhydrous calcium chloride or potassium hydroxide as required. Reactions were followed by TLC whenever possible.

6.2.0. Specific Experimental Procedures and Spectral Data

2,4,6,8-Tetracarbomethoxy-bicyclo[3.3.1]nonane-3,7-dione (26)

Malonaldehyde bis(dimethyl acetal) (49.35 mL, 0.3 mol) and 2N HCl (150 mL) were stirred at rt for 2 h. The pH of that solution was changed to 8 by the addition of 5N NaOH solution (105 mL) under nitrogen atmosphere. Dimethyl-1,3-acetonedicarboxylate (88.6 mL, 0.6 mol) and CH_3OH (150 mL) were also added. 5N NaOH solution (15 mL) was used to bring the red colored solution to pH 8-8.5. The mixture was stirred for 3 days. To the ice cooled, yellow colored reaction, cold 5N HCl (54 mL) was cautiously added. The reaction color disappeared and a somewhat gummy precipitate was obtained. CH_3OH (50 mL) was added into the reaction and it was stirred for 30 min. The precipitate formed was collected and washed with cold CH_3OH. The mother liquor was extracted with ether (3 × 150 mL). The combined extracts were washed with saturated aqueous NaCl solution, dried over $MgSO_4$ and concentrated under reduced pressure, affording an oily residue. Addition of CH_3OH (50 mL) initiated crystal formation, giving 75g (65%) of the title compound: mp 183-185°C.

^{1}H-NMR($CDCl_3$): δ 1.95 (t, 2H, 2.95 Hz), 3.24 (t, 2H, 2.83 Hz), 3.30 (s, 2H), 3.78 (s, 6H), 3.85 (s, 6H), 12.35 (s, 2H).

^{13}C-NMR($CDCl_3$): δ 22.4, 30.1, 50.3, 52.1, 52.6, 102.0, 168.1, 170.7, 171.8.

IR($CHCl_3$): ν_{max} 3010, 2955, 1728, 1660, 1622, 1440, 1360, 1270, 1110, 1070, 1000 cm^{-1}.

2,4,6,8-Tetracarbomethoxy-tetracyclo[3.3.1.$0^{2,8}$.$0^{4,6}$]nonane-3,7-dione (27)

Compound **27** was prepared from compound **26** in two steps. Compound **26** (12.85 g, 33.0 mmol) in 100 mL of dry $CHCl_3$ was brominated at rt by adding a solution of Br_2 (4 mL, 12.4 g, 77.6 mmol) in dry $CHCl_3$ (50 mL), over a period of 4 h. The reaction mixture was stirred at rt overnight. 2% Sodium bisulfite solution (50 mL) was added in order to remove excess Br_2. When saturated aqueous Na_2CO_3 solution (50 mL) was cautiously added into the organic layer, a white colored precipitate was obtained and collected. The organic layer was dried over $MgSO_4$ and concentrated by using a rotary evaporator. The resulting residue was crystallized from methanol to give 9.0 g (74%) of the title compound: mp 245-246°C.

^{1}H-NMR ($CDCl_3$): δ 2.59 (t, 2H, 2.45 Hz), 3.41 (t, 2H, 2.41 Hz), 3.79 (s, 12H).

^{13}C-NMR ($CDCl_3$): δ 16.0, 39.2, 49.1, 53.8, 164.0, 186.8.

IR($CHCl_3$): ν_{max} 3018, 2955, 1745, 1700, 1610, 1440, 1310, 1250, 1170, 1045, 980 cm^{-1}.

Anal. Calcd for $C_{17}H_{16}O_{10}$: C, 53.67; H, 4.24. Found: C, 53.44; H, 4.28.

2,4,6,8-Tetracarbomethoxy-tetracyclo[3.3.1.$0^{2,8}$.$0^{4,6}$]nonane-3,7-diol (28-a)

An ice-cooled suspension of 7.6 g (20 mmol) of **27** in 300 mL of dry toluene was stirred under argon. A solution of $Al(iBu)_3$ in toluene {25% wt. (1.0 M) solution} (50 mL) was added. The slightly cloudy solution was stirred overnight. After cooling the clear light yellow solution in an ice-bath, cold 4N H_2SO_4 (100 mL) was cautiously added and stirred, and a white colored precipitate was obtained. Stirring was continued for about 2 h. The crude precipitate was then filtered off, and the organic layer was washed with saturated aqueous $NaHCO_3$ (2 × 75 mL), dried over $MgSO_4$ and concentrated by reduced pressure. Recrystallization of the residue from ethyl acetate, afforded 6.0 g (79%) of exo,exo-adduct **28-a**: mp 185-186°C.

^{1}H-NMR ($CDCl_3$): δ 2.46 (t, 2H, 2.34 Hz), 2.50 (m, 2H), 3.19 (bs, 2H), 3.71 (s, 12H), 5.23 (s, 2H).

IR($CHCl_3$): ν_{max} 3580, 3010, 2960, 2860, 1720, 1440, 1360, 1250, 1175, 1065, 1030, 975 cm^{-1}.

Diphosphorus Tetraiodide

PCl_3 (2.61 mL, 4.11 g, 0.03 mol) was cautiously added with stirring to a slurry of KI (16.6 g, 0.1 mol) in anhydrous ether (150 mL) under argon. The reaction mixture was refluxed for 2 days at 40°C. An orange colored solution, the title compound in ether, was obtained.

Alternatively, P_2I_4 could be prepared by addition of solid I_2 (64.7 g, 0.255 mol) all at once to white phosphorus (7.85 g, 0.253 atom g, washed with acetone) in CS_2 solution (170 mL) under argon and maintained at 0°C. The I_2 dissolved after a few minutes producing a deep violet solution which turned orange after stirring at 10°C for 2 h. The solution was stored cold overnight, filtered off by suction under argon and washed with some CS_2, and gave 45.0 g (62%) of orange gold colored, needle shaped crystals of P_2I_4: mp 123-125.5°C.

2,4,6,8-Tetracarbomethoxy-tricyclo[3.3.1.$0^{2,8}$]nona-3,6-diene (2,4,6,8-Tetracarbomethoxybarbaralane) (18)

2,4,6,8-Tetracarbomethoxy-bicyclo[3.3.1]nona-3,7-diene (2,4,6,8-Tetracarbomethoxy-dihydrobarbaralane) (30)

2,4,6-Tricarbomethoxy-tricyclo[3.3.1.$0^{2,8}$]nona-3,6-diene (2,4,6-Tricarbomethoxybarbaralane) (31-a)

Exo,exo-diol **28-a** (10.56 g, 27.5 mmol) was dissolved in a solution containing P_2I_4 (31.33 g, 55 mmol) in a mixture of ether 400 mL and dry pyridine (500 mL) under argon. The reaction was stirred at 80°C overnight. Most of the pyridine was then distilled off, and the residue was poured into ice water (500 mL) containing concentrated HCl (100 mL). The pyridine smell disappeared and the solution became slightly acidic. Then, 4% sodium bisulfite solution (200 mL) was added, and the reaction mixture was extracted with ether (4 × 300 mL). The combined organic extracts were washed with saturated aqueous $NaHCO_3$ (2 × 100 mL) and dried over $MgSO_4$. Concentration under reduced pressure and column chromatography on silica gel, eluting with 20% EtOAc in hexane,

afforded 3.4 g (35%) of compound **18**: mp 99-100°C, along with 0.22 g (2%) of compound **30**: mp 158-159°C and 0.22 g (3%) of compound **31-a**: mp 106-107°C.

^{1}H-NMR ($CDCl_3$) **18**: δ 1.33 (t, 2H, 2.6 Hz), 3.79 (s, 12H), 3.82 (t, 2H, 2.6 Hz), 7.07 (s, 2H).

^{13}C-NMR ($CDCl_3$) **18**: δ 16.2, 27.9, 52.6, 87.9, 129.2, 166.7.

IR (CCl_4) **18**: ν_{max} 3000, 2950, 1720, 1630, 1450, 770 cm^{-1}.

UV (EtOH) **18**: λ_{max} 238nm (ε 12808) with a characteristic shoulder at 250nm.

MS (70 eV) **18**: m/z 350 (M^+), 291, 259, 247, 221, 169, 143, 129, 71, 44.

Anal. Calcd for $C_{17}H_{18}O_8$ **18**: C, 58.28; H, 5.18. Found: C, 59.04; H, 5.39.

^{1}H-NMR ($CDCl_3$) **30**: δ 1.84 (t, 2H, 2.92 Hz), 3.28 (d, 2H, 5.06 Hz), 3.41 (bs, 2H), 3.76 (s, 6H), 3.77 (s, 6H), 7.03 (d, 5.04 Hz).

^{13}C-NMR ($CDCl_3$) **30**: δ 23.3, 28.7, 45.6, 52.0, 52.5, 133.9, 135.8, 166.3, 171.1.

IR (CCl_4) **30**: ν_{max} 3000, 2950, 1720, 1645, 1435, 1240, 1170, 1060, 1010 cm^{-1}.

UV (EtOH) **30**: λ_{max} 213nm (ε 8374).

Anal. Calcd for $C_{17}H_{20}O_8$ **30**: C, 57.95; H, 5.72. Found: C,57.33, H, 5.75.

^{1}H-NMR ($CDCl_3$) **31-a**: δ 1.32 (AB, 2H), 3.06 (m, 1H), 3.12 (m, 1H), 3.76 (s, 3H), 3.78 (s, 3H), 3.82 (s, 3H), 4.08 (bs, 1H), 6.82 (d, 1H, 6.6 Hz), 7.41 (s, 1H).

^{13}C-NMR ($CDCl_3$) **31-a**: δ 17.6, 27.3, 28.3, 34.7, 34.9, 51.7 (for 2C's), 52.5, 129.4, 130.3, 130.7, 131.8, 164.7, 164.8, 170.4.

IR (CCl_4) **31-a**: ν_{max} 3000, 2950, 1720, 1630, 1440, 1250, 1220, 1060cm^{-1}

4,6-Dicarbomethoxy-tricyclo[3.3.1.0^{2,8}]nona-3,6-diene-2,8-dicarboximide (4,6-Dicarbomethoxy-barbaralane-2,8-dicarboximide) (57)

4,6-Dicarboxamido-tricyclo[3.3.1.0^{2,8}]nona-3,6-diene-2,8-dicarboximide (4,6-Dicarboxamido-barbaralane-2,8-dicarboximide) (58)

2,4,6,8-Tetracarbomethoxybarbaralane **18** (1.0 g, 2.86 mmol) in 75 mL of dry CH_3OH was saturated with anhydrous NH_3 at 0°C for 4 h. The reaction mixture was allowed to warm to rt and then heated at 50°C for 3 days. Concentration under reduced pressure and recrystallization from CH_3OH afforded two different kinds of crystals, 220 mg (25%) of big

crystal **57**: mp 267-269°C and 45 mg (6%) of small crystal **58**: mp >300°C.

^{1}H-NMR (DMSO) **57**: δ 1.38 (t, 2H, 2 Hz), 3.66 (s, 6H), 3.73 (d, 1H, 1.92 Hz), 3.98 (bs, 1H), 6.96 (s, 2H), 11.11 (bs, 1H).
^{13}C-NMR (DMSO) **57**: δ 19.8, 28.4, 41.8, 52.3, 127.9, 129.5, 164.3, 173.2.

IR (KBr) **57**: ν_{max} 3240, 2940, 1700, 1625, 1435, 1375, 1255, 1120 cm^{-1}.

^{1}H-NMR (DMSO) **58**: δ 1.35 (t, 2H, 1.65 Hz), 3.63 (d, 1H, 1.83 Hz), 3.67 (m, 1H), 6.88 (s, 2H), 7.28 (bs, 2H), 8.13 (bs, 2H), 11.05 (bs, 1H).

2,6-Dicarboxy-4,8-dicarbomethoxy-bicyclo[3.3.1]nonane-3,7-dione (76)

Tetracarbomethoxy-Weiss compound **26** (41.0 g, 106.8 mmol) was mixed with 50% aqueous KOH solution (250 mL) and stirred at rt for 12 h. The reaction mixture was then cooled in an ice bath and the reaction was hydrolyzed with ice-cooled HCl solution (concentrated HCl 150 mL in distilled water 600 mL). The white colored precipitate which formed was filtered off by suction and washed with ice water to give 29.0 g (77%) of the title compound: mp 115-140°C.

^{1}H-NMR(DMSO): δ 1.85 (bs, 2H), 3.18 (m, 4H), 3.75 (s, 6H), 12.18 (bs, 2H), 12.95 (bs, 2H).

2,6-Dicarbomethoxy-bicyclo[3.3.1]nonane-3,7-dione (67)

A mixture of tetracarbomethoxy-Weiss compound **26** (1.92 g, 5 mmol) and freshly prepared $NaOCH_3$ (2.7 g, 50 mmol) in 75 mL of DMSO containing 10 mol % CH_3OH (3.4 g, 4.3 mL, 0.106 mol) was stirred at 55°C for 21 h. The cloudy light brown colored reaction was acidified to pH 4 using ice-cooled dilute HCl solution. The precipitate formed was collected and sublimed to give 550 mg (41%) of the title compound: mp 149-151°C.

Alternatively, the title compound **67** could be obtained by heating 2.0 g (5.62 mmol) of diacid-diester-Weiss compound **76** to 170°C followed by digestion with hot methanol. This process produced 1.4 g (92%) of the shiny crystals **67**: mp 149-151°C.

^{1}H-NMR ($CDCl_3$): δ 1.75 (t, 2H, 3.25 Hz), 2.41 (AB, 4H), 3.00 (m, 2H), 3.78 (s, 6H), 12.25 (s, 2H).

^{13}C-NMR ($CDCl_3$): δ 26.0, 29.2, 36.2, 51.5, 100.9, 172.3, 172.4.

2,6-Dicarbomethoxy-triasterane-3,7-dione (68)

Diacid-diester-Weiss compound **76** (1.84 g, 5.17 mmol) was stirred in 100 mL of dry CH_2Cl_2 at 0°C for 30 min under nitrogen. A cloudy solution was obtained. Dry NEt_3 (8.65 mL, 62.02 mmol) was added dropwise by dropping funnel. The mixture was stirred for 2 h, then Br_2 (1.2 mL, 3.72 g, 23.27 mmol) in 20 mL of CH_2Cl_2 was added dropwise during a period of 30 min at 0°C. After being stirred for 17 h, the brown

colored reaction mixture was poured into ice water containing 15 mL of 10% HCl. The organic layer was washed with 40mL of 10% Na_2SO_3 to remove excess Br_2, then it was washed successively with H_2O, saturated aqueous NaCl and saturated aqueous $NaHCO_3$, and dried over $MgSO_4$. The solvent was removed under vacuum and the crude compound was purified by passage through a short silica column using 90% EtOAc in hexane as eluent, giving rise to 1.03 g (76%) of the adduct **68**: mp 133-135°C.

In an alternative approach to **68**, dry NEt_3 (33.4 mL, 240 mmol) was added dropwise into a solution of the diester-Weiss compound **67** in 500 mL of dry CH_2Cl_2 at 0°C. The reaction mixture was stirred for an hour, and Br_2 (7.2 mL, 22.3 g, 140 mmol) in 100 mL of dry CH_2Cl_2 was added dropwise during a period of 1.5 h at 0°C. A precipitate formed and the reaction mixture changed from white to yellow and then to orange brown. After being stirred overnight, the dark-brown colored reaction was hydrolyzed with a mixture of 88 mL of 10% HCl in 200 mL of brine. The organic layer was washed once with 180 mL of ice-cooled 10% aqueous Na_2SO_3 to remove excess Br_2, then successively with 250 mL of brine, 150 mL of saturated aqueous $NaHCO_3$, and finally with ice water (2 × 300 mL), then dried over $MgSO_4$. The solvent was removed under reduced pressure and recrystallization of the residue from dry CH_3OH afforded 9.6 g (91%) of the title compound: mp 133-135°C.

^{1}H-NMR ($CDCl_3$ with a drop of benzene): δ 2.49 (t, 2H, 2.4 Hz), 2.87 (m, 4H), 3.77 (s, 6H).

2,6-Dicarbomethoxy-3,7-diphenyl-tetracyclo[3.3.1.$0^{2,8}$.$0^{4,6}$]-nonane-3,7-diol (81)

CuCN (0.63 g, 7 mmol) was stirred in a solvent mixture of 50 mL of anhydrous ether and 30 mL of dry THF at −78°C under nitrogen. C_6H_5Li (7.8 mL, 14 mmol) was added dropwise by syringe. After being stirred for a while, the reaction mixture became deep red and the dry ice-bath was removed. A solution of diester-triasterane-dione **68** (0.792 g, 3 mmol) in 25 mL of dry THF was added dropwise into the reaction mixture at 0°C via a dropping funnel. The reaction mixture turned to a yellow color and some precipitate was formed. After being stirred for 5 h, the reaction mixture was hydrolyzed with a solution of 15 mL of 10% HCl in 75 mL of ice-water. The organic layer was washed with brine and dried over $MgSO_4$. After solvent was removed by rotary evaporation, the residue was chromatographed on silica gel with 33% EtOAc/hexane as eluent, providing 365 mg (29%) of the title compound.

^{1}H-NMR ($CDCl_3$): δ 2.12 (d, 2H, 8.72 Hz), 2.26 (m, 2H), 2.41 (bs, 2H), 3.51 (s, 6H), 5.05 (bs, 2H), 7.40 (m, 10H).

2,6-Dicarbomethoxy-tetracyclo[3.3.1.$0^{2,8}$.$0^{4,6}$]nonane-3,7-diol (85-c)

An ice cooled suspension of 5.28 g (20 mmol) of tetracyclic diketo diester **68** in 240 mL of dry toluene was stirred under argon. A solution of $Al(iBu)_3$ in toluene (80 mL) was added dropwise. After being stirred for 2.5 h, the reaction mixture was hydrolyzed with a solution of 16.8 mL of 5N HCl in 75 mL of saturated aqueous NaCl solution. The organic layer

was washed with 50 mL of saturated aqueous $NaHCO_3$, dried over $MgSO_4$ and concentrated to afford 4.32 g (81%) of crude compound **85-c**. This was recrystallized from ethyl acetate to give 1.7 g (32%) of endo,endo-adduct **85-c**: mp 143-145°C.

^{1}H-NMR ($CDCl_3$): δ 1.90 (m, 2H), 2.11 (t, 2H, 2.7 Hz), 2.19 (m, 2H), 3.71 (s, 6H), 4.92 (d, 2H, 3.92 Hz).

2,6-Dicarbomethoxy-tricyclo[3.3.1.0^{2,8}]nona-3,6-diene (2,6-Dicarbomethoxybarbaralane) (23)

To an ice cooled solution of diol mixture **85** (2.75 g, 10.26 mmol) and NEt_3 (10 mL, 7.26 g, 71.82 mmol) in 100 mL of dry CH_2Cl_2, a solution of CH_3SO_2Cl (1.75 mL, 2.59 g, 22.57 mmol) in 20 mL of dry CH_2Cl_2 was added dropwise during a period of 40 min under nitrogen. After being stirred for 3 h, the red colored reaction mixture was hydrolyzed with a solution of 15 mL 5N HCl in ice water 225 mL. The organic layer was washed, first with 200 mL of ice water including some solid NaCl, second with 200 mL of brine, third with 100 mL of saturated aqueous $NaHCO_3$, then dried over $MgSO_4$. Concentration under reduced pressure afforded 3.35 g (77%) of brown colored liquid which appeared to be a mixture of bismesylates **86**.

In a later attempt at mesylation under similar condition, 6.06 g (86%) of an orange colored liquid, quite likely a mixture of dichlorides (**88**) was obtained.

The mixture of dimesylates (**86**) (3.35 g, 7.9 mmol) and NaI (18 g, 120 mmol) and K_2CO_3 (0.5 g) were mixed with 50 mL of dry acetone and stirred at rt under nitrogen. After being stirred for 25 h, the red-brown colored reaction mixture was quenched with 200 mL of ice water, then washed with 90 mL of 10% aqueous Na_2SO_3 to remove excess I_2 and extracted with ether (4 × 200 mL). The combined ether extracts were washed with 50 mL of saturated aqueous $NaHCO_3$ and dried over $MgSO_4$. The concentrated extract was chromatographed on silica gel using 25% EtOAc in hexane as eluent, and gave rise to 515 mg (28%) of diesterbarbaralane **23** as a yellowish liquid, along with 893 mg (31%) of rearranged chloro-mesylate **87** as a white solid: mp 130-133°C.

When we used the mixture of dichlorides (**88**) as a precursor in the NaI induced Grob-fragmentation, we obtained 1.5 g (32%) of the title compound **23** as a yellowish liquid along with 0.5 g (8%) of rearranged dichlorinated compound **89**, as a white solid: mp 96-98°C.

^{1}H-NMR ($CDCl_3$): δ 1.22 (t, 2H, 2.35 Hz), 3.22 (m, 2H), 3.77 (s, 6H), 4.46 (t, 2H, 7.55 Hz), 6.49 (d, 2H, 8.27 Hz).

^{13}C-NMR (THF-d_8): δ 18.0, 28.7, 52.0, 80.8, 84.0, 125.5, 168.6.

6,9-Dibromo-1,4-dicarbomethoxy-tricyclo[3.3.1.0^{2,8}]nona-3-ene (91)

Dicarbomethoxybarbaralane **23** (440 mg, 1.88 mmol) was dissolved in 50 mL of dry CH_2Cl_2 and the solution was chilled in an ice

bath under nitrogen. 2% v/v bromine solution in CH_2Cl_2 (5.9 mL, 2.3 mmol) was added dropwise during a period of 24 min. After the reaction mixture was stirred for 3.5 h, the golden orange colored mixture was washed with ice water containing 3 mL of 10% aqueous Na_2SO_3 to remove excess Br_2. The organic layer was washed with saturated aqueous $NaHCO_3$, dried over $MgSO_4$ and concentrated under reduced pressure. Digestion of the residue with anhydrous ether yielded 533 mg (72%) of the rearranged brominated compound **91**: mp 121-123°C.

^{1}H-NMR ($CDCl_3$): δ 2.23 (m, 1H), 2,45 (m, 2H), 2.65 (m, 1H), 3.60 (m, 1H), 3.80 (s, 3H), 3.84 (s, 3H), 4.41 (m, 1H), 5.72 (t, 1H, 1.5 Hz), 7.32 (d, 1H, 6.29 Hz).

2,6-Dicarboxamido-tricyclo[3.3.1.0^{2,8}]nona-3,6-diene (2,6-Dicarboxamidobarbaralane) (94)

2-Carboxamido-6-carbomethoxy-tricyclo[3.3.1.0^{2,8}]nona-3,6-diene (2-Carboxamido-6-carbomethoxybarbaralane) (95-a)

An ice cooled solution of dicarbomethoxybarbaralane 23 (1.1 g, 4.7 mmol) in 75 mL of CH_3OH was saturated with NH_3 for 6 h. The reaction mixture was allowed to warm to rt and a catalytic amount of 80% NaH was cautiously added. The mixture was stirred overnight, then solvent was removed under reduced pressure and the residue was chromatographed on silica gel with 75% EtOAc/hexane as eluent, affording 130 mg (12%) of unreacted starting compound **23**, 330 mg (34%) of 2,6-dicarboxamido analogue **94**: mp >280°C and 530 mg (51%) of carboxamido-ester analogue **95-a**: mp 165-166°C.

^{1}H-NMR (DMSO) **94**: δ 1.00 (bs, 2H), 2.96 (m, 2H), 4.21 (t, 2H, 7.59 Hz), 6.25 (d, 2H, 8.25 Hz), 7.01 (bs, 2H), 7.39 (bs, 2H).

^{1}H-NMR (DMSO) **95-a**: δ 1.06 (t, 2H, 2.46 Hz), 3.01 (m, 2H), 3.66 (s, 3H), 4.25 (t, 1H, 7.66 Hz), 4.39 (t, 1H, 7.70 Hz), 6.27 (d,1H, 8.24 Hz), 6.39 (d, 1H, 8.22 Hz), 7.07 (bs, 1H), 7.44 (bs, 1H).

^{13}C-NMR (THF-d_8) **95-a**: δ 18.0, 28.3, 28.8, 51.9, 76.1, 83.1, 84.8, 87.4, 122.0, 126.3, 168.6, 170.3.

Methyl (chlorosulfonyl) carbamate (98)

Inner Salt of Methyl (carboxysulfamoyl)triethylammonium hydroxide (Burgess Reagent) (99)

A dry, three necked, 300 mL round bottomed flask was fitted with a magnetic stirring bar, a 25 mL pressure equalizing dropping funnel and a reflux condenser to which was attached a $CaCl_2$ drying tube. The flask was charged with a solution of 25.0 g (15.36 mL, 176.5 mmol) of chlorosulfonyl isocyanate **97** in 53.5 mL of anhydrous benzene. A solution of 5.7 g (7.2 mL, 178 mmol) of anhydrous CH_3OH in 8.9 mL of anhydrous benzene was placed in the dropping funnel. The flask was immersed in a water bath, stirring was begun, and the methanol-benzene solution was added dropwise during 30 min. Ice water was added to the bath as required to maintain a temperature of 18-22°C. The reaction mixture was stirred for an additional 30 min, and then 50 mL of hexane was added from the addition funnel during a 5 min period while the

flask was cooled to 0-5°C with an ice-bath. The moisture sensitive product was removed by filtration, washed with hexane, and dried under reduced pressure to give 30.34 g (99%) of methyl (chlorosulfonyl) carbamate **98** as white crystals.

A three-necked, 1L. round bottomed flask was fitted with a magnetic stirring bar, a 250 mL pressure equalizing dropping funnel, and a condenser to which a $CaCl_2$ drying tube was attached. A solution of 39.82 g (54.85 mL, 393.5 mmol) of anhydrous NEt_3 in 87.5 mL of anhydrous benzene was placed in the flask, stirring was begun, and a solution of 30.34 g (174.9 mmol) of methyl (chlorosulfonyl) carbamate **98** in 315 mL of dried benzene was added dropwise during 2.5 h. During addition, the flask was cooled with a water bath maintained at 10-15°C. The resulting mixture was stirred at 20-25°C overnight. The reaction was then filtered to remove triethylammonium chloride. Evaporation of the filtrate under reduced pressure left 43.5 g of a vanilla colored solid, mp 76-78°C. This was dissolved in 215 mL of anhydrous THF at 25°C. On cooling the solution deposited 30.34 g (72%) of the inner salt of methyl (carboxysulfamoyl)triethylammonium hydroxide **99** as light tan colored crystals.

^{1}H-NMR ($CDCl_3$): δ 1.42 (t, 9H), 3.45 (q, 6H), 3.66 (s, 3H).

2,6-Dicyano-tricyclo[3.3.1.$0^{2,8}$]nona-3,6-diene (2,6-Dicyanobarbaralane) (5-a)

A suspension of dicarboxamidobarbaralane **94** (200 mg, 0.98 mmol) in 6 mL of dry CH_2Cl_2 was stirred at rt under argon. The Burgess reagent was added in ten 0.233 g portions (2.33 g, 9.8 mmol) during 2 h. Light brown colored suspension was refluxed at 43°C for 15 min, cooled and applied directly to a silica gel column. Flash chromatography with 50% EtOAc in hexane as eluent afforded 130 mg (81%) of the title compound, mp 100-102°C, as a white crystalline solid.

^{1}H-NMR($CDCl_3$): δ 1.36 (t, 2H, 2.6 Hz), 2.98 (m, 2H), 4.54 (t, 2H, 7.8 Hz), 6.18 (d, 2H, 8.2 Hz).

FT-IR (KBr): ν_{max} 3059, 2968, 2942, 2236, 2210, 1627, 1607 cm^{-1}.

2-Carbomethoxy-tricyclo[3.3.1.$0^{2,8}$]nona-3,6-diene-6-carbonitrile (2-Carbomethoxy-barbaralane-6-carbonitrile) (96-a)

A suspension of 2-carboxamido-6-carbomethoxybarbaralane **95-a** (350 mg, 1.6 mmol) in 7 mL of dry CH_2Cl_2 was stirred at rt under argon. The Burgess reagent was added in five 0.4 g portions (2 g, 8.4 mmol) during 40 min. A clear brown solution was obtained within 30 min after the addition of the Burgess reagent, and reaction was complete within 2 h. The mixture was applied directly to a silica gel column. Flash chromatography with 75% EtOAc in hexane as eluent gave rise to 291 mg (91%) of the title compound **96-a**: mp 107-108°C.

^{1}H-NMR ($CDCl_3$): δ 1.27 (m, 2H), 2.93 (m, 1H), 3.02 (m, 1H), 3.21 (t, 1H, 7.32 Hz), 3.78 (s, 3H), 5.78 (dd, 1H, 9.30 and 9.37 Hz), 6.37 (d, 1H, 9.37 Hz), 6.41 (d, 1H, 7.2 Hz).

^{13}C-NMR ($CDCl_3$): δ 16.6, 26.8, 31.1, 41.0, 43.7, 52.5, 104.3, 117.4, 118.6, 121.8, 134.3, 170.4.

FT-IR (CCl_4): ν_{max} 2953, 2214, 1729, 1618, 1609, 1438, 1273, 1233, 1108 cm^{-1}.

Bicyclo[3.3.1]nonane-3,7-dione (102)

2,4,6,8-Tetracarbomethoxy-bicyclo[3.3.1]nonane-3,7-dione **26** (38.4 g, 0.1 mol) was refluxed with 6N HCl (700 mL) for 26 h. A clear orange solution was obtained which was neutralized with cold concentrated NaOH (155 g) solution and extracted with CH_2Cl_2 (4 × 225 mL). The combined organic layers were washed with brine (2 × 150 mL), dried over $MgSO_4$ and evaporated under reduced pressure. The crude residue was triturated with CCl_4 affording **102** in 7.46 g (49%): mp 215–220°C.

^{1}H-NMR ($CDCl_3$): δ 2.2 (m, 2H), 2.5 (m, 8H), 2.85 (m, 2H).

^{13}C-NMR ($CDCl_3$): δ 31.3, 32.6, 47.7, 208.4.

2,6-Dibromo-triasterane-3,7-dione (104)

2,4-Dibromo-triasterane-3,7-dione (105)

To a stirred slurry of 33.84 g (90 mmol) of phenyltrimethyl-ammonium tribromide in 150 mL of CH_2Cl_2 was added, all at once, 3.04 g (20 mmol) of bicyclo[3.3.1]nonane-3,7-dione **102**. The reaction mixture color turned from orange to clear red. Stirring was continued for 1 h, then 150 mL of water was added and the resulting two phases were shaken and discolored (from red to cloudy yellow) with an aliquot of 15% aqueous sodium bisulfite (100 mL). The CH_2Cl_2 layer was separated and the aqueous layer was extracted with more CH_2Cl_2 (3 × 75 mL). The combined CH_2Cl_2 extracts were washed with H_2O (3 × 125 mL), dried over $MgSO_4$ and evaporated to yield 8.34 g of amber colored oil. This was dissolved in 150 mL of dry THF and the solution was stirred, while 27.88 mL (20.24 g, 200 mmol) dry triethylamine in 60 mL of dry THF was added during a period of 15 min. The resulting amber colored solution turned cloudy yellow. After being stirred for 1 h, the mixture was evaporated under reduced pressure leaving a light brown colored residue. This was dissolved in CH_2Cl_2 (250 mL) and washed with water. The organic layer was dried over $MgSO_4$ and evaporated to afford 5.6 g (92%) of white crude solid compound (**104** and **105**). Recrystallization from benzene/hexane solvent mixture provided 1.02 g (17%) of **104** as an only isomer: mp 203-205°C.

^{1}H-NMR ($CDCl_3$) **104 and 105**: δ 2.40 (m), 2.60 (t), 2.66-3.17 (m).

^{1}H-NMR ($CDCl_3$) **104**: δ 2.60 (t, 2H, 2.64 Hz), 2.92 (m, 2H), 3.07 (d, 2H, 8.54 Hz).

1,2,4,5,6,8-Hexacarbomethoxy-bicyclo[3.3.0]octane-3,7-dione (114)

2-Oxa-bicyclo[3.3.0]oct-7-ene-1,4,5,6,8-pentacarbomethoxy-3-carbomethoxymethylene-3,7-diol (115)

To 180 mL of pH 5 aqueous buffer solution , 7.64 mL (9.05 g, 52mmol) of dimethyl acetone-1,3-dicarboxylate **24** and freshly distilled dimethyl diketosuccinate **113** (5.16 g, 25.05 mmol) were added and the mixture was stirred at rt for 5 days. Part of the reaction mixture stuck in the flask and all the solvent was decanted. The sticking compound was digested with CH_3OH, giving 660 mg (6%) of **114**: mp 210-213°C.

The solvent that was removed from the flask was extracted with EtOAc (3 × 200 mL), washed with ice-water (2 × 100 mL), dried over $MgSO_4$ and evaporated, giving 1.38 g (11%) of **115**: mp 174-175°C.

^{1}H-NMR ($CDCl_3$) **114**: δ 3.66 (s, 6H), 3.68 (s, 6H), 3.69 (s, 6H), 4.90 (s, 2H), 10.55 (bs, 2H).
^{13}C-NMR ($CDCl_3$) **114**: δ 29.6, 51.5, 52.2, 53.1, 54.6, 65.0, 102.0, 168.1, 170.9, 171.6.

^{1}H-NMR ($CDCl_3$) **115**: δ 3.18 (AB, 2H), 3.58 (s, 3H), 3.73 (s, 3H), 3.76 (s, 3H), 3.77 (s, 3H), 3.78 (s, 3H), 3.89 (s, 3H), 4.73 (s, 1H), 5.13 (s, 1H), 6.21 (s, 1H), 10.55 (bs, 1H).

^{13}C-NMR ($CDCl_3$) **115**: δ 41.7, 51.3, 51.9 (for 2C's), 52.5, 52.7, 53.1, 54.1, 55.6, 64.6, 94.0, 103.7, 106.0, 167.6, 167.9, 168.2, 169.1, 170.4, 171.0, 174.1.

^{1}H-NMR Spectra of Selected Compounds

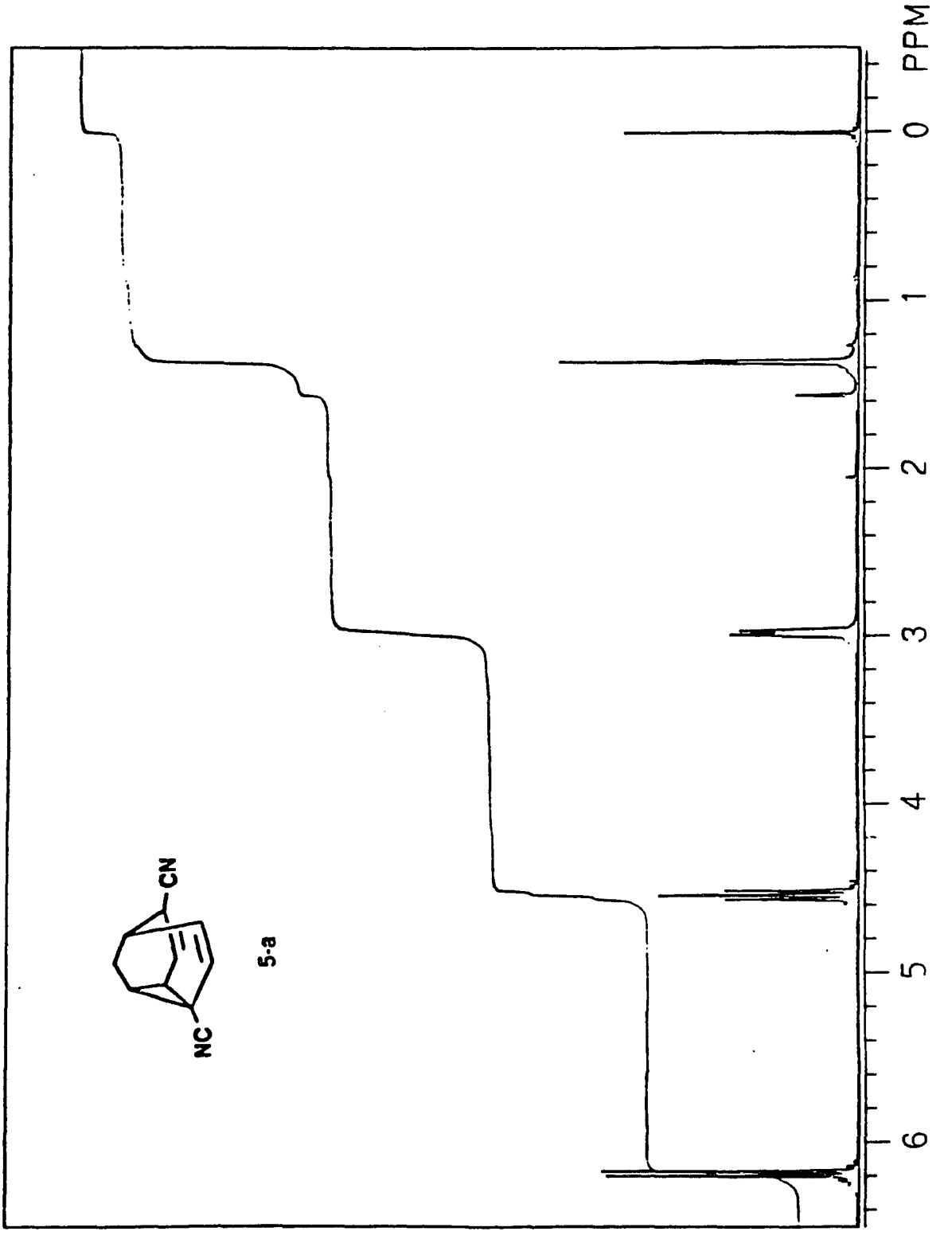
PPM
0
1
2
3
4
5
6
CN
NC
5-a

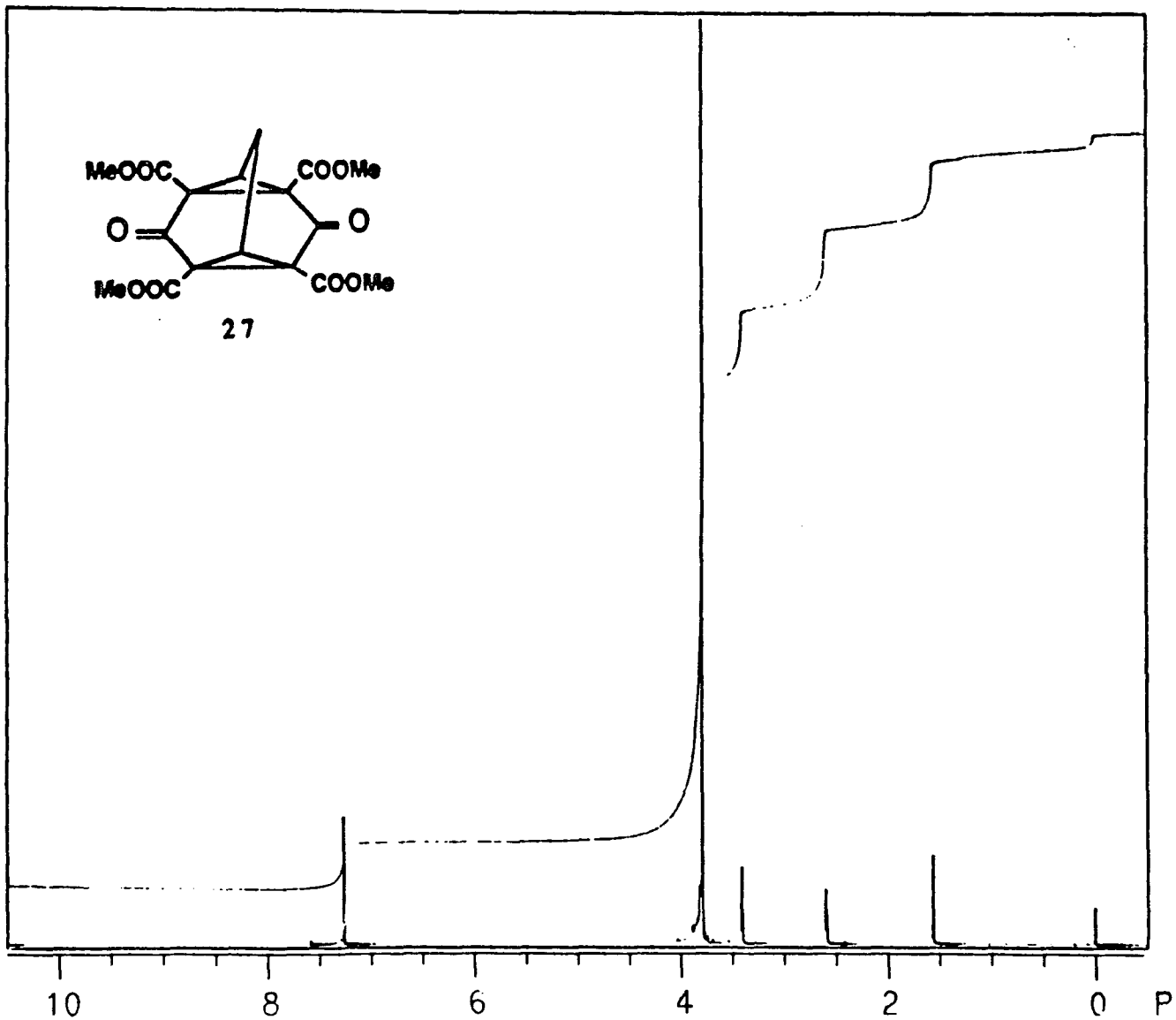
MeOOC
COOMe
O
O
MeOOC
COOMe
27
10
8
6
4
2
0
PPM

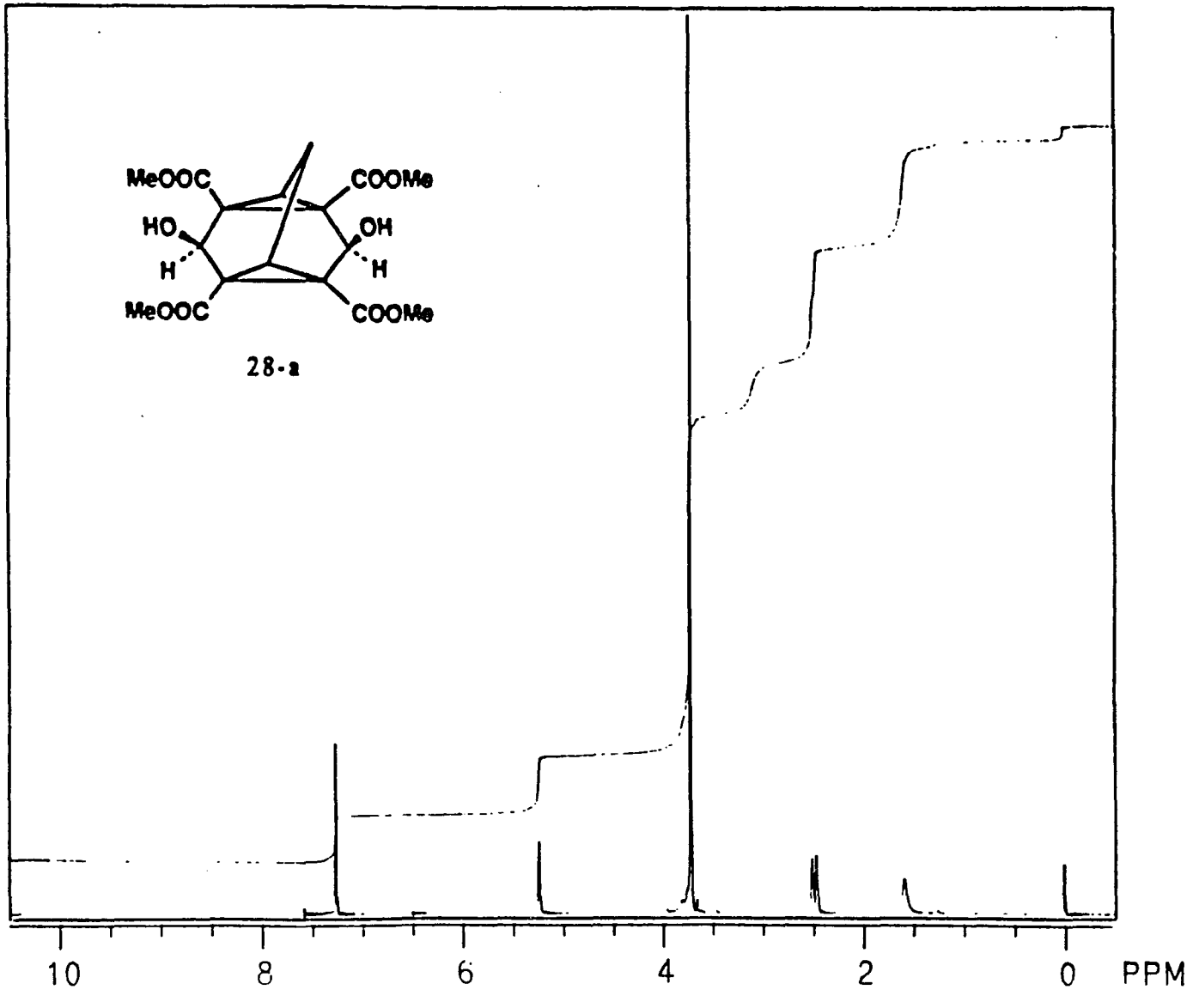
MeOOC
COOMe
HO
OH
H
H
MeOOC
COOMe
28-a
10
8
6
4
2
0
PPM

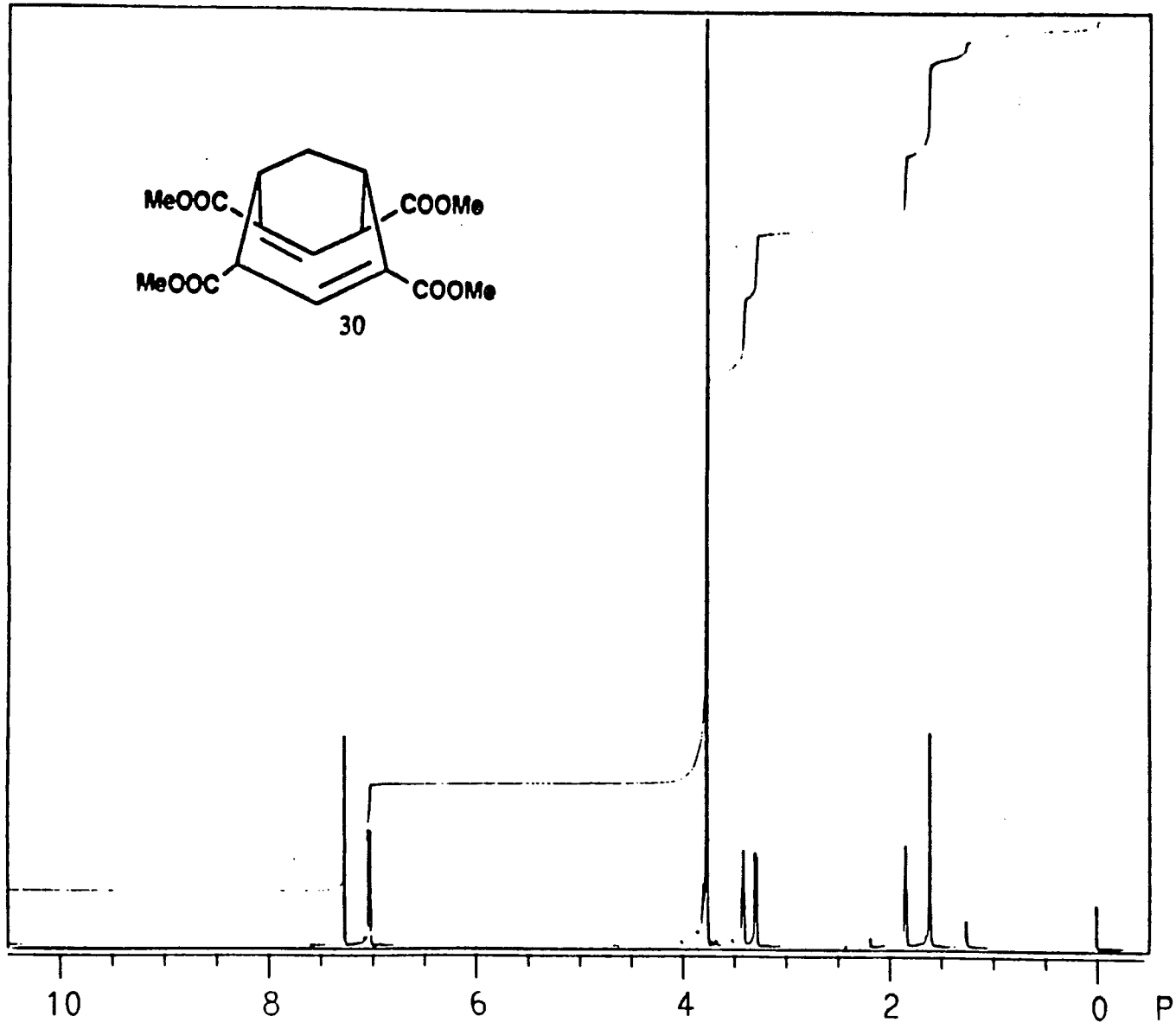
MeOOC
COOMe
MeOOC
COOMe
30
10
8
6
4
2
0
PPM

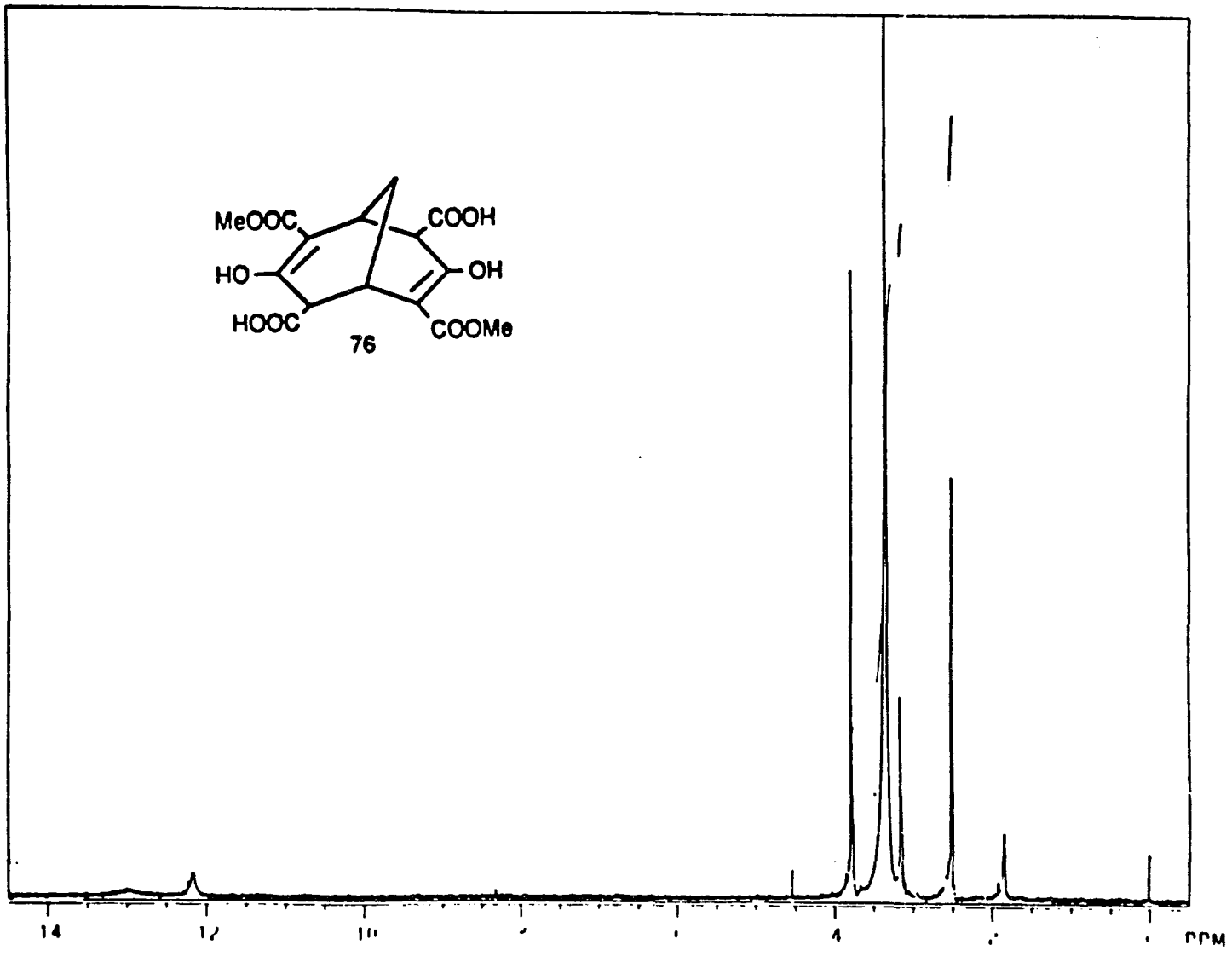
MeOOC
COOH
HO
OH
HOOC
COOMe
76
14
12
10
4
PPM

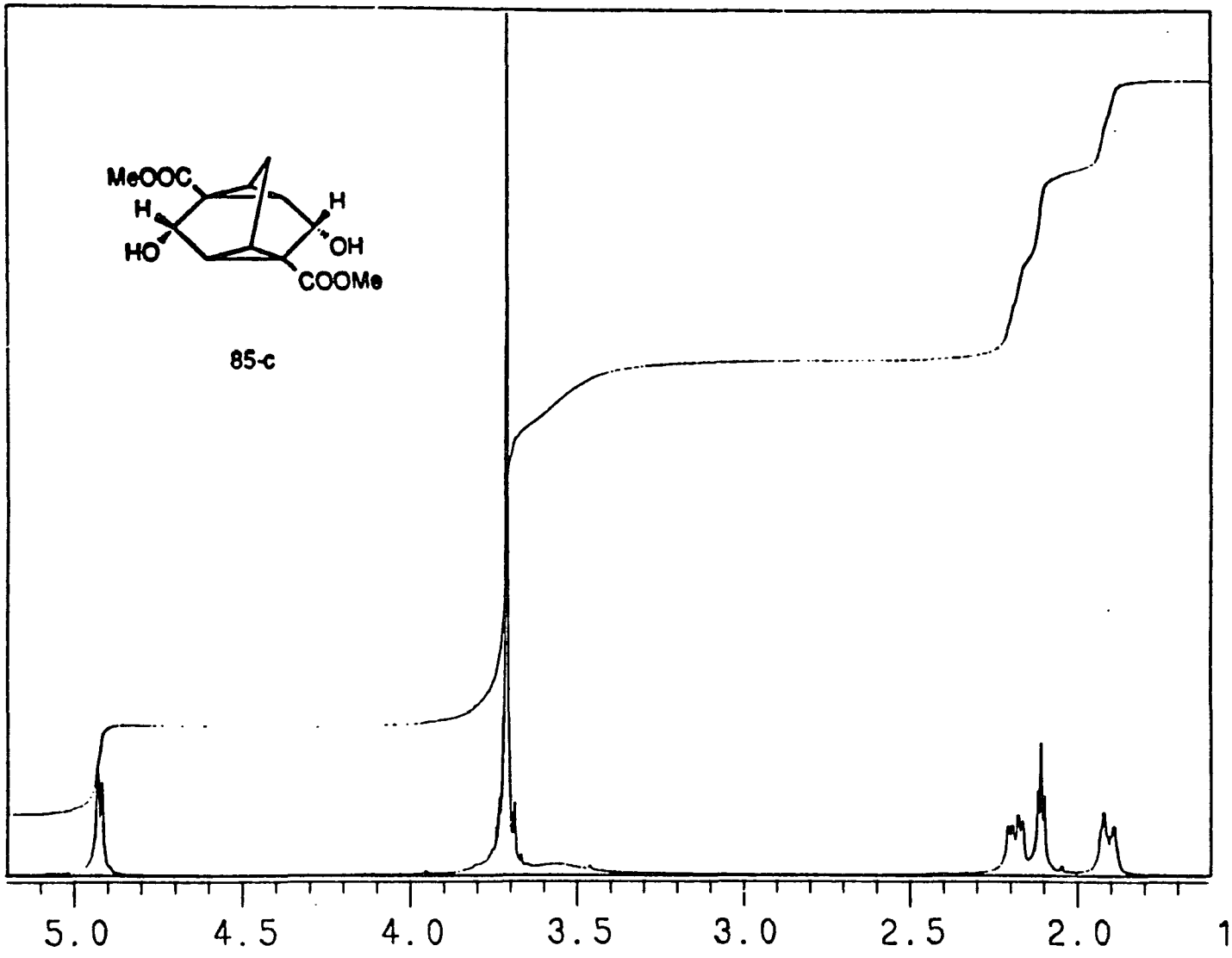
MeOOC
H
HO
H
OH
COOMe
85-c
5.0
4.5
4.0
3.5
3.0
2.5
2.0
1.5
PPM

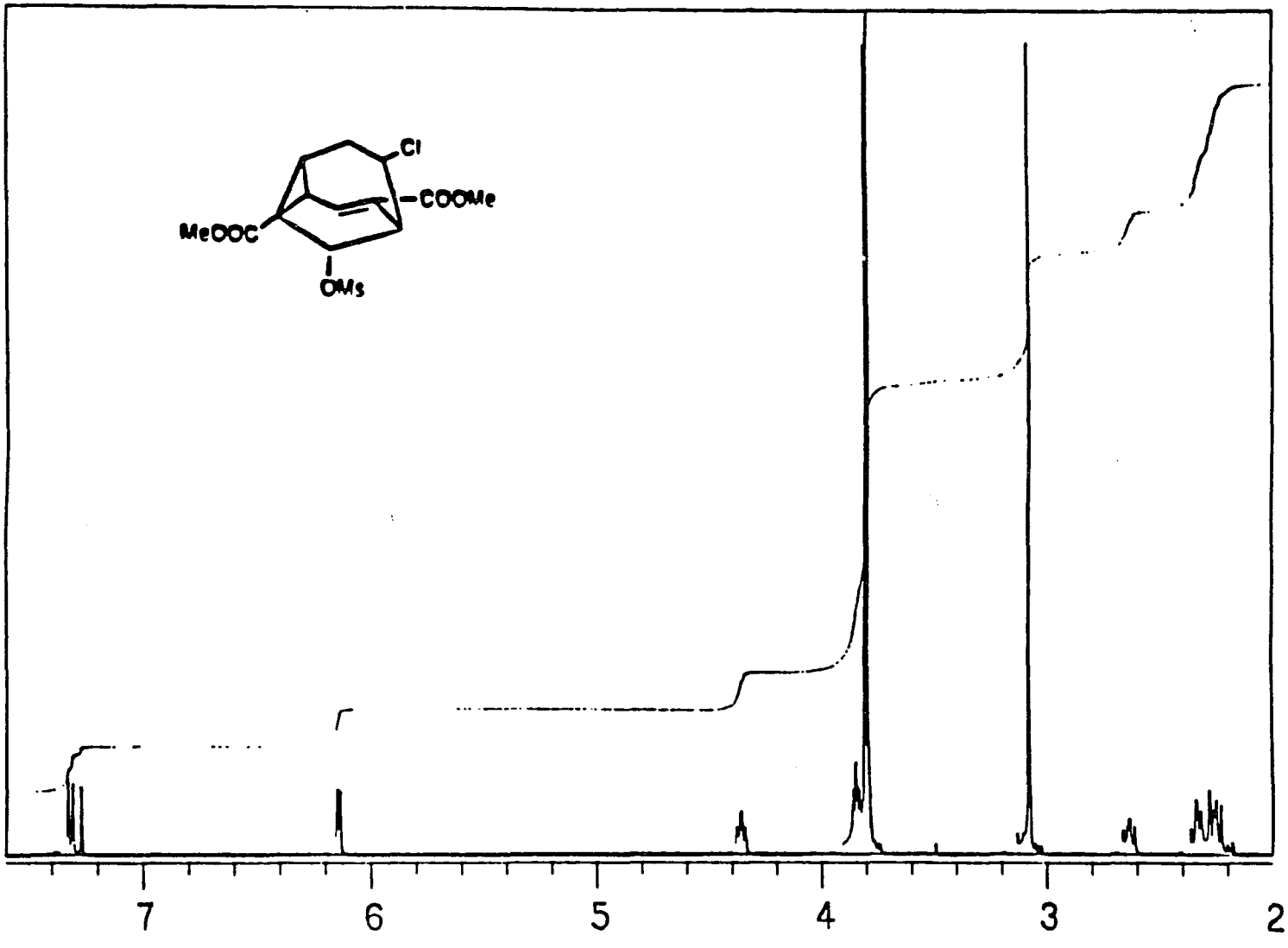
Cl
COOMe
MeOOC
OMs
7
6
5
4
3
2
PPM

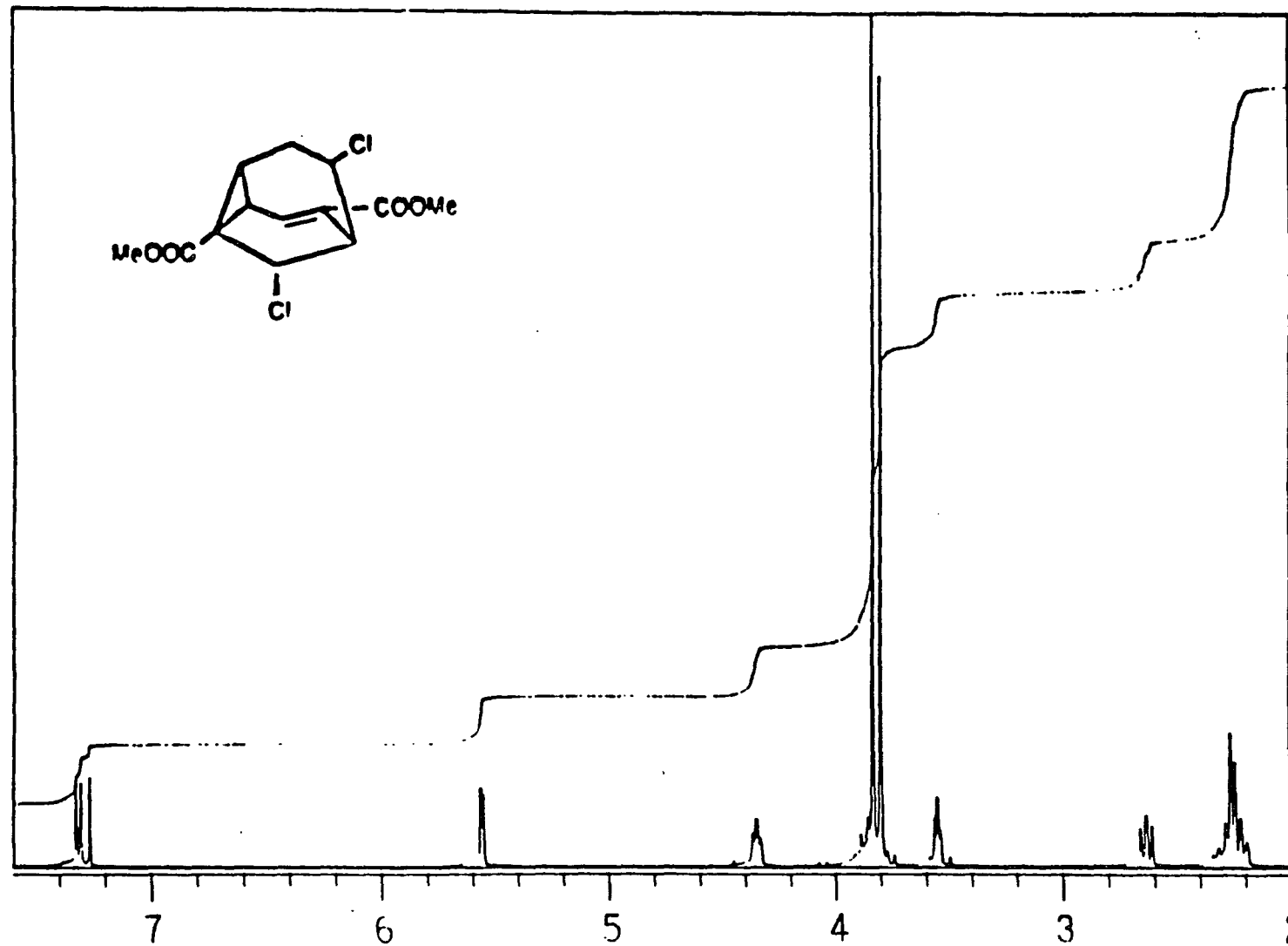
Cl
COOMe
MeOOC
Cl
7
6
5
4
3
2
PPM

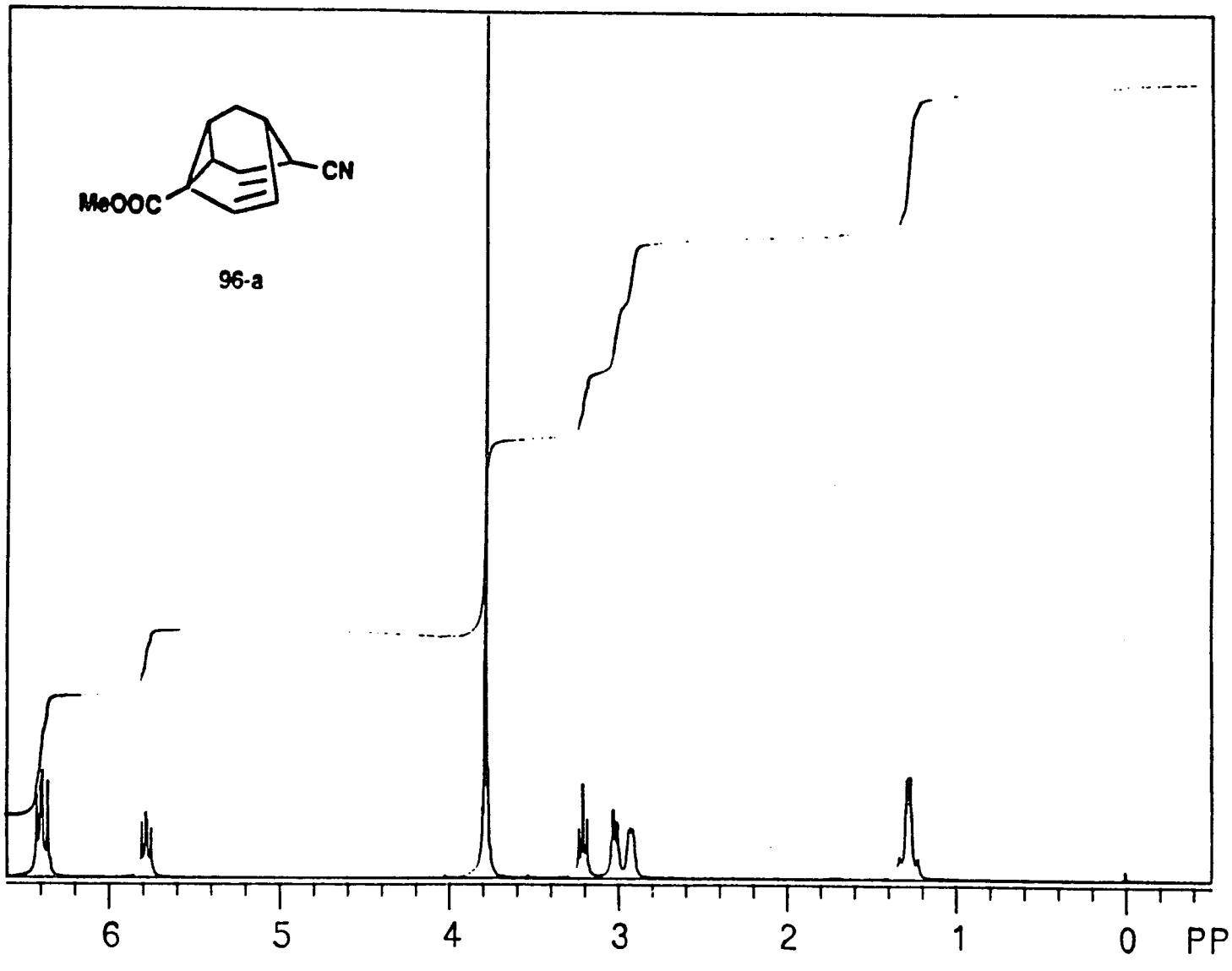
MeOOC
CN
96-a
6
5
4
3
2
1
0
PPM

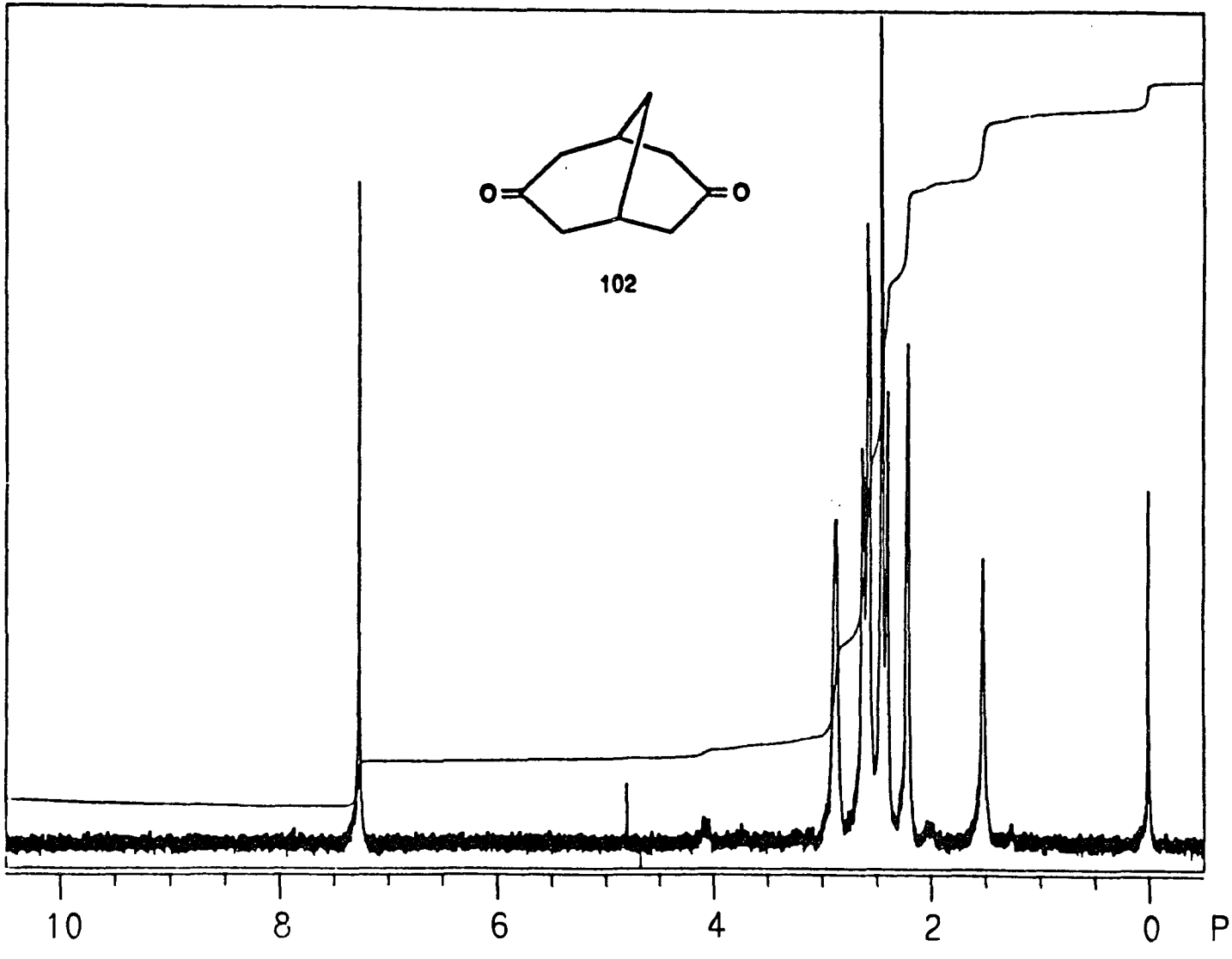
O
O
102
10
8
6
4
2
0
PPM

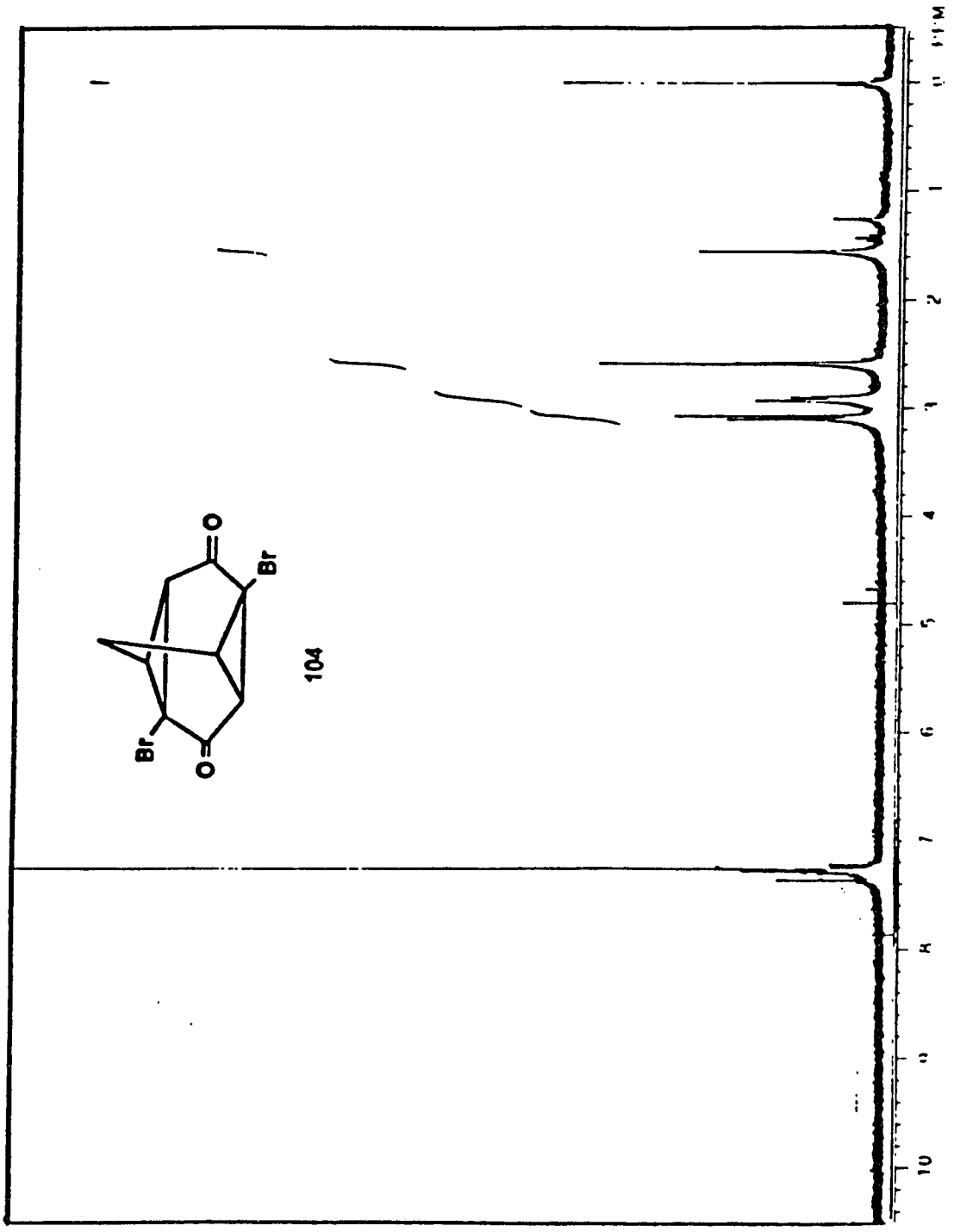
O
Br
Br
O
104

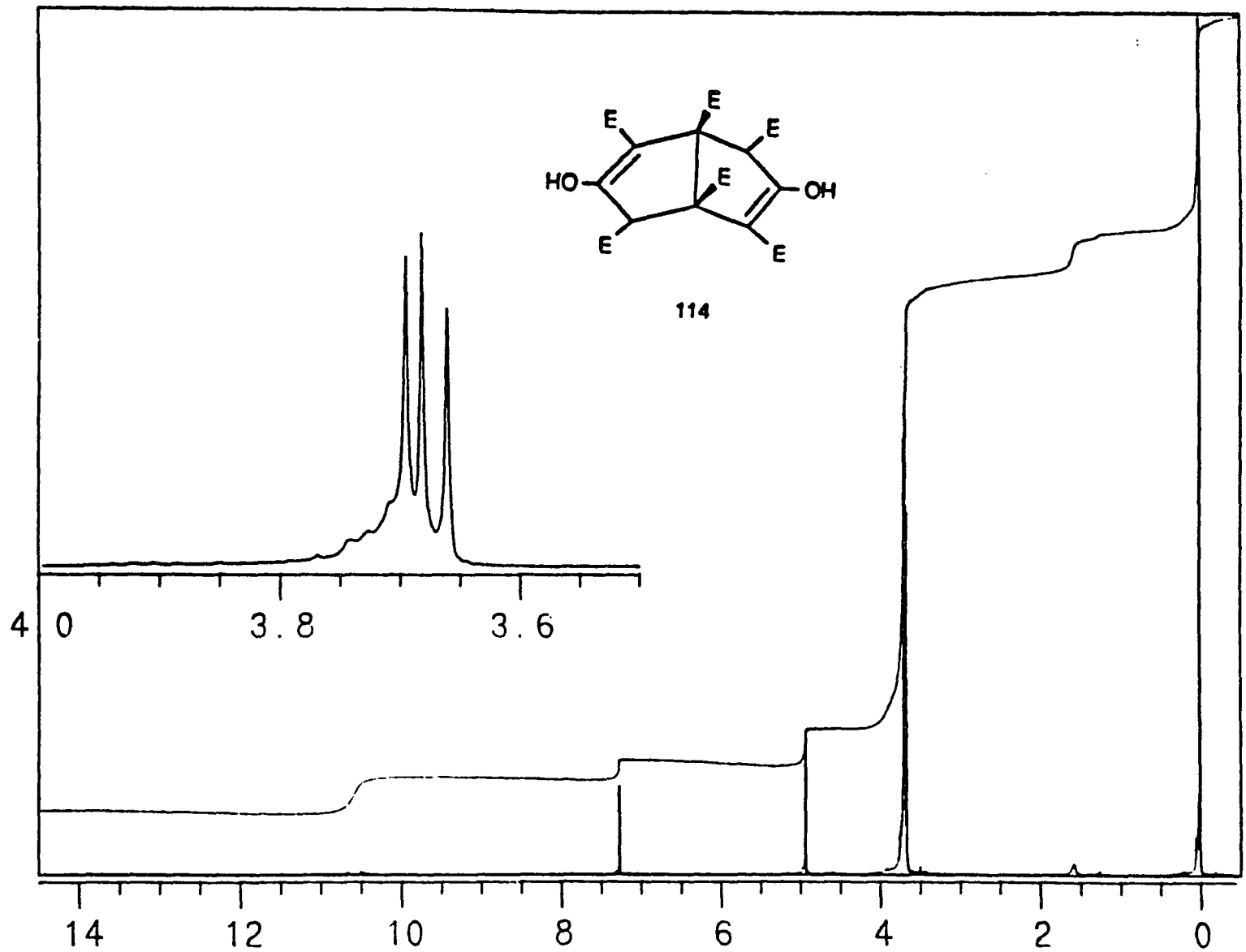
E
E
E
E
HO
E
OH
E
E
114
4.0
3.8
3.6
14
12
10
8
6
4
2
0
PPM

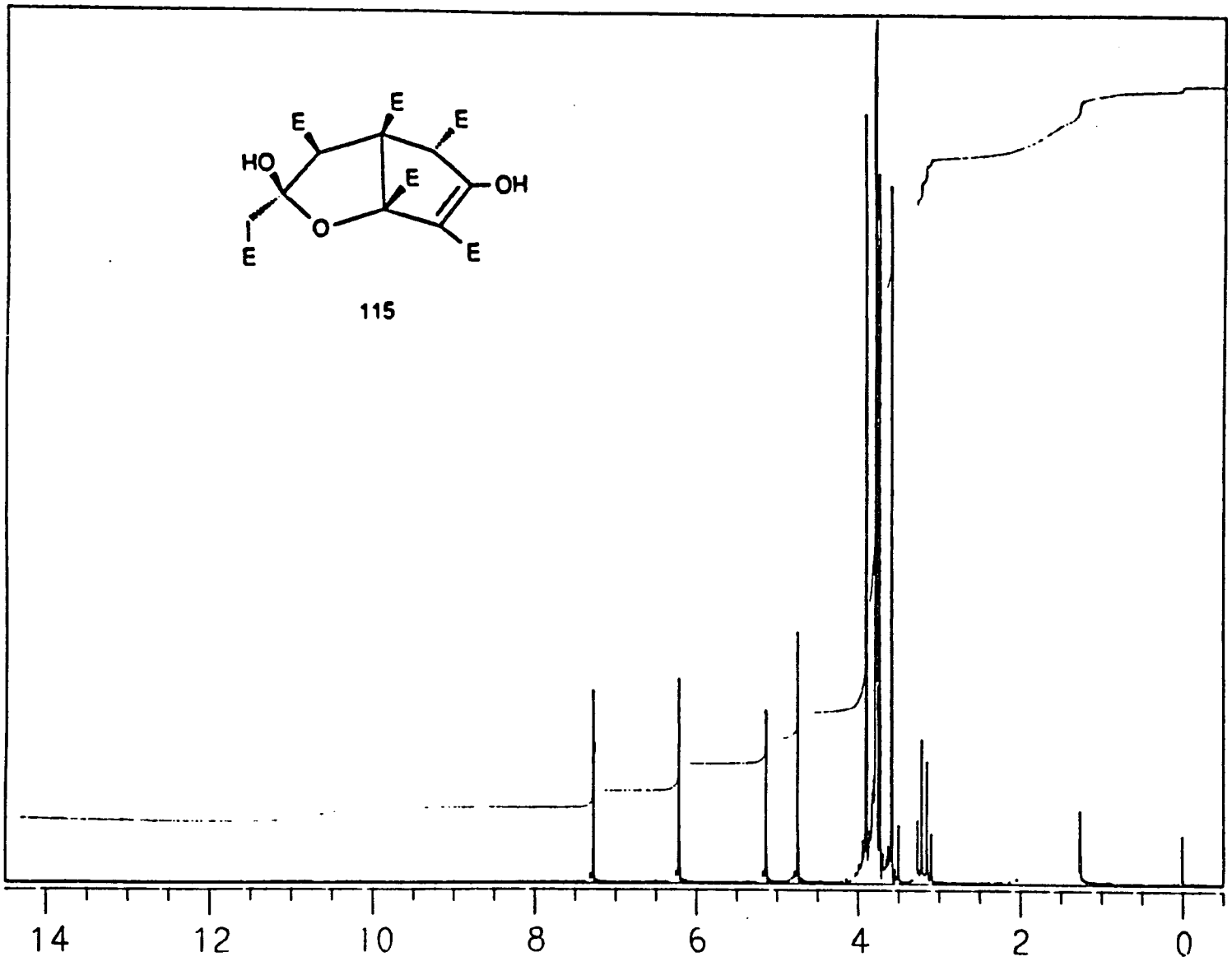

115

^{13}C-NMR Spectra of Selected Compounds

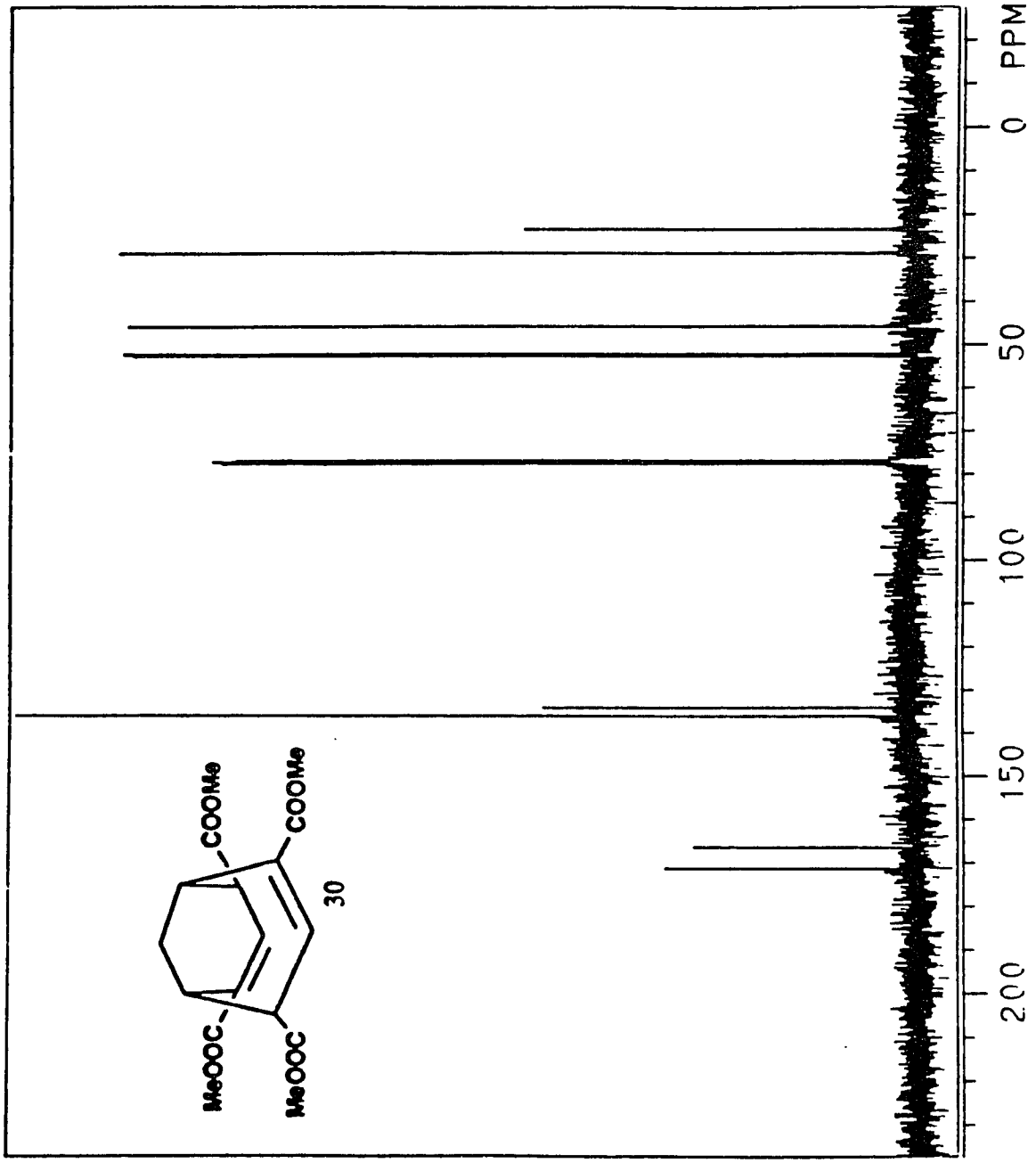
COOMe
COOMe
MeOOC
MeOOC
30
200
150
100
50
0
PPM

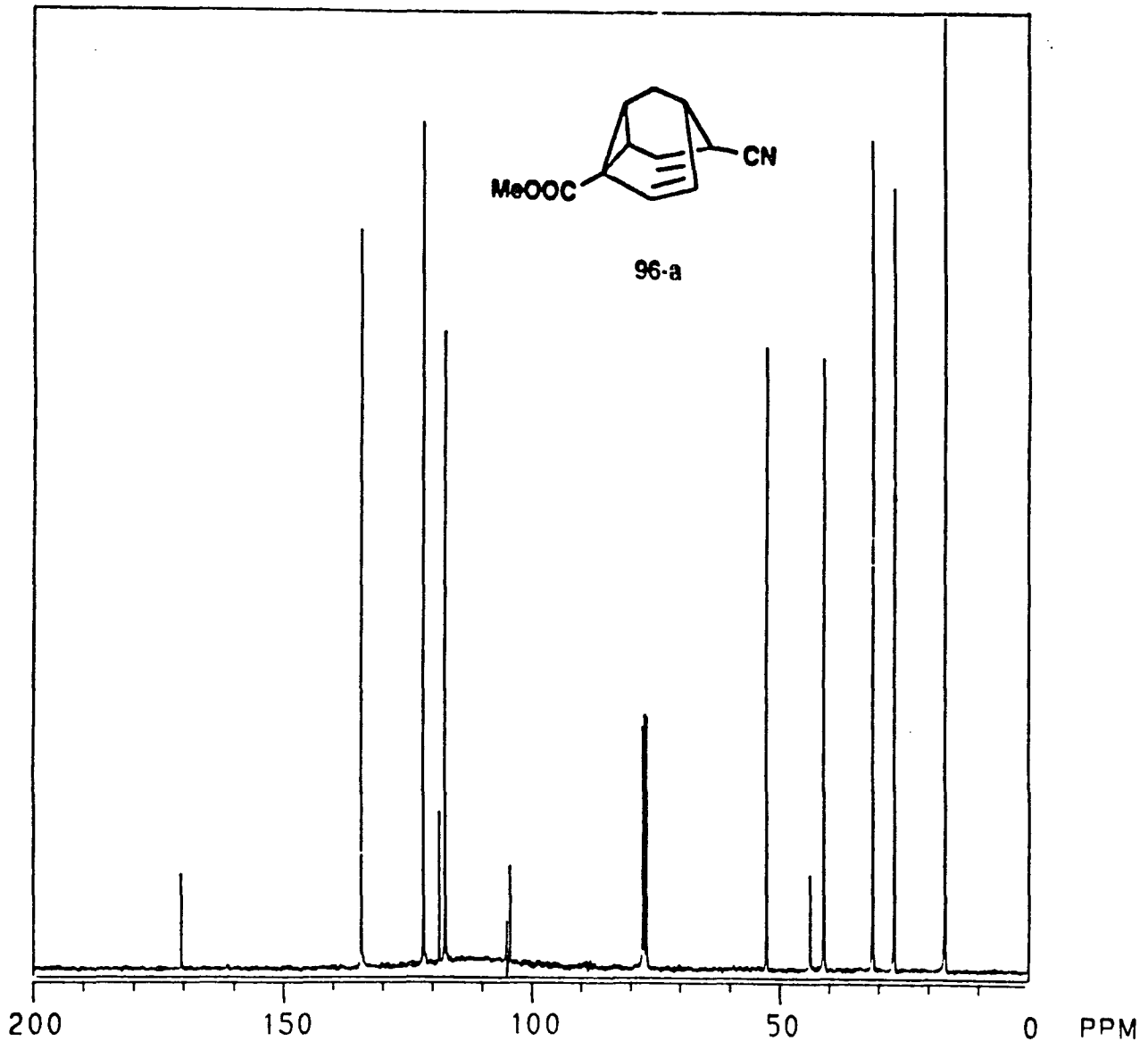
MeOOC
CN
96-a
200
150
100
50
0
PPM

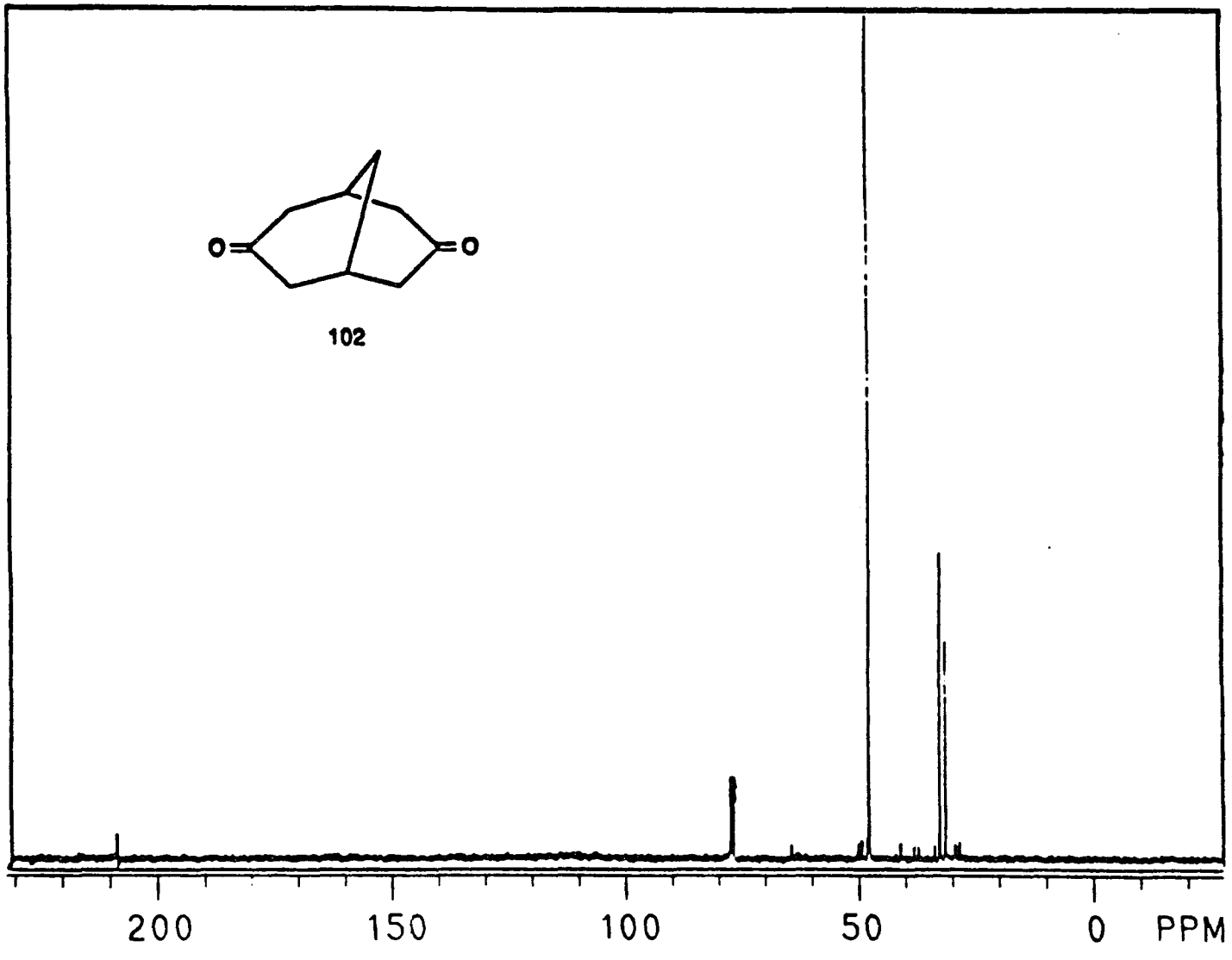

102

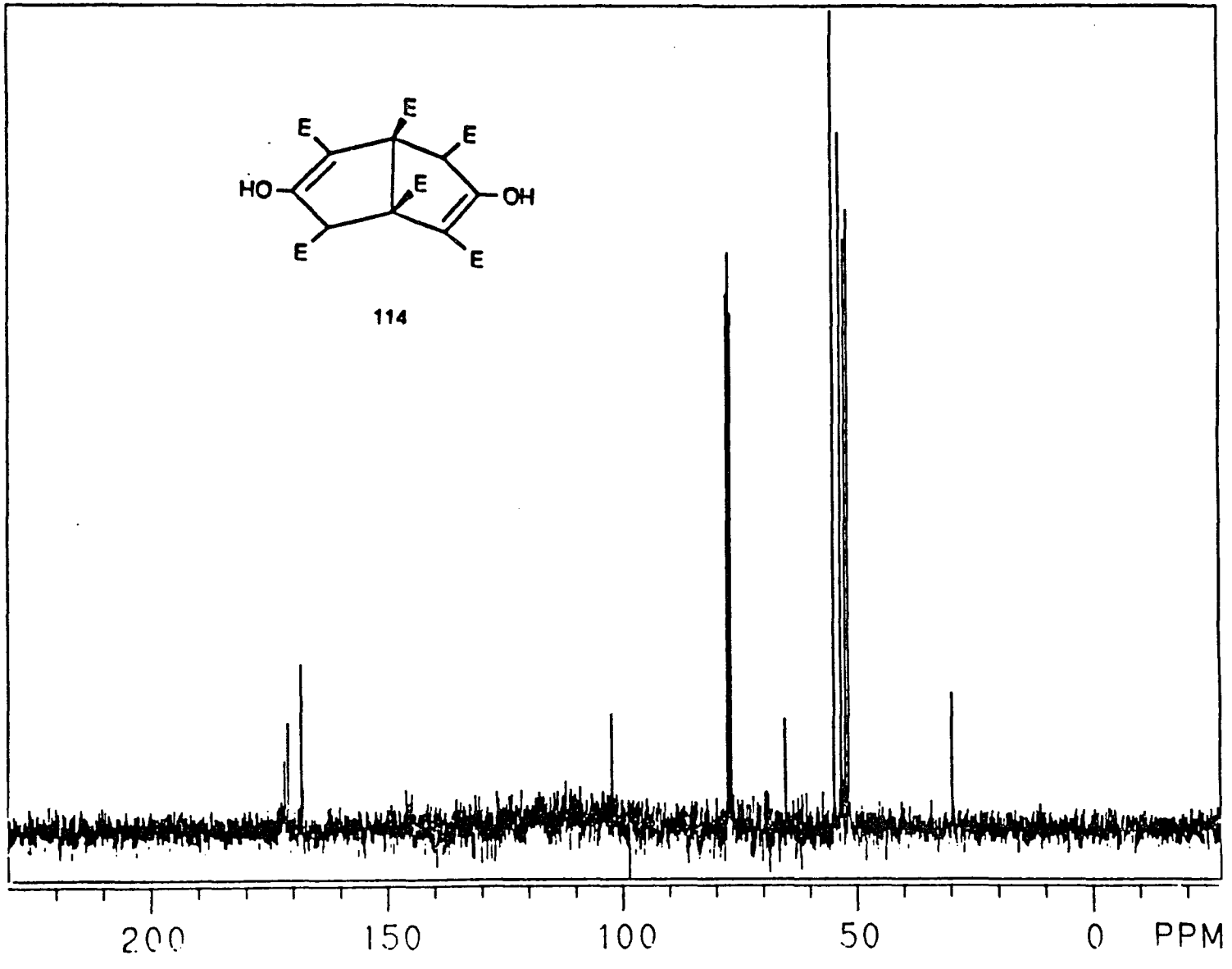

114

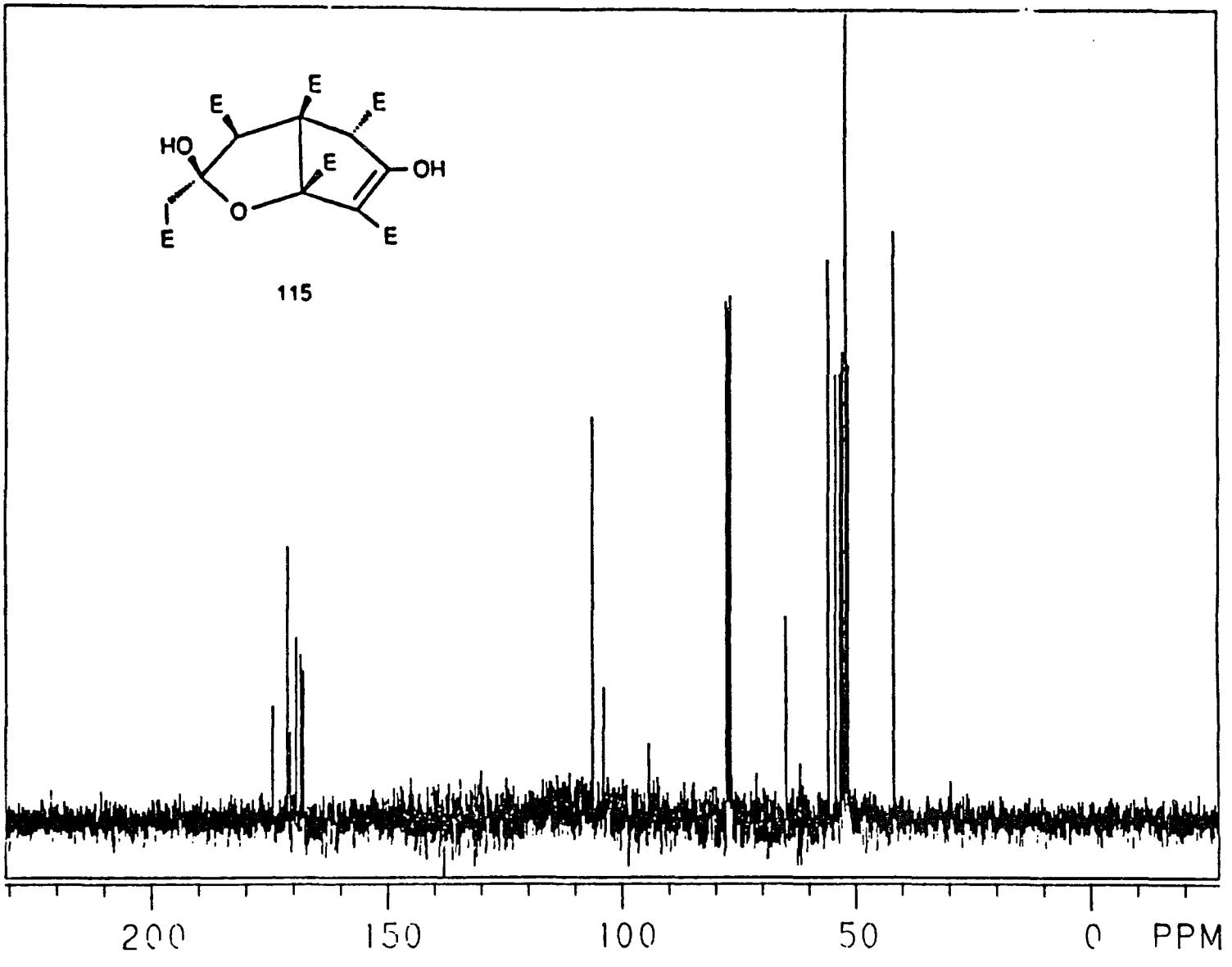
E
E
E
E
HO
E
OH
O
E
E
E
115
200
150
100
50
0
PPM

IR Spectra of Selected Compounds

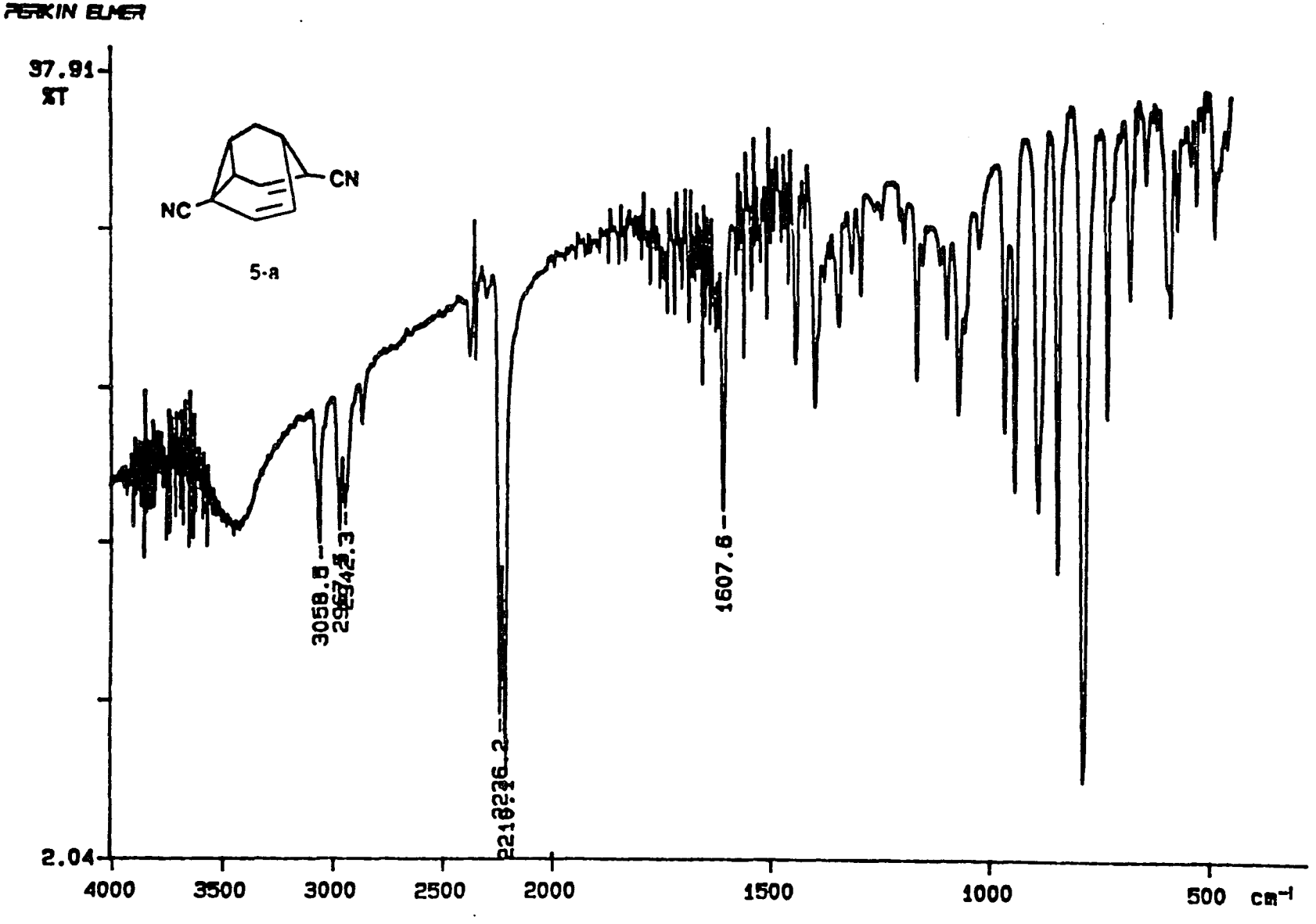
PERKIN ELMER
97.91
%T
NC
CN
5-a
3058.8
2942.3
2216.2
1607.6
2.04
4000
3500
3000
2500
2000
1500
1000
500
cm-1

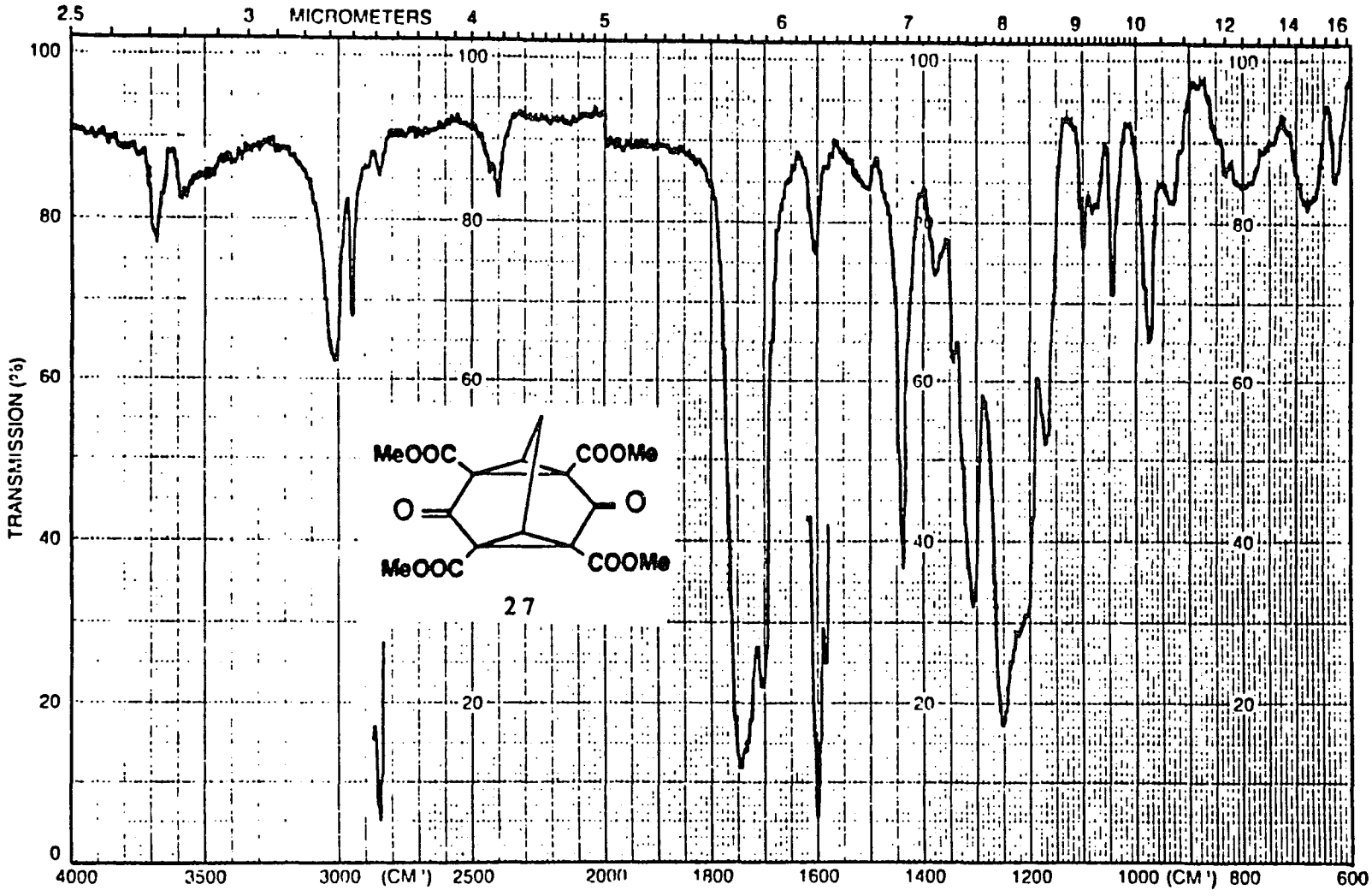
2.5
3
MICROMETERS
4
5
6
7
8
9
10
12
14
16
100
80
60
40
20
0
TRANSMISSION (%)
4000
3500
3000
(CM ')
2500
2000
1800
1600
1400
1200
1000 (CM ')
800
600
MeOOC
COOMe
O
O
MeOOC
COOMe

27

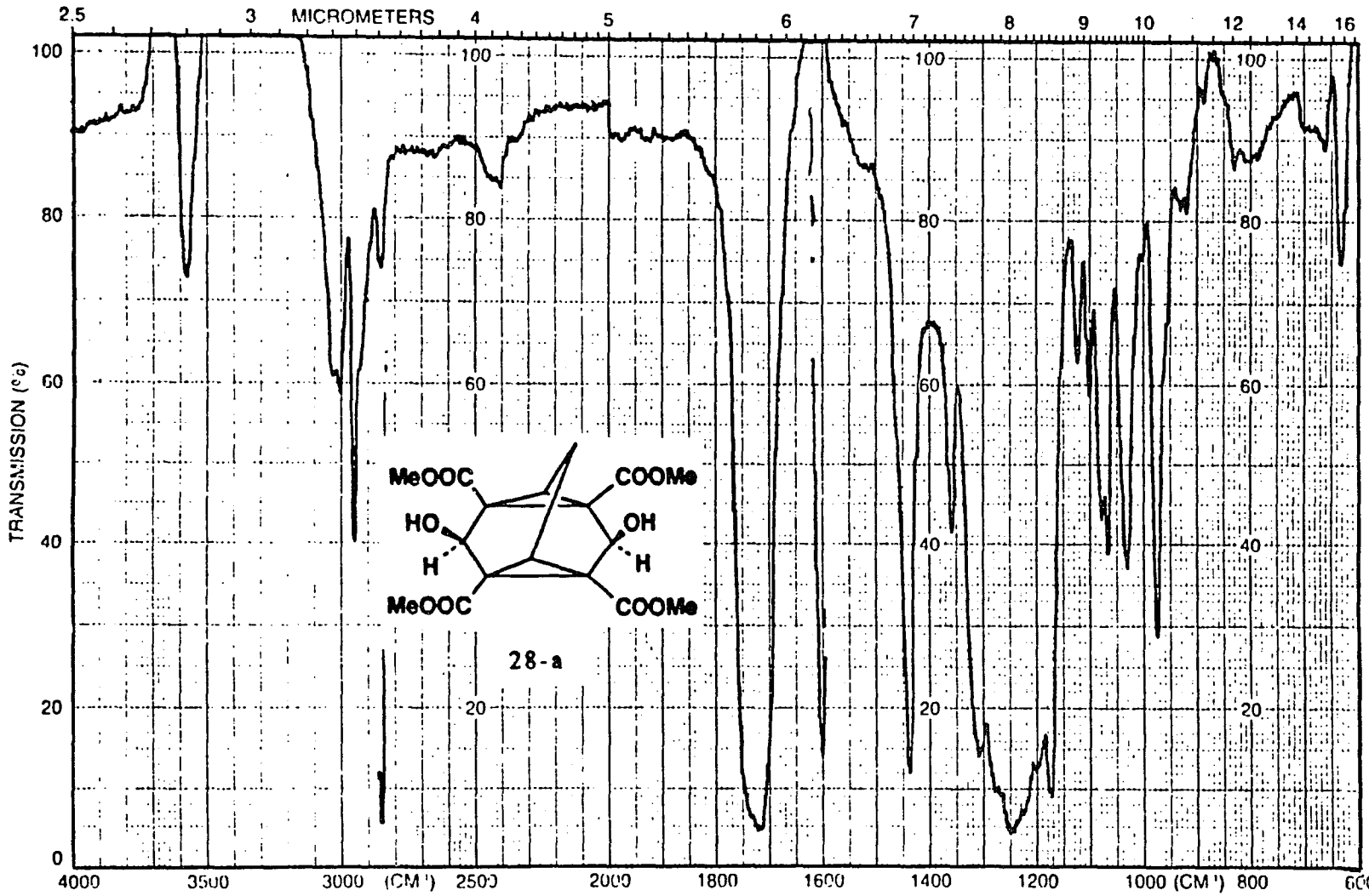
2.5
3
MICROMETERS
4
5
6
7
8
9
10
12
14
16
100
80
60
40
20
0
TRANSMISSION (%)
4000
3500
3000
(CM⁻¹)
2500
2000
1800
1600
1400
1200
1000 (CM⁻¹)
800
600
MeOOC
COOMe
HO
OH
H
H
MeOOC
COOMe
28-a

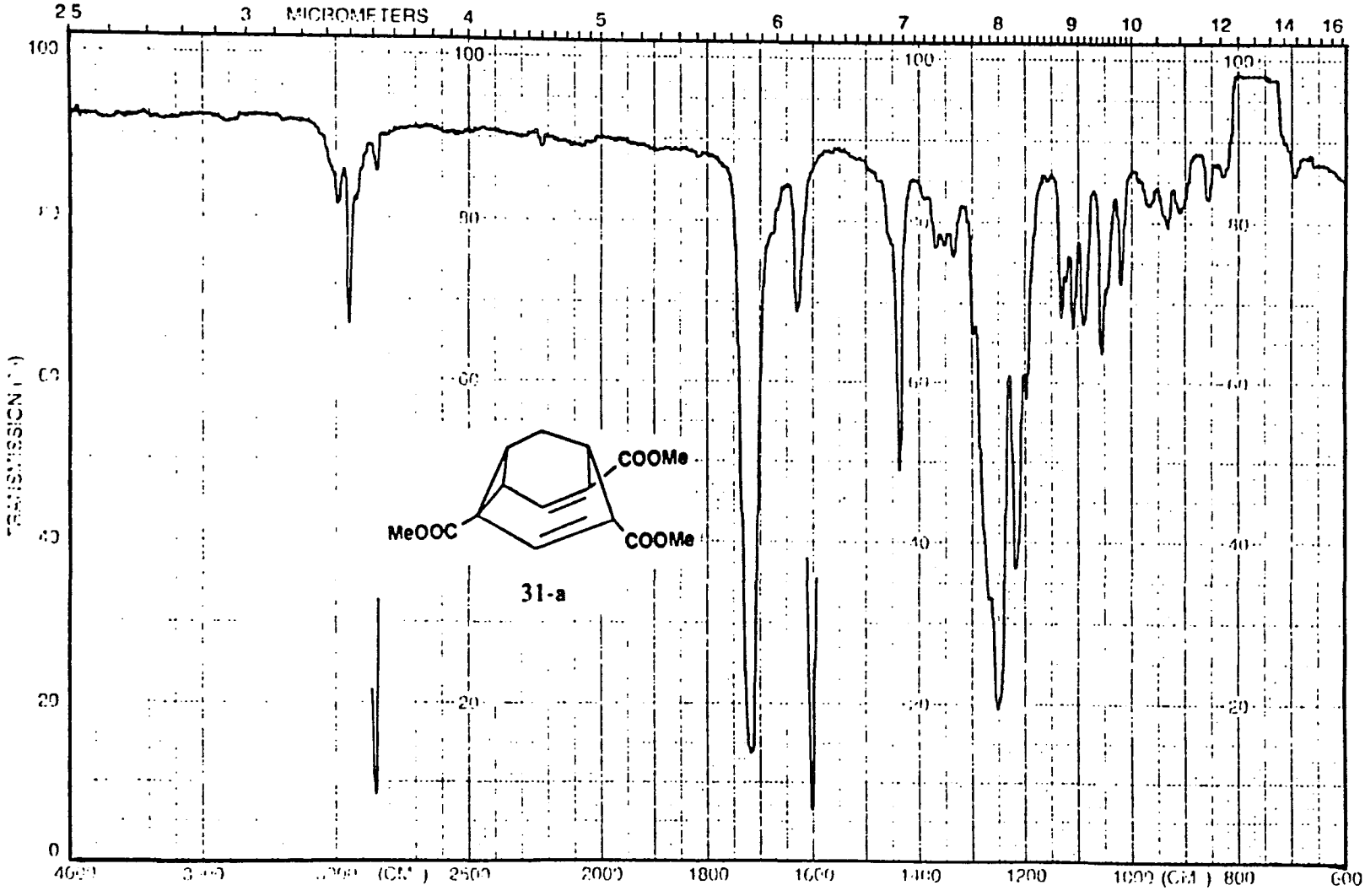
MICROMETERS
TRANSMISSION (%)
COOMe
MeOOC
COOMe
31-a

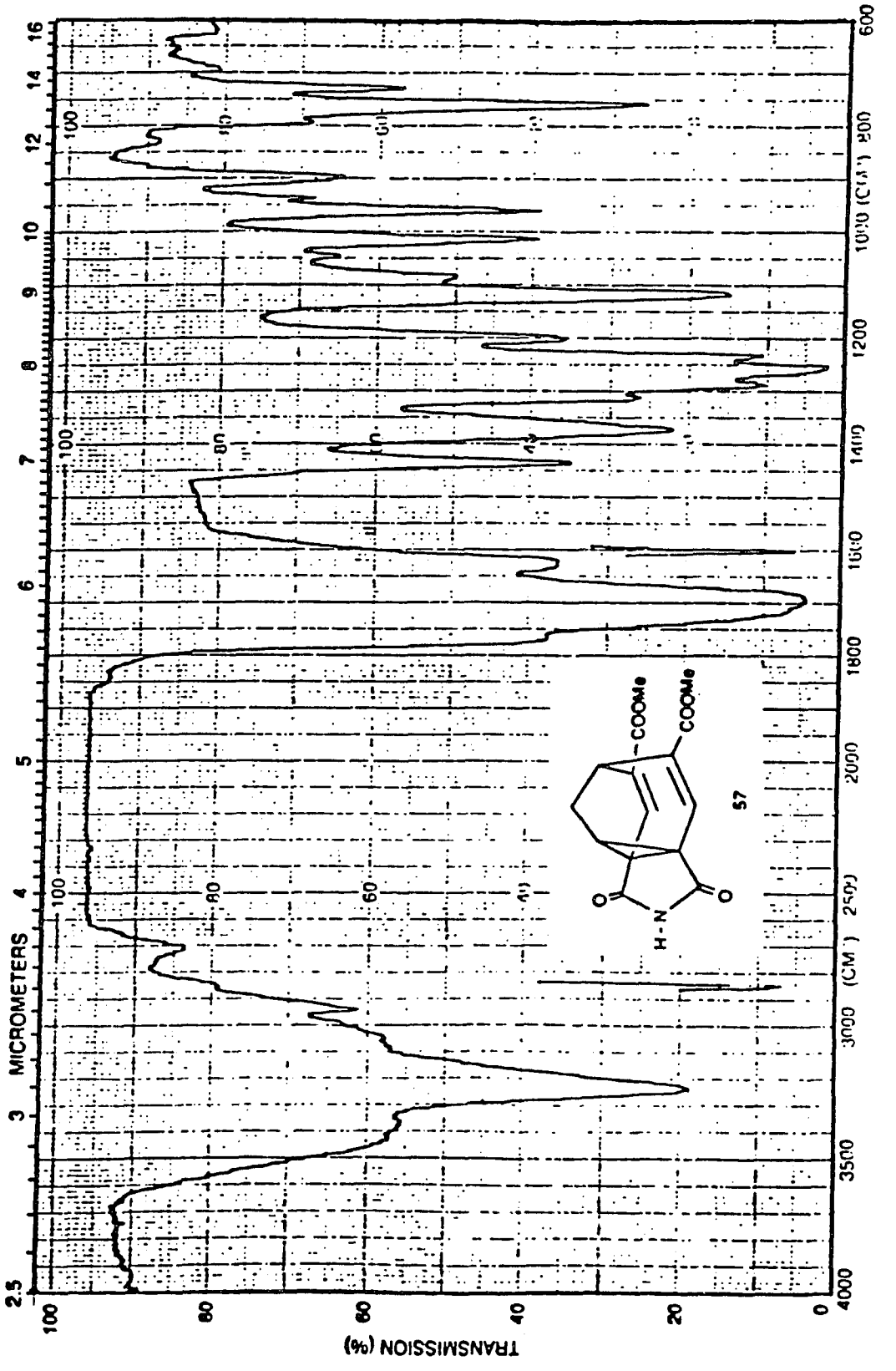
MICROMETERS
TRANSMISSION (%)
COOMe
COOMe
H-N
O
O
57

X-Ray Data of Selected Compounds

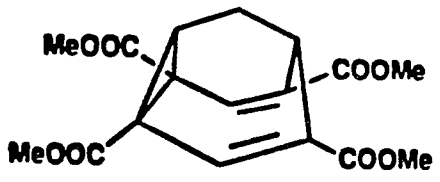
MeOOC
COOMe
MeOOC
COOMe

18

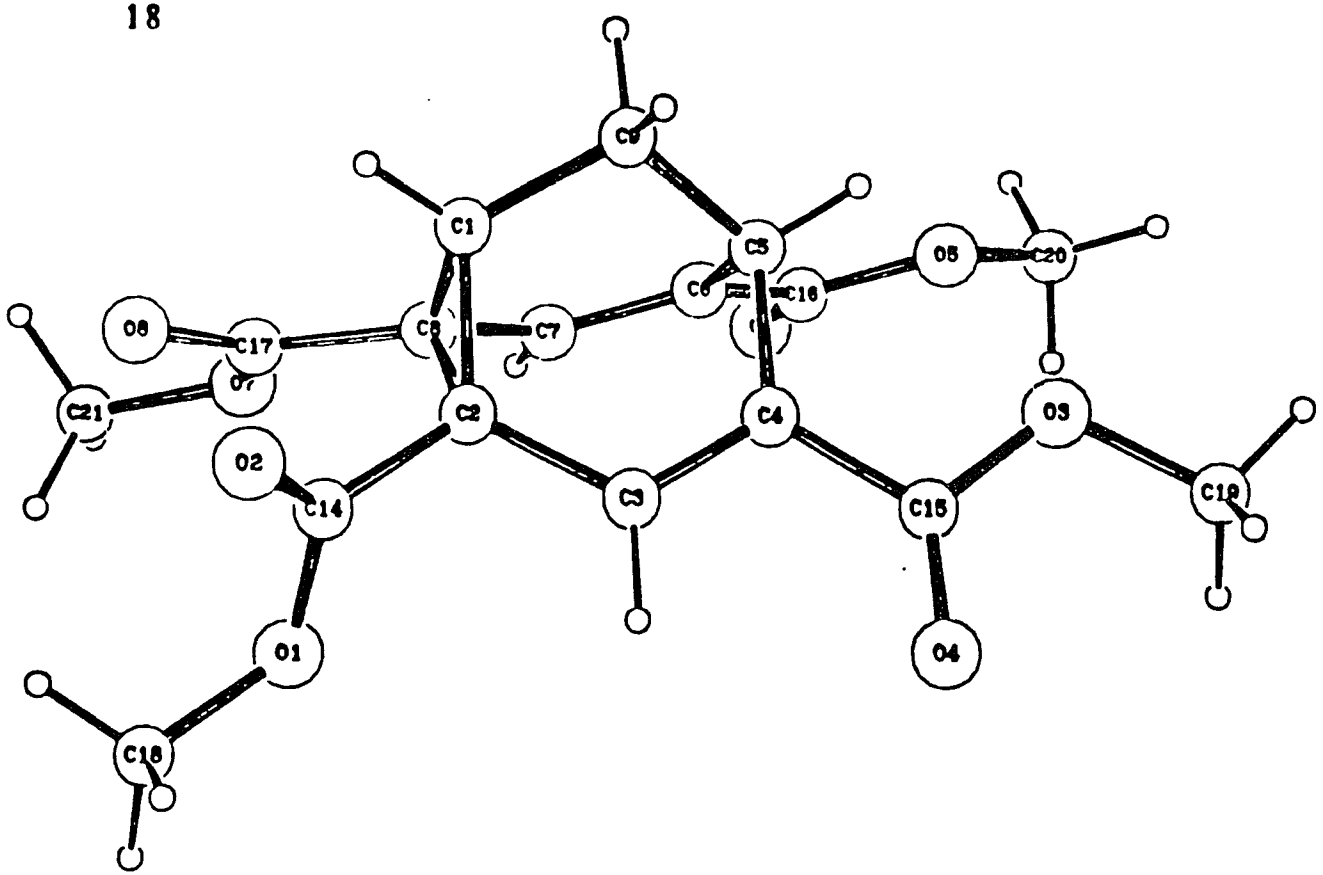
C9
C1
C5
C6
C16
O5
C20
O8
C17
C8
C7
O7
C21
C2
C4
O3
O2
C14
C3
C15
C19
O1
O4
C18

Table 6: Crystal Data for Compound 18

Formula		$C_{17}H_{18}O_8$	
Formula weight		350.33	
Temperature (K)	295		110
Crystal size (mm)		0.10 x 0.36 x 0.50	
Crystal system		Monoclinic	
Space group		$P2_1/c$	
a (Å)	7.854(1)		7.757(1)
b (Å)	16.206(2)		16.101(5)
c (Å)	12.982(2)		12.866(3)
β (°)	90.64(1)		90.08(1)
Cell volume (Å^3)	1652.3		1606.9
Z		4	
d_{calc} (g cm^{-3})	1.408		1.448
μ(Cu Kα) (cm^{-1})	9.2		9.4

Table 7: Experimental Details for Compound **18**

Temperature (K)	295	110
Maximum θ (°)	75	75
Number of unique reflections	3401	3314
Number of observed reflections [$I > 3\sigma(I)$]	2735	2888
Absorption correction	no	no
Least-square refinement	full matrix	full matrix
Nonhydrogen atoms	anisotropic	anisotropic
Hydrogen atoms	isotropic (fixed)	isotropic (fixed)
Final R	0.046	0.044
Final wR	0.059	0.059
Largest peak of final difference map (e $Å^{-3}$)	0.2	0.4

Table 8: Final Atomic Parameters for Compound 18 at 295K

Atom	x	y	z	B(A2)
O1	0.2411(2)	0.42427(9)	0.87540(9)	3.80(3)
O2	0.4506(2)	0.33047(9)	0.8817(1)	4.21(3)
O3	-0.0046(2)	0.2492(1)	0.4500(1)	4.52(3)
O4	-0.1120(2)	0.2466(1)	0.6082(1)	5.00(3)
O5	0.1152(2)	0.40867(9)	0.9340(1)	3.91(3)
O6	0.1288(2)	0.53870(8)	0.3919(1)	4.26(3)
O7	0.4229(2)	0.59253(7)	0.7060(1)	3.84(3)
O8	0.5680(2)	0.49999(8)	0.8004(1)	3.97(3)
C1	0.4874(2)	0.3714(1)	0.6518(1)	2.55(3)
C2	0.3338(2)	0.37204(9)	0.7181(1)	2.50(3)
C3	0.1796(2)	0.3294(1)	0.6809(1)	2.64(3)
C4	0.1582(2)	0.31033(9)	0.5814(1)	2.59(3)
C5	0.2884(2)	0.33974(9)	0.5044(1)	2.52(3)
C6	0.2538(2)	0.43096(9)	0.4924(1)	2.38(3)
C7	0.3008(2)	0.48260(9)	0.5681(1)	2.48(3)
C8	0.3961(2)	0.45376(9)	0.6587(1)	2.41(3)
C9	0.4687(2)	0.3276(1)	0.5497(1)	2.65(3)
C14	0.3539(2)	0.3728(1)	0.8337(1)	2.90(3)
C15	-0.0002(2)	0.2662(1)	0.5503(1)	3.15(3)
C16	0.1600(2)	0.4664(1)	0.4027(1)	2.79(3)
C17	0.4731(2)	0.5162(1)	0.7297(1)	2.79(3)
C18	0.2500(4)	0.4321(2)	0.9862(2)	5.68(6)
C19	-0.1559(3)	0.2082(2)	0.4114(2)	6.38(6)
C20	0.0244(3)	0.4381(2)	0.2439(2)	4.80(5)
C21	0.4819(4)	0.6570(1)	0.7749(2)	5.04(5)
H1	0.600	0.367	0.688	3.0
H3	0.089	0.314	0.731	3.1
H5	0.281	0.309	0.438	3.0
H7	0.270	0.542	0.563	2.9
H9A	0.490	0.267	0.560	3.1
H9B	0.554	0.350	0.501	3.1
H18A	0.161	0.472	1.010	6.8
H18B	0.230	0.377	1.018	6.8
H18C	0.365	0.453	1.007	6.8
H19A	-0.145	0.199	0.335	7.6
H19B	-0.170	0.154	0.447	7.6
H19C	-0.258	0.244	0.424	7.6
H20A	-0.003	0.391	0.198	5.7
H20B	-0.083	0.466	0.265	5.7
H20C	0.097	0.479	0.206	5.7
H21A	0.437	0.712	0.750	6.0
H21B	0.440	0.646	0.846	6.0
H21C	0.609	0.658	0.776	6.0

The parameters of the hydrogen atoms were not refined.

Standard deviations are in parentheses.

Anisotropically refined atoms are given in the form of the isotropic equivalent displacement parameter defined as:
(4/3) * [a2*B(1,1) + b2*B(2,2) + c2*B(3,3) + ab(cos gamma)*B(1,2) + ac(cos beta)*B(1,3) + bc(cos alpha)*B(2,3)]

Table 9: Final Anisotropic Thermal Parameters (U's) for

Compound 18 at 295K

Atom	U(1,1)	U(2,2)	U(3,3)	U(1,2)	U(1,3)	U(2,3)
O1	0.0575(7)	0.0600(8)	0.0270(5)	0.0118(6)	-0.0005(5)	-0.0035(6)
O2	0.0630(8)	0.0540(7)	0.0428(6)	0.0109(6)	-0.0119(6)	0.0133(6)
O3	0.0460(6)	0.0793(9)	0.0484(7)	-0.0151(7)	-0.0040(6)	-0.0179(7)
O4	0.0538(7)	0.0804(9)	0.0557(8)	-0.0298(7)	0.0027(7)	0.0038(8)
O5	0.0634(7)	0.0522(7)	0.0325(6)	0.0037(6)	-0.0165(5)	-0.0019(6)
O6	0.0691(8)	0.0421(6)	0.0502(7)	0.0120(6)	-0.0107(7)	0.0090(6)
O7	0.0693(8)	0.0277(5)	0.0488(7)	-0.0018(6)	-0.0148(6)	-0.0074(5)
O8	0.0618(7)	0.0441(6)	0.0446(6)	-0.0060(6)	-0.0189(6)	-0.0028(6)
C1	0.0326(7)	0.0298(7)	0.0345(7)	0.0025(6)	-0.0027(6)	0.0018(6)
C2	0.0376(7)	0.0276(7)	0.0297(7)	0.0002(6)	-0.0018(6)	0.0025(6)
C3	0.0376(7)	0.0278(7)	0.0349(7)	-0.0020(6)	0.0003(6)	0.0041(6)
C4	0.0357(7)	0.0254(6)	0.0371(7)	-0.0011(6)	-0.0020(6)	0.0019(6)
C5	0.0379(7)	0.0270(7)	0.0307(7)	0.0010(6)	-0.0007(6)	-0.0009(6)
C6	0.0325(7)	0.0294(7)	0.0284(6)	0.0009(6)	0.0003(6)	0.0027(6)
C7	0.0367(7)	0.0268(7)	0.0308(7)	0.0004(6)	0.0006(6)	0.0031(6)
C8	0.0356(7)	0.0268(6)	0.0291(6)	-0.0019(6)	-0.0016(6)	-0.0001(6)
C9	0.0354(7)	0.0301(7)	0.0353(7)	0.0043(6)	0.0020(6)	-0.0007(6)
C14	0.0429(8)	0.0348(7)	0.0326(7)	-0.0027(7)	-0.0042(7)	0.0049(6)
C15	0.0395(8)	0.0343(8)	0.0456(9)	-0.0033(7)	-0.0050(7)	-0.0006(7)
C16	0.0361(7)	0.0390(8)	0.0309(7)	0.0025(6)	0.0007(6)	0.0040(6)
C17	0.0401(8)	0.0319(7)	0.0340(7)	-0.0048(6)	0.0003(6)	-0.0007(6)
C18	0.097(2)	0.093(2)	0.0256(8)	0.010(1)	0.001(1)	-0.008(1)
C19	0.048(1)	0.122(2)	0.072(1)	-0.023(1)	-0.009(1)	-0.038(1)
C20	0.061(1)	0.085(2)	0.0364(9)	0.006(1)	-0.0164(8)	0.004(1)
C21	0.091(1)	0.0329(9)	0.067(1)	-0.007(1)	-0.019(1)	-0.0178(9)

The form of the anisotropic displacement parameter is:
exp[-2PI2[h2a2U(1,1) + k2b2U(2,2) + l2c2U(3,3) + 2hkabU(1,2) + 2hlacU(1,3) + 2klbcU(2,3)]] where a,b, and c are reciprocal lattice constants.

Table 10: Bond Distances (Å) for Compound 18 at 295K

Atom 1	Atom 2	Distance
O1	C14	1.336(2)
O1	C18	1.445(2)
O2	C14	1.194(2)
O3	C15	1.331(2)
O3	C19	1.446(3)
O4	C15	1.204(2)
O5	C16	1.337(2)
O5	C20	1.444(3)
O6	C16	1.205(2)
O7	C17	1.333(2)
O7	C21	1.448(3)
O8	C17	1.205(2)
C1	C2	1.490(2)
C1	C8	1.518(2)
C1	C9	1.509(2)
C2	C3	1.473(2)
C2	C8	1.611(2)
C2	C14	1.507(2)
C3	C4	1.337(2)
C4	C5	1.515(2)
C4	C15	1.487(2)
C5	C6	1.511(2)
C5	C9	1.539(2)
C6	C7	1.339(2)
C6	C16	1.487(2)
C7	C8	1.464(2)
C8	C17	1.492(2)

Standard deviations are in parentheses.

Table 11: Bond Angles (°) for Compound 18 at 295K

Atom 1	Atom 2	Atom 3	Angle	Atom 1	Atom 2	Atom 3	Angle
C14	O1	C18	115.7(2)	C3	C4	C15	117.9(1)
C15	O3	C19	116.5(2)	C5	C4	C15	122.8(1)
C16	O5	C20	115.6(2)	C4	C5	C6	104.7(1)
C17	O7	C21	115.8(1)	C4	C5	C9	109.5(1)
C2	C1	C8	64.8(1)	C6	C5	C9	109.1(1)
C2	C1	C9	116.1(1)	C5	C6	C7	119.2(1)
C8	C1	C9	115.1(1)	C5	C6	C16	123.1(1)
C1	C2	C3	118.4(1)	C7	C6	C16	117.6(1)
C1	C2	C8	58.5(1)	C6	C7	C8	121.6(1)
C1	C2	C14	119.9(1)	C1	C8	C2	56.8(1)
C3	C2	C8	118.8(1)	C1	C8	C7	118.1(1)
C3	C2	C14	114.0(1)	C1	C8	C17	116.4(1)
C8	C2	C14	116.1(1)	C2	C8	C7	119.4(1)
C2	C3	C4	121.3(1)	C2	C8	C17	112.6(1)
C3	C4	C5	119.1(1)	C7	C8	C17	118.7(1)

Atom 1	Atom 2	Atom 3	Angle
C1	C9	C5	110.8(1)
O1	C14	O2	124.6(2)
O1	C14	C2	110.2(1)
O2	C14	C2	125.0(2)
O3	C15	O4	123.0(2)
O3	C15	C4	112.1(1)
O4	C15	C4	124.8(2)
O5	C16	O6	123.5(2)
O5	C16	C6	112.1(1)
O6	C16	C6	124.4(2)
O7	C17	O8	123.8(2)
O7	C17	C8	111.7(1)
O8	C17	C8	124.4(2)

Standard deviations are in parentheses.

Table 12: Final Atomic Parameters for Compound 18 at 110K

Atom	x	y	z	B(A2)
O1	0.2381(1)	0.42302(7)	0.87604(8)	1.52(2)
O2	0.4513(1)	0.32827(7)	0.88163(9)	1.60(2)
O3	-0.0038(1)	0.24728(8)	0.44488(9)	1.86(2)
O4	-0.1145(2)	0.24272(8)	0.60609(9)	1.98(2)
O5	0.1136(1)	0.40917(7)	0.33044(8)	1.53(2)
O6	0.1275(2)	0.54062(7)	0.38981(9)	1.62(2)
O7	0.4244(1)	0.59365(6)	0.70614(9)	1.52(2)
O8	0.5674(1)	0.49908(7)	0.80172(9)	1.56(2)
C1	0.4908(2)	0.37085(9)	0.6492(1)	1.07(2)
C2	0.3343(2)	0.37083(9)	0.7167(1)	1.08(2)
C3	0.1790(2)	0.32736(9)	0.6793(1)	1.15(2)
C4	0.1586(2)	0.30841(9)	0.5784(1)	1.10(2)
C5	0.2908(2)	0.33928(9)	0.5005(1)	1.10(2)
C6	0.2545(2)	0.43116(9)	0.4898(1)	1.08(2)
C7	0.3006(2)	0.48292(8)	0.5665(1)	1.10(2)
C8	0.3968(2)	0.45342(9)	0.6574(1)	1.07(2)
C9	0.4734(2)	0.32723(9)	0.5462(1)	1.13(2)
C14	0.3534(2)	0.37121(9)	0.8331(1)	1.19(2)
C15	-0.0014(2)	0.26401(9)	0.5470(1)	1.34(2)
C16	0.1591(2)	0.46726(9)	0.4003(1)	1.16(2)
C17	0.4734(2)	0.51616(9)	0.7298(1)	1.15(2)
C18	0.2492(2)	0.4306(1)	0.9876(1)	2.19(3)
C19	-0.1564(2)	0.2053(1)	0.4073(2)	2.62(3)
C20	0.0225(2)	0.4403(1)	0.2406(1)	1.78(3)
C21	0.4833(2)	0.6572(1)	0.7774(1)	1.92(3)
H1	0.605	0.367	0.685	1.3
H3	0.087	0.312	0.730	1.4
H5	0.284	0.309	0.433	1.3
H7	0.269	0.543	0.562	1.3
H9A	0.495	0.267	0.556	1.3
H9B	0.560	0.350	0.497	1.3
H18A	0.159	0.470	1.013	2.6
H18B	0.230	0.375	1.020	2.6
H18C	0.366	0.452	1.007	2.6
H19A	-0.146	0.196	0.331	3.1
H19B	-0.169	0.151	0.466	3.1
H19C	-0.260	0.240	0.421	3.1
H20A	-0.006	0.393	0.193	2.1
H20B	-0.086	0.468	0.263	2.1
H20C	0.097	0.481	0.203	2.1
H21A	0.441	0.713	0.753	2.3
H21B	0.438	0.645	0.848	2.3
H21C	0.612	0.658	0.779	2.3

The parameters of the hydrogen atoms were not refined.

Standard deviations are in parentheses.

Anisotropically refined atoms are given in the form of the isotropic equivalent displacement parameter defined as:
(4/3) * [a2*B(1,1) + b2*B(2,2) + c2*B(3,3) + ab(cos gamma)*B(1,2) + ac(cos beta)*B(1,3) + bc(cos alpha)*B(2,3)]

Table 13: Final Anisotropic Thermal Parameters (U's) for Compound **18** at 110K

Atom	U(1,1)	U(2,2)	U(3,3)	U(1,2)	U(1,3)	U(2,3)
O1	0.0245(5)	0.0202(5)	0.0132(4)	0.0049(4)	-0.0009(4)	-0.0014(4)
O2	0.0232(5)	0.0174(5)	0.0202(5)	0.0016(4)	-0.0046(4)	0.0045(4)
O3	0.0186(5)	0.0300(6)	0.0221(5)	-0.0048(5)	-0.0025(4)	-0.0091(5)
O4	0.0232(5)	0.0272(6)	0.0249(5)	-0.0105(5)	-0.0008(5)	0.0024(5)
O5	0.0263(5)	0.0166(5)	0.0153(5)	0.0014(4)	-0.0065(4)	-0.0009(4)
O6	0.0260(5)	0.0135(5)	0.0220(5)	0.0037(4)	-0.0041(4)	0.0032(4)
O7	0.0281(5)	0.0078(4)	0.0217(5)	-0.0008(4)	-0.0058(4)	-0.0029(4)
O8	0.0241(5)	0.0158(5)	0.0193(5)	-0.0017(4)	-0.0067(4)	-0.0005(4)
C1	0.0157(6)	0.0091(6)	0.0157(6)	0.0010(5)	-0.0009(5)	0.0002(5)
C2	0.0174(6)	0.0089(6)	0.0148(6)	-0.0001(5)	-0.0012(5)	0.0007(5)
C3	0.0165(6)	0.0090(6)	0.0182(6)	-0.0000(5)	-0.0006(5)	0.0015(5)
C4	0.0159(6)	0.0080(6)	0.0180(6)	0.0005(5)	-0.0017(5)	0.0012(5)
C5	0.0172(6)	0.0095(6)	0.0151(6)	0.0001(5)	-0.0015(5)	-0.0002(5)
C6	0.0149(6)	0.0104(6)	0.0157(6)	0.0003(5)	-0.0009(5)	0.0017(5)
C7	0.0163(6)	0.0105(6)	0.0151(6)	-0.0001(5)	-0.0003(5)	0.0022(5)
C8	0.0176(6)	0.0083(6)	0.0147(6)	-0.0005(5)	-0.0012(5)	0.0003(5)
C9	0.0158(6)	0.0109(6)	0.0161(6)	0.0017(5)	0.0001(5)	-0.0011(5)
C14	0.0168(6)	0.0115(6)	0.0170(6)	-0.0024(5)	-0.0009(5)	0.0012(5)
C15	0.0191(6)	0.0107(6)	0.0210(7)	0.0003(5)	-0.0029(5)	0.0005(6)
C16	0.0155(6)	0.0138(6)	0.0146(6)	0.0004(5)	0.0000(5)	-0.0001(5)
C17	0.0178(6)	0.0098(6)	0.0161(6)	-0.0010(5)	0.0003(5)	-0.0002(5)
C18	0.0400(9)	0.0307(8)	0.0123(6)	0.0043(8)	-0.0005(6)	-0.0033(6)
C19	0.0203(7)	0.046(1)	0.0331(8)	-0.0081(7)	-0.0035(7)	-0.0171(8)
C20	0.0247(7)	0.0271(8)	0.0159(7)	0.0018(7)	-0.0060(6)	0.0017(6)
C21	0.0361(8)	0.0104(6)	0.0264(8)	-0.0025(6)	-0.0060(7)	-0.0069(6)

The form of the anisotropic displacement parameter is:
exp[-2PI2[h2a2U(1,1) + k2b2U(2,2) + l2c2U(3,3) + 2hkabU(1,2) + 2hlacU(1,3) + 2klbcU(2,3)]] where a,b, and c are reciprocal lattice constants.

Table 14: Bond Distances (Å) for Compound 18 at 110K

Atom 1	Atom 2	Distance	Atom 1	Atom 2	Distance
O1	C14	1.342(2)	O7	C17	1.339(2)
O1	C18	1.443(2)	O7	C21	1.448(2)
O2	C14	1.201(2)	O8	C17	1.209(2)
O3	C15	1.342(2)	C1	C2	1.494(2)
O3	C19	1.445(2)	C1	C8	1.520(2)
O4	C15	1.211(2)	C1	C9	1.505(2)
O5	C16	1.344(2)	C2	C3	1.473(2)
O5	C20	1.444(2)	C2	C8	1.608(2)
O6	C16	1.214(2)	C2	C14	1.505(2)

Atom 1	Atom 2	Distance
C3	C4	1.342(2)
C4	C5	1.519(2)
C4	C15	1.487(2)
C5	C6	1.512(2)
C5	C9	1.545(2)
C6	C7	1.340(2)
C6	C16	1.486(2)
C7	C8	1.466(2)
C8	C17	1.497(2)

Standard deviations are in parentheses.

Table 15: Bond Angles (°) for Compound 18 at 110K

Atom 1	Atom 2	Atom 3	Angle
C14	O1	C18	115.0(1)
C15	O3	C19	115.6(1)
C16	O5	C20	115.0(1)
C17	O7	C21	115.2(1)
C2	C1	C8	64.5(1)
C2	C1	C9	116.1(1)
C8	C1	C9	115.3(1)
C1	C2	C3	118.3(1)
C1	C2	C8	58.5(1)
C1	C2	C14	120.0(1)
C3	C2	C8	119.0(1)
C3	C2	C14	114.0(1)
C8	C2	C14	116.1(1)
C2	C3	C4	121.3(1)
C3	C4	C5	119.0(1)
C3	C4	C15	117.9(1)
C5	C4	C15	122.8(1)
C4	C5	C6	104.7(1)
C4	C5	C9	109.1(1)
C6	C5	C9	109.1(1)
C5	C6	C7	119.5(1)
C5	C6	C16	123.1(1)
C7	C6	C16	117.3(1)
C6	C7	C8	121.4(1)
C1	C8	C2	57.0(1)
C1	C8	C7	118.1(1)
C1	C8	C17	116.3(1)
C2	C8	C7	119.6(1)
C2	C8	C17	112.5(1)
C7	C8	C17	118.6(1)
C1	C9	C5	110.9(1)
O1	C14	O2	124.4(1)
O1	C14	C2	110.3(1)
O2	C14	C2	125.2(1)
O3	C15	O4	123.3(1)
O3	C15	C4	111.9(1)
O4	C15	C4	124.8(1)
O5	C16	O6	123.4(1)
O5	C16	C6	112.1(1)
O6	C16	C6	124.5(1)
O7	C17	O8	123.8(1)
O7	C17	C8	112.0(1)
O8	C17	C8	124.1(1)

Standard deviations are in parentheses.

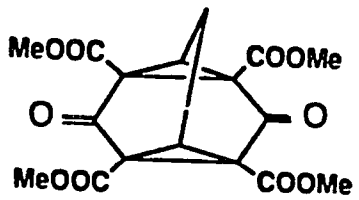
MeOOC
COOMe
O
O
MeOOC
COOMe

27

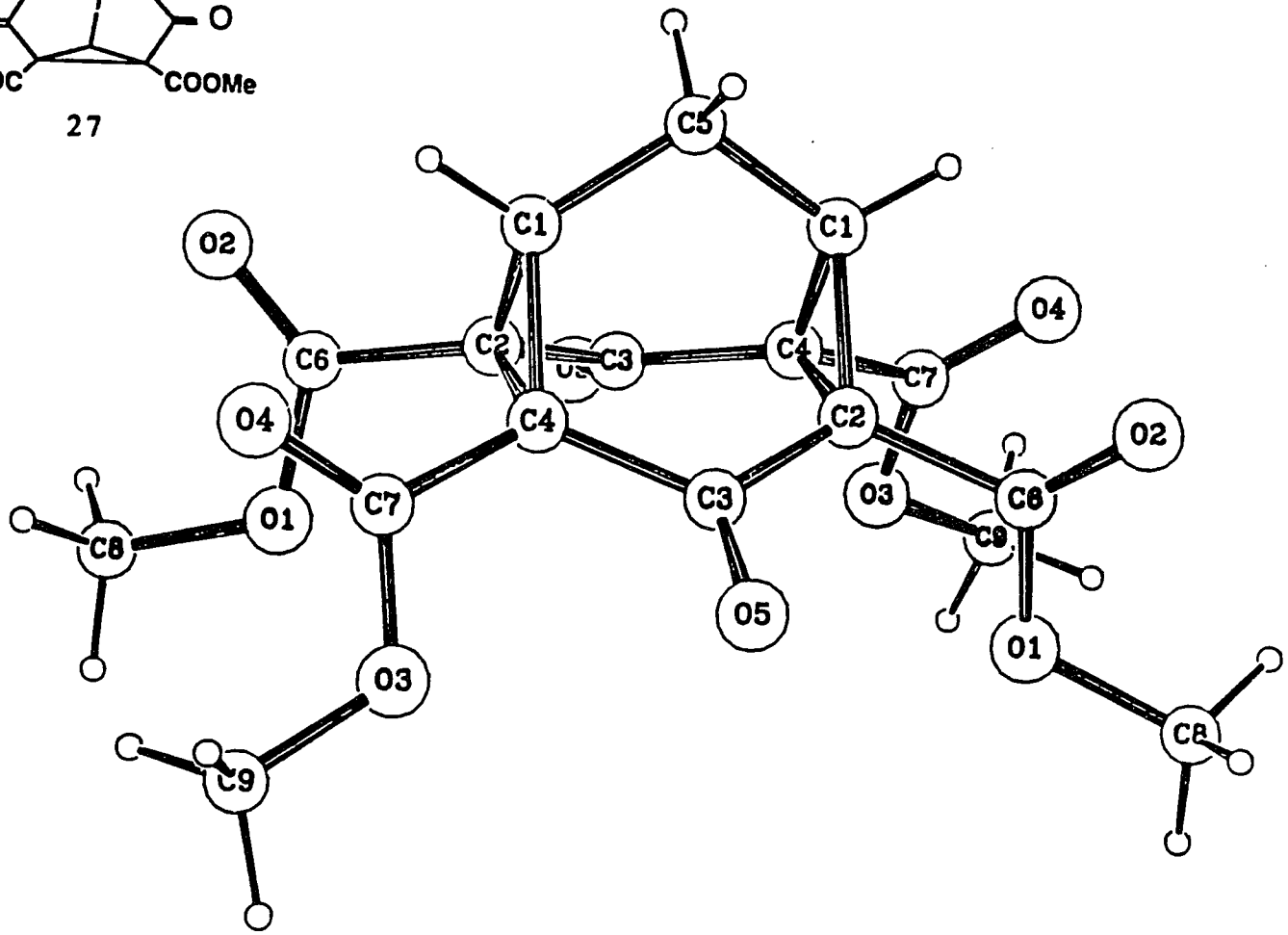
C5
C1
C1
02
04
C6
C2
C3
C4
C7
04
C4
C2
02
01
C7
C3
03
C8
C8
C9
05
01
03
C8
C9

Table 16: Crystal Data for Compound 27

Formula	$C_{17}H_{16}O_{10}$
Formula weight	380.31
Crystal system	monoclinic
Space group	C2/c
a	20.832(2) Å
b	5.911(1) Å
c	13.877(2) Å
β	99.76(1)°
Z	4
d_{calc}	1.500 g cm^{-3}
μ(Cu Kα)	10.4 cm^{-1}

Table 17: Final Atomic Parameters for Compound 27

Atom	x	y	z	B(A2)
O1	0.35259(8)	0.1988(3)	0.1822(2)	3.54(4)
O2	0.31803(9)	0.5485(4)	0.1395(2)	4.61(5)
O3	0.58670(9)	0.2004(4)	0.0885(2)	4.04(4)
O4	0.64606(9)	0.5154(4)	0.1185(2)	4.46(5)
O5	0.45787(9)	0.3404(4)	0.0639(2)	4.08(5)
C1	0.4422(1)	0.7056(5)	0.2650(2)	3.40(6)
C2	0.4299(1)	0.4893(4)	0.2087(2)	2.81(5)
C3	0.4768(1)	0.4234(4)	0.1435(2)	2.94(5)
C4	0.5463(1)	0.4848(4)	0.1790(2)	2.91(5)
C5	0.500	0.8478(7)	0.250	4.1(1)
C6	0.3600(1)	0.4205(5)	0.1725(2)	3.02(5)
C7	0.5982(1)	0.4074(5)	0.1236(2)	3.14(5)
C8	0.2860(1)	0.1149(6)	0.1538(3)	4.44(7)
C9	0.6368(2)	0.1010(7)	0.0410(3)	5.04(8)
H1	0.402	0.792	0.275	4.0
H5	0.487	0.945	0.191	4.9
H8A	0.285	-0.053	0.164	5.3
H8B	0.257	0.189	0.195	5.3
H8C	0.270	0.151	0.083	5.3
H9A	0.623	-0.054	0.017	6.0
H9B	0.643	0.197	-0.016	6.0
H9C	0.679	0.092	0.089	6.0

The parameters of the hydrogen atoms were not refined.

Standard deviations are in parentheses.

Anisotropically refined atoms are given in the form of the isotropic equivalent displacement parameter defined as:
(4/3) * [a2*B(1,1) + b2*B(2,2) + c2*B(3,3) + ab(cos gamma)*B(1,2) + ac(cos beta)*B(1,3) + bc(cos alpha)*B(2,3)]

Table 18: Final Anisotropic Thermal Parameters (U's) for Compound 27

Atom	U(1,1)	U(2,2)	U(3,3)	U(1,2)	U(1,3)	U(2,3)
O1	0.0328(8)	0.0297(9)	0.070(1)	-0.0036(8)	0.0023(8)	0.003(1)
O2	0.0388(9)	0.042(1)	0.087(2)	0.0051(9)	-0.011(1)	0.013(1)
O3	0.0518(9)	0.041(1)	0.065(1)	-0.0080(9)	0.0225(9)	-0.008(1)
O4	0.0421(9)	0.054(1)	0.076(1)	-0.0135(9)	0.0175(9)	-0.003(1)
O5	0.0451(9)	0.060(1)	0.047(1)	-0.011(1)	0.0018(8)	-0.001(1)
C1	0.035(1)	0.024(1)	0.068(2)	0.002(1)	0.003(1)	-0.002(1)
C2	0.030(1)	0.026(1)	0.049(1)	-0.001(1)	0.000(1)	0.005(1)
C3	0.034(1)	0.028(1)	0.047(1)	-0.007(1)	0.001(1)	0.009(1)
C4	0.033(1)	0.028(1)	0.047(1)	-0.003(1)	0.002(1)	0.004(1)
C5	0.041(2)	0.023(2)	0.089(3)	0	0.002(2)	0
C6	0.032(1)	0.033(1)	0.048(1)	0.000(1)	0.002(1)	0.004(1)
C7	0.036(1)	0.039(1)	0.043(1)	-0.005(1)	0.004(1)	0.005(1)
C8	0.039(1)	0.044(2)	0.084(2)	-0.013(1)	0.005(1)	-0.006(2)
C9	0.069(2)	0.059(2)	0.071(2)	-0.003(2)	0.034(1)	-0.009(2)

The form of the anisotropic displacement parameter is:
exp[-2PI2(h2a2U(1,1) + k2b2U(2,2) + l2c2U(3,3) + 2hkabU(1,2) + 2hlacU(1,3) + 2klbcU(2,3))] where a,b, and c are reciprocal lattice constants.

Table 19: Bond Distances (Å) for Compound 27

Atom 1	Atom 2	Distance	Atom 1	Atom 2	Distance
O1	C6	1.329(3)	C1	C4	1.517(4)
O1	C8	1.462(3)	C1	C5	1.512(3)
O2	C6	1.188(3)	C2	C3	1.491(4)
O3	C7	1.323(4)	C2	C4	1.553(4)
O3	C9	1.450(4)	C2	C6	1.514(3)
O4	C7	1.197(3)	C3	C4	1.493(3)
O5	C3	1.211(3)	C4	C7	1.500(4)
C1	C2	1.498(4)			

Standard deviations are in parentheses.

Table 20: Bond Angles (°) for Compound 27

Atom 1	Atom 2	Atom 3	Angle	Atom 1	Atom 2	Atom 3	Angle
C6	O1	C8	115.4(2)	C1	C4	C2	58.4(2)
C7	O3	C9	116.3(2)	C1	C4	C3	116.0(2)
C2	C1	C4	62.0(2)	C1	C4	C7	117.4(2)
C2	C1	C5	118.2(2)	C2	C4	C3	117.5(2)
C4	C1	C5	119.3(2)	C2	C4	C7	112.6(2)
C1	C2	C3	117.9(2)	C3	C4	C7	119.9(2)
C1	C2	C4	59.6(2)	C1	C5	C1	112.4(3)
C1	C2	C6	118.1(2)	O1	C6	O2	125.2(2)
C3	C2	C4	118.3(2)	O1	C6	C2	110.7(2)
C3	C2	C6	114.9(2)	O2	C6	C2	124.2(3)
C4	C2	C6	117.0(2)	O3	C7	O4	124.9(3)
O5	C3	C2	120.9(2)	O3	C7	C4	111.7(2)
O5	C3	C4	123.2(3)	O4	C7	C4	123.2(3)
C2	C3	C4	115.7(2)				

Standard deviations are in parentheses.

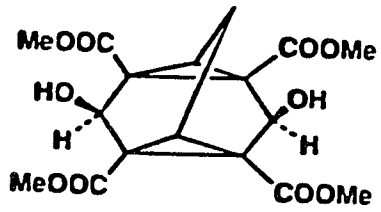
MeOOC
COOMe
HO
OH
H
H
MeOOC
COOMe

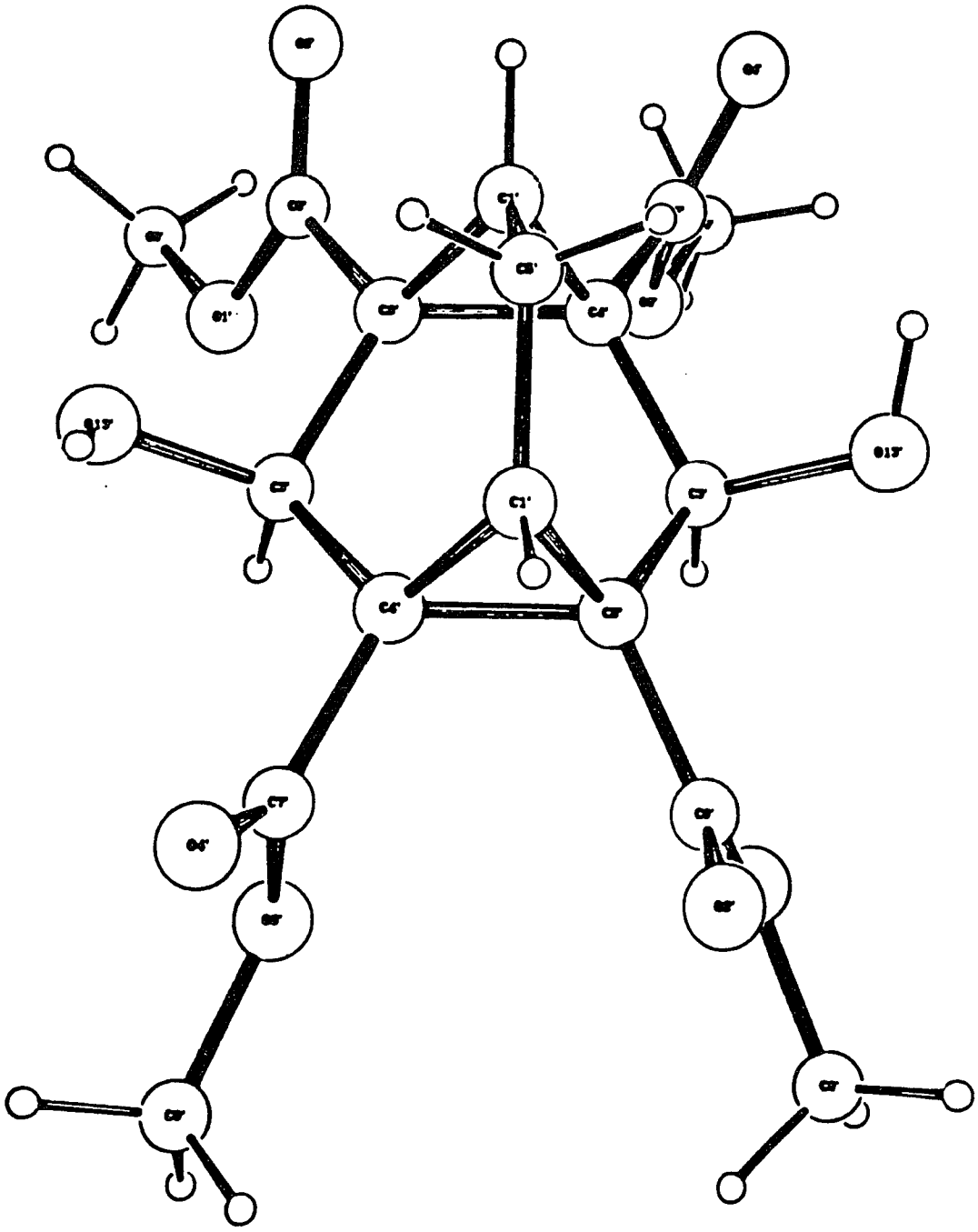

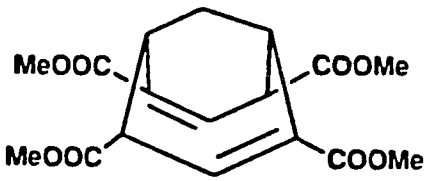
MeOOC
COOMe
MeOOC
COOMe

30

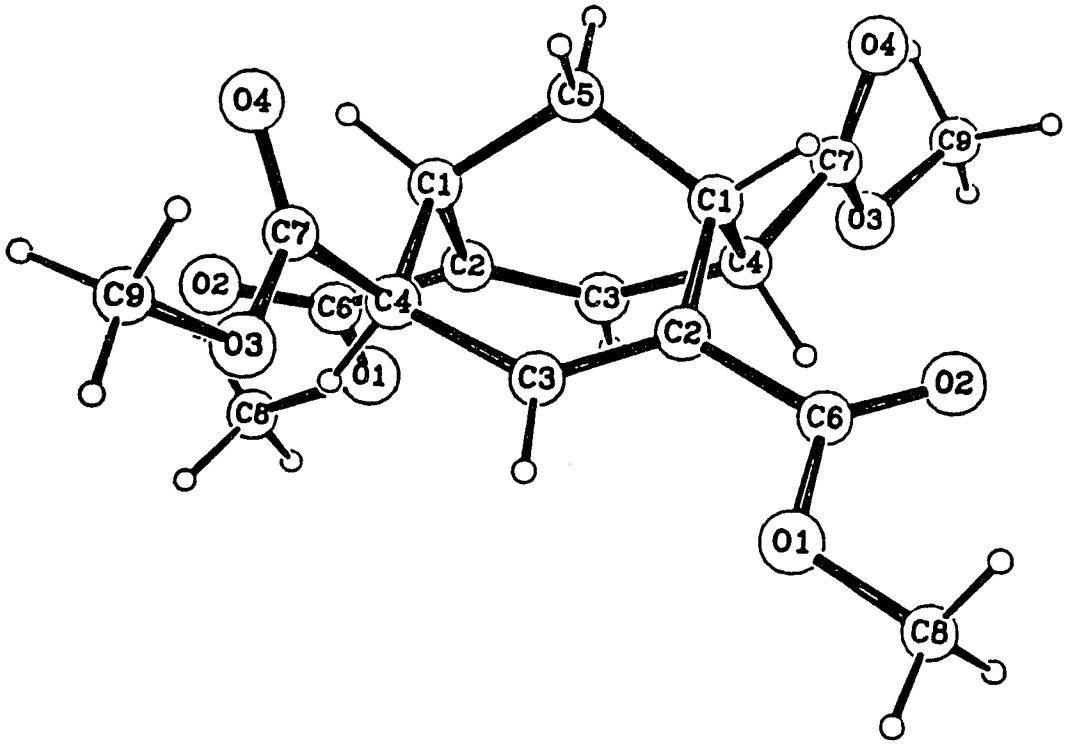
O4
C5
O4
C1
C7
C9
C1
C7
O3
C9
O2
C6
C4
C2
C3
C4
O3
C2
O1
C3
O2
C6
C6
O1
C8

Table 21: Crystal Data for Compound **30**

Formula	$C_{17}H_{20}O_8$
Formula weight	352.34
Crystal system	orthorhombic
Space group	Ac2a
a	10.083(1) Å
b	9.925(1) Å
c	17.742(1) Å
Z	4
d_{calc}	1.318 g cm^{-3}
μ(Cu Kα)	8.5 cm^{-1}

Table 22: Final Atomic Parameters for Compound 30

Atom	x	y	z	B(A2)
O1	0.2846(3)	0.200	0.1566(2)	5.89(6)
O2	0.4548(3)	0.3108(5)	0.2059(2)	7.34(8)
O3	0.8798(2)	0.3606(4)	0.0825(2)	5.94(7)
O4	0.7727(3)	0.5504(3)	0.1059(2)	6.07(6)
C1	0.5215(3)	0.4393(4)	0.0686(2)	3.63(6)
C2	0.4070(3)	0.3424(4)	0.0759(2)	3.53(6)
C3	0.6696(3)	0.3074(4)	-0.0191(2)	3.43(6)
C4	0.6509(3)	0.3579(4)	0.0603(2)	3.34(5)
C5	0.500	0.5289(5)	0.000	3.80(9)
C6	0.3862(3)	0.2853(4)	0.1530(2)	4.36(7)
C7	0.7730(3)	0.4369(4)	0.0850(2)	3.74(6)
C8	0.2557(6)	0.1420(7)	0.2309(2)	7.7(1)
C9	1.0028(4)	0.4219(7)	0.1103(3)	7.1(1)
H1	0.528	0.498	0.114	4.4
H3	0.744	0.244	-0.029	4.1
H4	0.642	0.279	0.095	4.0
H5	0.580	0.587	-0.008	4.6
H8A	0.178	0.080	0.227	9.2
H8B	0.335	0.091	0.249	9.2
H8C	0.234	0.216	0.267	9.2
H9A	1.077	0.356	0.106	8.5
H9B	1.024	0.504	0.080	8.5
H9C	0.991	0.448	0.164	8.5

The parameters of the hydrogen atoms were not refined.

Standard deviations are in parentheses.

Anisotropically refined atoms are given in the form of the isotropic equivalent displacement parameter defined as:
(4/3) * [a2*B(1,1) + b2*B(2,2) + c2*B(3,3) + ab(cos gamma)*B(1,2) + ac(cos beta)*B(1,3) + bc(cos alpha)*B(2,3)]

Table 23: Final Anisotropic Thermal Parameters (U's) for Compound 30

Atom	U(1,1)	U(2,2)	U(3,3)	U(1,2)	U(1,3)	U(2,3)
O1	0.066(2)	0.094(2)	0.063(1)	-0.012(2)	0.011(1)	0.024(2)
O2	0.091(2)	0.135(3)	0.053(1)	-0.021(2)	-0.010(2)	0.010(2)
O3	0.037(1)	0.071(2)	0.118(2)	0.005(1)	-0.012(1)	-0.026(2)
O4	0.064(2)	0.053(1)	0.114(2)	-0.004(1)	-0.016(2)	-0.025(2)
C1	0.041(2)	0.045(1)	0.052(2)	0.002(1)	0.001(1)	-0.007(2)
C2	0.038(1)	0.048(2)	0.048(2)	0.004(1)	0.007(1)	0.003(1)
C3	0.035(1)	0.044(1)	0.052(2)	0.001(1)	0.002(1)	-0.005(1)
C4	0.037(1)	0.040(1)	0.050(1)	0.001(1)	-0.001(1)	-0.005(1)
C5	0.045(2)	0.036(2)	0.063(3)	0	-0.000(2)	0
C6	0.050(2)	0.067(2)	0.049(2)	0.006(2)	0.008(2)	0.004(2)
C7	0.040(2)	0.053(2)	0.049(1)	-0.002(2)	-0.001(1)	-0.006(2)
C8	0.097(3)	0.123(4)	0.073(2)	-0.010(4)	0.029(2)	0.034(2)
C9	0.038(2)	0.125(4)	0.105(3)	-0.001(2)	-0.016(2)	-0.025(3)

The form of the anisotropic displacement parameter is:
exp[-2PI2(h2a2U(1,1) + k2b2U(2,2) + l2c2U(3,3) + 2hkabU(1,2) + 2hlacU(1,3) + 2klbcU(2,3))] where a,b, and c are reciprocal lattice constants.

Table 24: Bond Distances (Å) for Compound 30

Atom 1	Atom 2	Distance	Atom 1	Atom 2	Distance
O1	C6	1.333(4)	C1	C4	1.542(5)
O1	C8	1.466(5)	C1	C5	1.523(4)
O2	C6	1.194(5)	C1	C5	1.523(4)
O3	C7	1.318(4)	C2	C3	1.317(4)
O3	C9	1.466(6)	C2	C6	1.494(5)
O4	C7	1.186(5)	C3	C4	1.507(5)
C1	C2	1.509(5)	C4	C7	1.524(5)

Standard deviations are in parentheses.

Table 25: Bond Angles (°) for Compound **30**

Atom 1	Atom 2	Atom 3	Angle	Atom 1	Atom 2	Atom 3	Angle
C6	O1	C8	116.4(3)	C1	C4	C7	112.7(3)
C7	O3	C9	116.2(4)	C3	C4	C7	109.9(3)
C2	C1	C4	108.8(3)	C1	C5	C1	108.6(4)
C2	C1	C5	109.4(2)	O1	C6	O2	122.9(4)
C4	C1	C5	110.5(2)	O1	C6	C2	113.2(3)
C1	C2	C3	123.4(3)	O2	C6	C2	123.9(4)
C1	C2	C6	115.4(3)	O3	C7	O4	123.9(3)
C3	C2	C6	121.2(3)	O3	C7	C4	110.8(3)
C2	C3	C4	123.7(3)	O4	C7	C4	125.3(3)
C1	C4	C3	111.7(3)				

Standard deviations are in parentheses.

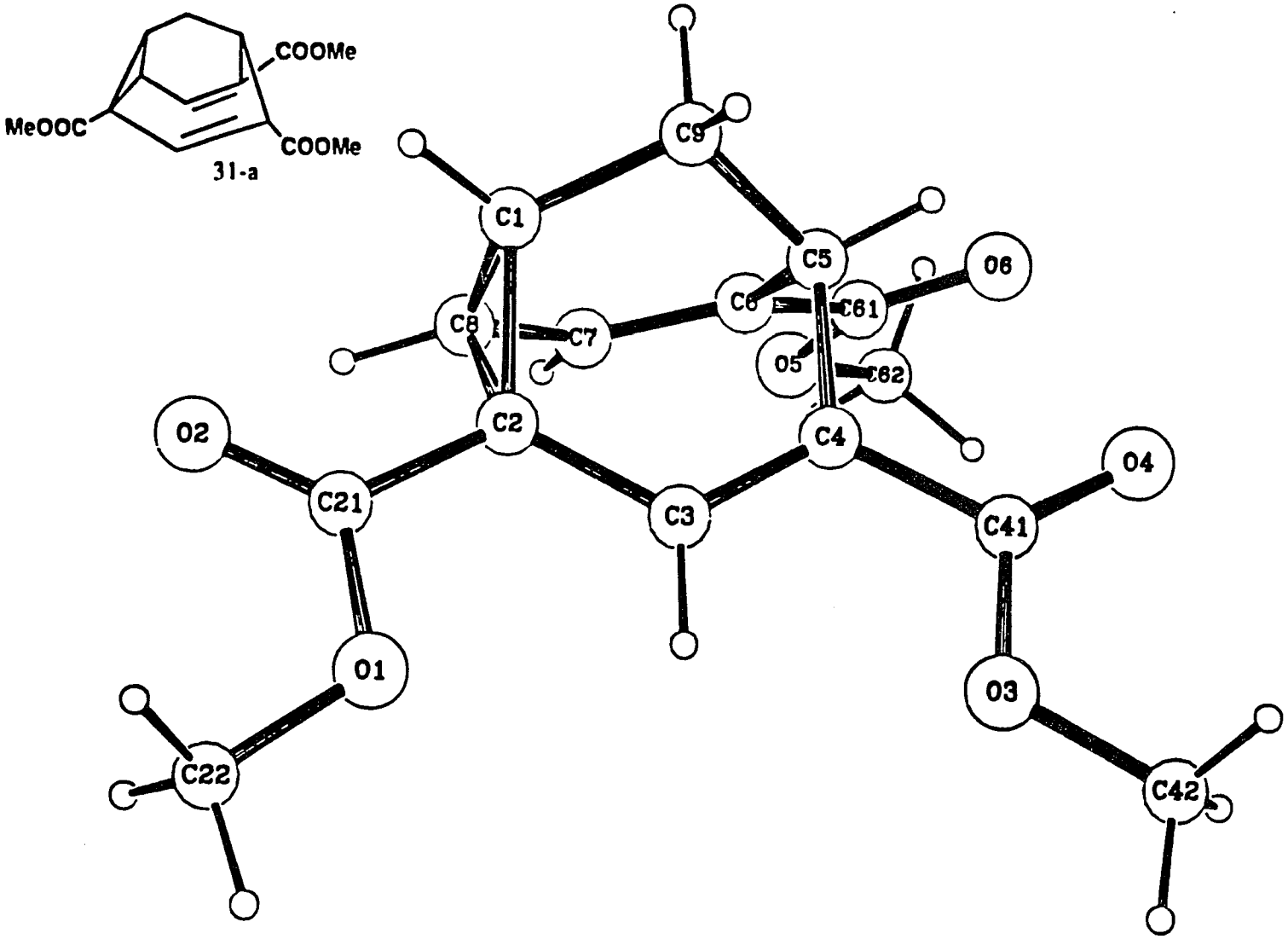
COOMe
MeOOC
COOMe
31-a
C9
C1
C5
O6
C6
C61
C8
C7
O5
C62
O2
C2
C4
O4
C21
C3
C41
O1
O3
C22
C42

Table 26: Crystal Data for Compound 31-a

Formula	$C_{15}H_{16}O_6$
Formula weight	292.29
Crystal system	orthorhombic
Space group	$Pc2_1b$
a	6.765(1) Å
b	9.512(1) Å
c	21.735(1) Å
Z	4
d_{calc}	1.388 g cm^{-3}
μ(Cu Kα)	8.7 cm^{-1}

Table 27: Final Atomic Parameters for Compound 31-a

Atom	x	y	z	B(A2)
O1	0.1913(3)	1.016	0.3524(1)	-3.77(4)
O2	0.0457(3)	0.9024(3)	0.2747(1)	4.50(5)
O3	0.7826(3)	0.8854(3)	0.4482(1)	4.16(4)
O4	0.9548(3)	0.6974(3)	0.4188(1)	4.96(5)
O5	0.4621(4)	0.3194(3)	0.4159(1)	5.24(5)
O6	0.7749(4)	0.3686(3)	0.3928(2)	5.86(6)
C1	0.3925(4)	0.7211(4)	0.2630(1)	3.20(5)
C2	0.3369(4)	0.8065(3)	0.3200(1)	2.85(5)
C3	0.4925(4)	0.8302(3)	0.3659(1)	2.93(5)
C4	0.6521(4)	0.7469(3)	0.3688(1)	2.82(5)
C5	0.6652(4)	0.6213(3)	0.3267(1)	3.11(5)
C6	0.5213(4)	0.5146(3)	0.3528(1)	3.03(5)
C7	0.3283(4)	0.5347(3)	0.3445(1)	3.09(5)
C8	0.2566(4)	0.6518(3)	0.3072(1)	3.06(5)
C9	0.6011(4)	0.6654(4)	0.2617(1)	3.61(6)
C21	0.1761(4)	0.9115(3)	0.3119(1)	3.25(5)
C22	0.0337(5)	1.1197(4)	0.3521(2)	4.61(7)
C41	0.8126(4)	0.7703(3)	0.4139(1)	3.14(5)
C42	0.9342(6)	0.9156(5)	0.4936(2)	5.28(8)
C61	0.6027(4)	0.3960(4)	0.3888(2)	3.51(6)
C62	0.5261(7)	0.2016(4)	0.4530(2)	6.08(9)
H1	0.335	0.753	0.223	3.8
H3	0.479	0.910	0.396	3.5
H5	0.802	0.582	0.324	3.7
H7	0.232	0.469	0.364	3.7
H8	0.109	0.668	0.304	3.6
H9A	0.692	0.740	0.246	4.3
H9B	0.607	0.582	0.234	4.3
H22A	0.060	1.193	0.384	5.5
H22B	0.027	1.165	0.310	5.5
H22C	-0.095	1.072	0.361	5.5
H42A	0.899	1.003	0.517	6.4
H42B	0.945	0.835	0.523	6.4
H42C	1.064	0.930	0.472	6.4
H62A	0.407	0.153	0.471	7.2
H62B	0.602	0.134	0.427	7.2
H62C	0.612	0.236	0.487	7.2

The parameters of the hydrogen atoms were not refined.

Standard deviations are in parentheses.

Anisotropically refined atoms are given in the form of the isotropic equivalent displacement parameter defined as:
(4/3) * [a^2*B(1,1) + b^2*B(2,2) + c^2*B(3,3) + ab(cosγ)*B(1,2) + ac(cosβ)*B(1,3) + bc(cosα)*B(2,3)]

Table 28: Final Anisotropic Thermal Parameters (U's) for Compound **31-a**

Atom	U(1,1)	U(2,2)	U(3,3)	U(1,2)	U(1,3)	U(2,3)
O1	0.046(1)	0.042(1)	0.056(1)	0.016(1)	-0.004(1)	-0.002(1)
O2	0.052(1)	0.053(1)	0.065(1)	0.008(1)	-0.022(1)	0.004(1)
O3	0.058(1)	0.047(1)	0.053(1)	0.002(1)	-0.022(1)	-0.009(1)
O4	0.049(1)	0.067(2)	0.073(1)	0.019(1)	-0.023(1)	-0.008(1)
O5	0.062(1)	0.047(1)	0.090(2)	0.014(1)	0.008(1)	0.024(1)
O6	0.052(1)	0.059(2)	0.112(2)	0.014(1)	-0.015(1)	0.015(2)
C1	0.043(1)	0.045(1)	0.034(1)	-0.003(1)	-0.002(1)	-0.002(1)
C2	0.036(1)	0.034(1)	0.038(1)	0.003(1)	-0.003(1)	-0.001(1)
C3	0.037(1)	0.035(1)	0.039(1)	0.001(1)	-0.002(1)	0.000(1)
C4	0.033(1)	0.034(1)	0.040(1)	-0.003(1)	-0.001(1)	-0.000(1)
C5	0.029(1)	0.039(1)	0.051(1)	0.002(1)	0.003(1)	-0.007(1)
C6	0.041(1)	0.028(1)	0.046(1)	0.003(1)	0.003(1)	-0.007(1)
C7	0.040(1)	0.034(1)	0.044(1)	-0.000(1)	0.001(1)	-0.004(1)
C8	0.034(1)	0.038(1)	0.044(1)	-0.001(1)	-0.003(1)	-0.003(1)
C9	0.043(1)	0.053(2)	0.041(2)	-0.000(2)	0.006(1)	-0.009(1)
C21	0.038(1)	0.038(1)	0.048(1)	0.000(1)	-0.000(1)	0.006(1)
C22	0.049(2)	0.055(2)	0.071(2)	0.021(1)	0.005(2)	0.008(2)
C41	0.038(1)	0.035(1)	0.046(1)	-0.003(1)	-0.003(1)	0.004(1)
C42	0.069(2)	0.074(3)	0.057(2)	-0.014(2)	-0.026(2)	-0.004(2)
C61	0.046(1)	0.034(1)	0.054(2)	0.007(1)	-0.001(1)	-0.009(1)
C62	0.093(3)	0.045(2)	0.093(2)	0.017(2)	0.001(3)	0.025(2)

The form of the anisotropic displacement parameter is:
$\exp[-2\pi^2(h^2a^2U(1,1) + k^2b^2U(2,2) + l^2c^2U(3,3) + 2hkabU(1,2) + 2hlacU(1,3) + 2klbcU(2,3))]$ where a,b, and c are reciprocal lattice constants.

Table 29: Bond Distances (Å) for Compound 31-a

Atom 1	Atom 2	Distance	Atom 1	Atom 2	Distance
O1	C21	1.336(3)	C2	C3	1.468(4)
O1	C22	1.449(4)	C2	C8	1.593(4)
O2	C21	1.199(4)	C2	C21	1.488(4)
O3	C41	1.339(4)	C3	C4	1.341(4)
O3	C42	1.453(4)	C4	C5	1.508(4)
O4	C41	1.190(4)	C4	C41	1.480(4)
O5	C61	1.335(4)	C5	C6	1.517(4)
O5	C62	1.445(5)	C5	C9	1.535(4)
O6	C61	1.197(4)	C6	C7	1.332(4)
C1	C2	1.528(4)	C6	C61	1.480(4)
C1	C8	1.484(4)	C7	C8	1.461(4)
C1	C9	1.507(4)			

Standard deviations are in parentheses.

Table 30: Bond Angles (°) for Compound 31-a

Atom 1	Atom 2	Atom 3	Angle	Atom 1	Atom 2	Atom 3	Angle
C21	O1	C22	116.5(2)	C6	C5	C9	110.2(2)
C41	O3	C42	115.6(3)	C5	C6	C7	118.8(3)
C61	O5	C62	117.1(3)	C5	C6	C61	118.0(2)
C2	C1	C8	63.8(2)	C7	C6	C61	123.1(3)
C2	C1	C9	115.6(2)	C6	C7	C8	120.7(3)
C8	C1	C9	115.8(3)	C1	C8	C2	59.4(2)
C1	C2	C3	117.1(2)	C1	C8	C7	119.5(2)
C1	C2	C8	56.7(2)	C2	C8	C7	119.6(2)
C1	C2	C21	116.2(2)	C1	C9	C5	110.1(2)
C3	C2	C8	120.4(2)	O1	C21	O2	123.7(3)
C3	C2	C21	120.1(3)	O1	C21	C2	111.6(2)
C8	C2	C21	110.5(2)	O2	C21	C2	124.7(3)
C2	C3	C4	121.3(3)	O3	C41	O4	123.3(3)
C3	C4	C5	119.1(2)	O3	C41	C4	112.3(2)
C3	C4	C41	122.2(3)	O4	C41	C4	124.3(3)
C5	C4	C41	118.6(2)	O5	C61	O6	122.9(3)
C4	C5	C6	105.3(2)	O5	C61	C6	112.6(3)
C4	C5	C9	109.0(3)	O6	C61	C6	124.5(3)

Standard deviations are in parentheses.

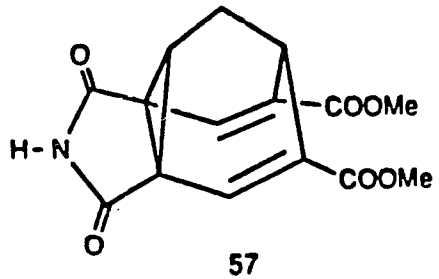
O
H-N
O
COOMe
COOMe

57

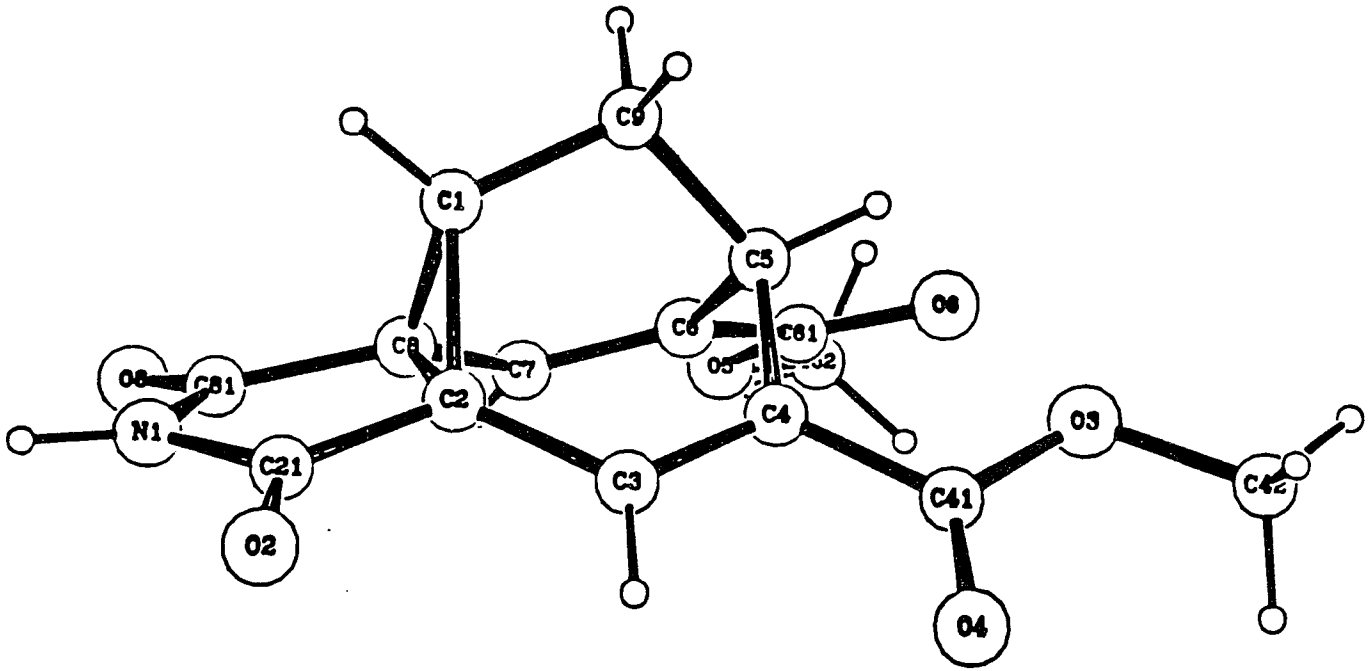
C9
C1
C5
O6
C61
C8
C7
C6
O5
O2
C61
O8
C2
C4
O3
N1
C21
C3
C41
O2
O4

Table 31: Crystal Data for Compound 57

Formula	$C_{15}H_{13}NO_6$
Formula weight	303.27
Crystal system	triclinic
Space group	$P\bar{1}$
a	6.863(1) Å
b	9.977(1) Å
c	10.404(1) Å
α	92.36(1)°
β	106.09(1)°
γ	98.92(1)°
Z	2
d_{calc}	1.495 g cm^{-3}
μ(Cu Kα)	9.5 cm^{-1}

Table 32: Final Atomic Parameters for Compound 57

Atom	x	y	z	B(A2)
O2	0.2514(3)	0.7902(2)	0.5391(2)	-5.02(5)
O3	0.1931(3)	0.1342(2)	0.4735(2)	3.78(4)
O4	0.2093(3)	0.2976(2)	0.3342(2)	4.35(4)
O5	0.7497(3)	0.2586(2)	0.9297(2)	3.67(4)
O6	0.4960(3)	0.1096(2)	0.7881(2)	4.35(4)
O8	0.6591(3)	0.7698(2)	0.9598(2)	3.72(4)
N1	0.4299(3)	0.8108(2)	0.7635(2)	3.51(4)
C1	0.2051(3)	0.5483(2)	0.7712(2)	2.81(4)
C2	0.2987(3)	0.5917(2)	0.6600(2)	2.78(4)
C3	0.2754(3)	0.4925(2)	0.5475(2)	2.84(4)
C4	0.2498(3)	0.3595(2)	0.5643(2)	2.67(4)
C5	0.2494(3)	0.3148(2)	0.7018(2)	2.59(4)
C6	0.4680(3)	0.3438(2)	0.7938(2)	2.60(4)
C7	0.5574(3)	0.4728(2)	0.8397(2)	2.71(4)
C8	0.4388(3)	0.5831(2)	0.8045(2)	2.67(4)
C9	0.1190(3)	0.3990(2)	0.7614(2)	2.99(5)
C21	0.3180(4)	0.7401(2)	0.6420(3)	3.38(5)
C41	0.2172(4)	0.2634(2)	0.4451(2)	2.93(4)
C42	0.1454(6)	0.0329(3)	0.3614(3)	5.27(8)
C61	0.5704(4)	0.2251(2)	0.8338(2)	2.92(4)
C62	0.8506(4)	0.1462(3)	0.9797(3)	4.58(6)
CB1	0.5272(4)	0.7289(2)	0.8562(2)	3.03(5)
HN1	0.439	0.906	0.782	4.2
H1	0.133	0.614	0.807	3.4
H3	0.279	0.524	0.458	3.4
H5	0.191	0.215	0.693	3.1
H7	0.704	0.493	0.897	3.3
H9A	-0.026	0.382	0.702	3.6
H9B	0.121	0.371	0.853	3.6
H42A	0.131	-0.060	0.394	6.3
H42B	0.014	0.044	0.295	6.3
H42C	0.259	0.045	0.318	6.3
H62A	0.982	0.182	1.051	5.5
H62B	0.758	0.083	1.019	5.5
H62C	0.880	0.096	0.904	5.5

The parameters of the hydrogen atoms were not refined.

Standard deviations are in parentheses.

Anisotropically refined atoms are given in the form of the isotropic equivalent displacement parameter defined as:
(4/3) * [a^2*B(1,1) + b^2*B(2,2) + c^2*B(3,3) + ab(cosγ)*B(1,2) + ac(cosβ)*B(1,3) + bc(cosα)*B(2,3)]

Table 33: Final Anisotropic Thermal Parameters (U's) for Compound 57

Atom	U(1,1)	U(2,2)	U(3,3)	U(1,2)	U(1,3)	U(2,3)
O2	0.078(1)	0.0360(8)	0.066(1)	0.0141(8)	-0.001(1)	0.0188(7)
O3	0.072(1)	0.0276(7)	0.0426(8)	0.0061(7)	0.0154(7)	0.0008(6)
O4	0.087(1)	0.0394(8)	0.0438(8)	0.0122(8)	0.0250(8)	0.0074(7)
O5	0.0421(8)	0.0333(7)	0.0595(9)	0.0148(6)	0.0027(7)	0.0052(7)
O6	0.068(1)	0.0251(7)	0.061(1)	0.0135(7)	-0.0009(9)	-0.0042(7)
O8	0.0498(9)	0.0339(7)	0.0504(9)	0.0004(7)	0.0073(7)	-0.0030(7)
N1	0.049(1)	0.0223(7)	0.060(1)	0.0094(7)	0.0102(9)	0.0024(8)
C1	0.035(1)	0.0281(8)	0.043(1)	0.0085(8)	0.0098(9)	0.0020(8)
C2	0.036(1)	0.0250(8)	0.043(1)	0.0079(7)	0.0075(9)	0.0063(8)
C3	0.037(1)	0.0280(9)	0.041(1)	0.0060(8)	0.0070(9)	0.0050(8)
C4	0.034(1)	0.0269(8)	0.038(1)	0.0054(8)	0.0057(8)	0.0034(8)
C5	0.035(1)	0.0227(8)	0.038(1)	0.0024(7)	0.0064(8)	0.0023(7)
C6	0.037(1)	0.0255(8)	0.0373(9)	0.0082(7)	0.0103(8)	0.0058(7)
C7	0.037(1)	0.0256(8)	0.039(1)	0.0074(7)	0.0072(8)	0.0037(8)
C8	0.034(1)	0.0239(8)	0.040(1)	0.0055(7)	0.0054(8)	0.0015(8)
C9	0.036(1)	0.0331(9)	0.044(1)	0.0049(8)	0.0119(9)	0.0048(9)
C21	0.043(1)	0.0263(9)	0.057(1)	0.0097(8)	0.008(1)	0.0082(9)
C41	0.041(1)	0.0292(9)	0.040(1)	0.0059(8)	0.0093(9)	0.0038(8)
C42	0.118(2)	0.030(1)	0.051(1)	0.005(1)	0.028(1)	-0.005(1)
C61	0.044(1)	0.0280(8)	0.040(1)	0.0111(8)	0.0114(9)	0.0028(8)
C62	0.059(1)	0.050(1)	0.066(2)	0.033(1)	0.006(1)	0.010(1)
C81	0.042(1)	0.0266(9)	0.047(1)	0.0059(8)	0.0142(9)	0.0011(8)

The form of the anisotropic displacement parameter is:
$\exp[-2\pi^2(h^2a^2U(1,1) + k^2b^2U(2,2) + l^2c^2U(3,3) + 2hkabU(1,2) + 2hlacU(1,3) + 2klbcU(2,3))]$ where a,b, and c are reciprocal lattice constants.

Table 34: Bond Distances (Å) for Compound 57

Atom 1	Atom 2	Distance	Atom 1	Atom 2	Distance
O2	C21	1.203(3)	C2	C3	1.458(3)
O3	C41	1.330(3)	C2	C8	1.558(3)
O3	C42	1.442(3)	C2	C21	1.491(3)
O4	C41	1.205(3)	C3	C4	1.336(3)
O5	C61	1.337(2)	C4	C5	1.516(3)
O5	C62	1.449(3)	C4	C41	1.480(3)
O6	C61	1.205(2)	C5	C6	1.516(3)
O8	C81	1.207(2)	C5	C9	1.546(4)
N1	C21	1.381(3)	C6	C7	1.343(3)
N1	C81	1.386(3)	C6	C61	1.485(3)
C1	C2	1.518(3)	C7	C8	1.468(3)
C1	C8	1.524(3)	C8	C81	1.502(3)
C1	C9	1.503(3)			

Standard deviations are in parentheses.

Table 35: Bond Angles (°) for Compound **57**

Atom 1	Atom 2	Atom 3	Angle	Atom 1	Atom 2	Atom 3	Angle
C41	O3	C42	116.1(2)	C7	C6	C61	122.9(2)
C61	O5	C62	115.8(2)	C6	C7	C8	119.4(2)
C21	N1	C81	113.3(2)	C1	C8	C2	59.0(1)
C2	C1	C8	61.6(1)	C1	C8	C7	118.0(2)
C2	C1	C9	114.9(2)	C1	C8	C81	114.4(2)
C8	C1	C9	115.2(2)	C2	C8	C7	122.7(2)
C1	C2	C3	118.7(2)	C2	C8	C81	104.2(2)
C1	C2	C8	59.4(1)	C7	C8	C81	122.1(2)
C1	C2	C21	114.4(2)	C1	C9	C5	110.1(2)
C3	C2	C8	123.3(2)	O2	C21	N1	125.7(2)
C3	C2	C21	120.8(2)	O2	C21	C2	126.2(2)
C8	C2	C21	104.9(2)	N1	C21	C2	108.1(2)
C2	C3	C4	119.9(2)	O3	C41	O4	123.7(2)
C3	C4	C5	119.0(2)	O3	C41	C4	112.2(2)
C3	C4	C41	117.4(2)	O4	C41	C4	124.1(2)
C5	C4	C41	123.6(2)	O5	C61	O6	123.3(2)
C4	C5	C6	108.9(2)	O5	C61	C6	113.1(2)
C4	C5	C9	109.2(2)	O6	C61	C6	123.5(2)
C6	C5	C9	107.9(2)	O8	C81	N1	125.1(2)
C5	C6	C7	119.6(2)	O8	C81	C8	127.0(2)
C5	C6	C61	117.4(2)	N1	C81	C8	107.9(2)

Standard deviations are in parentheses.

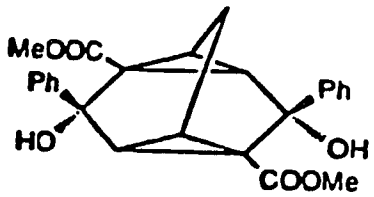
MeOOC
Ph
HO
Ph
OH
COOMe

81

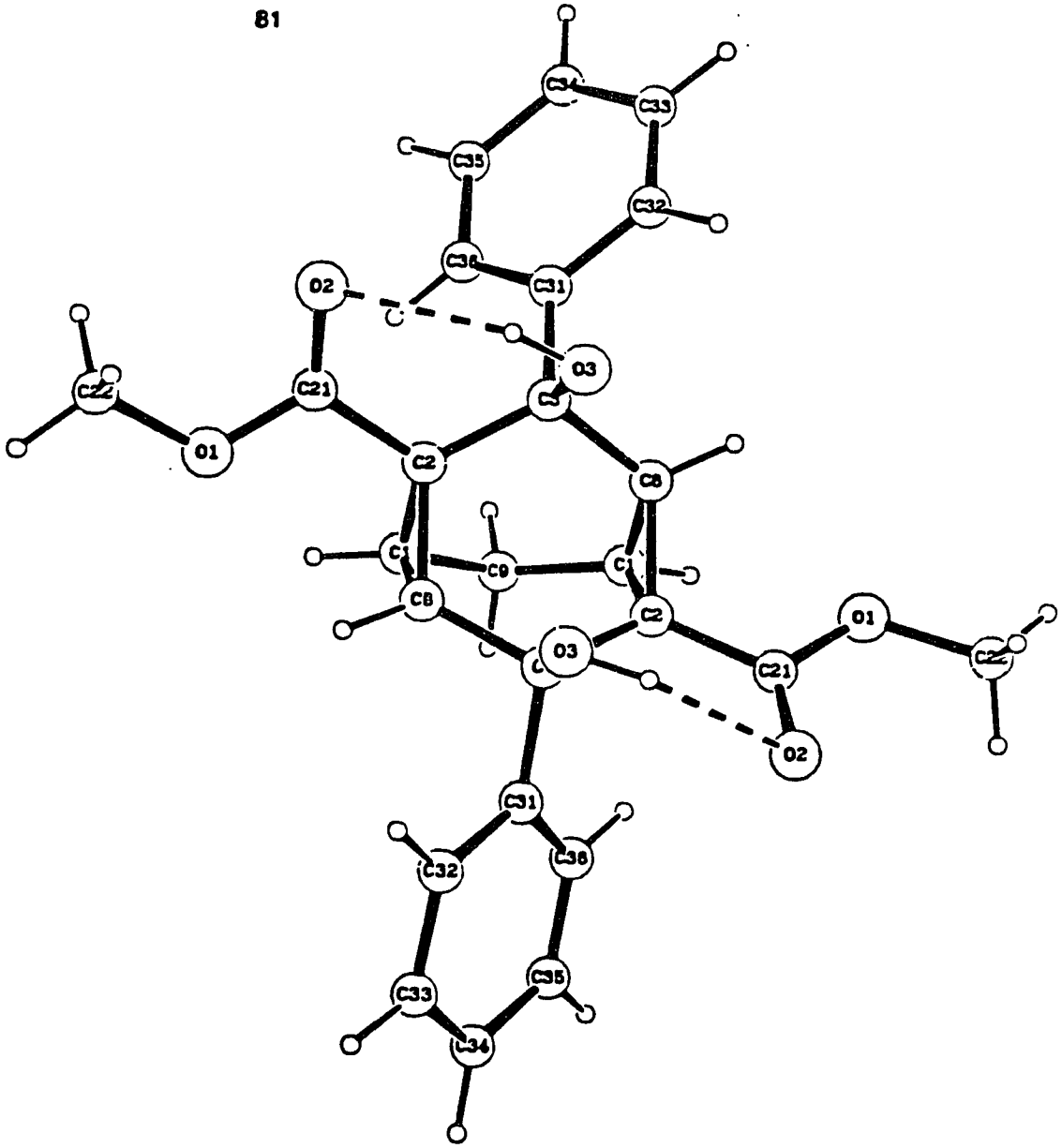
C34
C33
C35
C32
C36
C31
O2
O3
C22
C21
C5
O1
C2
C6
C1
C9
C8
C2
O1
O3
C21
C22
O2
C31
C32
C36
C33
C35
C34

Table 36: Crystal Data for Compound 81

Formula	$C_{25}H_{24}O_6$
Formula weight	420.47
Crystal system	monoclinic
Space group	C2/c
a	21.992(1) Å
b	8.941(1) Å
c	10.664(1) Å
β	106.92(1)°
Z	4
d_{calc}	1.392 g cm^{-3}
μ(Cu Kα)	7.7 cm^{-1}

Table 37: Final Atomic Parameters for Compound 81

Atom	x	y	z	B(A2)
O1	0.14211(7)	0.2203(2)	0.5353(2)	4.78(4)
O2	0.16750(8)	0.1102(2)	0.3701(2)	5.09(4)
O3	0.05051(7)	0.0284(2)	0.1763(2)	3.99(4)
C1	0.0408(1)	0.3840(3)	0.3608(2)	3.57(5)
C2	0.06814(9)	0.2373(3)	0.3262(2)	3.21(5)
C3	0.05135(9)	0.1895(3)	0.1838(2)	3.14(5)
C8	0.01483(9)	0.2406(3)	0.3919(2)	3.30(5)
C9	0.000	0.4785(4)	0.250	4.11(8)
C21	0.1310(1)	0.1826(3)	0.4096(2)	3.57(5)
C22	0.1994(1)	0.1601(4)	0.6249(3)	5.34(7)
C31	0.09717(9)	0.2496(3)	0.1122(2)	3.43(5)
C32	0.0951(1)	0.1889(4)	-0.0086(3)	5.03(7)
C33	0.1349(1)	0.2415(4)	-0.0789(3)	6.21(8)
C34	0.1777(1)	0.3531(4)	-0.0279(3)	5.50(7)
C35	0.1799(1)	0.4170(3)	0.0914(3)	5.00(7)
C36	0.1392(1)	0.3664(3)	0.1606(3)	4.12(6)
H03	0.087	0.002	0.235	4.8
H1	0.069	0.440	0.437	4.3
H22A	0.203	0.195	0.716	6.4
H22B	0.198	0.048	0.622	6.4
H22C	0.237	0.195	0.599	6.4
H8	0.028	0.213	0.487	4.0
H9	0.028	0.543	0.215	4.9
H32	0.065	0.106	-0.046	6.0
H33	0.132	0.198	-0.167	7.5
H34	0.207	0.388	-0.077	6.6
H35	0.211	0.500	0.128	6.0
H36	0.140	0.414	0.246	4.9

The parameters of the hydrogen atoms were not refined.

Standard deviations are in parentheses.

Anisotropically refined atoms are given in the form of the isotropic equivalent displacement parameter defined as:
$(4/3) * [a^2*B(1,1) + b^2*B(2,2) + c^2*B(3,3) + ab(\cos\gamma)*B(1,2) + ac(\cos\beta)*B(1,3) + bc(\cos\alpha)*B(2,3)]$

Table 38: Final Anisotropic Thermal Parameters (U's) for

Compound 81

Atom	U(1,1)	U(2,2)	U(3,3)	U(1,2)	U(1,3)	U(2,3)
O1	0.0342(7)	0.086(1)	0.0500(9)	0.0080(9)	-0.0055(7)	0.000(1)
O2	0.0435(8)	0.085(1)	0.061(1)	0.0223(9)	0.0094(7)	0.011(1)
O3	0.0406(8)	0.0402(9)	0.064(1)	0.0002(7)	0.0048(7)	0.0002(9)
C1	0.0298(9)	0.047(1)	0.051(1)	-0.004(1)	-0.0004(9)	-0.006(1)
C2	0.0235(8)	0.047(1)	0.046(1)	-0.002(1)	0.0008(8)	0.001(1)
C3	0.0286(9)	0.039(1)	0.047(1)	-0.0014(9)	0.0028(9)	0.001(1)
C8	0.0264(8)	0.051(1)	0.044(1)	-0.001(1)	0.0029(8)	-0.001(1)
C9	0.037(2)	0.044(2)	0.066(2)	0	0.001(2)	0
C21	0.0276(9)	0.051(1)	0.051(1)	-0.002(1)	0.0031(9)	0.008(1)
C22	0.034(1)	0.103(2)	0.053(2)	0.007(1)	-0.007(1)	0.019(2)
C31	0.0280(8)	0.047(1)	0.052(1)	0.004(1)	0.0067(9)	0.007(1)
C32	0.056(1)	0.068(2)	0.075(2)	-0.005(1)	0.032(1)	-0.012(1)
C33	0.074(1)	0.083(2)	0.095(2)	-0.003(2)	0.050(1)	-0.004(2)
C34	0.047(1)	0.078(2)	0.092(2)	0.012(1)	0.034(1)	0.025(2)
C35	0.037(1)	0.062(2)	0.082(2)	-0.003(1)	0.002(1)	0.029(1)
C36	0.034(1)	0.057(2)	0.056(1)	-0.005(1)	-0.002(1)	0.013(1)

The form of the anisotropic displacement parameter is:
$\exp[-2\pi^2(h^2a^2U(1,1) + k^2b^2U(2,2) + l^2c^2U(3,3) + 2hkabU(1,2) + 2hlacU(1,3) + 2klbcU(2,3))]$ where a,b, and c are reciprocal lattice constants.

Table 39: Bond Distances (Å) for Compound 81

Atom 1	Atom 2	Distance	Atom 1	Atom 2	Distance
O1	C21	1.334(3)	C2	C21	1.492(3)
O1	C22	1.446(3)	C3	C8	1.515(3)
O2	C21	1.199(3)	C3	C31	1.528(4)
O3	C3	1.442(3)	C31	C32	1.387(4)
C1	C2	1.532(3)	C31	C36	1.391(3)
C1	C8	1.480(4)	C32	C33	1.388(5)
C1	C9	1.517(3)	C33	C34	1.371(4)
C2	C3	1.516(3)	C34	C35	1.383(4)
C2	C8	1.531(3)	C35	C36	1.390(4)

Standard deviations are in parentheses.

Table 40: Bond Angles (°) for Compound **81**

Atom 1	Atom 2	Atom 3	Angle	Atom 1	Atom 2	Atom 3	Angle
C21	O1	C22	116.0(2)	C1	C8	C2	61.1(2)
C2	C1	C8	61.1(2)	C1	C8	C3	121.0(2)
C2	C1	C9	118.3(2)	C2	C8	C3	119.7(2)
C8	C1	C9	118.5(2)	C1	C9	C1	112.2(3)
C1	C2	C3	119.0(2)	O1	C21	O2	123.0(2)
C1	C2	C8	57.8(2)	O1	C21	C2	112.5(2)
C1	C2	C21	119.8(2)	O2	C21	C2	124.5(2)
C3	C2	C8	117.9(2)	C3	C31	C32	118.6(2)
C3	C2	C21	114.7(2)	C3	C31	C36	122.9(2)
C8	C2	C21	115.7(2)	C32	C31	C36	118.5(2)
O3	C3	C2	109.4(2)	C31	C32	C33	120.9(3)
O3	C3	C8	106.1(2)	C32	C33	C34	120.0(3)
O3	C3	C31	108.9(2)	C33	C34	C35	120.1(3)
C2	C3	C8	111.4(2)	C34	C35	C36	119.9(3)
C2	C3	C31	113.4(2)	C31	C36	C35	120.6(3)
C8	C3	C31	107.4(2)				

Standard deviations are in parentheses.

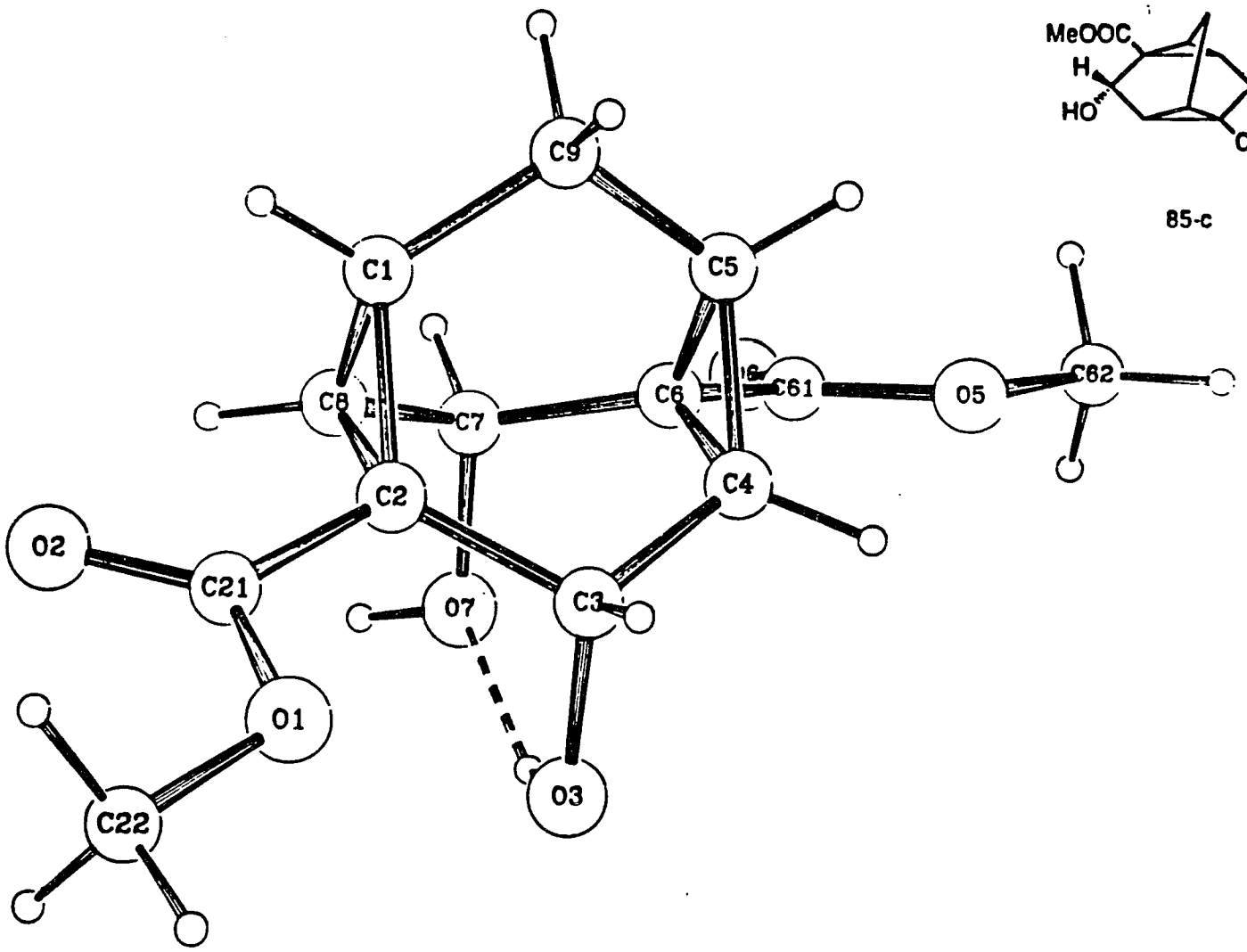
C9
C1
C5
C8
C7
C6
C61
05
C62
C2
C4
02
C21
07
C3
01
03
C22

MeOOC
H
HO
H
OH
COOMe

85-c

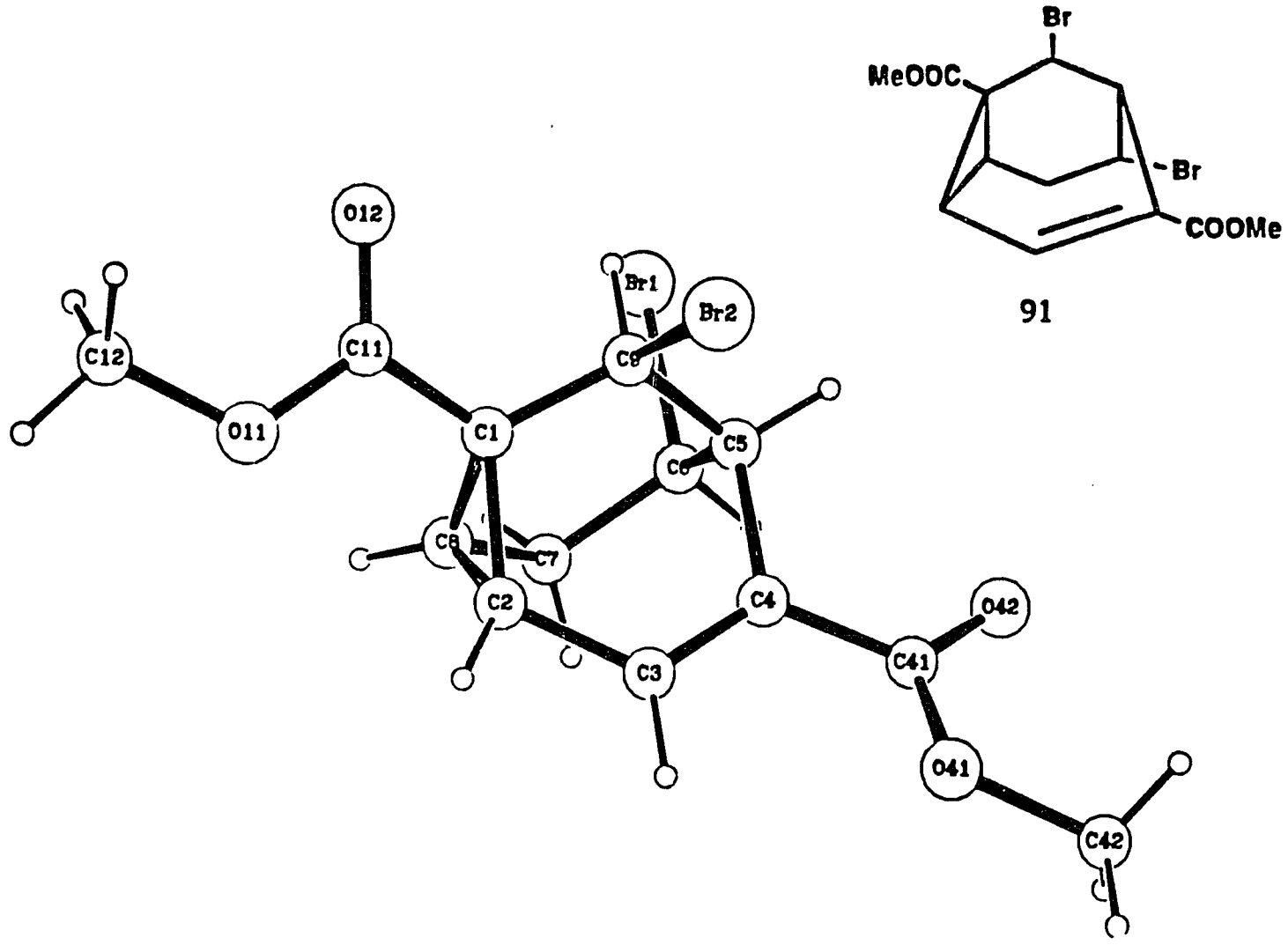
Br
MeOOC
Br
COOMe
O12
Br1
Br2
C12
C11
C9
O11
C1
C5
C6
C8
C7
C2
C4
O42
C41
C3
O41
C42

91

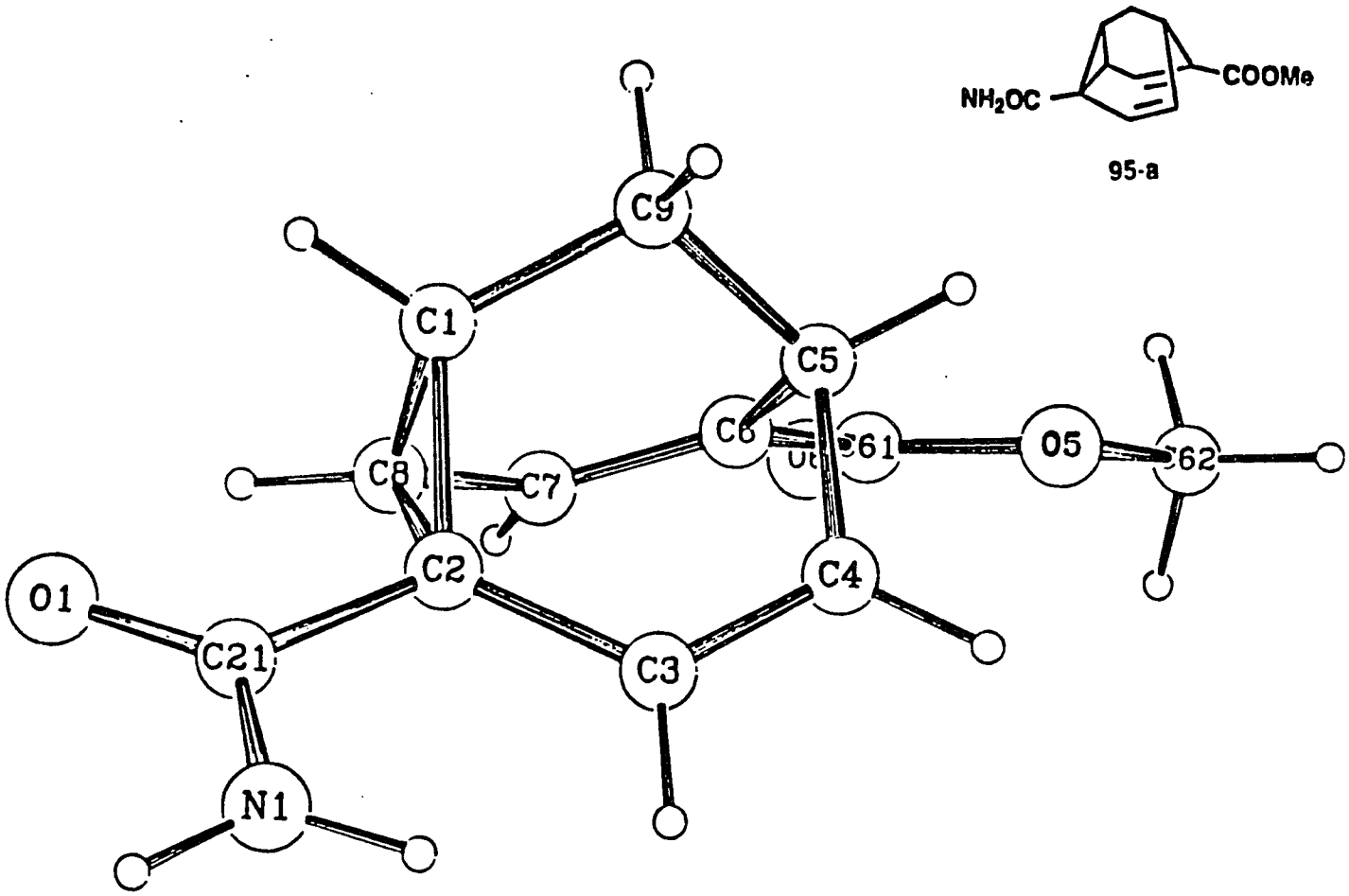

95-a

Table 41: Crystal Data for Compound 95-a

Formula	$C_{12}H_{13}NO_3$
Formula weight	219.24
Crystal system	monoclinic
Space group	$P2_1/c$
a	7.373(1) Å
b	17.066(2) Å
c	8.321(1) Å
β	96.86(1)°
Z	4
d_{calc}	1.401 g cm^{-3}
μ(Cu Kα)	7.9 cm^{-1}

Table 42: Final Atomic Parameters for Compound 95-a

Atom	x	y	z	B(A2)
O1	0.9984(3)	0.0384(2)	0.2059(3)	4.46(6)
O5	0.2397(3)	0.1672(2)	0.6480(3)	4.01(5)
O6	0.4131(4)	0.0851(2)	0.8060(3)	4.62(6)
N1	0.7782(4)	0.0523(2)	-0.0053(3)	3.64(6)
C1	0.8155(5)	0.1602(2)	0.3728(4)	3.31(7)
C2	0.7200(5)	0.0939(2)	0.2595(3)	2.81(7)
C3	0.5272(5)	0.1097(2)	0.2069(4)	3.23(7)
C4	0.4211(5)	0.1557(2)	0.2862(4)	3.35(8)
C5	0.5058(5)	0.1965(2)	0.4395(4)	3.15(7)
C6	0.5196(5)	0.1317(2)	0.5652(4)	2.84(7)
C7	0.6496(5)	0.0775(2)	0.5614(4)	2.97(7)
C8	0.7844(5)	0.0815(2)	0.4463(4)	3.02(7)
C9	0.6969(5)	0.2261(2)	0.4178(4)	3.65(8)
C21	0.8448(5)	0.0595(2)	0.1537(4)	3.07(7)
C61	0.3884(5)	0.1251(2)	0.6852(4)	2.97(7)
C62	0.1047(5)	0.1632(3)	0.7625(5)	4.81(9)
HN1A	0.657	0.069	-0.041	4.0
HN1B	0.851	0.030	-0.080	4.0
H1	0.953	0.168	0.375	3.6
H3	0.471	0.082	0.108	3.5
H4	0.289	0.163	0.246	3.7
H5	0.426	0.240	0.470	3.4
H7	0.654	0.033	0.640	3.2
H8	0.894	0.047	0.470	3.3
H9A	0.687	0.267	0.330	4.0
H9B	0.753	0.250	0.522	4.0
H62A	-0.002	0.197	0.723	5.2
H62B	0.063	0.108	0.771	5.2
H62C	0.161	0.182	0.871	5.2

The parameters of the hydrogen atoms were not refined.

Standard deviations are in parentheses.

Anisotropically refined atoms are given in the form of the isotropic equivalent displacement parameter defined as:
$(4/3) * [a^2*B(1,1) + b^2*B(2,2) + c^2*B(3,3) + ab(\cos\gamma)*B(1,2) + ac(\cos\beta)*B(1,3) + bc(\cos\alpha)*B(2,3)]$

Table 43: Final Anisotropic Thermal Parameters (U's) for

Compound **95-a**

Atom	U(1,1)	U(2,2)	U(3,3)	U(1,2)	U(1,3)	U(2,3)
O1	0.051(1)	0.090(2)	0.029(1)	0.019(1)	0.008(1)	-0.017(1)
O5	0.057(1)	0.063(2)	0.035(1)	0.011(1)	0.018(1)	0.001(1)
O6	0.071(2)	0.083(2)	0.024(1)	0.006(2)	0.016(1)	0.015(1)
N1	0.062(2)	0.061(2)	0.018(1)	0.010(2)	0.012(1)	-0.003(1)
C1	0.055(2)	0.046(2)	0.026(2)	-0.002(2)	0.011(1)	-0.004(2)
C2	0.049(2)	0.045(2)	0.014(1)	0.003(2)	0.008(1)	-0.002(1)
C3	0.055(2)	0.051(2)	0.018(1)	0.005(2)	0.007(1)	0.002(1)
C4	0.056(2)	0.052(2)	0.020(2)	0.012(2)	0.008(1)	0.007(1)
C5	0.062(2)	0.038(2)	0.021(1)	0.008(2)	0.012(1)	0.000(1)
C6	0.052(2)	0.041(2)	0.016(1)	0.004(2)	0.008(1)	-0.001(1)
C7	0.055(2)	0.043(2)	0.015(1)	0.003(2)	0.003(1)	-0.001(1)
C8	0.049(2)	0.047(2)	0.018(1)	0.009(2)	0.004(1)	0.001(1)
C9	0.071(2)	0.041(2)	0.029(2)	-0.001(2)	0.016(2)	-0.003(2)
C21	0.048(2)	0.045(2)	0.025(2)	0.003(2)	0.011(1)	-0.002(1)
C61	0.050(2)	0.042(2)	0.022(1)	-0.001(2)	0.007(1)	-0.006(1)
C62	0.056(2)	0.079(3)	0.053(2)	-0.001(2)	0.030(2)	-0.013(2)

The form of the anisotropic displacement parameter is:
$\exp[-2\pi^2(h^2a^2U(1,1) + k^2b^2U(2,2) + l^2c^2U(3,3) + 2hkabU(1,2) + 2hlacU(1,3) + 2klbcU(2,3))]$ where a,b, and c are reciprocal lattice constants.

Table 44: Bond Distances (Å) for Compound 95-a

Atom 1	Atom 2	Distance	Atom 1	Atom 2	Distance
O1	C21	1.218(4)	C2	C8	1.597(4)
O5	C61	1.317(4)	C2	C21	1.506(5)
O5	C62	1.460(5)	C3	C4	1.336(5)
O6	C61	1.211(4)	C4	C5	1.520(4)
N1	C21	1.360(4)	C5	C6	1.517(5)
C1	C2	1.524(5)	C5	C9	1.528(5)
C1	C9	1.498(5)	C6	C61	1.475(5)
C1	C8	1.504(5)	C6	C7	1.335(5)
C2	C3	1.449(5)	C7	C8	1.462(5)

Standard deviations are in parentheses.

Table 45: Bond Angles (°) for Compound 95-a

Atom 1	Atom 2	Atom 3	Angle	Atom 1	Atom 2	Atom 3	Angle
C61	O5	C62	115.7(3)	C5	C6	C7	118.6(3)
C2	C1	C8	63.7(2)	C5	C6	C61	121.8(3)
C2	C1	C9	115.4(3)	C7	C6	C61	119.6(3)
C8	C1	C9	116.5(3)	C6	C7	C8	121.9(3)
C1	C2	C3	117.6(3)	C1	C8	C2	58.8(2)
C1	C2	C8	57.6(2)	C1	C8	C7	117.2(3)
C1	C2	C21	113.5(3)	C2	C8	C7	120.0(3)
C3	C2	C8	119.0(3)	C1	C9	C5	110.8(3)
C3	C2	C21	121.8(3)	O1	C21	N1	122.2(3)
C8	C2	C21	110.8(3)	O1	C21	C2	122.0(3)
C2	C3	C4	122.5(3)	N1	C21	C2	115.7(3)
C3	C4	C5	118.5(3)	O5	C61	O6	122.8(3)
C4	C5	C6	103.4(3)	O5	C61	C6	113.2(3)
C4	C5	C9	110.2(3)	O6	C61	C6	124.0(3)
C6	C5	C9	109.6(3)				

Standard deviations are in parentheses.

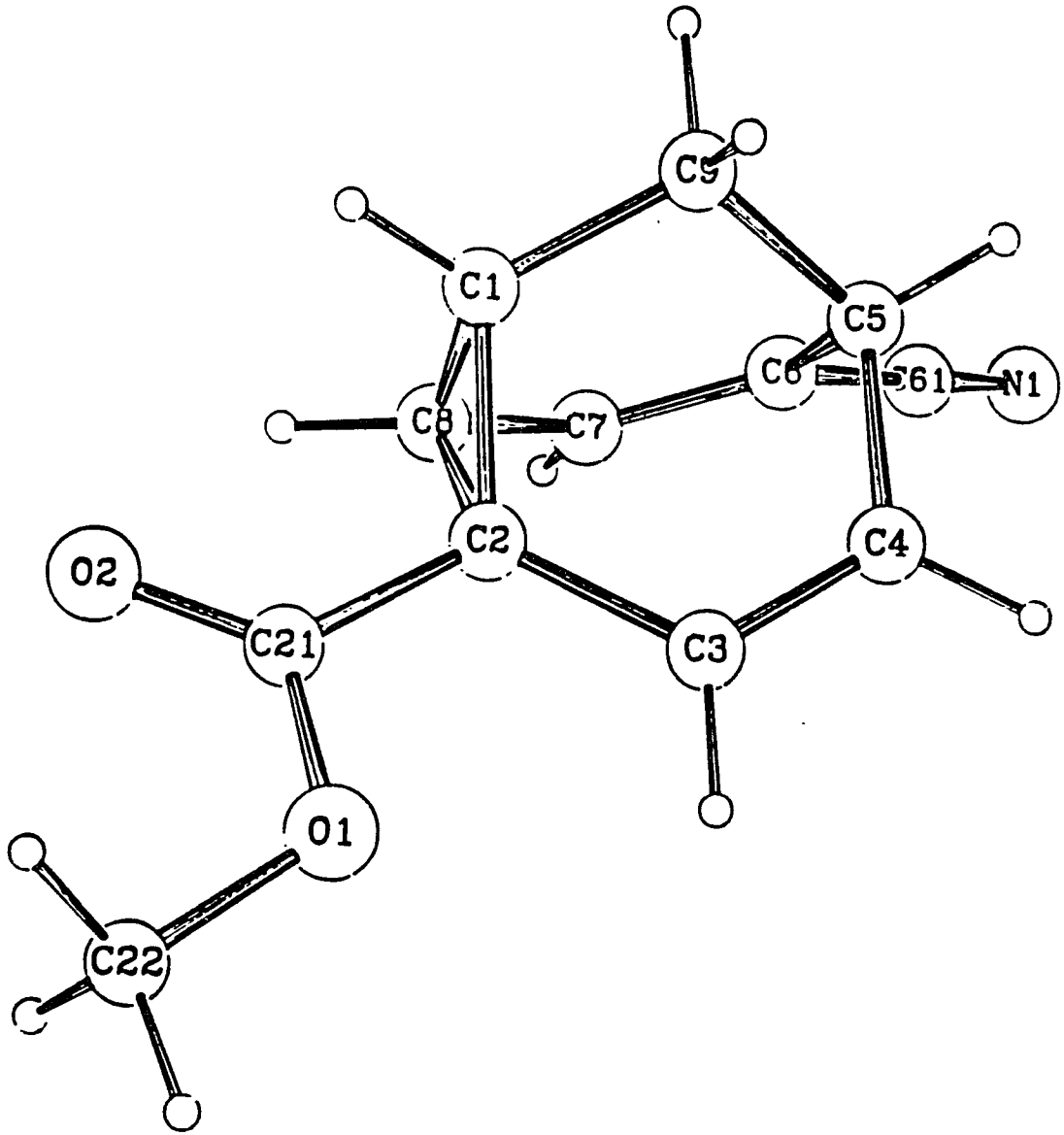

96-a

Table 46: Crystal Data for Compound 96-a

Formula	$C_{12}H_{11}NO_2$
Formula weight	201.23
Crystal system	monoclinic
Space group	C2/c
a	22.584(2) Å
b	6.044(1) Å
c	14.828(2) Å
β	97.65(1)°
Z	8
d_{calc}	1.333 g cm^{-3}
μ(Cu Kα)	7.1 cm^{-1}

Table 47: Final Atomic Parameters for Compound 96-a

Atom	x	y	z	B(A2)
O1	0.06541(6)	0.9523(2)	0.31926(8)	3.74(3)
O2	0.05560(6)	0.6063(2)	0.36862(9)	4.75(3)
N1	0.30398(8)	0.4052(4)	0.0738(1)	6.70(6)
C1	0.08717(8)	0.4519(3)	0.1944(1)	3.36(4)
C2	0.10659(7)	0.6686(3)	0.2398(1)	2.96(3)
C3	0.13032(8)	0.8400(3)	0.1839(1)	3.41(4)
C4	0.15025(8)	0.7903(3)	0.1060(1)	3.68(4)
C5	0.15147(8)	0.5517(3)	0.0765(1)	3.66(4)
C6	0.20413(8)	0.4541(3)	0.1374(1)	3.43(4)
C7	0.19974(8)	0.4132(3)	0.2249(1)	3.48(4)
C8	0.14289(8)	0.4437(3)	0.2605(1)	3.25(4)
C9	0.09364(9)	0.4344(3)	0.0953(1)	3.95(4)
C21	0.07384(7)	0.7340(3)	0.3162(1)	3.23(4)
C22	0.0365(1)	1.0310(4)	0.3944(1)	4.64(5)
C61	0.26005(9)	0.4272(4)	0.1026(1)	4.43(5)
H1	0.051	0.381	0.214	4.0
H3	0.131	0.997	0.205	4.1
H4	0.164	0.910	0.067	4.3
H5	0.155	0.536	0.010	4.3
H7	0.236	0.361	0.266	4.1
H8	0.139	0.373	0.321	3.9
H9A	0.058	0.506	0.058	4.7
H9B	0.095	0.275	0.078	4.7
H22A	0.032	1.196	0.390	5.5
H22B	-0.004	0.962	0.392	5.5
H22C	0.061	0.990	0.453	5.5

The parameters of the hydrogen atoms were not refined.

Standard deviations are in parentheses.

Anisotropically refined atoms are given in the form of the isotropic equivalent displacement parameter defined as:
$(4/3) * [a^2*B(1,1) + b^2*B(2,2) + c^2*B(3,3) + ab(\cos\gamma)*B(1,2) + ac(\cos\beta)*B(1,3) + bc(\cos\alpha)*B(2,3)]$

Table 48: Final Anisotropic Thermal Parameters (U's) for Compound 96-a

Atom	U(1,1)	U(2,2)	U(3,3)	U(1,2)	U(1,3)	U(2,3)
O1	0.0546(7)	0.0412(7)	0.0480(7)	0.0086(6)	0.0130(6)	0.0007(6)
O2	0.0791(8)	0.0484(7)	0.0585(7)	-0.0080(7)	0.0289(6)	0.0030(7)
N1	0.054(1)	0.131(2)	0.072(1)	0.013(1)	0.0193(9)	0.010(1)
C1	0.0425(9)	0.0383(9)	0.046(1)	-0.0069(8)	0.0050(8)	-0.0047(8)
C2	0.0406(8)	0.0323(9)	0.0393(8)	-0.0013(8)	0.0036(7)	0.0026(8)
C3	0.0476(9)	0.0342(9)	0.0482(9)	0.0010(8)	0.0073(8)	0.0066(8)
C4	0.050(1)	0.044(1)	0.0462(9)	0.0044(9)	0.0082(8)	0.0120(9)
C5	0.048(1)	0.053(1)	0.0382(9)	0.0023(9)	0.0057(8)	-0.0005(9)
C6	0.0426(9)	0.0389(9)	0.049(1)	0.0011(8)	0.0075(8)	-0.0030(8)
C7	0.0432(9)	0.0379(9)	0.049(1)	0.0043(8)	-0.0001(8)	0.0014(8)
C8	0.0492(9)	0.0307(9)	0.0436(9)	0.0024(8)	0.0064(8)	0.0040(8)
C9	0.047(1)	0.054(1)	0.048(1)	-0.0040(9)	0.0020(8)	-0.0097(9)
C21	0.0398(8)	0.0397(9)	0.0422(9)	-0.0025(8)	0.0024(7)	-0.0005(8)
C22	0.066(1)	0.058(1)	0.056(1)	0.014(1)	0.0191(9)	-0.008(1)
C61	0.049(1)	0.066(1)	0.053(1)	0.003(1)	0.0067(9)	0.002(1)

The form of the anisotropic displacement parameter is:
$\exp[-2\pi^2(h^2a^2U(1,1) + k^2b^2U(2,2) + l^2c^2U(3,3) + 2hkabU(1,2) + 2hlacU(1,3) + 2klbcU(2,3))]$ where a,b, and c are reciprocal lattice constants.

Table 49: Bond Distances (Å) for Compound 96-a

Atom 1	Atom 2	Distance	Atom 1	Atom 2	Distance
O1	C21	1.335(2)	C2	C21	1.487(2)
O1	C22	1.444(3)	C3	C4	1.329(3)
O2	C21	1.206(2)	C4	C5	1.509(3)
N1	C61	1.139(3)	C5	C6	1.514(2)
C1	C2	1.510(2)	C5	C9	1.544(3)
C1	C8	1.489(2)	C6	C7	1.336(3)
C1	C9	1.500(3)	C6	C61	1.436(3)
C2	C3	1.471(3)	C7	C8	1.463(3)
C2	C8	1.596(2)			

Standard deviations are in parentheses.

Table 50: Bond Angles (°) for Compound 96-a

Atom 1	Atom 2	Atom 3	Angle	Atom 1	Atom 2	Atom 3	Angle
C21	O1	C22	115.6(1)	C6	C5	C9	109.2(2)
C2	C1	C8	64.3(1)	C5	C6	C7	119.8(2)
C2	C1	C9	115.9(2)	C5	C6	C61	119.2(2)
C8	C1	C9	117.3(2)	C7	C6	C61	120.7(2)
C1	C2	C3	117.8(1)	C6	C7	C8	120.6(2)
C1	C2	C8	57.2(1)	C1	C8	C2	58.5(1)
C1	C2	C21	115.2(1)	C1	C8	C7	118.2(2)
C3	C2	C8	119.5(1)	C2	C8	C7	119.4(1)
C3	C2	C21	119.8(2)	C1	C9	C5	109.9(1)
C8	C2	C21	112.0(1)	O1	C21	O2	123.2(2)
C2	C3	C4	121.4(2)	O1	C21	C2	112.1(1)
C3	C4	C5	119.3(2)	O2	C21	C2	124.6(2)
C4	C5	C6	104.0(1)	N1	C61	C6	179.0(2)
C4	C5	C9	109.7(2)				

Standard deviations are in parentheses.

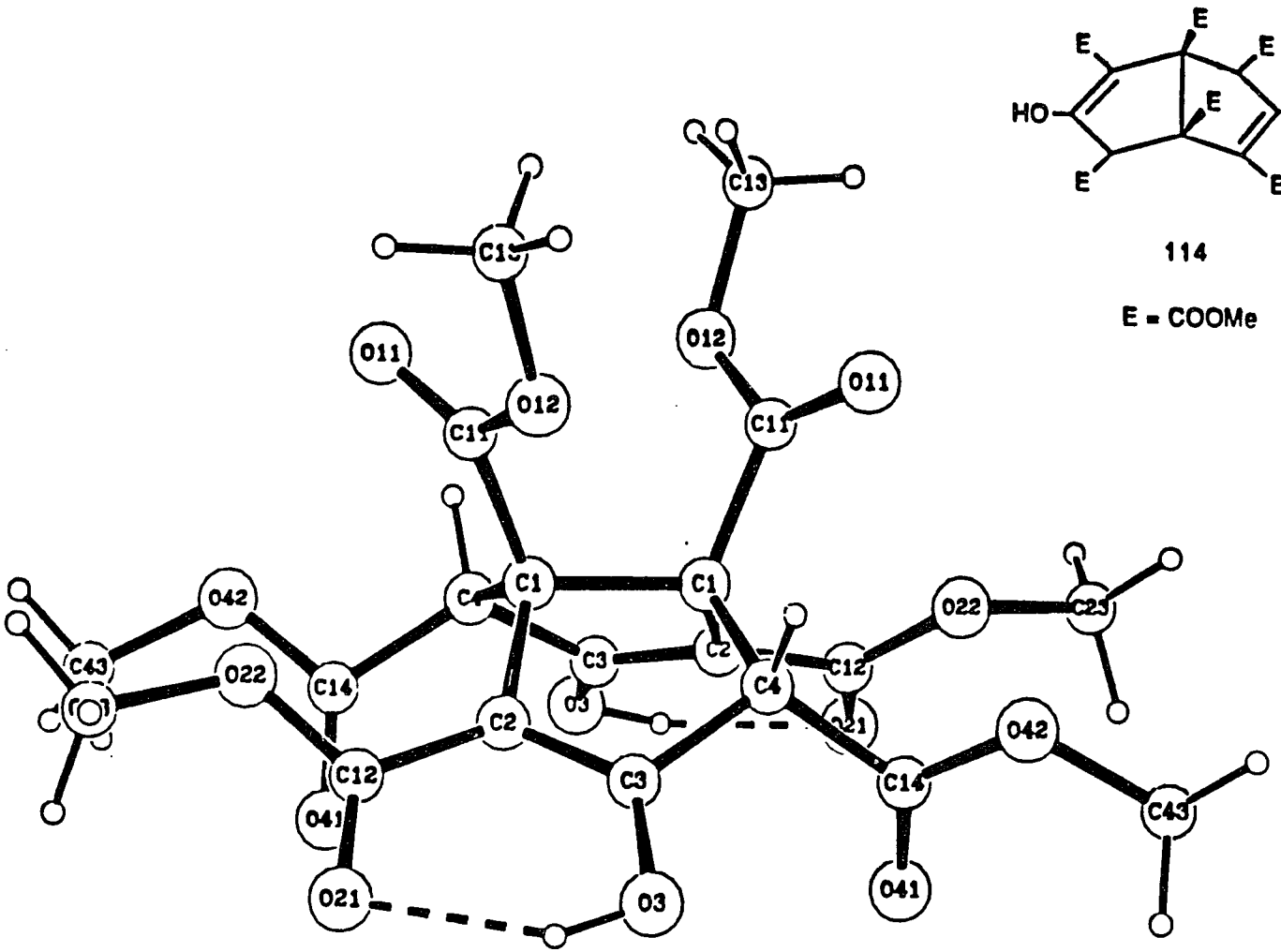
C13
C15
011
012
C11
012
011
C11
042
C43
022
C14
C1
C1
C2
C3
C4
C12
022
C25
O3
C2
C12
C3
C14
042
C43
041
021
O3
041

E
E
E
HO
E
OH
E
E

114

E = COOMe

Table 51: Crystal Data for Compound **114**

Formula	$C_{20}H_{22}O_{14}$
Formula weight	486.39
Crystal system	monoclinic
Space group	C2/c
a	19.375(2) Å
b	8.189(1) Å
c	14.841(2) Å
β	110.82(1)°
Z	4
d_{calc}	1.468 g cm^{-3}
μ(Cu Kα)	10.5 cm^{-1}

Table 52: Final Atomic Parameters for Compound 114

Atom	x	y	z	B(A2)
O3	0.54638(7)	0.6592(2)	0.07902(8)	3.15(3)
O11	0.37784(7)	0.1816(2)	0.1858(1)	4.28(3)
O12	0.47190(7)	0.1847(2)	0.1326(1)	3.77(3)
O21	0.39974(8)	0.6693(2)	-0.01121(9)	3.58(3)
O22	0.33655(7)	0.4819(2)	0.03967(9)	3.50(3)
O41	0.65084(8)	0.7236(2)	0.2983(1)	4.29(3)
O42	0.71382(6)	0.5062(2)	0.2770(1)	3.77(3)
C1	0.45718(8)	0.4190(2)	0.2158(1)	2.01(3)
C2	0.45807(8)	0.5312(2)	0.1354(1)	2.30(3)
C3	0.52705(8)	0.5690(2)	0.1412(1)	2.27(3)
C4	0.58561(8)	0.4824(2)	0.2204(1)	2.22(3)
C11	0.42931(9)	0.2489(2)	0.1774(1)	2.54(3)
C12	0.39590(9)	0.5701(2)	0.0485(1)	2.71(3)
C13	0.4555(2)	0.0178(3)	0.0999(2)	6.11(6)
C14	0.65293(9)	0.5868(2)	0.2705(1)	2.79(3)
C23	0.2730(1)	0.4996(4)	-0.0482(2)	5.74(7)
C43	0.7831(1)	0.5905(4)	0.3228(2)	5.53(6)
H03	0.503	0.687	0.033	3.8
H4	0.602	0.386	0.192	2.7
H13A	0.490	-0.018	0.068	7.4
H13B	0.461	-0.055	0.156	7.4
H13C	0.404	0.011	0.053	7.4
H23A	0.232	0.427	-0.045	6.9
H23B	0.256	0.616	-0.055	6.9
H23C	0.287	0.469	-0.105	6.9
H43A	0.825	0.518	0.324	6.7
H43B	0.784	0.693	0.286	6.7
H43C	0.789	0.619	0.391	6.7

The parameters of the hydrogen atoms were not refined.

Standard deviations are in parentheses.

Anisotropically refined atoms are given in the form of the isotropic equivalent displacement parameter defined as:
(4/3) * [a2*B(1,1) + b2*B(2,2) + c2*B(3,3) + ab(cos gamma)*B(1,2) + ac(cos beta)*B(1,3) + bc(cos alpha)*B(2,3)]

Table 53: Final Anisotropic Thermal Parameters (U's) for

Compound **114**

Atom	U(1,1)	U(2,2)	U(3,3)	U(1,2)	U(1,3)	U(2,3)
O3	0.0447(6)	0.0428(7)	0.0367(5)	-0.0019(5)	0.0198(4)	0.0097(5)
O11	0.0499(6)	0.0488(7)	0.0740(8)	-0.0216(6)	0.0342(5)	-0.0180(7)
O12	0.0530(6)	0.0393(6)	0.0615(6)	-0.0081(6)	0.0329(4)	-0.0197(6)
O21	0.0502(7)	0.0503(7)	0.0323(5)	0.0088(6)	0.0109(5)	0.0127(6)
O22	0.0308(5)	0.0651(8)	0.0302(5)	-0.0037(6)	0.0025(4)	0.0037(6)
O41	0.0519(7)	0.0445(7)	0.0654(8)	-0.0161(6)	0.0192(6)	-0.0133(7)
O42	0.0262(5)	0.0685(9)	0.0497(6)	-0.0092(6)	0.0147(4)	-0.0096(7)
C1	0.0241(6)	0.0284(7)	0.0241(5)	0.0006(6)	0.0088(4)	-0.0004(6)
C2	0.0306(6)	0.0305(7)	0.0256(6)	0.0005(6)	0.0090(5)	0.0012(6)
C3	0.0337(6)	0.0285(7)	0.0258(6)	-0.0008(6)	0.0125(5)	0.0005(6)
C4	0.0260(6)	0.0307(7)	0.0290(6)	-0.0019(6)	0.0112(4)	-0.0002(6)
C11	0.0298(6)	0.0341(8)	0.0312(6)	-0.0015(6)	0.0093(5)	-0.0033(6)
C12	0.0362(7)	0.0391(8)	0.0270(6)	0.0067(7)	0.0105(5)	0.0008(6)
C13	0.103(1)	0.045(1)	0.102(1)	-0.015(1)	0.059(1)	-0.036(1)
C14	0.0327(7)	0.0436(9)	0.0311(6)	-0.0092(7)	0.0132(5)	-0.0005(7)
C23	0.037(1)	0.126(2)	0.039(1)	-0.005(1)	-0.0059(9)	0.008(1)
C43	0.0305(8)	0.106(2)	0.071(1)	-0.026(1)	0.0148(8)	-0.013(1)

The form of the anisotropic displacement parameter is:
exp[-2PI2(h2a2U(1,1) + k2b2U(2,2) + l2c2U(3,3) + 2hkabU(1,2) + 2hlacU(1,3) + 2klbcU(2,3))] where a,b, and c are reciprocal lattice constants.

Table 54: Bond Distances (Å) for Compound 114

Atom 1	Atom 2	Distance	Atom 1	Atom 2	Distance
03	C3	1.336(2)	042	C43	1.446(3)
011	C11	1.184(2)	C1	C1	1.608(2)
012	C11	1.337(3)	C1	C2	1.511(2)
012	C13	1.448(3)	C1	C4	1.553(2)
021	C12	1.223(2)	C1	C11	1.529(2)
022	C12	1.324(2)	C2	C3	1.344(2)
022	C23	1.447(2)	C2	C12	1.453(2)
041	C14	1.200(2)	C3	C4	1.491(2)
042	C14	1.325(2)	C4	C14	1.515(2)

Standard deviations are in parentheses.

Table 55: Bond Angles (°) for Compound **114**

Atom 1	Atom 2	Atom 3	Angle	Atom 1	Atom 2	Atom 3	Angle
C11	012	C13	115.9(2)	C2	C3	C4	113.7(1)
C12	022	C23	117.7(2)	C1	C4	C3	102.6(1)
C14	042	C43	116.8(2)	C1	C4	C14	116.3(1)
C1	C1	C2	101.5(1)	C3	C4	C14	113.5(1)
C1	C1	C4	105.7(1)	011	C11	012	124.2(2)
C1	C1	C11	112.6(1)	011	C11	C1	125.6(2)
C2	C1	C4	115.9(1)	012	C11	C1	110.2(1)
C2	C1	C11	111.2(1)	021	C12	022	124.4(1)
C4	C1	C11	109.7(1)	021	C12	C2	122.9(2)
C1	C2	C3	112.3(1)	022	C12	C2	112.6(2)
C1	C2	C12	126.6(1)	041	C14	042	125.3(2)
C3	C2	C12	119.9(2)	041	C14	C4	124.5(2)
03	C3	C2	126.8(1)	042	C14	C4	110.1(2)
03	C3	C4	119.1(1)				

Standard deviations are in parentheses.

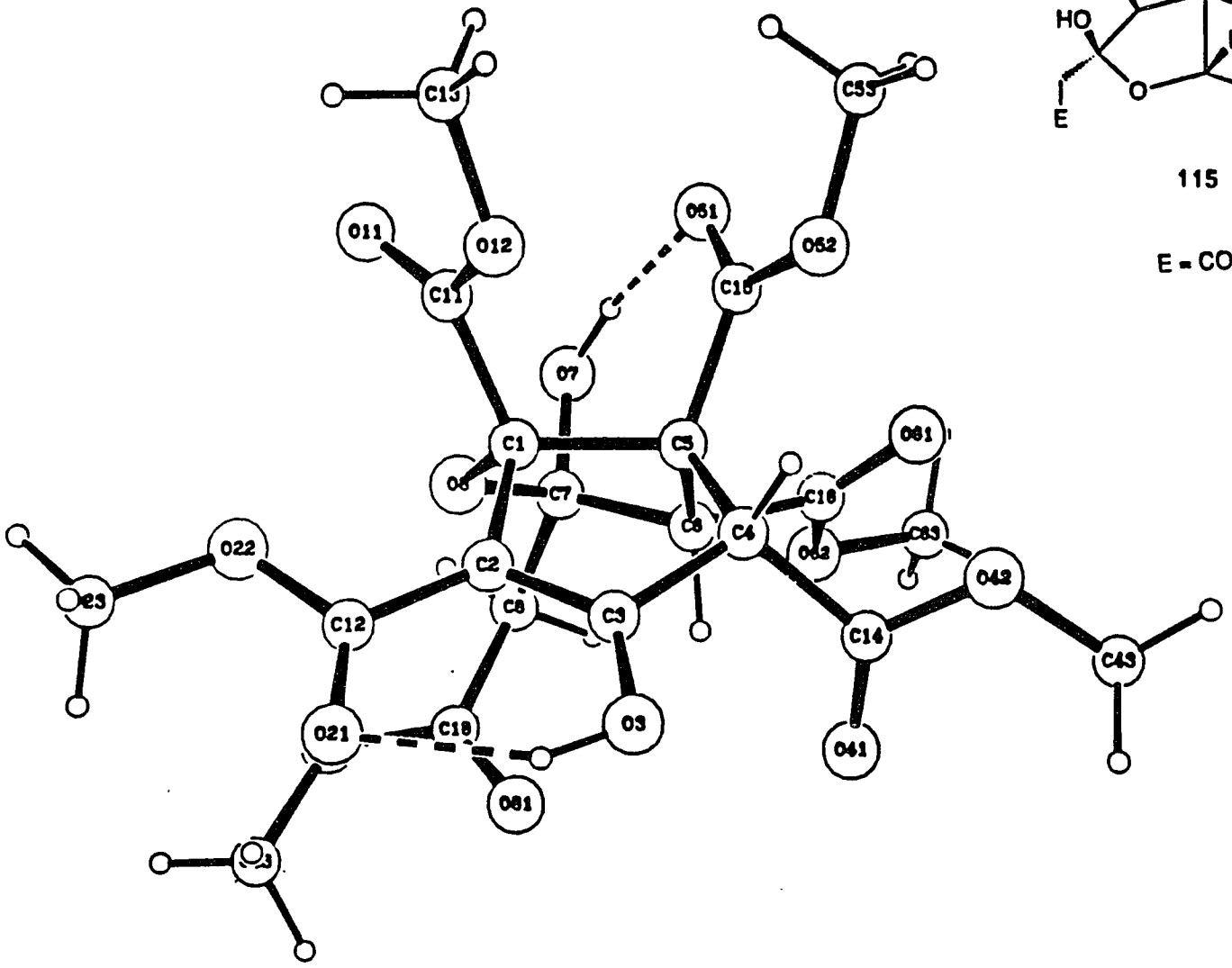
C13
C55
011
012
061
062
C11
C16
07
C1
C5
081
06
C7
C8
C4
C16
022
C2
082
C83
042
023
C12
C6
C3
C14
C43
021
C18
03
041
081
O3

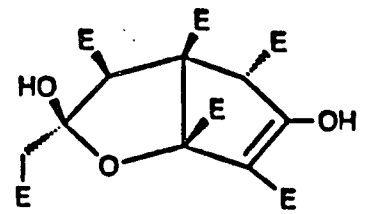
E
E
E
HO
E
OH
O
E
E

115

E = COOMe

Table 56: Crystal Data for Compound 115

Formula	$C_{20}H_{24}O_{15}$
Formula weight	504.41
Crystal system	monoclinic
Space group	$P2_1/c$
a	16.699(1) Å
b	8.073(1) Å
c	16.931(1) Å
β	90.19(1)°
Z	4
d_{calc}	1.468 g cm^{-3}
μ(Cu Kα)	10.7 cm^{-1}

Table 57: Final Atomic Parameters for Compound 115

Atom	x	y	z	B(A2)
O3	0.29253(8)	0.8876(2)	0.56426(8)	3.10(3)
O7	0.22613(9)	0.3208(2)	0.30747(8)	3.42(3)
O8	0.17818(8)	0.4763(2)	0.41337(8)	2.65(2)
O11	0.0808(1)	0.6487(2)	0.3191(1)	4.38(3)
O12	0.14687(9)	0.8847(2)	0.34178(9)	3.45(3)
O21	0.14261(9)	0.7966(3)	0.60861(9)	4.24(4)
O22	0.06521(8)	0.6815(2)	0.51525(9)	3.80(3)
O41	0.42833(9)	0.6542(2)	0.5111(1)	3.80(3)
O42	0.46563(8)	0.8362(2)	0.4189(1)	3.80(3)
O51	0.2637(1)	0.6206(2)	0.23888(8)	3.68(3)
O52	0.32129(9)	0.8567(2)	0.27768(8)	3.25(3)
O61	0.4268(1)	0.5231(2)	0.3070(1)	4.99(4)
O62	0.40354(9)	0.2713(2)	0.35470(9)	3.72(3)
O81	0.2697(1)	0.3353(2)	0.5620(1)	4.76(4)
O82	0.15852(9)	0.1859(2)	0.54606(9)	3.92(3)
C1	0.1965(1)	0.6478(2)	0.4063(1)	2.14(3)
C2	0.1988(1)	0.7310(2)	0.4860(1)	2.34(3)
C3	0.2700(1)	0.8025(2)	0.5006(1)	2.28(3)
C4	0.3273(1)	0.7925(2)	0.4332(1)	2.16(3)
C5	0.2878(1)	0.6619(2)	0.3778(1)	2.05(3)
C6	0.3154(1)	0.4829(2)	0.3935(1)	2.14(3)
C7	0.2406(1)	0.3729(2)	0.3850(1)	2.35(3)
C8	0.2398(1)	0.2164(3)	0.4354(1)	2.84(4)
C11	0.1341(1)	0.7232(3)	0.3503(1)	2.54(3)
C12	0.1338(1)	0.7394(3)	0.5429(1)	2.79(4)
C13	0.0945(2)	0.9702(3)	0.2867(2)	4.66(5)
C14	0.4124(1)	0.7505(3)	0.4598(1)	2.55(3)
C15	0.2909(1)	0.7090(3)	0.2902(1)	2.49(3)
C16	0.3875(1)	0.4308(3)	0.3458(1)	2.73(4)
C18	0.2258(1)	0.2542(3)	0.5211(1)	2.78(4)
C23	-0.0027(1)	0.6863(4)	0.5687(2)	5.46(7)
C43	0.5487(1)	0.7962(4)	0.4350(2)	5.39(7)
C53	0.3154(2)	0.9242(3)	0.1982(1)	4.67(5)
C63	0.4713(2)	0.2057(3)	0.3119(2)	4.72(5)
C83	0.1365(2)	0.2181(5)	0.6275(2)	6.61(8)

Table 57 (cont.): Final Atomic Parameters for Compound 115

Atom	x	y	z	B(A2)
H03	0.250	0.882	0.597	3.7
H07	0.236	0.408	0.276	4.1
H4	0.335	0.900	0.406	2.6
H6	0.337	0.471	0.448	2.6
H8A	0.293	0.159	0.430	3.4
H8B	0.196	0.142	0.416	3.4
H13A	0.109	1.090	0.285	5.6
H13B	0.100	0.921	0.233	5.6
H13C	0.037	0.959	0.305	5.6
H23A	-0.051	0.640	0.541	6.6
H23B	0.010	0.618	0.617	6.6
H23C	-0.013	0.803	0.585	6.6
H43A	0.584	0.867	0.402	6.5
H43B	0.561	0.817	0.492	6.5
H43C	0.558	0.677	0.423	6.5
H53A	0.340	1.037	0.197	5.6
H53B	0.343	0.850	0.160	5.6
H53C	0.257	0.934	0.183	5.6
H63A	0.478	0.084	0.324	5.7
H63B	0.463	0.221	0.254	5.7
H63C	0.522	0.265	0.329	5.7
H83A	0.085	0.161	0.640	8.0
H83B	0.179	0.175	0.663	8.0
H83C	0.130	0.340	0.636	8.0

The parameters of the hydrogen atoms were not refined.

Standard deviations are in parentheses.

Anisotropically refined atoms are given in the form of the isotropic equivalent displacement parameter defined as:
(4/3) * [a2*B(1,1) + b2*B(2,2) + c2*B(3,3) + ab(cos gamma)*B(1,2) + ac(cos beta)*B(1,3) + bc(cos alpha)*B(2,3)]

Table 58: Final Anisotropic Thermal Parameters (U's) for

Compound **115**

Atom	U(1,1)	U(2,2)	U(3,3)	U(1,2)	U(1,3)	U(2,3)
O3	0.0409(7)	0.0426(8)	0.0342(7)	-0.0069(6)	0.0007(6)	-0.0106(6)
O7	0.0617(9)	0.0391(8)	0.0292(6)	-0.0149(7)	-0.0028(6)	-0.0057(6)
O8	0.0298(6)	0.0260(6)	0.0447(7)	-0.0051(5)	0.0040(5)	0.0011(6)
O11	0.0517(8)	0.052(1)	0.0625(9)	-0.0126(8)	-0.0259(7)	0.0068(8)
O12	0.0514(8)	0.0309(7)	0.0487(8)	0.0004(6)	-0.0169(6)	0.0051(7)
O21	0.0469(8)	0.080(1)	0.0347(7)	-0.0073(8)	0.0072(6)	-0.0169(8)
O22	0.0288(6)	0.071(1)	0.0447(8)	-0.0078(7)	0.0058(6)	-0.0102(8)
O41	0.0430(7)	0.0485(9)	0.0531(8)	0.0014(7)	-0.0106(7)	0.0128(7)
O42	0.0288(6)	0.0562(9)	0.0594(9)	-0.0080(7)	-0.0002(7)	0.0122(8)
O51	0.0656(9)	0.0465(8)	0.0275(6)	-0.0143(8)	-0.0038(7)	0.0017(6)
O52	0.0558(8)	0.0346(7)	0.0332(6)	-0.0110(7)	-0.0029(6)	0.0110(6)
O61	0.0576(8)	0.0447(9)	0.088(1)	0.0043(8)	0.0413(7)	0.0152(9)
O62	0.0492(7)	0.0321(7)	0.0601(9)	0.0097(6)	0.0209(7)	0.0011(7)
O81	0.074(1)	0.064(1)	0.0431(8)	-0.0223(9)	-0.0112(8)	-0.0054(8)
O82	0.0508(8)	0.060(1)	0.0376(7)	-0.0119(8)	0.0085(7)	0.0013(7)
C1	0.0273(7)	0.0230(8)	0.0309(8)	-0.0029(7)	0.0007(7)	-0.0005(7)
C2	0.0309(8)	0.0295(9)	0.0286(8)	0.0001(7)	-0.0001(7)	-0.0012(8)
C3	0.0325(8)	0.0256(8)	0.0284(8)	0.0003(7)	-0.0017(7)	-0.0010(7)
C4	0.0277(7)	0.0241(8)	0.0301(8)	-0.0027(7)	-0.0013(7)	-0.0007(7)
C5	0.0272(7)	0.0235(8)	0.0270(8)	-0.0018(7)	0.0001(6)	0.0009(7)
C6	0.0302(8)	0.0224(8)	0.0287(8)	-0.0011(7)	0.0015(7)	-0.0005(7)
C7	0.0344(8)	0.0257(8)	0.0291(8)	-0.0031(7)	0.0014(7)	-0.0034(7)
C8	0.048(1)	0.0250(9)	0.0352(9)	-0.0044(8)	0.0053(8)	-0.0010(8)
C11	0.0294(8)	0.034(1)	0.0328(8)	-0.0018(8)	-0.0015(7)	0.0006(8)
C12	0.0311(8)	0.040(1)	0.0350(9)	-0.0014(8)	0.0015(7)	0.0001(9)
C13	0.069(1)	0.049(1)	0.058(1)	0.010(1)	-0.023(1)	0.014(1)
C14	0.0306(8)	0.0292(9)	0.0372(9)	-0.0031(7)	-0.0014(7)	-0.0044(8)
C15	0.0316(8)	0.0328(9)	0.0303(8)	-0.0023(8)	0.0026(7)	0.0038(8)
C16	0.0357(9)	0.0309(9)	0.0372(9)	-0.0003(8)	0.0057(8)	-0.0019(8)
C18	0.0416(9)	0.0298(9)	0.0344(9)	0.0004(8)	-0.0016(8)	0.0037(8)
C23	0.036(1)	0.107(2)	0.065(1)	-0.010(1)	0.018(1)	-0.011(2)
C43	0.029(1)	0.091(2)	0.085(2)	-0.007(1)	-0.002(1)	0.009(2)
C53	0.087(2)	0.053(1)	0.038(1)	-0.015(1)	-0.004(1)	0.022(1)
C63	0.055(1)	0.050(1)	0.075(2)	0.017(1)	0.027(1)	-0.003(1)
C83	0.102(2)	0.102(2)	0.048(1)	-0.017(2)	0.031(1)	-0.011(2)

The form of the anisotropic displacement parameter is:
exp[-2PI2(h2a2U(1,1) + k2b2U(2,2) + l2c2U(3,3) + 2hkabU(1,2) + 2hlacU(1,3) + 2klbcU(2,3))] where a,b, and c are reciprocal lattice constants.

Table 59: Bond Distances (Å) for Compound 115

Atom 1	Atom 2	Distance	Atom 1	Atom 2	Distance
O3	C3	1.332(2)	O62	C63	1.446(3)
O7	C7	1.398(2)	O81	C18	1.201(3)
O8	C1	1.423(2)	O82	C18	1.323(3)
O8	C7	1.420(2)	O82	C83	1.451(3)
O11	C11	1.194(3)	C1	C2	1.508(3)
O12	C11	1.329(3)	C1	C5	1.604(2)
O12	C13	1.451(3)	C1	C11	1.534(3)
O21	C12	1.213(3)	C2	C3	1.343(3)
O22	C12	1.322(2)	C2	C12	1.455(3)
O22	C23	1.455(3)	C3	C4	1.493(3)
O41	C14	1.195(3)	C4	C5	1.556(3)
O42	C14	1.324(2)	C4	C14	1.527(3)
O42	C43	1.450(3)	C5	C6	1.540(3)
O51	C15	1.212(2)	C5	C15	1.533(3)
O52	C15	1.314(2)	C6	C7	1.540(3)
O52	C53	1.454(3)	C6	C16	1.511(3)
O61	C16	1.192(3)	C7	C8	1.525(3)
O62	C16	1.324(3)	C8	C18	1.502(3)

Standard deviations are in parentheses.

Table 60: Bond Angles (°) for Compound 115

Atom 1	Atom 2	Atom 3	Angle	Atom 1	Atom 2	Atom 3	Angle
C1	08	C7	112.7(1)	C5	C6	C7	106.4(1)
C11	012	C13	116.0(2)	C5	C6	C16	114.1(2)
C12	022	C23	116.6(2)	C7	C6	C16	115.9(2)
C14	042	C43	115.4(2)	07	C7	08	111.7(1)
C15	052	C53	117.7(2)	07	C7	C6	113.5(2)
C16	062	C63	117.2(2)	07	C7	C8	105.9(2)
C18	082	C83	116.6(2)	08	C7	C6	103.0(1)
08	C1	C2	111.3(1)	08	C7	C8	106.9(1)
08	C1	C5	107.4(1)	C6	C7	C8	115.7(2)
08	C1	C11	106.9(1)	C7	C8	C18	112.0(2)
C2	C1	C5	102.5(1)	011	C11	012	124.5(2)
C2	C1	C11	113.1(1)	011	C11	C1	125.2(2)
C5	C1	C11	115.5(1)	012	C11	C1	110.3(2)
C1	C2	C3	112.0(2)	021	C12	022	124.1(2)
C1	C2	C12	126.6(2)	021	C12	C2	122.4(2)
C3	C2	C12	121.4(2)	022	C12	C2	113.4(2)
03	C3	C2	128.1(2)	041	C14	042	124.8(2)
03	C3	C4	117.8(2)	041	C14	C4	124.3(2)
C2	C3	C4	113.9(2)	042	C14	C4	110.9(2)
C3	C4	C5	103.0(1)	051	C15	052	124.3(2)
C3	C4	C14	112.6(2)	051	C15	C5	122.3(2)
C5	C4	C14	114.8(1)	052	C15	C5	113.3(2)
C1	C5	C4	105.5(1)	061	C16	062	124.0(2)
C1	C5	C6	99.6(1)	061	C16	C6	124.2(2)
C1	C5	C15	110.1(1)	062	C16	C6	111.8(2)
C4	C5	C6	113.9(1)	081	C18	082	124.1(2)
C4	C5	C15	113.5(1)	081	C18	C8	124.8(2)
C6	C5	C15	112.9(1)	082	C18	C8	111.0(2)

Standard deviations are in parentheses.

REFERENCES

(1) Hansen, H. J.; Schmidt, H. *Tetrahedron* **1974**, 30, 1959.

(2) (a) Hurd, C. D.; Pollack, M. A. *J. Org. Chem.* **1939**, 3, 550.
(b) Levy, H.; Cope, A. C. *J. Am. Chem. Soc.* **1944**, 66, 1684.
(c) Gajewski, J.J. *Hydrocarbon Thermal Isomerizations*, Academic Press, **1981**, 166.

(3) Doering, W. v. E.; Roth, W. R. *Tetrahedron* **1963**, 19, 715.

(4) Günther, H.; Runsink, J.; Schmickler, H.; Schmitt, P. *J. Org. Chem.* **1985**, 50, 289.

(5) Kessler, H.; Ott, W. *J. Am. Chem. Soc.* **1976**, 98, 5014.

(6) Gajewski, J. J.; Conrad, N. D. *Ibid.* **1979**, 101, 6693.

(7) Dewar, M. J. S.; Wade, L. E. Jr. *Ibid.* **1977**, 99, 4417.

(8) Doering, W. v. E.; Roth, W. R. *Tetrahedron* **1962**, 18, 67.

(9) Hoffmann, R.; Woodward, R. B. *J. Am. Chem. Soc.* **1965**, 87, 4389.

(10) Doering, W. v. E.; Toscano, V., unpublished work, but see footnote 9 in Berson, J. A.; Jones, M. Jr. *Ibid.* **1964**, 86, 5017.

(11) (a) Wehrli, R.; Schmidt, H.; Bellus, D.; Hansen, H. J. *Helv. Chim. Acta* **1977**, 60, 1325.
(b) Doering, W. v. E.; Troise, C. A. *J. Am. Chem. Soc.* **1985**, 107, 5739.
(c) Dewar, M. J. S.; Jie, C. *Ibid.* **1987**, 109, 5893.
(d) Dewar, M. J. S.; Jie, C. *J. Chem. Soc., Chem. Commun.* **1987**, 1451.

(12) Allerhand, A.; Gutowsky, H. S. *J. Am. Chem. Soc.* **1965**, 87, 4092.

(13) Doering, W. v. E.; Ferrier, B. M.; Hartenstein, J. H.; Jones, M. Jr.; Klumpp, G.; Rubin, R. M.; Saunders, M. *Tetrahedron* **1967**, 23, 3943.

(14) (a) Zimmerman, H. E.; Binkley, R. W.; Givens, R. S.; Grunwald, G. L.; Sherwin, M. A. *J. Am. Chem. Soc.* **1969**, 91, 3316.
(b) Cheng, A. K.; Anet, F. A. L.; Mioduski, J.; Meinwald, J. *Ibid.* **1974**, 96, 2887.

(c) Macho, V.; Miller, R. D.; Yannoni, C. S. *Ibid.* **1983**, 105, 3735.
(d) Günther, H.; Moskau, D.; Aydin, R.; Leber, W.; Quast, H.; Martin, H.-D.; Hassenrück, K.; Miller, L. S.; Grohmann, K. *Chem. Ber.* **1989**, 122, 925.

(15) Hoffmann, R.; Stohrer, W.-D. *J. Am. Chem. Soc.* **1971**, 93, 6941.

(16) (a) Doering, W, v. E.; Laber, G.; Vonderwahl, R.; Chamberlain, N. F.; Williams, R. B. *Ibid.* **1956**, 78, 5448.
(b) Winstein, S. J. *Ibid*, **1959**, 81, 6524.
(c) Winstein, S. J. *Special Publication, Chem. Soc.* (London) **1967**, 21, 5.

(17) (a) Warner, P. M. *Topics in Nonbenzenoid Aromatic Chemistry* (Edited by Nozoe, T.; Breslow, R.; Hafner, K.; Ito, S.; Murata, I.) **1977**, 2, 283, Hirokawa, Tokyo.
(b) Paquette, L. A. *Angew. Chem., Int. Ed. Engl.* **1978**, 17, 106.
(c) Childs, R. F. *Accts. Chem. Res.* **1984**, 17, 347.

(18) Dewar, M. J. S.; Schoeller, W. W. *J. Am. Chem. Soc.* **1971**, 93, 1481.

(19) Dewar, M. J. S.; Lo, D. H. *Ibid.* **1971**, 93, 7201.

(20) Anet, F. A. L.; Schenck, G. E. *Tetrahedron Lett.* **1970**, 48, 4237.

(21) Oth, J. F. M.; Gilles, J.-M., unpublished work, but see footnote 27 in Schröder, G.; Oth, J. F. M. *Angew. Chem., Int. Ed. Engl.* **1967**, 6, 414.

(22) Grohmann, K.; Miller, L. S.; Dannenberg, J. J. *J. Am. Chem. Soc.* **1983**, 105, 6862.

(23) (a) Miller, L. S.; Todaro, L. J.; Dannenberg, J. J.; Grohmann, K. *Ibid.* **1981**, 103, 6249.
(b) Miller, L. S. *Ph. D. Thesis*, City Univ. of New York, **1982**.

(24) (a) Quast, H.; Görlach, Y.; Stawitz, J. *Angew. Chem., Int. Ed. Engl.* **1981**, 20, 93.
(b) Jackman, L. M.; Ibar, G.; Freyer, A. J.; Görlach, Y.; Quast, H. *Chem. Ber.* **1984**, 117, 1671.

(25) Quast, H.; Geissler, E.; Mayer, A.; Jackman, L. M.; Colson, K. L. *Tetrahedron* **1986**, 42, 1805.

(26) Busch, A.; Hoffmann, H. M. R. *Tetrahedron Lett.* **1976**, 2379.

(27) Gompper, R.; Nöth, H.; Spes, P. *Ibid.* **1988**, 29, 3639.

(28) Barton, T. J.; Juvet, M. *Ibid.* **1975**, 2561.

(29) Anastassiou, A. G.; Reichmanis, E.; Winston, A. E. *Angew. Chem., Int. Ed. Engl.* **1976**, 88, 382.

(30) Lambert, J. B. *Tetrahedron Lett.* **1963**, 1901.

(31) Anastassiou, A. G.; Chao, B. Y.-H. *J. Chem. Soc., Chem. Commun.* **1972**, 277.

(32) Katz, T. J.; Carnahan, J. C. Jr.; Clarke, G. M.; Acton, N. *J. Am. Chem. Soc.* **1970**, 92, 734.

(33) (a) Biethan, V.; Klusacek, H.; Musso, H. *Angew. Chem., Int. Ed. Engl.* **1967**, 6, 176.
(b) Goldstein, M. J.; Odell, B. G. *J. Am. Chem. Soc.* **1967**, 89, 6356.
(c) Tsuruta, H.; Kurabayashi, K.; Mukai, T. *Tetrahedron Lett.* **1967**, 3775.
(d) Daub, J.; Schleyer, P. v. R. *Angew. Chem., Int. Ed. Engl.* **1968**, 7, 468.

(34) Baxter, S. G.; Weissman, S. A. *J. Am. Chem. Soc.* **1986**, 108, 529.

(35) Dewar, M. J. S.; Náhlovská. Z.; Náhlovsky, B. D. *J. Chem. Soc., Chem. Commun.* **1971**, 1377.

(36) (a) Paquette, L. A.; Volz, W. E.; Beno, M. A.; Christoph, G. G. *Ibid.* **1975**, 97, 2562.
(b) Christoph, G. G.; Beno, M. A. *Ibid.* **1978**, 100, 3156.
(c) Quast, H.; Görlach, Y.; Meichsner, G.; Peters, K.; Peters, E.-M.; Schnering, H. G. *Tetrahedron Lett.* **1982**, 23, 4677.
(d) Quast, H.; Görlach, Y.; Christ, J.; Perters, E.-M.; Peters, K.; Schnering, H. G.; Jackman, L. M.; Ibar, G.; Freyer, A.J. *Ibid.* **1983**, 24, 5595.

(37) Quast, H.; Görlach, Y.; Stawitz, J.; Peters, E.-M.; Peters, K.; Schnering, H. G. *Ibid.* **1984**, 117, 2745.

(38) (a) Vogel, E.; Reel, H. *J. Am. Chem. Soc.* **1972**, 94, 4388.
(b) Vogel, E.; Brinker, U. H.; Nachtkamp, K.; Wassen, J.; Müllen, K. *Angew. Chem.* **1973**, 85, 758.
(c) Günther, H.; Vogel, E.; Schmickler, H.; Brinker, U. H.; Nachtkamp, K.; Wassen, J. *Ibid.* 760.

(39) Williams, R. V.; Kurtz, H. A. *J. Org, Chem.* **1988**, 53, 3626.

(40) (a) Iyengar, R. *Ph. D. Thesis*, City Univ. of New York, **1987**.
(b) Iyengar, R.; Piña, R.; Grohmann, K.; Todaro, L. J. *J. Am. Chem. Soc.* **1988**, 110, 2643.

(41) Bertz, S. H. *J. Org. Chem.* **1985**, 50, 3585.

(42) Sands, R. D. *Ibid.* **1983**, 48, 3362.

(43) Roberts, M.; Parsons, W.; Schlessinger, R. *Ibid.* **1978**, 43, 3970.

(44) Birladeanu, L.; Chamot, E.; Fristad, W. E.; Paquette, L. A.; Winstein, S. *Ibid.* **1977**, 42, 3260.

(45) Dong, D. C.; Edwards, J. T. *Can. J. Chem.* **1980**, 58, 1324.

(46) Marchand, A. P.; Chou, T.-C.; Ekstrand, J. D.; Vanderhelm, D. *J. Org. Chem.* **1976**, 41, 1438.

(47) Smith, E. C.; Barborak, J. C. *Ibid.* 1433.

(48) Grob, C. A. *Angew. Chem., Int. Ed. Engl.* **1969**, 8, 535.

(49) Kessler, H.; Ott, W. *Tetrahedron Lett.* **1974**, 15, 1383.

(50) Birladeanu, L.; Harris, D. L.; Winstein, S. *J. Am. Chem. Soc.* **1970**, 92, 6387.

(51) Hanafusa, T.; Imai, S.; Ohkata K.; Suzuki, H.; Suzuki, Y. *J. Chem. Soc., Chem. Commun.* **1974**, 73.

(52) (a) Kuhn, R.; Winterstein, A. *Helv. Chim. Acta* **1928**, 11, 87.
(b) Kuhn, R.; Wallenfels, K. *Chem, Ber.* **1938**, 71, 1889 and references cited therein.

(53) Newkome, G. R.; Sauer, J. D.; Erbland, M. L. *J. Chem. Soc., Chem. Commun.* **1975**, 885.

(54) (a) Germann, F. E. E.; Traxler, R. N. *J. Am. Chem. Soc.* **1927**, 49, 307.
(b) Lauwers, M.; Regnier, B.; Eenoo, M. V.; Denis, J. N.; Krief, A. *Tetrahedron Lett.* **1979**, 20, 1801.

(55) Tsuruta, H.; Kurabayashi, K.; Mukai, T. *Ibid.* **1967**, 3775.

(56) (a) Lythgoe et al. *Am. Soc.* 1956, 4060.
(b) Dev et al. *J. Indian Chem. Soc.* **1956**, 33, 773.

(57) (a) Hoffmann, R. *Tetrahedron Lett.* **1970**, 2907.
(b) Günther, H. *Ibid.* 5173.

(58) (a) Paquette, L. A.; Volz, W. E. *J. Am. Chem. Soc.* **1976**, 98, 2910.
(b) Hoffmann, R. W.; Hauel, N.; Frickel, F.; Kempf, M.; Kessler, H. *Chem. Ber.* **1979**, 112, 2894.

(59) Müllen, K.; Trinks, R. *Chem. Ber.* **1987**, 120, 1481.

(60) Cookson, R. C.; Friedrich, K. R. *Org. Chem. Section C*, **1966**, 1641.

(61) Sellner, I.; Schuster, H.; Sichert, H.; Sauer, J.; Nöth, H. *Chem. Ber.* **1983**, 116, 3751.

(62) Gaylord, N. G. *Reduction with Complex Metal Hydrides*, Interscience, New York, **1956**, 391-531.

(63) (a) Müller, P. in Patai, *The Chemistry of Functional Groups, Supplement E*, Wiley, New York, **1980**, 469- 538.
(b) Cullis, C. F.; Fish, A. in Patai, *The Chemistry of the Carbonyl Group*, Interscience, New York, **1966**, 1, 129-157.

(64) Sandler, S. R.; Karo, W. *Organic Functional Group Preparations*, Academic Press, New York, **1972**, 3, 372-381.

(65) (a) Foley, P. J. Jr. *J. Org. Chem.* **1969**, 34, 2805.
(b) Chakrabarti, J. K.; Hotten, T. M. *J. Chem. Soc., Chem. Commun.* **1972**, 1226.

(66) (a) Wrobel, J.; Takahashi, K.; Honkan, V.; Lannoye, G.; Cook, J. M.; Bertz, S. H. *J. Org. Chem.* **1983**, 48, 139.
(b) Bertz, S. H.; Dabbagh, G.; Cook, J. M.; Honkan, V. *Ibid.* **1984**, 49, 1739.

(67) Bhatnagar, S. P.; Weiss, U.; Highet, R. J. *J. Org. Chem.* **1977**, 42, 3089.

(68) Findlay, S. P. *J. Am. Chem. Soc.* **1957**, 22, 1385.

(69) Connelly, M. *Ph. D. Thesis*, City Univ. of New York, **1993**.

(70) (a)Yates, P.; Stevens, K. E. *Tetrahedron* **1981**, 37, 4401.
(b) Trost, B. M.; Taber, D. F.; Alper, J. B. *Tetrahedron Lett.* **1976**, 3857.
(c) Clark, R. D.; Heathcock, C. H. *Ibid.* **1975**, 529.
(d) Corey, E. J.; Fuchs, P. L. *J. Am. Chem. Soc.* **1972**, 94, 4014.

(e) Alexakis, A.; Cahiez, G.; Normant, J. F. Tetrahedron **1980**, 36, 1961.

(71) Paquette, L. A.; Birnberg, G. H. *J. Chem. Soc., Chem. Commun.* **1973**, 129.

(72) Askani, R.; Sonmez, H. *Tetrahedron Lett.* **1973**, 20, 1751.

(73) (a) Taft, R. W. Jr. *J. Am. Chem. Soc.* 1957, 79, 1045.
(b) Jaffé, H. H. *Chem. Rev.* **1953**, 53, 191.

(74) (a) Burgess, E. M.; Penton, H. R. Jr.; Taylor, E. A.; Williams, W. M. *Org. Syntheses* **1988**, 56, 40.
(b) Burgess, E. M.; Penton, H. R. Jr.; Taylor, E. A. *J. Org. Chem.* **1973**, 38, 26.
(c) Claremon, D. A.; Phillips, B. T. *Tetrahedron Lett.* **1988**, 29, 2155.

(75) (a) Harrison, C. R.; Hodge, P. Rogers, W. J. *Synthsis*, **1977**, 41.
(b) Appel, R.; Kleinstück, R.; Ziehn, K. *Chem. Ber.* **1971**, 104, 1030.

(76) Lehnert, W. *Tetrahedron Lett.* **1971**, 1501.

(77) Monson, R. S.;Priest, D. N. *Can. J. Chem.* **1971**, 49, 2897.

(78) Yokoyama, M.; Yoshida, S.; Imamoto, T. *Synthesis* **1982**, 591.

(79) McDonald, I. A.; Dreiding, A. S.; Hutmacher, H.-M.; Musso, H. *Helv. Chim. Acta* **1973**, 56, 1385.

(80) Weiss, U.; Edwards, J. M. *Tetrahedron Lett.* **1968**, 47, 4885.

(81) Fox, H. H. *J. Org. Chem.* **1947**, 12, 535.

(82) Quast, H.; Röschert, H.; Peters, E.-M.; Peters, K.; Schnering, H. G. *Chem. Ber.* **1989**, 122, 523.

(83) (a) Camps, P.; Figueredo, M. *Can. J. Chem.* **1984**, 62, 1184.
(b) Camps, P.; Iglesias, C.; Rodrjguez, M. J.; Grancha, M. D.; Gregori, M. E.; Lozano, R.; Miranda, M. A.; Figueredo, M.; Linares, A. *Chem. Ber.* **1988**, 121, 647.

(84) Sutton, L. E. *Spec. Publ. Chem. Soc.* **1958**, 11, 1965.

(85) (a) Ermer, O. *Angew. Chem., Int. Ed. Engl.* 1987, 26, 782.
(b) Grob, C. A. Acc. Chem. Res. **1983**, 16, 426.

(86) Todaro, L. J. *Ph. D. Thesis*, City Univ. of New York, **1993**.

(87) These measurements were carried out in collaboration with C. S. Yannoni at IBM (San Jose) and with L. M. Jackman at Pennsylvania State University.

(88) (a) Quast, H.; Carlsen, J.; Janiak, R.; Peters, E.-M.; Peters, K.; Schnering, H. G. *Chem. Ber.* **1992**, 125, 955.
(b) Jackman, L. M.; Benesi, A.; Mayer, A.; Quast, H.; Peters, E.-M.; Peters, K.; Schnering, H. G. *J. Am. Chem. Soc.* **1989**, 111, 1512.

(89) Anet, F. A. L.; Anet, R. *Configuration and Conformation by NMR*, in Nachod, F. C.; Zuckerman, J. J. (eds.) *Determination of Organic Structures by Physical Methods*, Academic Press, New York, London, **1971**, 3, Chapter 7.

(90) Breitmaier, E.; Voelter, W. *Carbon-13 NMR Spectrtscopy*, 3rd Ed.,VCH Publishers, **1987**, 127.

(91) (a) Kessler, H. *Angew. Chem.* **1970**, 82, 237.
(b) Kessler, H. *Angew. Chem., Int. Ed. Engl.* **1970**, 9, 158, 219 and references cited there in.

(92) Still, W. C.; Kahn, M.; Mitra, A. *J. Org. Chem.* **1978**, 43, 2923.

(93) Instruction manual for chromatotron model 8924, Harrison Research, CA, dated 88-11-07, recipe 1, page 20.

(94) Langrebe, J. A. *Theory and Practice in the Organic Laboratory*, 2nd Ed., D. C. Heath and Co., **1977**, Chapter 7.7.

(95) Aldrich Chem. Co., Technical Information Bulletin, No. AL-136.